The Role of Bile Acids and Farnesoid X Receptor in Ileal Crohn's Disease

Dr R Alexander Speight MA (cantab.), MBBS (hons.), MRCP

Institute of Cellular Medicine

Submitted in partial fulfillment of the degree Doctor of Medicine

December 2015

Surely mankind must believe in something, or at least seek for the truth, otherwise life is just emptiness.

To live and not to know why the cranes fly, why children are born, why there are stars in the sky… Either you must know why you live, or everything is trivial – just dust in the wind.

The Three Sisters (Act 2), Anton Chekhov

Table of Contents

List of Figures and Tables v

List of Abbreviations ix

Acknowledgements xi

Thesis Abstract xiii

Chapter 1 – Introduction 1

1.1 Crohn's disease 2

1.1.1 Epidemiology 3

1.1.2 Aetiopathology 3

1.1.3 Treatment 5

1.2 Environmental risk factors for Crohn's disease 5

1.2.1 Diet 6

1.2.2 Gut microbiota 7

1.2.3 Association between diet and microbiota 9

1.2.4 Microbiota and intestinal homeostasis 10

1.2.5 Bile acid dysmetabolism 10

1.2.6 Short chain fatty acids (SCFAs) 12

1.2.7 Obesity and tight junction proteins 12

1.2.8 Specific pathobionts 13

1.3 Bile acids 14

1.3.1 Synthesis and structure 14

1.3.2 Entero-hepatic circulation 16

1.3.3 Bile Acids as signalling molecules 16

1.4 Farnesoid X receptor 17

1.4.1 Structure and function 17

1.4.2 FXR is a key regulator of bile acid metabolism 19

1.4.3 FXR and IBD 20

1.4.4 FXR agonists 23

1.4.5 TGR5 24

1.5 Small bowel epithelium 24

1.5.1 The epithelial barrier 25

1.5.2 Epithelial barrier dysfunction in Crohn's disease 26

1.5.3 Tight junctions 27

1.5.4 Innate immune dysfunction and IBD 28

1.6 Cytokine profiles in Crohn's disease 31

1.6.1 T-helper cell phenotype in Crohn's disease 31

1.6.2 Effect of pro-inflammatory cytokines on the gut epithelial barrier 33

1.7 Hypothesis and Aims 36

Chapter 2 – FXR Agonism and Gut Epithelial Barrier Function in Human Cell Lines 39

2.1 Abstract 39

2.2 Introduction and aims 40

2.3 Methods 42

2.3.1 The Caco-2 and HT29 cell lines 42

2.3.2 Optimisation of a Caco-2 polarised epithelial monolayer 43

2.3.3 Mycoplasma 45

2.3.4 Lactate dehydrogenase release assay 47

2.3.5 Measurement of trans-epithelial electrical resistance 47

2.3.6 Measurement of Lucifer Yellow monolayer flux 49

2.3.7 Imaging Caco-2 cell monolayers 50

2.3.8 HT29 cell culture ... 51
2.3.9 Enzyme-linked immunosorbent assay (ELISA) ... 51
2.3.10 BSA protein assay ... 54
2.3.11 RNA extraction ... 54
2.3.12 Phenol-based RNA extraction ... 55
2.3.13 Phenol-based method combined with spin column-based RNA extraction ... 56
2.3.14 RNA quantity and quality ... 57
2.3.15 Complementary DNA (cDNA) synthesis ... 60
2.3.16 Real-time reverse transcription polymerase chain reaction (RT-PCR) ... 61
2.3.17 RT-PCR quality control ... 64
2.3.18 Threshold cycle and relative quantification ... 67
2.3.19 Fold change calculations and statistical analyses ... 68
2.4 Results ... 70
2.4.1 Optimisation of a Caco-2 polarised monolayer model ... 70
2.4.2 6-ECDCA and GW4064 agonise FXR in both Caco-2 and HT29 cells ... 75
2.4.3 Activation of FXR does not maintain Caco-2 monolayer permeability when disrupted with inflammatory cytokines ... 79
2.4.4 Activation of FXR maintains Caco-2 cell morphology ... 84
2.4.5 Activation of FXR may inhibit cytokine induced upregulation of MLCK ... 91
2.4.6 Optimisation of HT29 as a model of IL-8 secretion ... 92
2.4.7 FXR agonism reduces the IL-8 response induced by TNFα in HT29 cells ... 93
2.5 Discussion ... 97

Chapter 3 – The Effect of FXR Agonism on Ileal Inflammation in a Mouse Model of Metabolic Syndrome ... 103
3.1 Abstract ... 103
3.2 Introduction and aims ... 104
3.3 Methods ... 106
3.3.1 Animal care ... 106
3.3.2 Mouse strain – C3H/He ... 106
3.3.3 Study design ... 107
3.3.4 Ileal preparation ... 111
3.3.5 RNA isolation ... 112
3.3.6 RNA quantity and quality ... 113
3.3.7 mRNA reverse transcription (cDNA synthesis) ... 114
3.3.8 Real-time reverse transcription polymerase chain reaction (RT-PCR) ... 115
3.3.9 RT-PCR quality control ... 116
3.3.10 Relative quantification and statistical analyses ... 120
3.4 Results ... 122
3.4.1 Study animals ... 122
3.4.2 Mice fed a HF/HS diet were heavier with more visceral fat ... 125
3.4.3 Increased body fat is associated with higher levels of inflammatory cytokine expression in the ileum ... 125
3.4.4 There is evidence that FXR activity is decreased in the ileum of mice fed a HF/HS diet ... 128
3.4.5 There is a trend to suggest that Ileal inflammatory cytokine gene expression is elevated in mice fed a HF/HS diet ... 130
3.4.6 High dose, but not low dose, FXR agonist induced FXR activation ... 131
3.4.7 There is a trend suggesting attenuated levels of ileal cytokine expression in HF/HS fed mice when treated with an FXR agonist ... 135
3.4.8 High dose FXR agonist may cause an increase in ileal cytokine expression ... 138
3.5 Discussion ... 141

Chapter 4 – FXR Activity In Patients With Ileal Crohn's Disease ... 145
4.1 Abstract ... 145
4.2 Introduction and aims ... 146
4.3 Methods ... 148

4.3.1 Ethics and consent 148
4.3.2 Patient recruitment and control group 148
4.3.3 *Ex-vivo* organ culture of ileal mucosa 149
4.3.4 Final protocol 150
4.3.5 Real-time reverse transcription polymerase chain reaction (RT-PCR) 152
4.3.6 Detection of pro-inflammatory cytokines using a multi-array, electro-chemical luminescence assay 157
4.3.7 Statistics 158
4.4 Results 160
4.4.1 Study patient demographics 160
4.4.2 FXR expression and FXR activity is decreased in patients with ileal Crohn's disease 163
4.4.3 There is a trend to increased levels of inflammatory cytokine in the ileal mucosa of patients with Crohn's disease 163
4.4.4 Short-term, *ex-vivo* ileal explant culture is biologically viable 166
4.4.5 Pilot data suggests that FXR agonism does not ameliorate the pro-inflammatory milieu associated with TNFα stimulation 174
4.5 Discussion 177
Chapter 5 – Conclusions 181
5.1 Introduction 181
5.2 The overarching hypothesis 182
5.2.1 Data to support the hypothesis 184
5.2.2 Data against the hypothesis 186
5.3 Limitations of the thesis 187
5.4 Questions arising from the data and future work 189
5.5 From bench to bedside 191
Appendix 193
Publications 203
References 213

List of Figures and Tables

Chapter 1 – Introduction

Figure 1.1; The structure of primary and secondary bile acids 15

Figure 1.2; Schematic to demonstrate the enterohepatic circulation of primary BAs 17

Figure 1.3; Schematic representation of the FXR receptor 19

Figure 1.4; A diagram to demonstrate intercellular protein complexes controlling the transcellular movement of water, solutes and micro-organisms 26

Figure 1.5; The dysregulated cytokine profile in Crohn's disease 33

Figure 1.6; A schematic diagram to represent the re-arrangement of the cytoskeletal actin-myosin ring 35

Figure 1.7; A schematic diagram to represent the original hypothesis 36

Chapter 2 – FXR Agonism and Gut Epithelial Barrier Function in Human Cell Lines

Figure 2.1; A schematic to represent the conditions required for culture of Caco-2 cells as a polarised epithelial monolayer 43

Figure 2.2; Change in TEER with time, presented to demonstrate the deleterious effect of Mycoplasma infection on Caco-2 45

Figure 2.3; The Millicell ERS-2 voltohmeter and chopstick electrodes 47

Figure 2.4; A schematic diagram representing the process of a sandwich ELISA 51

Figure 2.5; Examples of spectrophotometer readings for purified RNA 58

Figure 2.6; Examples of electrophoresis gels for purified RNA used in chapter 2 59

Figure 2.7; A representation of a single cycle of PCR using a TaqMan probe-based assay 62

Table 2.1; List of genes of interest and TaqMan primer/probes used in chapter 2 63

Table 2.2; Primer efficiency and goodness of fit (R^2) for primers used in chapter 2 64

Figure 2.8; Primer validation experiments for primers used in chapter 2 65

Figure 2.9; An example of an RT-PCR amplification plot to demonstrate the concept of threshold cycle (Ct) 66

Figure 2.10; Mean TEER of Caco-2 polarised monolayers with time 69

Figure 2.11; Mean change in TEER over time for monolayers exposed to IL-6, IFNγ or TNFα in comparison to control 70

Table 2.3: A table to demonstrate the results of unpaired Student's t-tests for different concentrations of cytokine versus control 71

Figure 2.12; Mean TEER of monolayers at 48 hours after stimulation with different concentrations of CD associated cytokines 72

Figure 2.13; LDH release assay for monolayers stimulated with IL-6, TNFα or IFNγ. 73

Figure 2.14; The relative gene expression of FXR, SHP and IBABP, in Caco-2 treated with 6-ECDCA or GW4064 76

Figure 2.15; The relative gene expression of FXR, SHP and IBABP, in HT29 treated with 6-ECDCA or GW4064 77

Figure 2.16; Mean TEER for Caco-2 treated with IL-6 +/- 6-ECDCA 79

Figure 2.17; Mean TEER for Caco-2 treated with IFNγ +/- 6-ECDCA 80

Figure 2.18; Mean TEER for Caco-2 treated with TNFα +/- 6-ECDCA 81

Figure 2.19; Lucifer yellow flux assay in Caco-2 after exposure to TNFα, IL-6 or IFNγ +/- 6-ECDCA or vehicle 82

Figure 2.20; Bright-field microscopy of in-situ Caco-2 following treatment with vehicle, 6-ECDCA, IFNγ, IL-6, TNFα or 1% Triton-X 85-86

Figure 2.21; Number (%) of cell-cell fissures seen at TEM for Caco-2 stimulated with cytokine or vehicle +/- FXR agonist 87

Table 2.3; Number (absolute) of cell-cell fissures seen at TEM for Caco-2 stimulated with cytokine or vehicle +/- FXR agonist 87

Figure 2.22; TEM images demonstrating examples of Caco-2 treated with control, IFNγ, IL-6, IFNγ + 6-ECDCA, IL-6 + 6-ECDCA 88-89

Figure 2.23; Relative gene expression for MLCK in Caco-2 following exposure to vehicle, FXR agonist (6-ECDCA) and IL-6 +/- FXR agonist (6-ECDCA) 90

Figure 2.24; IL-8 production by HT29 cells when cultured with TNFα 91

Figure 2.25; The concentration and gene expression of IL-8 in HT29 cultured with TNFα and/or GW4064 93

Figure 2.26; The concentration and gene expression of IL-8 in HT29 cultured with TNFα and/or 6-ECDCA 95

Chapter 3 – The Effect of FXR Agonism on Ileal Inflammation in a Mouse Model of Metabolic Syndrome

Figure 3.1; Schematic to represent study design for mouse feeding regimen 108

Table 3.1; Control diet constituents 109

Table 3.2; ALIOS diet constituents 109

Figure 3.2; Schematic representation of mouse ileum 110

Figure 3.3; An example of Nanodrop spectrophotometry for mouse ileum RNA 113

Figure 3.4; Gel electrophoresis of mouse ileum RNA 113

Table 3.3; List of the genes of interest and their TaqMan primer/probes 115

Figure 3.5; Amplification plot from RT-PCR experiment using an RNA only template to test for gDNA contamination 116

Table 3.4; Primer efficiency and goodness of fit (R^2) for primers used in ch 3 117

Figure 3.6; Primer validation experiments for primers used in chapter 3 118

Table 3.5; Contingency tables for quality of RNA versus control diet/ALIOS diet and FXR agonist/no FXR agonist 121

Table 3.6; Contingency tables for quality of RNA versus control diet/ALIOS diet and FXR agonist/no FXR agonist 121

Table 3.7; Mice characteristics 123

Figure 3.7; Body weight and visceral adipose tissue weight for mice fed control or ALIOS diet 124

Figure 3.8; Correlation between visceral adipose tissue weight and inflammatory cytokine expression 125

Figure 3.9; Correlation between body weight and inflammatory cytokine expression 126

Figure 3.10; FXR and downstream target gene expression in ALIOS versus control diet 128

Figure 3.11; Expression of inflammatory cytokine in ALIOS versus control diet 130

Figure 3.12; The effect of 1mg/kg or 5mg/kg FXR agonist on the expression of FXR, SHP and IBABP (fold change) 132

Figure 3.13; The effect of 1mg/kg or 5mg/kg FXR agonist on the expression of FXR, SHP and IBABP (ΔΔCt) 133

Figure 3.14; The effect of ALIOS diet with or without FXR agonist on the expression of TNFα, IFNγ, IL-6 and IL-8 (fold change) 135

Figure 3.15; The effect of ALIOS diet with or without FXR agonist on the expression of TNFα, IFNγ, IL-6 and IL-8 (ΔΔCt) 136

Figure 3.16; The effect of 1mg/kg or 5mg/kg FXR agonist on the expression of TNFα, IFNγ, IL-6 and IL-8 in control mice (fold change) 138

Figure 3.17; The effect of 1mg/kg or 5mg/kg FXR agonist on the expression of TNFα, IFNγ, IL-6 and IL-8 in control mice (ΔΔCt) 139

Chapter 4 – FXR Activity In Patients With Ileal Crohn's Disease

Figure 4.1 A) & B); Representations of organ culture dish with biopsy 151

Figure 4.2; Example spectrophotometer reading demonstrate the purity of RNA isolated from human ileal biopsy 153

Table 4.1; List of genes of interest and TaqMan primer/probes used in ch 4 154

Table 4.2; Primer efficiency and goodness of fit (R^2) for primers used in ch 4 154

Figure 4.3; Primer validation experiments for primers used in ch 4 155

Figure 4.4; A schematic demonstrating electro-luminescent detection assay 156

Tables 4.3 & Table 4.4; characteristics of patients enrolled in the studies of FXR activity in ileal mucosa 160-161

Figure 4.5; Relative mRNA levels of FXR, its downstream targets and inflammatory cytokines in the ileal mucosa of patients with CD 164

Figure 4.6; Relative mRNA levels of FXR, its downstream targets and inflammatory cytokine in the ileal mucosa of patients with CD (fold change) 165

Figure 4.7; H&E stains of ileal explant tissue culture optimisation 166

Figure 4.8 (a & b); The concentration of inflammatory cytokines in supernatant from ileal organ culture of patients with Crohn's disease versus control 168-169

Figure 4.9 (a & b); The concentration of inflammatory cytokines in supernatant from ileal organ culture with TNFα 171-172

Figure 4.10 (a & b); The concentration of inflammatory cytokines in supernatant from ileal organ culture after stimulation with TNFα in the presence or absence of 6-ECDCA 174-175 174-175

Chapter 5 – Conclusions

Figure 5.1; Diagram to represent potential role of impaired BA signalling in pathogenesis of CD 182

List of Abbreviations

AIEC	Adherent, Invasive Escheria Coli
AJ	Adherence junction
ASBT	Apical Sodium-dependent bile acid transporter
BA	Bile acid
BSH	Bile salt hydroxylase
CA	Cholic acid
CBC	Comparative Biology Centre
CD	Crohn's disease
CDCA	Chenodeoxycholic acid
Ct	Cycle threshold/threshold cycle
DBD	DNA binding domain
DAB	3, 3'-diaminobenzidine
DCA	Deoxycholic acid
DMEM	Dulbecco's Modified Eagle's Medium Nutrient Mixture
DSS	Dextran sodium sulphate
DTT	Dithiothreitol
ECM	Extracellular Matrix
EDTA	Ethylene diamine tetra acetic acid
ELISA	Enzyme-linked immunosorbent assay
EMT	Epithelial to mesenchymal transition
FCS	Foetal calf serum
FFPE	Formalin fixed, paraffin embedded
FITC	Fluorescin isothiocyanate
FGF	Fibroblast growth factor
FXR	Farnesoid-X receptor
g	Relative centrifugal force
GAPDH	Glyceraldehyde 3-phosphate dehydrogenase
GI	Gastrointestinal
GWAS	Genome wide association study
HBSS	Hanks Balanced Salt Solution
IBABP	Ileal Bile Acid Binding Protein
IBD	Inflammatory Bowel Disease
IHC	Immunohistochemistry
IFNγ	Interferon gamma
IL	Interleukin
iNOS	Inducible Nitrous Oxide Synthase
LBD	Ligand binding domain
LCA	Lithocholic acid
LDH	Lactate dehydrogenase
LP	Lamina propria
LPS	Lipopolysaccharide
MDP	N-acetyl muramyl dipeptide
MLCK	Myosin light chain kinase
mRNA	Messenger ribonucleic acid
n	Sample size
Nod 2	Nucleotide-binding oligomerization domain-containing protein 2
NF-κB	Nuclear factor kappa B
NTC	No template control
OST	Organic Solute Transporter

PAMP	Pathogen-associated molecular patterns
PBS	Phosphate buffered saline
PCR	Polymerase chain reaction
PRR	Pattern Recognition Receptors
RNase	Ribonuclease
RT-PCR	Reverse transcription polymerase chain reaction
RXR	Retinoic x receptor
S100A4	S100 calcium binding protein A4
SEM	Scanning electron microscopy *or* standard error of the mean
Sqstm1/p62	Sequestosome 1
SHP	Small Heterodimer Partner
α-SMA	Alpha Smooth Muscle Antigen
TBS	Tris buffered saline
TEER	Trans-epithelial electrical resistance
TEM	Transmission electron microscopy
TGFβ	Transforming growth factor beta
TGR5	Transmembrane G-protein coupled bile acid receptor
TJ	Tight junction
TLR	Toll Like Receptor
TNFα	Tumour necrosis factor alpha
Treg	T-regulatory cell
UC	Ulcerative colitis
UTR	untranslated region
Zo-1	Zonula Occludens Protein-1

Acknowledgements

I am extremely grateful for the expertise and support provided by several people not least my supervisors Dr John Mansfield and Prof John Kirby.

Additional thanks go to members of the 'Kirby lab' including Dr C Barker, Dr C A Lamb, Dr S Douglass and E Giannoudaki.

Professor Thwaites kindly provided the HT29 cell line used in chapter 2. Dr H Reeves and members of her team, Anna Whitehead and Gillian Pattman, set up the mouse model used in chapter 3. These people assisted by performing animal husbandry in its entirety. Dr J Palmer was particularly helpful in assisting with the MSD experiments in chapter 4.

Finally, my thanks go to members of the Departments of Gastroenterology and of Colorectal Surgery, Newcastle u Tyne Hospitals NHS Trust, for their interest and clinical assistance.

Thesis Abstract

The aetiopathogenesis of Crohn's disease (CD) is characterised by epithelial barrier dysfunction and immune dysregulation in a genetically susceptible host. Exposure to a western diet, a dysbiosis and bile acid (BA) dysmetabolism have also been implicated. The BA receptor, farnesoid-x receptor (FXR), is central to the crosstalk between the host and its microbiota. FXR acts to maintain the epithelial barrier and has an immuno-modulatory function although the mechanism is not fully understood.

The first aim of this study was to investigate the effect of FXR agonism using *in-vitro* models of cytokine-induced epithelial barrier dysfunction. Functional and morphological studies of Caco-2 cell monolayers demonstrated that FXR acts to maintain epithelial cell morphology, probably via a mechanism involving the regulation of myosin light chain kinase expression. FXR agonism was also able to abolish the IL-8 response of HT29 cells to stimulation with TNF α.

The second aim of this study was to investigate the link between a western-lifestyle diet, impaired BA signalling and ileal inflammation in a mouse model of obesity. Animals fed a western-lifestyle diet expressed more ileal inflammatory cytokine. There was a trend to suggest that supplementation with an FXR agonist reduced inflammatory cytokine expression.

Finally, this study aimed to both measure FXR activity in patients with ileal CD, but also to optimise an *ex-vivo* tissue culture model to assay the effect of FXR agonism on ileal mucosal cytokine production. FXR activity was significantly reduced in patients with ileal CD as compared with controls. An *ex-vivo* tissue culture model was optimised, but there was no evidence that FXR agonism could attenuate the response of primary tissue to stimulation with inflammatory cytokine.

In summary, the data presented support the hypothesis that disrupted bile acid signalling, via FXR, may predispose to the development of ileal CD by impairing gut epithelial immune homeostasis.

Chapter 1 – Introduction

This thesis is concerned with the role that disruption to bile acid (BA) signalling, via the nuclear receptor, farnesoid X receptor (FXR), may play in the aetiopathology of ileal Crohn's disease (CD).

This introductory chapter provides background information on CD, including our current understanding of environmental risk factors, the role of the microbiota and the role of the epithelial barrier in disease pathogenesis. The broader function of FXR, including BA metabolism and what's already known about its immuno-modulatory role, is also covered.

1.1 Crohn's disease

Crohn's disease (CD) was described by a number of different clinicians in the early 20th century, with case reports describing a 'regional enteritis' affecting mainly the small bowel, with no evidence of mycobacterial infection(Dalziel, 1913, Crohn et al., 1932, Licharowicz and Mayberry, 1988). The eponymous title of 'Crohn's disease' was adopted following the description of 14 cases of terminal ileal inflammation by Crohn, Ginzburg and Oppenheimer, in the Journal of the American Medical Association in 1932(Crohn et al., 1932). In an earlier description of what's now known as CD, the Scottish surgeon, Dalziel, writes that 'the etiology of the condition remains in obscurity, but I trust that ere long further consideration will clear up the difficulty'(Dalziel, 1913). Long, further consideration has indeed since occurred, but unfortunately, the aetiology of CD remains somewhat obscure.

CD is one of two major forms of inflammatory bowel diseases (IBD), with ulcerative colitis (UC) being the other form. IBD is characterised by chronic, relapsing inflammation of the gastrointestinal (GI) tract. Both diseases have distinct phenotypes and some shared presumed aetiological features. In UC, inflammation is limited to the superficial mucosal layers of the colon, classically more severely affecting the rectum, whereas the hallmark of CD is a deep, trans-mural inflammatory process affecting all levels of the gut wall. Normal and CD involved areas can occur in patches, known as skip lesions, throughout the gut. Whilst CD can affect any part of the gastrointestinal (GI) tract from the mouth to the anus, it occurs most often in the ileo-caecum. The chronic GI inflammation of CD can lead to complications such as neoplasia, strictures, abscesses or fistula.

1.1.1 Epidemiology

The incidence and prevalence of CD is highest in the Northern hemisphere, in the industrialised nations of Europe and North America(Molodecky et al., 2012). However, the incidence of IBD is increasing in the Middle East and in Asia, indicating the emergence of the disease as a global phenomenon(Leong et al., 2004). The prevalence of CD is approximately 32 per 1,000 persons in Europe and North America with an annual incidence of approximately 15-20 per 100,000 persons/year(Hanuer, 2006). Disease onset can occur at any age, but the peak is at 15 to 30 years of age with a second small peak between 50 and 70 years. Approximately 10% of patients will be diagnosed before the age of 18(Hedin et al., 2012). There are ethnic differences with the disease being more common in Caucasians and Ashkenazi Jews, although over recent years other ethnic groups, including African-Americans and Asians, have started to catch up(Hanuer, 2006). This finding, along with the fact that immigrants from low prevalence to high prevalence areas develop an increase risk for development of the disease(Probert et al., 1992), suggests that environmental factors are important in disease pathogenesis.

1.1.2 Aetiopathology

The aetiopathology of CD remains incompletely understood but is complex and multifactorial, involving defective epithelial function, immune dysregulation, bacterial dysbiosis and other environmental risk factors in a genetically susceptible host(Xavier and Podolsky, 2007). High estimates of heritability, with monozygotic twin concordances of 20% to 55% for CD and 15% to 18% for UC, highlight the importance of genetic susceptibility factors(Brant, 2011, Hedin et al., 2012). Several large genome wide association studies (GWAS) have identified over

160 genetic loci associated with IBD(Wellcome Trust Case Control Consortium, 2007, Jostins et al., 2012). Detailed study of these loci, many of which overlap between CD and UC, has revealed novel molecular mechanisms in the pathogenesis of IBD. These mechanisms include dysfunction within the epithelial barrier, impaired autophagy and impairment of the Th17/IL-23 axis(Lees et al., 2011).

Other experimental evidence has implicated defective barrier function in the pathogenesis of CD. Several studies using non-invasive techniques have demonstrated increased epithelial permeability in active CD(Soderholm et al., 2002, Soderholm et al., 2004, Keita et al., 2008). Recurrent bacterial translocation, presumably through a leaky epithelium, has been serially demonstrated(McGuckin et al., 2009). Alterations in epithelial tight-junction complexes and defensin production have been described(Muniz et al., 2012). Clinically unaffected first-degree relatives of patients with CD demonstrate increased epithelial permeability(Hedin et al., 2012). Finally, as demonstrated by confocal laser endoscopy, an increase in ileal epithelial permeability can detect disease relapse in patients with quiescent CD(Kiesslich et al., 2012).

It is not clear whether epithelial barrier function is a cause or consequence of the inflammation associated with the disease. The genetic predisposition to impaired barrier function suggested by GWAS and the findings in unaffected first-degree relatives would suggest the former. What is clear, is the central importance of the epithelial barrier in CD pathogenesis and the potential therapeutic role of maintaining epithelial homeostasis.

Despite these advances in our understanding of the pathogenesis of CD, much is still to be learned. Much of the heritability suggested by twin studies has not been explained by GWAS and the search for further genetic susceptibility factors goes on. The role of the environment, and particularly the microbiome, has become

increasingly recognised over the last few years(Xavier and Podolsky, 2007). However, the interaction of genetic susceptibility and environmental factors that leads to the development of CD is still unknown.

1.1.3 Treatment

The aims of treatment are to induce and maintain disease remission, to improve quality of life, to prevent the development of complications and to prevent or reduce the requirement for surgery. The chronic inflammation of CD results in areas of narrowed, irreversibly damaged bowel for which surgery is the only treatment. The formation of fistulas, para-enteric abscesses, perforations and even surgery itself can cause further bowel damage.

The current pharmaceutical armamentarium includes corticosteroids and immunomodulators such as azathioprine, 6-mercaptopurine (6-MP) and methotrexate. Over the last 20 years, biological therapy, in the form of antibodies to tumour necrosis factor-alpha (anti-TNFα) drugs, has revolutionised the treatment of CD. Unfortunately, approximately 50% of patients will fail to respond to optimal treatment with anti-TNFα drugs and therefore disease complications and associated morbidity remains common(Steenholdt et al., 2014). There remains the need for more efficacious and safer treatments.

1.2 Environmental risk factors for Crohn's disease

Epidemiological evidence suggests that lifestyle and environmental factors are important in the aetiopathology of CD. The overall incidence of CD has increased in keeping with dietary changes in Europe and North America(Gibson and Shepherd, 2005, Richman and Rhodes, 2013). In addition, whilst disease prevalence in the developing world is lower than in the developed world, in countries undergoing industrialisation, such as India and The People's Republic of

China, the prevalence is increasing(Ananthakrishnan, 2013). Finally, disease risk increases for immigrants moving from an area of low prevalence to an area of high prevalence(Probert et al., 1992, Richman and Rhodes, 2013).

Several environmental risk factors are associated with CD, including diet, the intestinal flora and fauna (gut microbiota), exposure to non-steroidal anti-inflammatory drugs, vitamin-D deficiency and smoking(Cosnes, 2004, Ananthakrishnan, 2013). CD is a complex, heterogeneous disease and it is likely that multiple risk factors, in association with host genetic risk factors, are important in disease pathogenesis.

The importance of the gut microbiota has been highlighted by multiple large studies that have identified an association between CD and a disruption to the microbiome, known as a dysbiosis (Manichanh et al., 2006, Sokol et al., 2006, Joossens et al., 2011). Alterations in dietary intake have been shown to alter the constituents and diversity of the host microbiota(G.D. Wu et al., 2011, Albenberg et al., 2012, Leone et al., 2013). Microbes within the GI tract perform important metabolic functions for the host, leading to the adoption of the term 'super-organism' to describe the host and its attendant microbiota(Swann et al., 2011). Bile acids (BA's) have been shown to act as signalling molecules between the microbiota and the host(Martin et al., 2007, de Aguiar Vallim et al., 2013). Therefore, the dysbiosis demonstrated in CD may be associated with a disruption to this BA signalling pathway.

1.2.1 Diet

A western diet is typically considered to be high in animal fat and sugar, but low in fruit and vegetables. The evidence linking dietary constituents to the development of CD is varied and should be approached with some caution; much of it is based

on retrospective, case-control studies that are fraught with recall bias. However, there is a strikingly conserved finding of an increase in the consumption of refined carbohydrates both in patients pre-disease or pre-diagnosis and for those patients with established CD in comparison to healthy controls. In one review, the authors describe 12 of 13 case-control studies in which refined sugars were found to be consumed in excess in patients with CD(Gibson and Shepherd, 2005). In a further systematic review of case-control studies a positive association between the diagnosis of IBD and high dietary intakes of total fats, polyunsaturated fatty acids, omega-6 fatty acids, and meat was described(Hou et al., 2011). Some studies have also suggested a protective effect for dietary fibre, fruits or vegetables in the development of IBD(Ananthakrishnan et al., 2012).

1.2.2 Gut microbiota

The human gut contains approximately 10^{14} bacterial cells with vast species diversity in health(Fava and Danese, 2011). A symbiotic relationship has evolved whereby the human host provides nutrients and an ecological niche for gut microbes, whilst in return, the microbiota perform metabolic functions for their host. In this regard, the intestinal bacteria can be viewed as an extra, 'virtual' mammalian organ performing metabolic functions for the host(Martin et al., 2007, Swann et al., 2011, Leone et al., 2013). Some researchers go further with this theme with Sonnenberg describing the human body as 'an elaborate vessel for the growth and spread of our microbial inhabitants'(Pollan, 2013). In health, the microbiota also act to maintain epithelial homeostasis via a variety of immune regulating pathways (see 1.2.4).

Disruption to the microbial ecosystem, with proliferation or loss of different functional groups, is termed dysbiosis. Dysbiosis has been implicated in many

diseases, including IBD, Type 2 diabetes mellitus, obesity, cardiovascular disease and inflammatory arthropathies(Cho and Blaser, 2012).

There is now a consensus view that a dysbiosis is central in the pathogenesis of IBD(Huttenhower et al., 2014). Evidence comes from several sources including animal models, human GWAS data, clinical observation and direct analysis of the microbiome. In multiple animal models of IBD, mice grown in germ free environments will not develop inflammation until enteric bacteria are introduced(Sellon et al., 1998, Leone et al., 2013). Many of the 160 identified host genetic risk variants for the development of CD, have implicated bacterial sensing pathways in the innate immune system(Jostins et al., 2012). An early and prominent breakthrough in understanding the pathogenesis of CD was the discovery that homozygous mutations within the nucleotide-binding oligomerization domain-containing protein 2 (NOD2), conferred a 20 fold increased risk for developing CD(Hugot et al., 2001). The common ligand for NOD2 is N-acetyl muramyl dipeptide (MDP), from peptidoglycan in bacterial cell walls. NOD2 activation is thought to impair innate immune cell function by decreasing nuclear-factor-kappa B (NF-κB) activation, impair autophagy pathways (important in handling intracellular bacteria) and modulate toll-like receptor (TLR) function(Fritz et al., 2011). In the early 1990's, Rutgeerts described a small cohort of patients in whom post-operative CD recurrence could be avoided by diverting the faecal stream away from the surgical anastomosis(Rutgeerts et al., 1991). This finding suggests that an element of the faecal stream, presumed to be bacteria, is required to drive the inflammation. Finally, several large studies have measured the microbiota in CD, both by bacterial culture techniques and by genetic sequencing from faecal samples and intestinal mucosal biopsies(Xavier and Podolsky, 2007, Sokol et al., 2008, Sokol et al., 2009, Joossens et al., 2011). Whilst

no single contributing organism has been discovered, several reproducible characteristics have emerged: an increase in the total bacterial load but with a loss of biodiversity, a proportional increase in the numbers of adherent bacteria (such as adherent invasive *Escherichia coli*) and a reduction in the phylum firmicutes(Joossens et al., 2011, Hedin et al., 2012). Firmicutes species include *Faecalibacterium prausnitzii*, which is thought to be protective via the production of the short chain fatty acid, butyrate (see below).

Most researchers accept that dysbiosis is associated with the development of CD. Less clear is whether the dysbiosis is a cause or consequence of chronic intestinal inflammation. The evidence presented above and the finding that innate immune dysfunction and epithelial barrier function defects are genetic risk factors for CD, suggest the central role for dysbiosis in CD pathogenesis.

1.2.3 Association between diet and microbiota

Recently, much research interest has focused on the dysbiosis associated with a high fat and/or high sugar diet. Turnbaugh et al developed a gnotobiotic mouse model, manipulated to harbour human intestinal microbes, and demonstrated that a change to a high fat/high sugar content western diet changed the microbial population within a single day(Turnbaugh et al., 2009). In humans, specific diet types (e.g. those high in carbohydrates or protein) are associated with certain microbial enterotypes(G.D. Wu et al., 2011). Faecal microbial studies of geographically diverse human populations, and with different dietary habits, demonstrate differences in microbiota ecology. African children, with a diet rich in fibre, demonstrate an increase in the bacterial enterotype *Prevotella*(De Filippo et al., 2010). In comparison, European children, with a diet rich in animal fats and protein, demonstrate an increase in *Bacteroidetes sp*.(Albenberg et al., 2012). High

fat/high sugar feeding of mice will lead to a dysbiosis that is comparable to that seen in human CD(Martinez-Medina et al., 2014).

Interestingly, when rats are fed a diet enhanced with the primary BA, cholic acid, changes in the caecal microbiota are induced similar to the changes associated with a diet rich in fat(Islam et al., 2011). BA's are important metabolites for certain gut microbial species. This finding suggests that the concentration of BA reaching the colon may be a mechanism by which a westernised diet can influence the microbiota.

1.2.4 Microbiota and intestinal homeostasis

The intestinal mucosa and microbiota are in close contact. Dendritic cells (an antigen presenting cell) sample gut bacteria by passing their dendrites through the tight junction (TJs) of gut epithelial cells. A host of intra-epithelial lymphocytes and T-regulatory cells (Treg) maintain immune homeostasis, whilst the epithelial barrier forms an impermeable barrier to the microbes. As discussed in the next sub-sections (1.2.5 to 1.2.8), several possible pathological mechanisms have been suggested by which dysbiosis is thought to disrupt this homeostatic balance. These mechanisms include bile acid dysmetabolism, a reduction in butyrate producing bacterial species, the role of tight junction proteins in obesity and specific pathological bacteria (pathobionts),

1.2.5 Bile acid dysmetabolism

An inter-relationship exists between dietary intake, BA metabolism and the microbiota. Microorganisms within the gut lumen metabolise BAs prior to re-uptake by the host. The production of secondary BAs, via the metabolism of primary BAs, by mammalian gut microbes is an example of 'mammalian–microbiotal co-metabolism'(Nicholson et al., 2005, Martin et al., 2007).

Changes to the diet or the microbiota have been shown to alter the metabolomic profile of a host organism in a variety of animal studies. As described above, rats fed cholic acid will demonstrate caecal microbial changes akin to feeding with a high fat diet(Islam et al., 2011). Germ free mice demonstrate an increase in certain bile acid metabolites on colonisation with gut microbes(Claus et al., 2011). In an animal model, antibiotic manipulation of the microbiota changes the systemic BA pool with an increase in the concentration of taurine-conjugated BAs in diverse organs such as the liver, kidney, heart and blood plasma(Swann et al., 2011).

Duboc et al studied faecal and serum concentrations of different BA species in patients with colonic IBD (CD and UC)(Duboc et al., 2013). Patients with active IBD demonstrated a BA dysmetabolism associated with the dysbiosis seen in IBD. In comparison with controls, patients with disease demonstrated impaired deconjugation, desulfation and transformation of BAs. The study by Duboc et al. is interesting in that it provides an association between active IBD, dysbiosis and BA dysmetabolism. The authors suggest that the increase in sulfated BAs reaching the colon is potentially pro-inflammatory.

However, an alternative explanation to the mechanistic conclusion by Duboc et al may be that a dysbiosis-induced disruption to BA signalling pathways provides a pro-inflammatory stimulus. BAs act as signalling molecules via the nuclear receptor, FXR and also the G-protein coupled receptor, TGR5. These signalling pathways are explored in more detail later in this chapter. However, activation of FXR is known to have diverse downstream effects, including regulation of BA metabolism, but also in immunomodulation(de Aguiar Vallim et al., 2013). Fascinatingly, in a study of diet–induced fatty liver disease, a group has recently demonstrated that an antibiotic-associated dysbiosis was able to alter the ileal BA

composition with subsequent inhibition of intestinal FXR signalling(Jiang et al., 2015).

This thesis is concerned with investigating further the role that disrupted BA signalling, via FXR, may play in the pathogenesis of ileal CD. It is possible that the dysmetabolism of BAs associated with an IBD dysbiosis disrupts this signalling pathway, predisposing to inflammation within the ileum.

1.2.6 Short chain fatty acids (SCFAs)

In the gut, certain bacterial species ferment dietary fibre to produce the short chain fatty acid (SCFA), butyrate. The dysbiosis associated with CD is characterised by a reduction in firmicutes phyla, including *Faecalibacterium prausnitzii, bifidobacteria* and *clostridia sp.*(Sokol et al., 2008, Joossens et al., 2011, Eeckhaut et al., 2013). These bacterial species are all butyrate producing.

SCFAs, including butyrate, are an important source of energy for colonocytes. In addition, butyrate is thought to maintain gut epithelial homeostasis by inducing the production of mucous by goblet cells within the epithelial layer, inducing the production of IgA, by facilitating Treg differentiation and by inhibiting NF-κB(Thorburn et al., 2014). Sokol and colleagues demonstrated that *F. prausnitzii* or its supernatant could inhibit the activation of NF-κB by IL-1β in a cell model and can attenuate colitis in the TNBS mouse model(Sokol et al., 2008).

1.2.7 Obesity and tight junction proteins

Like CD, obesity has been associated with a dysbiosis and is also recognised as a systemic inflammatory disorder, as measured by increased levels of circulating inflammatory cytokine such as TNFα(Hotamisligil et al., 1995). Both obese humans and obese mouse models demonstrate a dysbiosis, which incredibly is transmissible; GF mice colonised with obese mouse microbiota will gain more

body fat compared to normal controls(Turnbaugh et al., 2009). In animal studies, a high fat diet increased the amount of plasma circulating lipo-polysaccharide (LPS), a constituent of bacterial cell walls(Cani et al., 2007). On antibiotic manipulation of the microbiota, this endotoxaemia was abolished. Epithelial barrier dysfunction has been implicated in the aetiopathogenesis of CD. Interestingly, Cani et al, were able to demonstrate, in their obese mouse model, a reduction in the expression of genes encoding protein involved in the epithelial tight junction (TJ) complex, including zonulla-occludens (zo-1) and occludin(Cani et al., 2008). The reduction in these TJ proteins was associated with the observed endotoxaemia induced by high fat feeding and was again abolished with antibiotic treatment.

1.2.8 Specific pathobionts

Escherichia coli has been associated with CD by several research groups, particularly in ileal CD. *E coli* is found within granuloma in both early and chronic CD and has been described as adherent, invasive *E coli* (AIEC), given its ability to adhere and invade epithelial cell lines and also its ability to replicate within macrophages(Glasser et al., 1999, Roberts et al., 2010). Recently, AIEC has been shown to be able to induce a chronic colitis in a genetically susceptible mouse model (toll like receptor 5 deficient)(Chassaing et al., 2014). In addition, AIEC can also induce epithelial barrier dysfunction, by upregulation of the leaky tight junction protein claudin 2, in a transgenic mouse model, engineered to express human carcinoembryonic antigen-related cell adhesion molecule (CEACAM)(Denizot et al., 2012).

A molecular mechanism linking diet and dysbiosis to the development of IBD has been suggested by Devkota and colleagues(Devkota et al., 2012). Mice fed a diet rich in saturated milk fat, but not when fed polyunsaturated fat, demonstrated a

bloom in a novel pathobiont, *Bilophila wadsworthia*, mediated by an increase in taurine conjugated bile acids (BAs). An overgrowth of *B. wadsworthia* was able to induce a more severe, early onset colitis in the genetically susceptible IL-10 knockout mouse.

In summary, a high-fat/high-sugar western diet has been linked both epidemiologically and in case control studies with an increase in the risk of developing IBD. A western style diet induces changes to the microbiome and this dysbiosis has been implicated in the pathogenesis of IBD via a variety of different pathological mechanisms, including BA dysmetabolism, a reduction in butyrate producing bacteria, an increase in AIEC and epithelial barrier dysfunction due to alterations in TJ protein expression.

1.3 Bile acids

BAs are amphipathic (contain both hydrophobic and hydrophilic components), steroid compounds synthesised by the catabolism of cholesterol in the liver. BAs are a major constituent of bile juice, which also contains water, bile pigment, cholesterol and other fats. Traditionally, the physiological role of BAs has been viewed as simply that of a detergent molecule, facilitating the adsorption of dietary fats. Recently a broader role for BAs has emerged with the recognition that they can act as signaling molecules.

1.3.1 Synthesis and structure

New BAs are synthesised from cholesterol in the liver and are known as primary BAs, in the human being cholic acid (CA) and chenodeoxycholic acid (CDCA). Prior to excretion into the biliary canalicular network within the liver, primary BAs are conjugated to the amino-acids taurine or glycine, to increase their solubility(Gadaleta et al., 2010). The neosynthesis and subsequent conjugation of

BAs requires approximately 17 different enzymatic steps. On reaching the caecum, primary BAs are metabolised by enteric bacteria. Conjugated primary BAs are first deconjugated by bacterial bile salt hydrolase (BSH). Then, further dehydroxylation, dehydrogenation and sulfation reactions occur, to produce the secondary BAs deoxycholic acid (DCA) and lithocholic acid (LCA) (see figure 1.1)(Jones et al., 2008). The position of hydroxyl groups on the steroid ring structure determines BA classification and alters their chemical property in terms of hydrophobicity, but also in signalling capacity(Payne et al., 2008). CDCA (primary BA) demonstrates the highest affinity for FXR, with CA and the secondary BAs demonstrating less affinity(W. Wang et al., 1999).

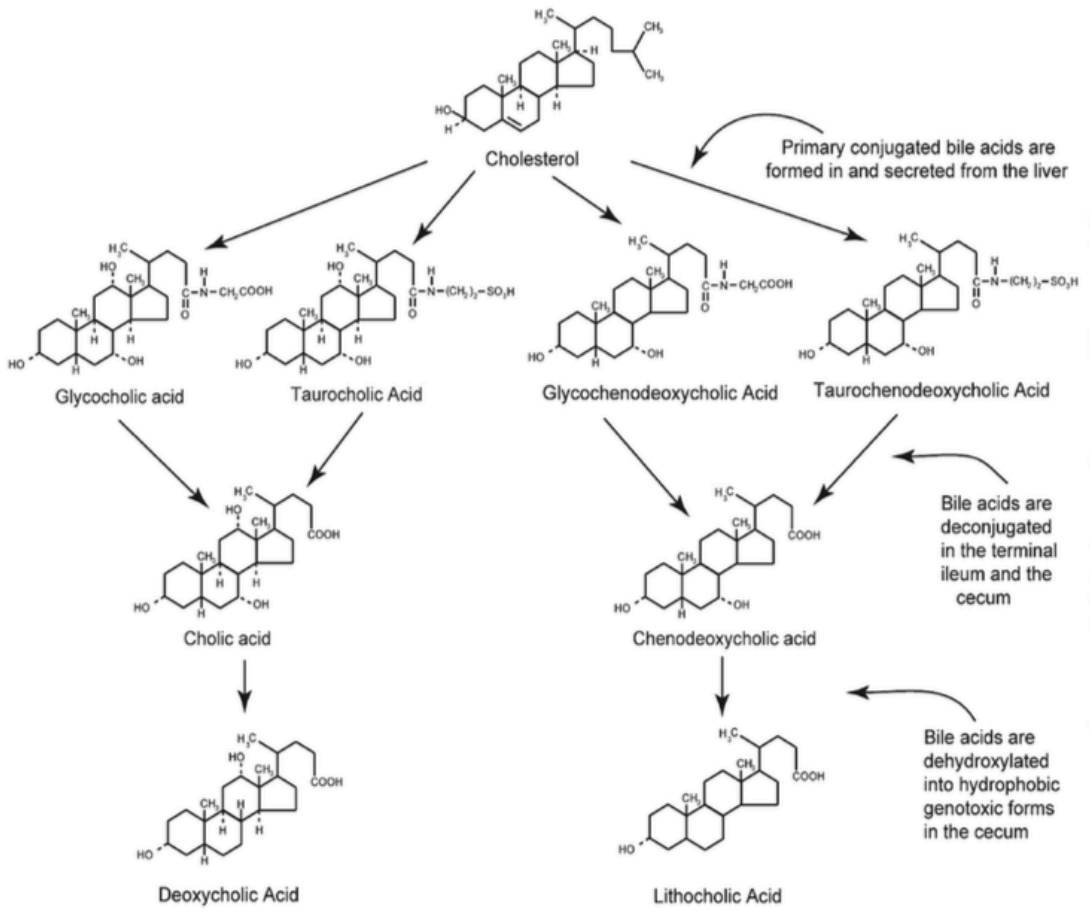

Figure 1.1; The structure of primary and secondary bile acids (BAs). Primary BAs (cholic acid and chenodeoxycholic acid) are synthesised and conjugated to either taurine or glycine in the liver. In the terminal ileum, a deconjugation reaction occurs. Primary BAs are subsequently metabolised to the secondary BAs deoxycholic acid and lithocholic acid by bacteria within the caecum (modified from Payne et al., Clinical and Experimental Gastroenterology, 2008)

1.3.2 Entero-hepatic circulation

Conjugated, primary BAs are avidly re-absorbed by enterocytes in the terminal ileum with 95-97% returning via the portal venous system back to the liver(Hofmann, 2009, Gadaleta et al., 2010). Absorption of BAs from the ileal lumen is driven by the Apical Sodium-dependent Bile acid Transporter (ASBT). BAs are transported through the enterocyte by the Ileal Bile Acid Binding Protein (IBABP) and secreted at the basolateral membrane by the heterodimeric Organic Solute Transporters (OSTα/OSTβ). Hepatocytes actively re-absorb BAs and re-circulate them back into the bile canaliculi. Individual bile salts complete this enterohepatic circulation several times a day (see figure 1.2).

Neosynthesis of BAs is a highly entropic pathway. The efficient re-circulation of BAs means that the total proportion of the BA pool that is newly synthesised is low. Interruption to the re-absorption of BAs increases production and also causes an irritant diarrhoea due to excess BA passing into the colon(Hofmann, 2009).

1.3.3 Bile Acids as signalling molecules

The discovery of BA receptors throughout the mammalian body revealed that these sterol compounds have important physiological roles as signalling molecules. The nuclear receptor, farnesoid X receptor (FXR) and the Transmembrane G-protein coupled bile acid receptor (TGR5) have been found to have important roles in controlling lipid and glucose homeostasis(Watanabe et al., 2004, Katsuma et al., 2005). The expression of FXR is concentrated in the liver and GI tract, particularly in the ileum. BA receptors have also been found in diverse organs including the kidneys, the heart and vascular endothelium(Khurana et al., 2011). The total signalling capacity of BAs throughout the whole organism, however, remains unknown(Swann et al., 2011).

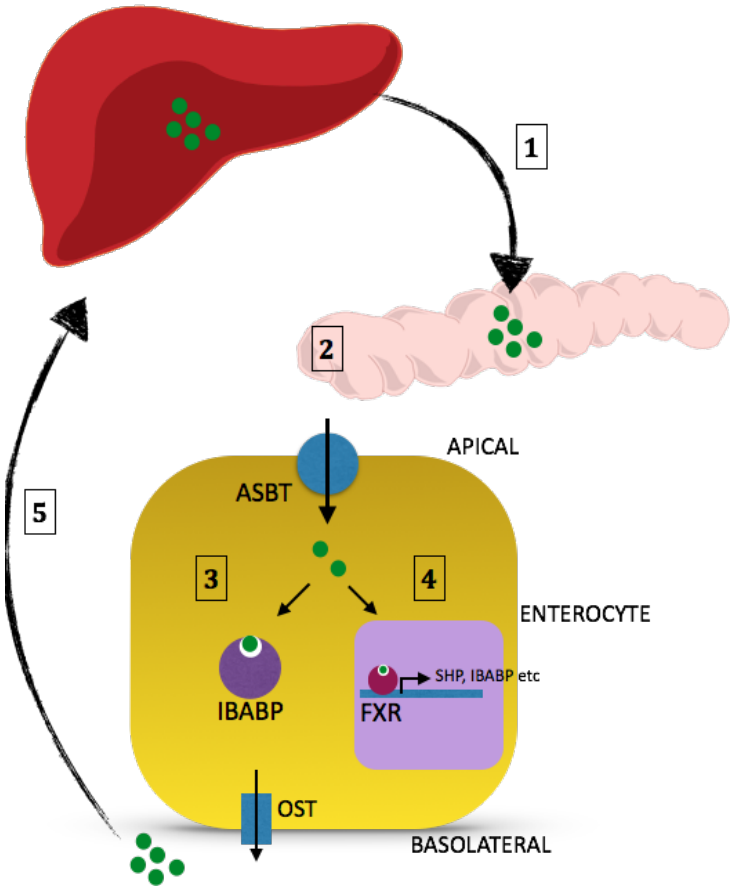

Figure 1.2; Schematic to demonstrate the enterohepatic circulation of primary BAs. BAs are excreted into the proximal small bowel via the biliary system (1); in the terminal ileum, BAs are actively re-absorbed by ASBT (2); BAs are transported through the enterocyte cytoplasm by the transport protein IBABP (3); BAs bind to FXR and are translocated to the nucleus where bound FXR acts as a transcription factor (4); BAs are exported to the portal system via OSTα/β heterodimer and return to the liver for re-circulation (5).

1.4 Farnesoid X receptor

1.4.1 Structure and function

The nuclear receptors are a superfamily of ligand-activated receptors that act as key regulators in a diverse range of cell function, including development, differentiation and metabolism(Mangelsdorf et al., 1995). On activation by lipophilic hormones, such as thyroxine, estrogen or vitamin D, the receptor localises to the nucleus to act as a transcription factor. The nuclear receptors are characterised by a conserved structure featuring a central DNA binding domain (DBD) which binds specific response elements, a C-terminal hormone specific

ligand binding domain (LBD) and an N-terminal transactivation domain (which interacts with other regulatory proteins).

FXR, identified in 1995 as an orphan receptor, was named when a supra-physiological concentration of farnesol, an intermediate in the mevalonate pathway, was found to demonstrate weak agonism(Modica et al., 2010). The discovery that primary bile acids were the natural, endogenous ligands for FXR was reported by several groups at the turn of the century(Makishima et al., 1999, Parks et al., 1999). Two genes, *NR1H4* and *NR1H5,* encode for two different FXR isoforms, FXRα/β, although the FXRβ isoform is a pseudogene in humans and primates and its physiological function remains unknown(Gadaleta et al., 2010). On activation by primary BA's, FXR forms an obligate heterodimer with retinoic x receptor (RXR) to become functional (see figure 1.3). The DBD recognises a motif of repeated inverted response elements of AGGTCA separated by a single nucleotide (the DNA response element).

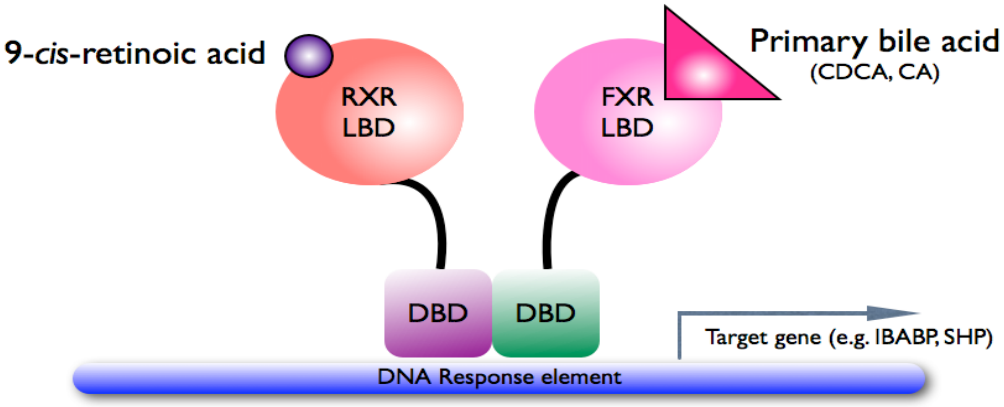

Figure 1.3; Schematic representation of the FXR receptor. FXR receptor acts as a heterodimer with RXR. Following activation by primary BA (CDCA or CA), which binds to the ligand binding domain (LBD), the receptor binds to its DNA binding domain (DBD) and acts as a transcription factor for multiple downstream genes (including IBABP and SHP). See text for more detail.

Activation of FXR by primary BA's has several downstream effects. FXR is a key regulator of BA metabolism. In addition, FXR is involved in the control of glucose metabolism, lipid metabolism and in attenuating inflammation (see section 1.4.3). FXR is most widely expressed in the liver and GI tract, with mRNA levels of FXR three times higher in the ileum, the site of active BA absorption, than elsewhere in the gut(Inagaki et al., 2006). Within the ileum, FXR is expressed in the villous epithelium, with highest levels in the inter-villous region, with little or no expression in the crypts.

1.4.2 FXR is a key regulator of bile acid metabolism

FXR is a key regulator of BA metabolism, acting to reduce BA production when activated by BAs in the terminal ileum(Modica et al., 2010). Activation of FXR

increases expression of IBABP, OSTα/β, fibroblast growth factor 19 (FGF19) and small heterodimer partner (SHP). The hormone FGF19 completes a negative feedback loop to the liver, where it acts to inhibit neosynthesis of BAs. FGF19 also inhibits the contraction of the gallbladder, and pancreatic exocrine function, to impair the excretion of further bile and digestive enzymes into the duodenum. This process has been described as the 'ileal brake', acting as a signal to represent progression from a fed to a fasting state. SHP is a nuclear receptor that acts as an inhibitory protein, via the enzymes CYP7A1 and CYP8B1, to downregulate the neosynthesis of BA's(Goodwin et al., 2000).

1.4.3 FXR and IBD

The observation that a decrease in bile acids within the small bowel leads to bacterial overgrowth has been recognised for many years(Berg, 1995). This observation has been demonstrated in a bile duct ligation model in mice, in which no bile acids reach the small bowel, and also in humans with liver cirrhosis who secrete smaller volumes of bile acid(Lorenzo-Zuniga et al., 2003, Ogata et al., 2003). In the bile duct ligation model, bacterial proliferation, mucosal injury and bacterial translocation is reversed by the oral administration of bile acids. Primary bile acids are only weakly bactericidal and therefore an alternative mechanism, by which BAs could control bacterial overgrowth, must be responsible.

In a landmark study, Inagaki et al were able to demonstrate that BAs could regulate an anti-inflammatory response via FXR in the terminal ileum(Inagaki et al., 2006). A genetically modified mouse with low levels of endogenous BA was treated with an FXR agonist and mRNA expression from the ileum was analysed. Included within several genes whose expression was increased by the FXR agonist, were pathways involved in mucosal defence including iNOS (inducible nitrous

oxide synthase), IL-18, Angiogenin and Carbonic anhydrase 12. In the bile duct ligation model, the FXR agonist also protected the epithelial barrier and decreased the number of bacteria isolated from mesenteric lymph nodes.

Studies of FXR knockout mice have provided further evidence as to the anti-inflammatory role of FXR(Vavassori et al., 2009). FXR knockout mice do not develop a de-novo colitis. However, as they age, histology of colonic mucosa demonstrates an increase in collagen deposition within the lamina propria and an increase in the number of infiltrating inflammatory cells, particularly macrophages. Cells isolated from the colon demonstrate an increase in the expression of several pro-inflammatory and pro-fibrotic genes including tumour necrosis factor-α (TNFα), interleukin-1β (IL-1β), interferon-γ (IFNγ), transforming growth factor-β (TGFβ), α1-collagen, tissue inhibitor of metalloproteinase-1 (TIMP-1) and α-smooth muscle actin (αSMA).

The two common mice models for colitis are the TNBS (intra-rectal administration of trinitrobenzenesulfonic acid) model and the DSS (oral adminsitration of dextransodiumsulfate) model. In these models, normal wild type (WT) mice will develop a relatively mild colitis. However, FXR knockout mice exposed to the irritant will develop a much more severe inflammatory condition(Vavassori et al., 2009). Gadaleta et al. were able to demonstrate that treatment with 6-ethyl-CDCA (INT-747, a semisynthetic FXR agonist) significantly reduced the inflammatory process in both of the colitis models in WT, but not FXR knockout mice(Gadaleta et al., 2011b). In the same paper, the authors also demonstrated that FXR activation rendered several different immune cell types (macrophages, peripheral blood mononuclear cells [PBMC], dendritic cells) refractory to stimulation with lipo-polysaccharide (LPS), a bacterial cell wall component, measured by a reduction in the production of TNFα. More recently, it has been demonstrated that FXR

agonism reduces the LPS-induced production of pro-inflammatory cytokines by macrophages, whilst maintaining the production of anti-inflammatory IL-10(Haselow et al., 2013).

In patients with Crohn's colitis, FXR mRNA levels were found to be lower in areas of macroscopically inflamed colon compared with areas that were normal(Vavassori et al., 2009). Additionally, the activity of FXR (by measurement of downstream gene target SHP) is reduced in the ilea of patients with quiescent colonic CD(Nijmeijer et al., 2011).

Particularly for patients with CD, fibrosis within the GI tract is a significant clinical problem. Progressive fibrosis leads to stenosis of the gut lumen causing obstruction, often-requiring recourse to surgical resection of the fibrosed area. As above, the antifibrotic properties of FXR are suggested in the observation by Vavasori et al that cells isolated from the colonic mucosa of FXR knockout mice demonstrate an increase in the expression of pro-fibrotic cytokines (e.g. TIMP-1, αSMA, TGFβ). Further evidence is provided by animal research in liver fibrosis on the function of hepatic stellate cells (HSCs)(Fiorucci et al., 2005, Renga et al., 2011). In response to an inflammatory insult, HSCs undergo a phenotypic change to an extracellular matrix producing, myofibroblast like cell. In a mouse model, treatment with an FXR agonist promoted a quiescent HSC phenotype, which more readily underwent apoptosis and was inhibited from becoming myofibroblast like.

Nuclear factor kappa B (NF-κB) is a central nuclear receptor in both acute and chronic inflammatory processes. NF-κB is activated via a variety of pathways, including stimulation with LPS and TNFα, to upregulate a variety of pro-inflammatory genes, such as IL-1β, IL-6, TNFα and IL-8. Activation of FXR inhibits the expression of these NF-κB controlled inflammatory genes in both cell line and primary tissue culture(Y. D. Wang et al., 2008). However, there is also interesting

data from cell-line and animal models to suggest that FXR and NF-κB mutually antagonise each other(Gadaleta et al., 2011a). In this model, increasing levels of NF-κB will inhibit FXR, leading to less repression of NF-κB and further inhibition of FXR, in a cycle representing chronic inflammation.

1.4.4 FXR agonists

The role of FXR in the metabolism of glucose, lipids and cholesterol and in inflammation, identify it as a potential therapeutic target. Several agonists have been developed, three of which are used in the experiments within this thesis. The most clinically advanced therapeutic FXR agonist is INT747 (Intercept Pharmaceuticals, New York, U.S.A.). INT747 is a steroidal, semi-synthetic BA, in which CDCA has been modified by the addition of an alkyl group (6α-ethyl chenodeoxycholic acid, 6-ECDCA) to form a more potent agonist (EC_{50} 0.1μM)(Pellicciari et al., 2002). INT747 has entered phase III trials in the treatment of primary biliary cirrhosis and demonstrated improved histological scoring in a phase II trial for the treatment of non-alcoholic fatty liver disease (NAFLD)(Nevens et al., 2014, Neuschwander-Tetri et al., 2015). INT747 was used in this thesis under a product licence from Intercept Pharmaceuticals. However, the compound is now commercially available as a generically produced molecule. Hence, 6-ECDCA, the biochemically correct notation, is used to represent the Intercept FXR agonist throughout the thesis.

Non-steroidal, fully synthetic agonists have also been developed, the first patent being GW4064 (GlaxoSMithKline) in 2000(Crawley, 2010). This compound is not in use in clinical trials, has greater potency than CDCA (EC_{50} 0.07μM) and can be commercially obtained from Sigma-Aldrich for experimental use. The final FXR agonist, used in chapter 3, is a non-steroidal compound, manufactured as a

modification of GW4064, known as Px-102 (Phenex Pharmaceuticals AG, Ludwigshafen, Germany). Px-102 has demonstrated some efficacy in the treatment of NAFLD in mouse models(Hambruch et al., 2013).

1.4.5 TGR5

The G-protein coupled, transmembrane receptor TGR5 is expressed mainly in adipose tissue and muscle, but expression has also been demonstrated in monocytes and rat colonocytes(Sato et al., 2008, Ward et al., 2013). In contrast to FXR, the major endogenous TGR5 ligands are the secondary BAs, LCA and DCA. BA signalling via TGR5 has been implicated in the modulation of energy expenditure, glucose metabolism and colonic motility(Thomas et al., 2009, Ward et al., 2013). An immuno-regulatory role has been suggested by the finding that TGR5 activated monocytes are less sensitive to LPS induced stress(Yoneno et al., 2013).

This thesis has not explored the role of TGR5 in the pathogenesis of CD. I have chosen to concentrate on the role of FXR alone as: i) there is more scientific evidence concerning the overall immuno-modulatory role of FXR, especially with respect to IBD; and ii) TGR5 is expressed in the colon, not the ileum, and so is less likely to be involved in the pathogenesis of ileal CD. However, the role of TGR5 in the potential pathogenesis of IBD deserves further research.

1.5 Small bowel epithelium

The epithelium of the GI tract is the largest surface area exposed to the external environment(Suzuki, 2013). Impressively, it functions as a single monolayer to control the absorption of nutrients, salts and water, whilst simultaneously acting as a physical barrier to the trillions of bacteria and other toxins within the gut lumen. The small bowel epithelium is organised into huge numbers of villi with crypts (of Lieberkuhn) spaced at the base of the villi(Tesori et al., 2013). The

epithelial lining has a high rate of turnover with enterocytes shedding approximately every five days. This high rate of turnover is controlled by multipotent columnar stem cells that reside in base of the crypt and divide to form daughter cells that differentiate as they migrate into the villi. Cells differentiate to form a variety of functionally distinct cell types. Enterocytes are the major cell type of the epithelium and are responsible for the absorption of nutrients and the formation of a selectively permeable physical barrier via tight cell-cell junctions. Goblet cells produce mucous which lines the apical surface of the epithelium throughout the GI tract. Enteroendocrine cells produce gut hormones that act either locally or on the enteric nervous system. Paneth cells remain within crypts, rather than migrating into the villous, and produce antimicrobial factors such as alpha-defensins. Specialised M (or microfold) cells, clustered over an aggregation of lymphoid tissue (a Peyer's patch), sample luminal antigens for presentation to the immune system.

1.5.1 The epithelial barrier

To function as a selectively permeable barrier, the epithelium transports substances via two routes. The cell membrane is relatively impermeable and nutrients, such as sugars, fats and amino acids, are actively absorbed via a transcellular route(Suzuki, 2013). Water and electrolytes, however, are absorbed via a paracellular route, the flow of which is controlled by an apical junction complex composed of tight junctions (TJ) and adherens junctions (AJ). The TJ protein complex consists of membrane spanning proteins, occludin and claudin, attached to cytosolic proteins, zonulla occludens 1 (Zo-1) and the cytoskeleton(Capaldo and Nusrat, 2009). The TJ forms around the apical border of the cell, facilitating polarisation of the epithelial layer by separating the apical and

basolateral surfaces. The TJ acts as a sophisticated barrier to the intercellular space by restricting the passage of gut bacteria, whilst allowing selective ion uptake. A 'leaky' epithelium may allow the transcellular passage of more gut bacteria. The AJ complex, composed of members of the cadherin family, provides adhesive bonds between cells and allows intercellular communication(Bruewer et al., 2003). A schematic representation of the apical junction complex is demonstrated in figure 1.4.

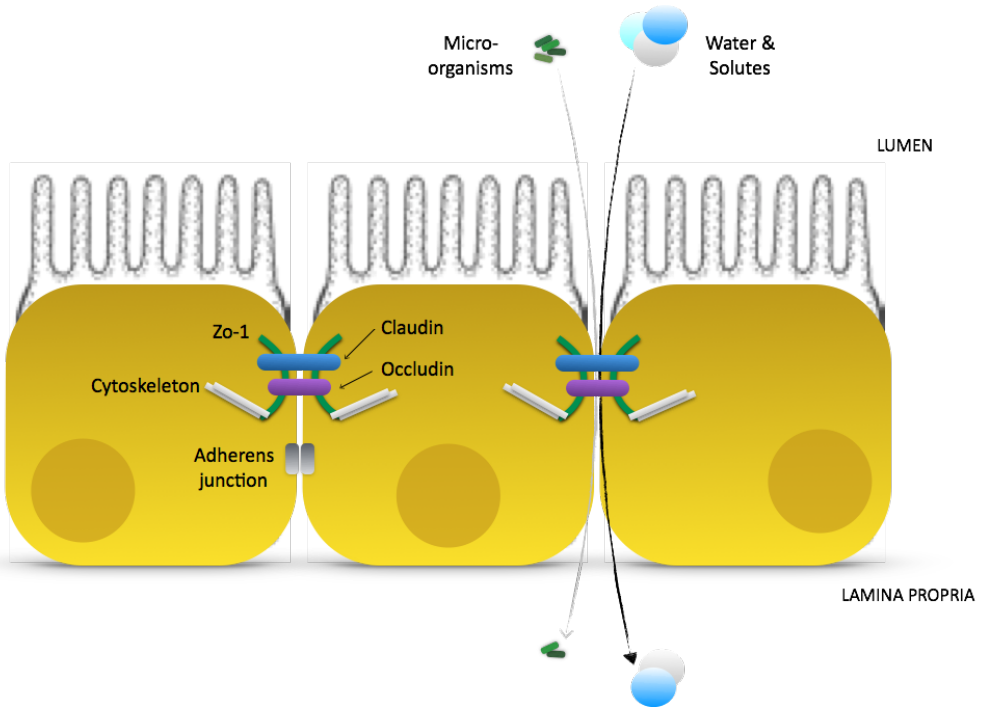

Figure 1.4; A diagram to demonstrate intercellular protein complexes controlling the transcellular movement of water, solutes and micro-organisms. The tight junction (TJ) complex is composed of membrance spanning occludin and a claudin protein anchored to the cell cytoskeleton via zonulla occludens 1 (Zo-1). The TJ complex controls the flow of water and electrolytes through the intercellular space. The expression of different claudin proteins alters the permeability of the epithelial barrier (see section 1.5.3). Under normal physiological conditions, the epithelium is impermeable to micro-organisms, but may become pathologically more permeable (see section 1.5.2)

1.5.2 Epithelial barrier dysfunction in Crohn's disease

Epithelial barrier function can be viewed both as a physical barrier alone, but also as a function of the physical barrier and the innate immune system. Maintaining the epithelial barrier is critical to health and dysfunction has been implicated in a

variety of diseases including IBD, autoimmune disease, sepsis and tumourigenesis(McGuckin et al., 2009, Su et al., 2009, Fasano, 2012, Runkle and Mu, 2013).

Impairment of the epithelial barrier is thought to be a major factor in the pathogenesis of CD(Soderholm et al., 2002, Ma et al., 2004, Zeissig et al., 2007, Fries et al., 2008, McGuckin et al., 2009, Su et al., 2009, Denizot et al., 2012). Intestinal permeability is increased in the first-degree relatives of patients with Crohn's disease(Hedin et al., 2012). GWAS studies have demonstrated an association between disease and barrier function gene loci variants, such as MUC19 and ITLN1(Franke et al., 2010, Khor et al., 2011). MUC19 is involved in the production of epithelial protective mucin, whilst ITLN1 (intelectin) is thought to act by stabilising the enterocyte brush border membrane(Van Limbergen et al., 2009). IBD associated inflammatory cytokines, such as TNFα, IFNγ and IL-6, increase epithelial permeability(Adams et al., 1993, Tazuke et al., 2003, Ma et al., 2004, Fries et al., 2008). In FXR knockout mice, defects in the epithelial barrier are seen with a loss of immunohistochemical (IHC) staining for occludin(Inagaki et al., 2006). Furthermore, FXR activation overcomes the increased intestinal permeability induced in an animal model of colitis(Gadaleta et al., 2011b). Finally, confocal endoscopy, in which intravascular fluorescein dye can be seen leaking from ileal villi, can predict relapse in patients with IBD, even when the disease is confined to the large bowel(Kiesslich et al., 2012, Turcotte et al., 2012).

1.5.3 Tight junctions

Bile duct ligation (BDL) mouse models, in which BA flow to the small bowel is disrupted, demonstrate epithelial barrier dysfunction, with bacterial translocation and decreased occludin at the TJ complex on IHC staining(Ogata et al., 2003,

Inagaki et al., 2006). However, occludin deficient mice have unperturbed barrier function. Therefore, presumably, other proteins within the TJ complex must be important in maintaining barrier function(Schulzke et al., 2005). Various studies have implicated changes in claudin expression in the pathogenesis of IBD.

The claudin family are trans-membrane spanning proteins that predominantly contribute to barrier function(Turksen and Troy, 2004). Some claudin proteins form very tight seals (known as 'seal forming'), whilst others are more permeable ('pore forming'). Zeissig et al demonstrated changes in the expression of claudin proteins in patients with active CD(Zeissig et al., 2007). The seal-forming claudins 5 and 8 were down regulated and displaced away from the TJ complex. However, the pore-forming claudin 2 was instead upregulated. Further studies have also suggested that the pathogenic *E. coli*, AIEC, can induce claudin 2 expression in an animal model of colitis(Denizot et al., 2012).

1.5.4 Innate immune dysfunction and IBD

Innate immune mechanisms that protect the epithelial barrier include the mucous layer and antimicrobial defensins(Ostaff et al., 2013). Epithelial cells recognise microorganisms by pattern recognition receptors (PRRs) stimulating the production of pro-inflammatory cytokines, such as the chemo-attractant IL-8, and can activate autophagy pathways to kill intracellular bacteria(Philpott and Girardin, 2004). Several genes involved in innate immune function have been positively associated with CD in GWAS studies(Wellcome Trust Case Control Consortium, 2007).

Mucous and defensins

The mucous layer, composed of structural mucins produced by goblet cells, coats the entire surface epithelium of the GI tract and contains defensins and IgA(Ostaff

et al., 2013). Defensins are small, antibacterial cationic proteins secreted into the mucous layer by Paneth cells in the small bowel (alpha-defensins), or by colonocytes (beta-defensins) in the large bowel. Defensins have a broad range of non-specific antimicrobial activity and function by forming microbial membrane disrupting pores. Several studies in IBD have demonstrated disruption in the mucous layer and in defensin production. Patients with IBD demonstrate various degrees of goblet cell loss(Sommers and Korelitz, 1975). Animal models deficient in their ability to produce mucin demonstrate increased intestinal permeability and spontaneously develop GI inflammation(Velcich et al., 2002). Some studies have demonstrated a reduction in alpha-defensin expression in ileal CD, although this was not replicated in a paediatric study(Wehkamp et al., 2005, Zilbauer et al., 2011). Similarly, a decrease in beta-defensin expression has been demonstrated in UC(Zilbauer et al., 2010).

NOD2

Pattern recognition receptors (PRRs) are an evolutionary conserved element of the innate immune system. They function by recognising particular microbial structural motifs, known as pathogen-associated molecular patterns (PAMPs), such as cell wall peptidoglycan or LPS(Philpott and Girardin, 2004). Cytoplasmic nucleotide-binding oligomerisation domain proteins (Nod 1 and Nod 2) and membrane bound toll-like receptors (TLRs) are two such PRRs.

Nod 2 has been strongly implicated in the pathogenesis of CD by both genetic and functional studies(Hugot et al., 2001, Maeda et al., 2005). Individuals who carry a homozygous mutation in the ligand-binding domain of NOD2 exhibit a twenty-fold increase in the risk for developing CD(Fritz et al., 2011). NOD2 is broadly expressed in macrophages and dendritic cells and its common ligand is N-acetyl

muramyl dipeptide (MDP), from peptidoglycan in bacterial cell walls(Kannegati et al., 2007). It functions to activate NF-κB, can modulate signalling by other TLRs and may be involved the stimulation of alpha-defensin secretion by Paneth cells(Fritz et al., 2011). The three most common mutations seen associated with CD are loss of function, suggesting that downregulation of the innate immune system at the epithelial barrier is a risk for development of the disease(Fritz et al., 2011). This story is, however, complicated by the finding that a gain of function mutation is also associated with CD, possibly via a mechanism that inhibits the production of anti-inflammatory interleukin-10 (IL-10)(Noguchi et al., 2009). The debate as to the exact mechanism by which NOD2 can predispose to CD remains unknown.

Autophagy

Autophagy is a fundamental cellular lysozymal degradation pathway in which damaged proteins and organelles can be recycled. It occurs during cell development, repair and under starvation conditions(Levine and Kroemer, 2008). Autophagy pathways are also activated to destroy intracellular pathogens and in this way act as an innate immune killing mechanism. Several autophagy genes have been strongly associated with the development of CD including ATG16L1 and IRGM(Van Limbergen et al., 2009). IRGM is required during the initiation of autophagy, whilst ATG16L1 recruits other proteins to the autophagosome, engulfing the content identified for degradation.

Interestingly, NOD2 also has a regulatory role in autophagy(Fritz et al., 2011). Bacterial activation of NOD2 leads to ATG16L1 dependent formation of autophagocytic vacuoles. NOD2 appears to recruit ATG16L1 to the cell membrane at site of bacterial entry.

There is a potential mechanism by which BA signalling via FXR could regulate autophagy and NOD2. Sequestosome 1 (Sqstm1/p62) is a cytosolic protein that ubiquitinates cellular proteins, targeting them for degradation by autophagy(Bjorkoy et al., 2005). Sqstm1/p62 also interacts with NOD2, enhancing its effects, probably by preventing NOD2 degradation(Park et al., 2013). Recent research has suggested that the expression of Sqstm1/p62 is upregulated by FXR activation(Williams et al., 2012). This is a potential mechanism by which BAs may promote innate immune function and may form the basis for future research.

1.6 Cytokine profiles in Crohn's disease

The chronic inflammatory response, that is the hallmark of CD, is driven by an inappropriate immune response to gut flora. An imbalance exists between pro-inflammatory and anti-inflammatory cytokines, driven largely by an imbalance in cytokine secreting T-lymphocytes (see figure 1.5).

1.6.1 T-helper cell phenotype in Crohn's disease

The differentiation of T-helper (Th) cells, either to IFNγ-producing Th1 cells or to IL4/IL5/IL13-producing Th2 cells, was described almost 30 years ago by Mosmann et al.(Mosmann et al., 1986). Th1 cells, induced by IL-12, are thought to protect against intracellular microorganisms, whereas Th2 cells are thought to be active against extracellular pathogens(Brand, 2009).

Traditionally, CD has been viewed as a Th1-cytokine mediated disease with high levels of both IL-12 and IFNγ found both in animal models and isolated from patients with CD(Fuss et al., 1996, Hart et al., 2005). In contrast, UC has been described as a Th2-like disease with associated high levels of interleukin-5 (IL-5) and interleukin-13 (IL-13) but with little or no IFNγ(Strober and Fuss, 2011). IL-

13 is a pro-fibrotic inflammatory cytokine and has been associated with collagen formation in the strictures of CD(J. R. Bailey et al., 2012).

Several, more recent studies have also identified interleukin-23 (IL-23) receptor positive, interleukin-17/interleukin-22 (IL17/IL22)-producing Th17 cells in association with CD(Brand, 2009). Transforming growth factor β (TGFβ) has traditionally been viewed as an anti-inflammatory cytokine, being anti-proliferative to T-lymphocytes, and by promoting the formation of T regulatory (Treg) cells by inducing Foxp3 (Forkhead Box protein 3) expression(Konkel and Chen, 2011). However, TGFβ in the presence of other inflammatory cytokines will also promote the differentiation of T cells to a Th17 phenotype(Wan and Flavell, 2007). Recently, so called 'Th17/Th1' cells have also been identified in CD, which secrete both IFNγ and IL-17A(Acosta-Rodriguez et al., 2007, Annunziato et al., 2008). Finally, in association with an increased proliferation of Th1 and Th17 cells, there is a reciprocal decrease in the number of anti-inflammatory Treg cells (see figure 1.5).

The effector cytokines of Th1 and Th17 lymphocytes, via stimulation of innate immune cells (such as antigen presenting cells and epithelial cells), lead to the production of secondary cytokines such as TNFα, IL-6 and IL-1 β(Strober and Fuss, 2011). Acting via NF-κB and mitogen activated protein (MAP) kinases, these secondary cytokines are responsible for many of the downstream inflammatory processes seen in CD.

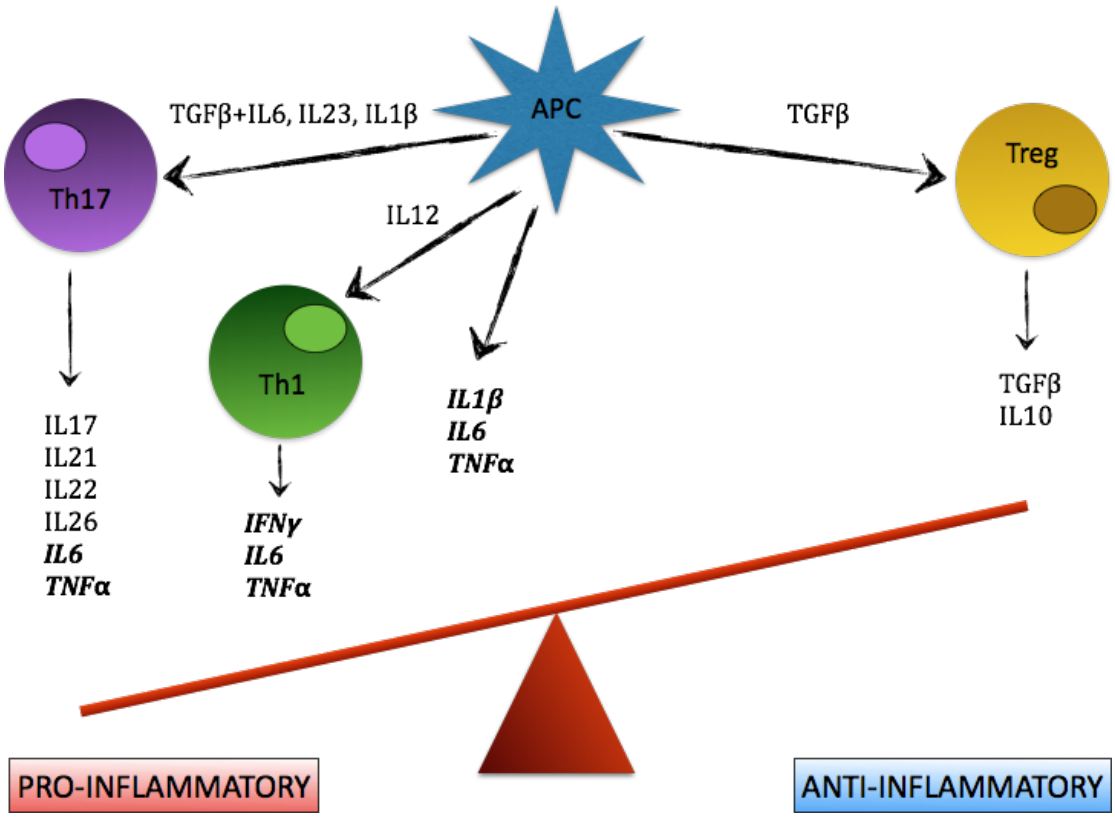

Figure 1.5; The dysregulated cytokine profile in Crohn's disease. Adapted from a figure by Brand S., Gut 2009;58. In CD, an exaggerated Th1 and Th17 response leads to the production of pro-inflammatory effector cytokines. TGFβ promotes the proliferation of Treg cells. However, in the presence of inflammation, TGFβ will promote the proliferation of Th17 cells. Effector cytokines in italic/bold are used in this thesis

The chemo-attractant cytokine, interleukin-8 (IL-8), is released by epithelial cells in response to stress, such as inflammatory cytokine activation or bacterial sensing(Eckmann et al., 1993). IL-8 is a potent chemo-attractant and activator of polymorphonucleocytes (PMNs), acting as a mechanism by which gut epithelial cells can alert the host immune defences following bacterial invasion.

1.6.2 Effect of pro-inflammatory cytokines on the gut epithelial barrier

Pro-inflammatory cytokines, such as TNFα, IFN γ and IL-6, increase the permeability of the gut epithelial barrier, demonstrated both in-vivo and in cell line models(Adams et al., 1993, Musch et al., 2002, Tazuke et al., 2003, Ma et al., 2004, Soderholm et al., 2004, Clark et al., 2005). Treatment with anti-TNFα therapy has been shown to reverse epithelial barrier defects in patients with

CD(Suenaert et al., 2002). The cellular mechanisms by which cytokines disrupt the epithelial barrier include changes to the TJ complex, re-arrangements of the cell cytoskeleton or increased epithelial cell shedding(Bruewer et al., 2003).

Exposure to IFN γ and TNFα have been shown, both independently and synergistically, to reduce epithelial electrical resistance (a marker of barrier function) in human cell-line models, including Caco-2(Bruewer et al., 2003, Ma et al., 2005, F. Wang et al., 2005). In these studies, researchers demonstrated changes to the TJ complex, with downregulation of both occludin and Zo-1, with cellular internalisation of these proteins away from the TJ complex.

Effector cytokines, particularly TNFα, disrupt the epithelial barrier via the upregulation of myosin light chain kinase (MLCK). Cell to cell junctions within the epithelium are diminished when the cellular actin - myosin ring contracts, 'shrinking' the cell away from its neighbouring cells(Cunningham and Turner, 2012). This cytoskeletal re-arrangement is mediated by MLCK, which acts to phosphorylate the myosin light chain (MLC) of myosin II, to contract the cytoskeleton (see figure 1.6)

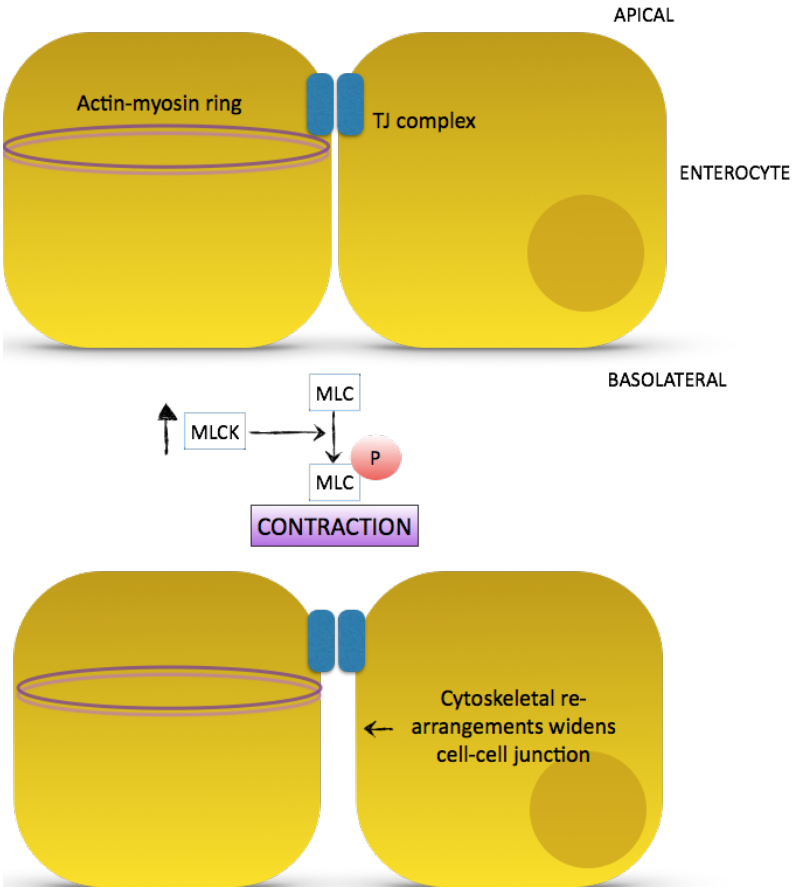

Figure 1.6; A schematic diagram to represent the re-arrangement of the cytoskeletal actin-myosin ring. Myosin light chain kinase (MLCK) acts to phosphorylate the light chain (MLC) of myosin II within the actin-myosin ring. The subsequent cytoskeletal contraction regulates epithelial barrier function.

TNFα increases the amount of MLCK protein, causing cell contraction, by upregulating its genetic transcription(Ma et al., 2005). A mouse model of systemic T-cell activation (via injection of anti-CD3 antibodies) causes diarrhea associated with increased levels of both TNFα and IFN γ (Musch et al., 2002). Clayburgh and colleagues demonstrated that phosphorylation of MLC increased immediately after T-cell activation and that diarrhea could be ameliorated via knocking out MLCK(Clayburgh et al., 2005). In a mouse model of ileal barrier dysfunction, anti-Il-6 antibody was found to reduce the phosphorylation of MLC(Zahs et al., 2013). These findings demonstrate the importance of cytoskeletal re-arrangement, via MLCK, in the disruption of the epithelial barrier.

1.7 Hypothesis and Aims

A better understanding of the aetiopathology of CD will help fulfill the need for more efficacious, less toxic treatments. The aetiopathogenesis is complex and multifactorial, but epithelial barrier dysfunction and dysbiosis are critical factors. A western diet is associated with dysbiosis and is also associated with an increased risk in the development of CD. The nuclear receptor FXR is central to signalling between the host and the microbiota. Evidence suggests that FXR is anti-inflammatory and helps to maintain an effective epithelial barrier.

The main hypothesis of this thesis is, therefore, that a diet-induced dysbiosis disrupts bile acid (BA) signalling, via FXR, predisposing to ileal Crohn's disease (CD)(see figure 1.7).

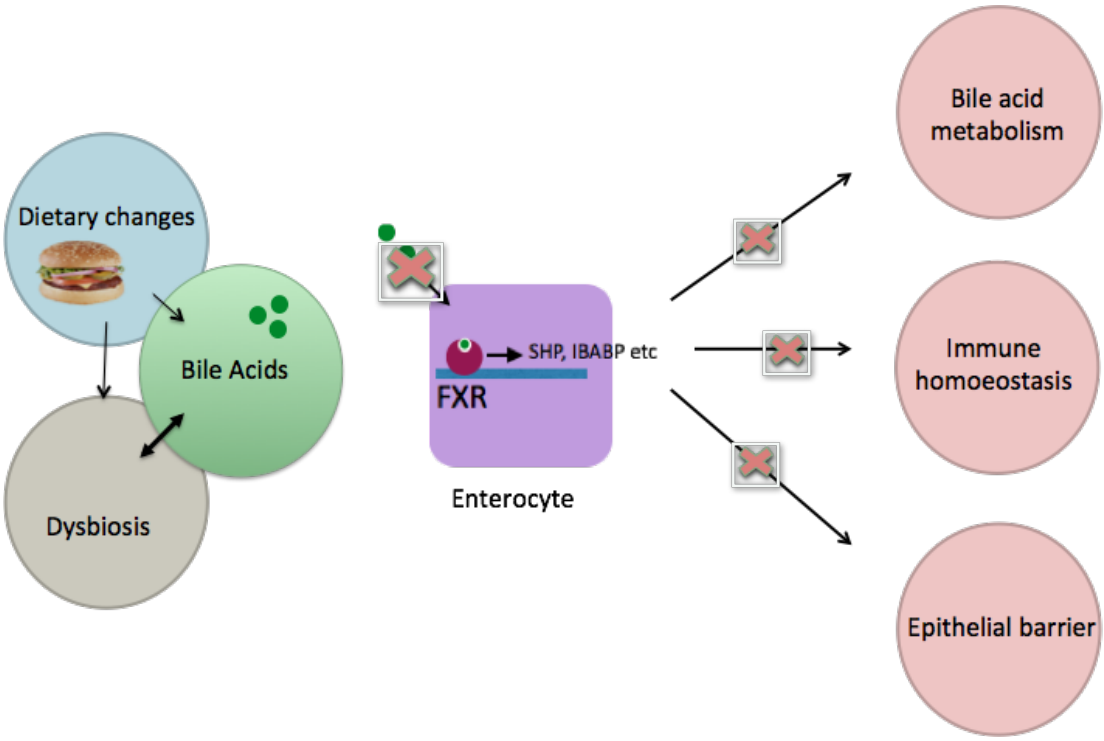

Figure 1.7; A schematic diagram to represent the original hypothesis. Dietary changes disrupt the microbiota and the bile acid pool (green dots) to impair FXR signalling. FXR has downstream effects on the maintenance of the epithelial barrier and on immune homeostasis, in addition to regulating BA metabolism in the liver. It is hypothesised that impaired FXR signalling in the ileum predisposes to gut inflammation.

Therefore, in order to investigate the role of FXR in the aetiopathogenesis of ileal CD, the broad aims of this thesis are:

1. To investigate the role of FXR agonism in maintaining an epithelial barrier using gut-derived, human cell lines.
2. To investigate the ability of FXR agonism to ameliorate the inflammation associated with high-fat/high-sugar feeding in a mouse model of obesity.
3. To investigate FXR activity in patients with ileal CD and to develop an *ex-vivo* ileal mucosa culture model to study FXR agonism and cytokine secretion.

Chapter 2 – FXR Agonism and Gut Epithelial Barrier Function in Human Cell Lines

2.1 Abstract

CD associated inflammatory cytokines induce epithelial barrier dysfunction and increase the leakiness of the gut mucosa(Bruewer et al., 2003, Suzuki, 2013). Farnesoid X receptor (FXR) agonism has been shown to maintain the epithelial barrier in a mouse model of colitis(Gadaleta et al., 2011b).

This chapter investigates the role of FXR in maintaining the epithelial barrier using human, gut derived cell lines. The aims were to optimise a model of cytokine induced barrier disruption and then to assay the effect of FXR agonism in this model. These experiments used the Caco-2 cell line as a model of the human small bowel epithelial barrier and HT29 cells as a model of the IL-8 secreting, immuno-phenotype of enterocytes.

Evidence is presented to demonstrate that FXR acts to maintain epithelial cell morphology after stress with inflammatory cytokine, possibly via the regulation of myosin light chain kinase (MLCK) expression. In addition, FXR activation is shown to ameliorate cytokine induced IL-8 secretion by gut epithelial cells.

2.2 Introduction and aims

The specialised epithelium of the GI tract is formed by a polarised cell monolayer in which intercellular TJ's control the paracellular flux of solutes, microorganisms and other toxins(Suzuki, 2013). As discussed in chapter 1, disruption to this epithelial barrier is central to the pathophysiology of IBD(Zeissig et al., 2007, Su et al., 2009, Hedin et al., 2012).

The effector inflammatory cytokine profile associated with CD increases epithelial permeability, probably by altering claudin protein expression and by cell cytoskeletal re-arrangement(Weber and Turner, 2007). Inflammatory cytokine induced expression and protein phosphorylation of MLCK leads to alterations in cell–cell junction morphology via re-arrangement of the apical cytoskeletal band(Cunningham and Turner, 2012).

A variety of innate immune mechanisms contribute to the maintenance of the epithelial barrier. When stressed by PAMPs, such as LPS, or by inflammatory cytokine, epithelial cells secrete IL-8, which acts as a chemo-attractant to circulating polymorphonucleocytes(Eckmann et al., 1993).

Gadaleta and co-workers have shown that activation of FXR can maintain the epithelial barrier both *in-vivo* and *in-vitro*, although the mechanism is not known. In a DSS colitis model, treatment with an FXR agonist maintained the epithelial barrier in WT, but not *Fxr-null* mice, as measured by the flux of FITC.dextran (a high molecular weight fluorescein) from the gut lumen to plasma(Gadaleta et al., 2011b). *In-vitro*, an FXR agonist was able to maintain an epithelial monolayer barrier, when exposed to DSS(Gadaleta et al., 2011b).

The aims of these cell line experiments were, therefore, to:

1. Optimise a model of inflammatory cytokine induced barrier dysfunction.
2. Assay the effect of FXR agonism on this induced epithelial barrier dysfunction.
3. Assay the effect of FXR agonism on the production of IL-8 by gut derived epithelial cells in response to cytokine stress.

2.3 Methods

2.3.1 The Caco-2 and HT29 cell lines

The Caco-2 and HT29 cell lines are well-characterised and often studied GI-derived, human epithelial cell models(Hidalgo et al., 1989, Jumarie and Malo, 1991, Dalmasso et al., 2008, Lee et al., 2008, Modica et al., 2008). Caco-2 is an immortalised epithelial cell line, originally isolated from a human colonic adenocarcinoma(Fogh and Trempe, 1975). Although originally of colonic tumour cell origin, on reaching maturity, Caco-2 cells exhibit characteristics of enterocyte differentiation. These enterocyte-like features include the growth of microvilli, attachment via tight junctions and the production of enterocyte specific enzymes including amino-peptidases, brush border enzymes and diamine oxidase(Jumarie and Malo, 1991). Caco-2 cells are well characterised in epithelial permeability studies due to their ability to form polarised monolayers(Hidalgo et al., 1989). The cells have a relatively slow doubling time, of approximately 60 hours, and reach full differentiation after maintenance in culture after approximately 21 days. Previous investigators have shown that FXR is only expressed and fully functional in fully differentiated, mature Caco-2 cells(Modica et al., 2008).

HT29 are an immortalised gut epithelial cell line, derived from an epithelial crypt-like cell from a colorectal adenocarcinoma(Fogh and Trempe, 1975). Like Caco-2 cells, HT29 will develop some enterocyte-like features, such as microvilli, on full differentiation after 7 days in culture. HT29 have been well characterised as a model of gut epithelial cytokine or chemokine secretion in response to stimulation with inflammatory cytokine or LPS(Riedel et al., 2006, Lee et al., 2008, Gadaleta et al., 2011b). Again, FXR has been shown to be expressed and functional in fully differentiated HT29 cells(Gadaleta et al., 2011b).

2.3.2 Optimisation of a Caco-2 polarised epithelial monolayer

New Caco-2 cells were purchased from the European Collection of Cell Culture (ECACC), thawed and re-suspended in Caco-2 growth media in a 25cm^2 flask (Greiner Bio One). All tissue culture was performed under a laminar flow hood using sterilised equipment. Caco-2 growth media consisted of Dulbecco's Modified Eagle's Medium (with 4500 mg/L glucose, 25 mM HEPES, sodium bicarbonate and phenol red; DMEM - Sigma), supplemented with 10% heat inactivated foetal calf serum (FCS -Biosera), 10% MEM Non-essential Amino Acid Solution (Sigma), 2mM L-glutamine, 100units/ml penicillin and 100µg/ml streptomycin (Sigma).

The concentrations of bile acid within a variety of manufacturers' FCS preparations was assayed (outsourced to Newcastle upon Tyne Foundation Hospitals Trust pathology laboratory), including dialysed FCS, and were found to be similar at levels from 8 to 9µmol/l. The ileal concentration of BA in humans is estimated to be approximately 1 x 10^4 µmol/l(Hofmann and Eckmann, 2006). Therefore, the low, relative concentration of BA in FCS was assumed to be of little biological importance in terms of confounding FXR agonism in comparison to either the in-vitro concentration of FXR agonist or the treatment of cells with an FXR agonist.

Cells were incubated in 5% CO^2 humidified atmosphere at 37^{o}C and cultured into 75cm^2 flask when they had reached 70% to 80% confluence. The growth media was changed every other day and cells were co-cultured, following washing with phosphate buffered saline (PBS) and removal with 5ml of trypsin-EDTA (Sigma), at a ratio of 1:6.

For growth as a polarised monolayer, Caco-2 cells were seeded into a hanging insert culture well, with high density 0.4 µm pore size, permeable, PET membrane (6 or 24-well Transwell Insert System, Corning Falcon), at a concentration of 50,000 cells/ml, as shown in figure 2.1. Cells were counted using a Neubauer

Improved haemocytometer by diffusing 10µl of cell containing growth media under a coverslip. A variety of different cell concentrations were used to determine the most efficient number of cells required for seeding.

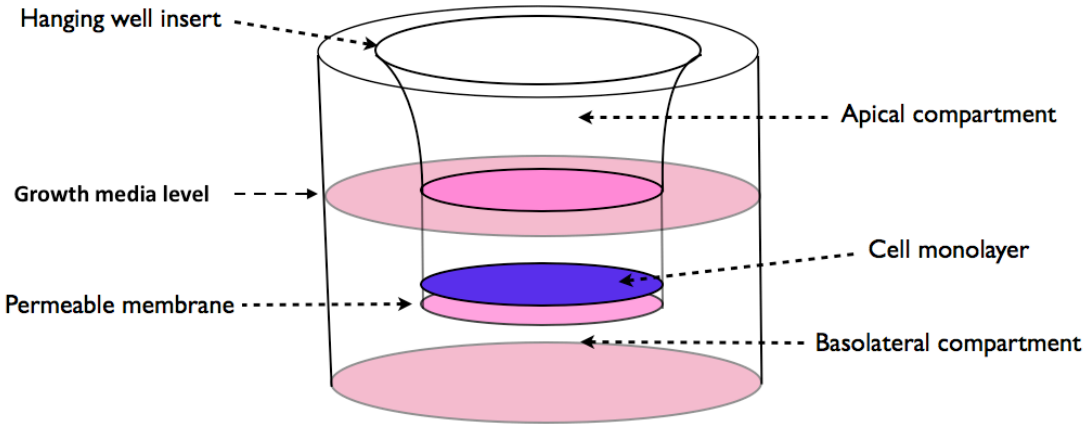

Figure 2.1; A schematic to represent the conditions required for culture of Caco-2 cells as a polarised epithelial monolayer. The cells are cultured on a permeable membrane, both covered by media and supported by a hanging well in media. As cells differentiate, apical and basolateral surfaces form, separated by apical tight junctions.

Use of 50,000 cells/ml reliably produced monolayers with stable and consistently high levels of trans-epithelial electrical resistance (TEER) after 21 days of differentiation. The measurement of TEER is described in section 2.2.3.

Cells in the 6-well system were cultured with 2ml of growth media in the apical chamber and 3ml of media in the basolateral chamber, whilst cells in the 24 –well system were cultured with 500µl of media in apical chamber and 800µl of media in the basolateral chamber. The growth media was changed every other day and

cells were allowed to mature for 21 days post seeding before experiments were performed.

For cytokine optimisation experiments, various concentrations (100ng/ml, 10ng/ml, 1ng/ml) of recombinant TNFα, IL-6 or IFNγ (R & D Systems) were added to the basolateral compartment. Previous studies have demonstrated that receptors for TNFα, IL-6 and IFNγ are expressed on the basolateral membrane in polarised Caco-2 cells(Adams et al., 1993, Tazuke et al., 2003, Ma et al., 2004). This panel of inflammatory cytokines was chosen due to the important role these particular cytokines play in the aetiopathology of CD, as described in chapter 1 (see figure 1.5).

Growth media was changed after 24 hours exposure to the cytokine. In subsequent experiments, 100ng/ml of cytokine was used. Optimisation experiments demonstrated that the upregulation of downstream FXR gene products was greater at 24 hours, rather than at 48 hours, post exposure to the FXR agonist (see results section 2.3.3). Therefore, in experiments utilising the FXR agonists, GW4064 and 6-ECDCA, dosing experiments with 1μM or 10μM of the compound were added to the apical cell monolayer compartment 24 hours prior to exposure to the cytokine. Experiments were replicated with a minimum of 3 different monolayers. TEER was measured every 24 hours as described below.

2.3.3 Mycoplasma

Initial attempts to culture the monolayers were hampered by unstable TEER measurements and the death of cells, which subsequently lifted off the well insert. Optimisation of growing conditions was performed by seeding different concentrations of cells, changing growth media constituents (e.g. 10% FCS versus

20% FCS), growing on a matrigel™ scaffold, growing on inserts coated with fibronectin and on inserts coated with rat tail collagen, but with no success.

An outbreak of a mycoplasma infection in the lab was eventually identified as the problem causing unstable monolayer formation. Figure 2.2 demonstrates an example of the change in TEER as the monolayer developed whilst infected with mycoplasma. Typically, an initial increase in TEER was not maintained and, often, whole Caco-2 monolayers would die before the end of the assay at 21 days.

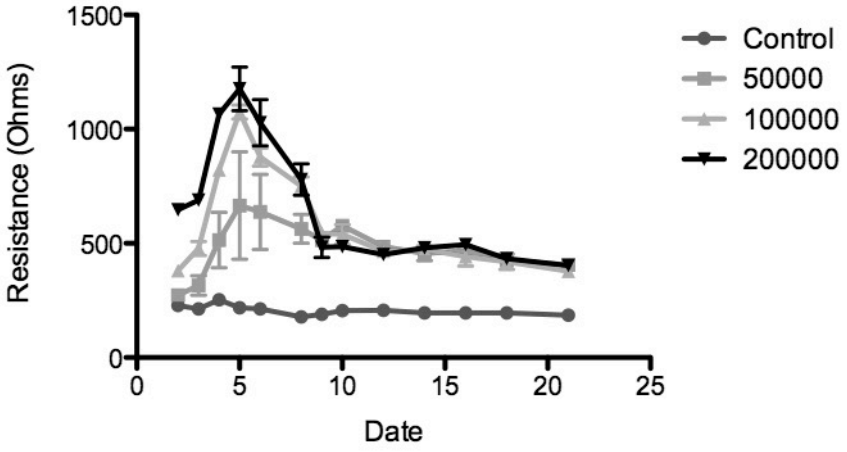

Figure 2.2; Chart of change in TEER with time for various seed concentrations of Caco-2 cells cultured in monolayers (50,000 cells/ml to 200,000 cells/ml). Presented here to demonstrate the deleterious effect of Mycoplasma infection on the ability of Caco-2 cells to form a polarised monolayer.

Mycoplasma are simple bacteria that lack a cell wall and are too small to be detected by light microscopy (0.3 to 0.8μm in diameter)(Robinson et al., 1956). They grow readily in cell culture media and can effect cell attachment, function, growth and metabolism. Mycoplasma infection is a common problem with 11% to 15% of cell lines tested in the U.S. being affected(Rottem and Barile, 1993).

A new cell line was purchased and the protocol for growing Caco-2 monolayers was changed to include a step to filter media (0.2μm pore, sterile filter) and to test for Mycoplasma every month. Mycoplasma testing of growth media and cell line media was performed using the enzyme-linked immunosorbent assay (ELISA)

Mycoalert testing kit from Lonza. Testing was performed according to the manufacturers instructions.

2.3.4 Lactate dehydrogenase release assay

To demonstrate that changes in TEER were due changes in paracellular flux, rather than monolayer disruption due to cell death, the level of lactate dehydrogenase (LDH) in the apical compartment was measured after exposure to inflammatory cytokine, FXR agonist, dimethyl sulfoxide (DMSO) as a vehicle control or Triton 1% (positive control). LDH is an abundant intracellular enzyme that converts pyruvate to lactate during anaerobic metabolism. Elevated levels of LDH within the supernatant would demonstrate cell lysis. DMSO is a common solvent used to re-suspend biologically active molecules. DMSO is toxic to cells at high concentrations (1-3%), but in these experiments was never used at concentrations greater than 0.025%. A DMSO (vehicle) control was used in all cell line experiments to control for the potential toxic effect of DMSO.

Supernatant from the apical compartment was analysed for LDH by the Newcastle upon Tyne Foundation Hospitals Trust pathology laboratory. The assay required phenol-red free growth media and so, for these experiments only, phenol-red free DMEM (Sigma-Aldrich) was used. Phenol-red is simply a pH indicator used in cell culture growth media to demonstrate metabolic activity. Growing Caco2 cells in phenol-red free media does not alter cell viability.

2.3.5 Measurement of trans-epithelial electrical resistance

Measurement of TEER provides a measure of epithelial barrier function. A volthometer measures the electrical current across the insert and the cell monolayer giving a result in ohms (Ω). Increasing levels of impendence to current

flow demonstrates that the cell monolayer is less permeable to the flow of charged ions and has formed a more effective barrier.

A Millicell ERS-2 voltohmeter with STX01 chopstick electrodes (both Merck Millipore, MA, USA) were used (see figure 2.3). Under a laminar flow hood, the chopstick electrodes were cleaned in 70% ethanol before being allowed to dry. The electrodes were then placed such that the short tip was in the insert culture well (apical compartment) and the long tip was in the basolateral compartment.

Reproducible positioning of the electrodes is important to provide reliable readings. Readings were always made with the electrodes perpendicular to the monolayer and after allowing the reading to settle for 3 to 4 seconds. Care was taken to measure different wells as quickly as possible to minimise changes in resistance measurements caused by cooling of monolayers to room temperature after removal from the incubator.

Figure 2.3; The Millicell ERS-2 voltohmeter and chopstick electrodes from the product literature of the manufacturers, Merk Millipore. To measure TEER, the electrodes are placed at a perpendicular angle to the surface of the monolayer, with the long chopstick arm in the basolateral well and the short chopstick arm in the apical well, just above the monolayer.

To calculate the monolayer resistance corrected for the area of the culture insert well (i.e. the unit area resistance) and for the resistance of the culture insert membrane ('control'), the following calculation was used:

Unit area resistance (Ω cm^2)= [Resistance sample (Ω) - Resistance control (Ω)] x effective membrane area (cm^2)

2.3.6 Measurement of Lucifer Yellow monolayer flux

Lucifer Yellow (LY) is a cell impermeable compound and measurement of its paracellular flux, from the apical compartment to the basolateral compartment, forms an alternative assay of monolayer permeability to TEER.

For the LY assay, monolayers grown on 24-well plate cell culture inserts were used. Cell media was removed from both apical and basolateral compartments and the monolayer was washed in transport buffer. Transport buffer consisted of Hank's Balanced Salt Solution (HBSS, Gibco, Life Technologies) supplemented with 140mg/l calcium chloride and 100mg/l magnesium chloride. 500 µl of LY, at a concentration of 100µM in transport buffer, was added to the apical compartment of each well, whilst 800µl of transport buffer, without LY, was added to the basolateral compartment. The monolayers were incubated in 5% CO^2 humidified atmosphere at 37^{o}C for 1.5 hours and then for 30 minutes on an orbital shaker at 37 ^{o}C, at 100 rpm. Following incubation, 200µl of supernatant from the basolateral compartment was transferred to a 96-well, black sided, clear-bottomed plate. Fluorescence was then measured in a Synergy HT plate reader (BioTek, U.S.A.) using a 485nm excitation filter and a 530nm emission filter. The fluorescence from serial dilutions of LY from 0.1 to 100µM was measured in order to produce a standard curve.

2.3.7 Imaging Caco-2 cell monolayers

Images of Caco-2 cells were recorded by both light microscopy (bright field) and electron microscopy for control and cytokine +/- FXR agonist treated monolayers. Bright-field microscopy was performed using the Cellix system. Fully differentiated Caco-2 monolayers in a 6-well Transwell Insert System were treated for 48 hours with basolateral inflammatory cytokine (100ng/ml TNFα, IFNγ or IL-6) with 24 hours of pre-treatment with apical FXR agonist (1μM 6-ECDCA) or 5μl DMSO as a vehicle control. 6-ECDCA was re-constituted in DMSO with 5μl of this solution in 2 ml of apical growth media being equivalent to 1μmolar. A 1% solution of Triton-X, a non-ionic surfactant, was also incubated in one of the apical compartments for 10 minutes to create a negative control. The Cellix incubator was pre-heated to 37°C and images were captured at 10x magnification.

For electron microscopy, fully differentiated 21 day monolayers were prepared in a 24-well Transwell Insert System. Monolayers were again exposed for 48 hours to basolateral inflammatory cytokine (100ng/ml TNFα, IFNγ or IL-6) with 24 hours of pre-treatment with apical FXR agonist (1μM 6-ECDCA) or 5μl of dimethyl sulfoxide (DMSO) as a vehicle control. Treated monolayers were then washed in PBS and resuspended in a 2% gluteraldehyde solution to fix the monolayers. The monolayers were then prepared and imaged for transmission and scanning electron microscopy (TEM and SEM) by the Electron Microscopy Research Services, Newcastle University.

For TEM, sections were prepared and imaged at random to demonstrate a cell-cell junction with its associated TJ complex. Sections were imaged at a magnification of 7900x to provide a representation of the full thickness of the cell monolayer. In this way, the majority of the cell-cell junction could be seen. In total, 20 junctions per intervention (e.g. control, TNFα, TNFα with FXR agonist etc.) were prepared.

The author and an independent researcher, who were both blinded as to the intervention, then reviewed the images. The presence or absence of cell-cell junction fissures was counted to provide evidence of the degree of cell cytoskeletal re-arrangement.

2.3.8 HT29 cell culture

A frozen cryovial of HT29 cells, gifted to the laboratory (courtesy of Professor Thwaites, Newcastle University), was re-suspended in 5 ml of warmed HT29 growth media in a 25cm^2 flask (Greiner Bio One). All tissue culture was performed under a laminar flow hood using sterilised equipment. HT29 growth media consisted of Dulbecco's Modified Eagle's Medium (with 4500 mg/L glucose, 25 mM HEPES, sodium bicarbonate and phenol red; DMEM - Sigma), supplemented with 10% heat inactivated foetal calf serum (FCS -Biosera), 10% MEM Non-essential Amino Acid Solution (Sigma), 2mM L-glutamine, 100units/ml penicillin and 100µg/ml streptomycin (Sigma).

Cells were incubated in 5% CO^2 humidified atmosphere at 37^{o}C and cultured into a 75cm^2 flask (Greiner, Bio One) when they had reached 80% confluence. For cytokine stimulation experiments 25cm^2 flasks were used. The growth media was changed every other day and cells were co-cultured, following washing with phosphate buffered saline (PBS) and removal with 5ml of trypsin-EDTA (Sigma), at a ratio of 1:4.

2.3.9 Enzyme-linked immunosorbent assay (ELISA)

An enzyme-linked immunosorbent assay (ELISA) is a laboratory technique used to quantify the concentration of a specific antigen or antibody within a biological substrate. In a ‘sandwich’ ELISA, the antigen of interest is sandwiched between a specific capture antibody and a biotinylated detection antibody, as seen in figure

2.4. A streptavidin conjugate is then added, which binds avidly to biotin (the binding of biotin to streptavidin is one of the strongest non-covalent interactions known in nature), the plate is developed and light absorbance measured against a known standard to calculate the concentration of the antigen of interest.

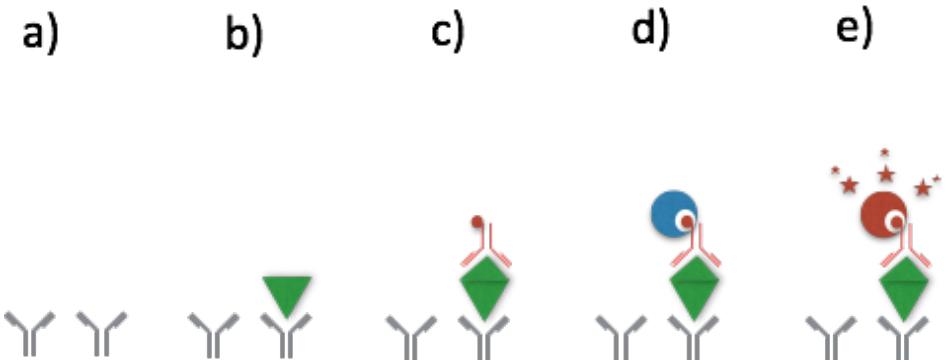

Figure 2.4; A schematic diagram representing the process of a sandwich ELISA: (a) Capture antibody coated plate, (b) addition of substrate containing antigen, (c) addition of specific biotinylated detection antibody, (d) addition of streptavidin which binds to biotin, (e) streptavidin is developed and absorbance is measured.

HT29 cells were grown in 25cm^2 flasks for 7 days. At full differentiation, cells were cultured with growth media containing 6-ECDCA (0.1, 1, 10µM), GW4064 (0.1, 1, 10µM), or DMSO (as vehicle control) for 24 hours. Some flasks were pre-treated for 24 hours with a growth media solution containing 100µM guggulsterone (Sigma Aldrich). Guggulsterone is a plant sterol compound that acts as an FXR antagonist(Urizar et al., 2002, J. Wu et al., 2002). Previous studies have demonstrated almost complete antagonism of FXR activity at doses of 100µM to 200µM(Capello et al., 2008). Following exposure to the FXR agonist +/- guggulsterone, HT29 cells were stimulated with growth media containing 100ng/ml TNFα for 24 hours. At the end of the experiments, growth media supernatant was collected to measure IL-8, secreted by the monolayer, and the cells were harvested for RNA extraction (see section 2.2.9).

An ELISA detection kit for IL-8 (PeproTech, NJ, USA) was used according to the manufacturers guidelines. Briefly, 100µl of a 0.5µg/ml solution of specific capture antibody was added to wells in a 96-well ELISA plate and stored at 4°C for 12 hours. The plate was washed in an automated plate washer (Thermo Fisher Scientific, MA, USA), using a wash buffer comprised of 1800ml water, 200ml 1% PBS and 1ml Tween-20. 150µl of block buffer (1g bovine serum albumin in 20ml PBS) was added to each well and left on an orbital shaker at room temperature for 1 hour. A standard 2000pg/ml solution of IL-8 was prepared and serially diluted 1:2 a further 7 times, using a diluent (1:10 solution of block buffer to wash buffer) to produce known samples for a standard curve. 100µl of standard or of cell supernatant was added to each well and left on an orbital shaker at 4°C for 12 hours. Each well was reproduced in triplicate. For some experiments, IL-8 levels were above the assay detection level (i.e. >2000pg/ml) and so cell supernatant samples were diluted to 1:10 and 1:100 using the diluent. After 12 hours incubation, 2 cycles of plate washing was performed, and 100µl of 0.25µg/ml biotinylated detection antibody was added before incubating on the orbital shaker at room temperature for 2 hours. The plate was then washed twice and 100µl of streptavidin-horseradish peroxidase (HRP) conjugate was added to each well and allowed to incubate at room temperature for 60 minutes. The plate was washed twice and developed with 100µl per well of a solution of 12.5ml citrate, 200µl o-Phenylenediamine (OPD), 5µl hydrogen peroxide (H_2O_2). The colour was allowed to develop sufficiently before terminating the reaction with 100µl per well of sulphuric acid. The absorbance in each well was then measured in a Synergy HT plate reader (BioTek, U.S.A.) at 492nm.

2.3.10 BSA protein assay

In order to determine the level of IL-8 in proportion to the number of cells in the monolayer, a measure of the protein content of the monolayer was made. Briefly, the monolayer was removed with 5ml of trypsin-EDTA and washed with PBS by centrifugation. The cell pellet was re-suspended in 150µl of cell-lysis buffer (10ml of Cell Lytic M cell lysis reagent, Sigma and one tablet of cOmplete, Mini, protease inhibitor cocktail, Roche), agitated and then incubated on ice for 10 minutes. The sample was then spun at 20,000 x g for 10 minutes, 4°C to pellet nucleic acid and debris. The remaining supernatant contained the protein fraction. Using a Pierce BCA Protein Assay kit (Thermo Scientific), a standard solution of 2mg/ml bovine serum albumin (BSA) was prepared and serially diluted 1:2, 7 times. In a black-walled 96-well plate, 10µl of sample or of standard BSA dilution was added in triplicate to each well. Again, sample supernatant was diluted 1:10 if the protein concentration was above the limit of assay. 200µl of reagent mix is then added to each well, allowed to incubate for 30minutes, 37°C on an orbital shaker. The absorbance at 492nm was then measured in a Synergy HT plate reader (BioTek, U.S.A.) and the protein concentration calculated as per the standard curve. The experiment was repeated for 3 different 25cm^2 flasks to give a mean average protein content per monolayer. ELISA results were then converted to IL-8 concentration per mass of cellular protein.

2.3.11 RNA extraction

RNA extraction from 25cm^2 Griener flask for Caco-2 and HT29 monolayers was performed using the phenol-based method described below.

RNA extraction for polarised, Caco-2 monolayers grown on cell culture inserts was more difficult to achieve and required several optimisation attempts in order to

extract RNA of sufficient quality. Optimisation steps included using polarised monolayers from both 24-well and then 6-well culture inserts (providing a greater concentration of genetic material), using 10mM EDTA to lift the cells or adding TRIzol directly to the inserts to remove the cells, using the total phenol-based method for RNA extraction or by using the spin column method for RNA extraction. Finally, a combination of both phenol-based and spin-column methods was used, as described below. An example of the spectrophotometer reading for contaminated Caco-2 RNA, prior to the optimisation of this process, is shown in figure 2.5.

2.3.12 Phenol-based RNA extraction

As described initially by Chomczynski and Sacchi, guanidinium-thiocyanate-phenol in the form of TRIzol reagent was used to extract RNA(Chomczynski and Sacchi, 1987). Experiments were performed using nuclease free, sterile equipment; surfaces were cleaned with RNase Zap (Life Technologies, UK), filter tips were used for pipetting and latex gloves were worn. The TRIzol reagent (Life Technologies) was used according to the manufacturers guidelines. Cells were removed from a 25cm^2 flask using 10mM EDTA, pH 8.0 and then resuspended in TRIzol at a concentration of 1ml per 10^6 cells. The TRIzol suspension was left for 5 minutes at room temperature before adding chloroform at a concentration of 20% of the total volume of TRIzol used. The suspension was mixed using a bench top vortex and then spun at 12,000 x g for 15 minutes, 4^{o}C. The aqueous phase was removed and the residual phenol was discarded. 2-propanol, at a concentration of 50% of the total volume of TRIzol used, was added to the aqueous phase and left for 11minutes at room temperature and spun at 12,000 x g for 10minutes, 4^{o}C to produce an RNA pellet. The supernatant was carefully removed and discarded.

The RNA pellet was then precipitated in 1ml 75% ethanol, spun at 7,500 x g for 5minutes, 4°C. The pellet was then allowed to dry before reconstitution in 50µl of RNAse free water.

2.3.13 Phenol-based method combined with spin column-based RNA extraction

Spin Columns use a solid phase extraction method in which RNA is purified by binding to silica within a manufactured tube(Boom et al., 1990). This method is more expensive than the phenol-based method, but is fast and produces a higher yield of RNA when the biological sample is small(Boom et al., 1990).

A protocol combining both the TRIzol and spin column methods was followed to extract RNA from polarised, monolayers. Again, RNA extraction was performed using nuclease free, sterile equipment. An RNeasy Mini-Kit (74104, Qiagen, Netherlands) was used as per the following protocol.

Fully differentiated polarised Caco-2 monolayers were grown on 6-well culture inserts as described in section 2.2.2. Growth media was changed every 48 hours. Monolayers were co-cultured for 24 hours with an apical growth media containing 1µM 6-ECDCA (FXR agonist) or equivalent vehicle (DMSO). Inflammatory cytokine (100ng/ml TNFα, IFNγ or IL-6) or PBS (vehicle) was then added to the basolateral media. Previous experiments had demonstrated that TEER reached a nadir at approximately 48 hours post exposure and, therefore, the monolayers were exposed to inflammatory cytokine for 48 hours in total. At the end of the experiment, the monolayers were washed in PBS and 700µl TRIzol was added directly to the culture insert. Experiments were performed in duplicate and the TRIzol/cell mixture from two identically treated culture inserts was then combined in a single Eppendorf. The TRIzol suspension was left for 5 minutes at room temperature before adding chloroform at a concentration of 20% of the total

volume of TRIzol used. The suspension was mixed using a bench top vortex and then spun at 12,000 x g for 15 minutes, 4°C. Approximately 600µl of the aqueous phase was removed and an equal volume of 70% ethanol was added and the sample mixed by pipetting. 700µl of the sample was transferred to a RNA spin column, in a 2ml collection tube, and spun at 8,000 x g for 15 seconds. The flow through was discarded and 700µl of buffer RW1 was added and spun at 8,000 x g for 15 seconds. The spin column was then washed with two cycles of 500µl buffer RPE, spun for 8,000 x g for 15 seconds and 2 minutes respectively. Finally, the RNA was precipitated in 30µl of nucleic acid and RNase-free water and spun for 8,000 x g for 1 minute to collect the RNA containing precipitate in a fresh, 1.5ml Eppendorf.

2.3.14 RNA quantity and quality

The efficiency of downstream assays depends on the purity of RNA isolated. The quantity and quality of RNA isolated by the above protocol was assessed using a spectrophotometer (Nanodrop ND-1000) and by gel electrophoresis.

The Nanodrop spectrophotometer measures the absorbance (A) of light at 260nm, to give an estimate of RNA quantity, and measures the absorbance of potential contaminants at 260nm and 280nm. Potential contaminants include organic solvents, such as phenol, peptides, carbohydrates, and salts such as guanidine thiocyanate(von Ahlfen and Schlumpberger, 2010). The ratio of A260/280nm and A260/230nm gives an estimate of nucleic acid purity, with ratios between 1.8 and 2.1 indicative of extremely pure RNA. No lower limits of acceptable contaminant ratios exist, but for the purposes of these experiments, A260/280nm and A260/230nm of 1.5 to 2.2 were accepted. Low levels of the A260/230nm ratio are usually due to contamination with guanidine thiocyanate, which is found in many

RNA extraction buffer reagents. A study has demonstrated that even high levels of guanidine thiocyanate contamination do not interfere with downstream RT-PCR reactions(von Ahlfen and Schlumpberger, 2010). Figure 2.5 demonstrates examples of spectrophotometer readings for poor quality Caco-2 RNA, purified Caco-2 RNA and purified HT29 RNA.

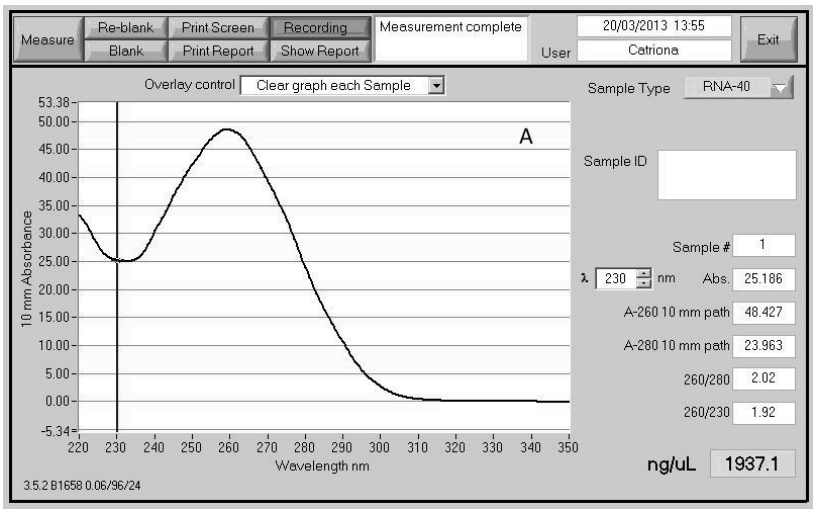

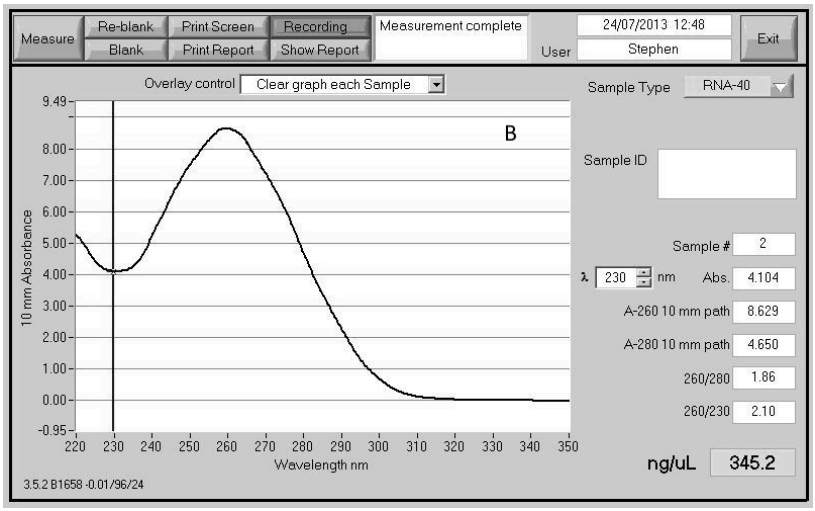

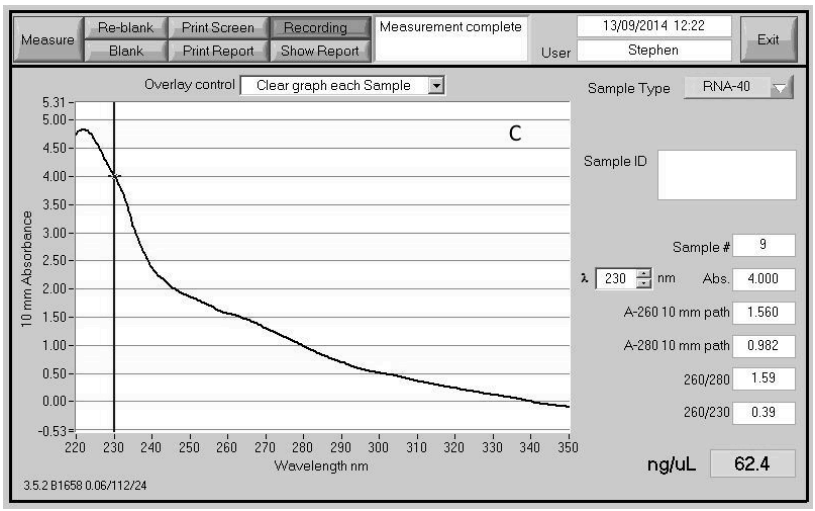

Figure 2.5; Examples of spectrophotometer readings for extracted RNA used in chapter 2 (A) Purified Caco-2 RNA, (B) purified HT29 RNA, (C) Poor quality RNA pre-optimisation of extraction technique. The Nanodrop ND 1000 provides a visual representation of absorbance at different wavelengths and calculates the A260/280 and A260/230 as described in the text. In addition, it provides an estimate of the concentration of RNA (ng/µl).

Gel electrophoresis of the RNA solute was performed by 120v electrophoresis, with 1xTAE buffer, on a 1.2% agarose, 0.5μg/ml ethidium bromide gel. 5μl of a 1kb DNA ladder control was loaded alongside 5μl of RNA, mixed with Orange G at a ratio of 1 in 10. RNA molecules have a negatively charged phosphate backbone and therefore move away from the negatively charged cathode. After 45 minutes, the electrophoresis was terminated and the gel was illuminated in a UV light box to highlight the ethidium bromide bound proteins. Pure RNA is demonstrated by the presence of discrete bands indicating the 18s and 28s subunits of ribosomal RNA. Gel electrophoresis was performed for optimisation steps and intermittently during RNA extraction to ensure RNA quality was maintained. Figure 2.6 demonstrates examples of UV light exposed electrophoresis gels run with purified RNA from Caco-2 and HT29 cells.

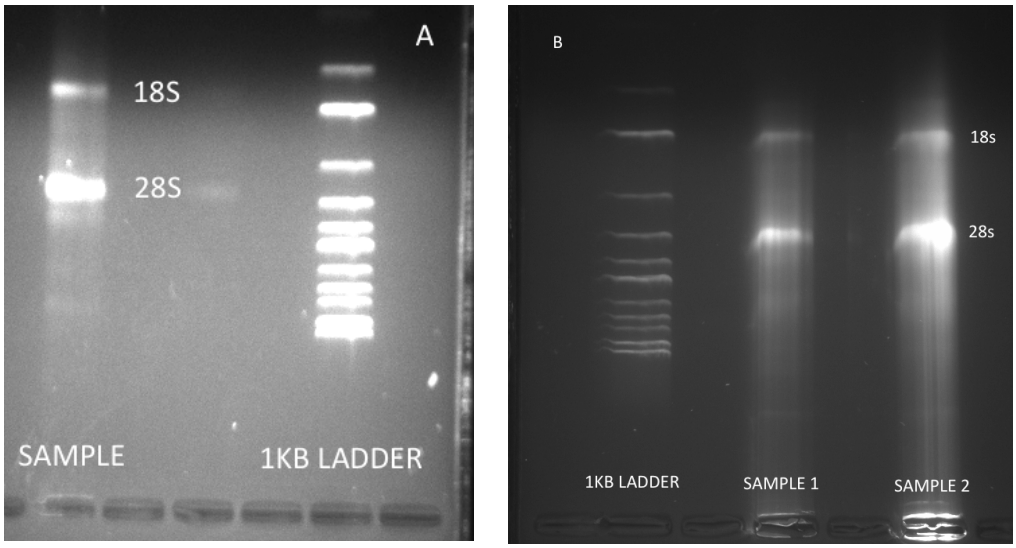

Figure 2.6; Examples of electrophoresis gels for purified RNA used in these experiments from A) Caco-2 cells and B) HT29 cells. The 28s and 18s ribosomal units can be clearly identified

2.3.15 Complementary DNA (cDNA) synthesis

Complementary DNA (cDNA) was prepared using the Tetro cDNA Synthesis Kit (Bioline) as per the manufacturers guidelines. As for RNA extraction, nuclease free equipment and reagents were used, surfaces were cleaned with RNase

decontamination solution (RNaseZap, Ambion, Life Technologies) and filter pipette tips were used. All procedures were performed on ice to minimize RNA degradation. A solution of isolated RNA was prepared in an autoclaved PCR tube representing up to 5µg of total RNA. To this was added 1µl of oligo dT primer; this recognises and binds only to the poly-A tail found on eukaryotic mRNA sequences. Then in sequence was added 1µl of 10mM dNTP mix, 4µl of 5x reverse transcriptase buffer, 1µl of Ribosafe RNase inhibitor and 1µl of Tetro reverse transcriptase. The solution was made up to 20µl using RNAse free water if necessary and run in a thermal cycler at 45°C for 30 minutes and then at 85°C for 5minutes to terminate the reaction. Samples were then stored at -20°C for later use in the second part of two-step RT-PCR experiments.

2.3.16 Real-time reverse transcription polymerase chain reaction (RT-PCR)

RNA isolated from Caco-2 and HT29 cells was used to measure the relative mRNA level of a variety of genes using RT-PCR via a TaqMan-based chemistry assay (Life Technologies). The relative mRNA level of FXR and its downstream targets, SHP and IBABP, was measured to assess the effect of FXR activity in both cell lines. The relative mRNA expression of IL-8 was measured in HT29 cells used in the IL-8 secretion experiments (section 2.2.7). In addition, the relative mRNA levels of myosin light chain kinase (MLCK) were measured in the RNA extracted from Caco-2 cells grown in polarised monolayers and treated with inflammatory cytokine +/- FXR agonist (section 2.2.9).

Polymerase chain reaction (PCR) is a wet-lab process by which small molecules of DNA are copied and amplified many times using sequence specific oligonucleotides and DNA polymerases in repeated cycles of heating and annealing. In a RT-PCR experiment, the amount of DNA is measured after each PCR cycle via fluorescent

dyes that produce increasing amounts of a fluorescent signal as the amount of replicated DNA increases. A variety of fluorescence reactions are available, but for these experiments a TaqMan assay was utilised(Holland et al., 1991). TaqMan chemistry is thought to be relatively specific and sensitive in comparison to other methods, such as SYBR Green(Cao and Shockey, 2012).

The TaqMan assay uses a pair of primers and a potentially fluorescent probe. Gene of interest specific, forward and reverse primers for taq DNA polymerase bind to a single strand of DNA to produce two copies. The probe is an oligonucleotide, containing a 5' fluorophore and a 3' quencher molecule that inhibits the fluorescence of the probe. The probe anneals to a specific single strand of DNA for the gene of interest within a region amplified by the taq polymerase primers. Whilst the fluorophore and quencher molecule are in close proximity, any fluorescence is absorbed. As it progesses, taq DNA polymerase cleaves the fluorophore from its quencher, increasing the overall fluorescence signal. The reaction continues to then release the residual probe from the DNA strand allowing DNA synthesis to be completed. In this way, with each cycle of PCR, the amount of fluorescence increases. Figure 2.7 demonstrates this process in a single cycle of PCR.

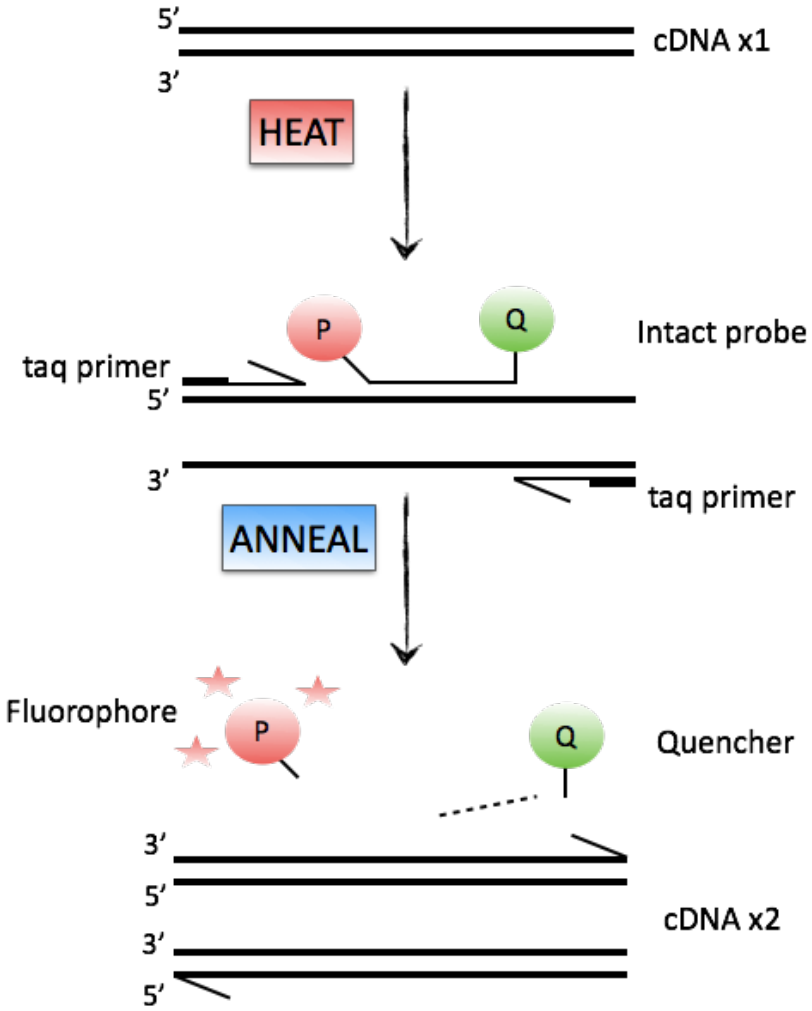

Figure 2.7; A representation of a single cycle of PCR using a TaqMan probe-based assay. Heating separates two strands of cDNA; the pair of taq polymerase primers bind and taq DNA polymerase replicates alternate strands of cDNA in a 5'-3' direction; the specific oligonucleotide probe binds, but does not fluoresce whilst the quencher portion is in close proximity to the fluorophore; as DNA replication progresses, the probe is cleaved, releasing the fluorescing portion; the new strands anneal to complete the cycle

Human specific, TaqMan Gene Expression Assays (pair of PCR primers and specific hydrolysis probe) to FXR, SHP, IBABP, IL-8, MLCK and GAPDH were purchased from Life Technologies. Table 2.1 lists the primer/probes and their targets used in these experiments. In order to avoid false positive detection of genomic DNA (gDNA), TaqMan primers/probes that span exon-exon junctions (intron-splice sites) were used in these experiments where possible.

Protein	Gene	Exon spanning	Primer/Probe
FXR	NR1H4	yes	Hs01026590_m1
SHP	NR0B2	yes	Hs00222677_m1
IBABP	FABP6	yes	Hs01031183_m1
IL-8	IL8	yes	Hs00174103_m1
MLCK	MYLK	yes	Hs00364926_m1
GAPDH	GAPDH	yes	Hs02758991_g1

Table 2.1; List of genes of interest and TaqMan primer/probes used in chapter 2

In a 96-well PCR plate, 10µl of 2x mastermix (SensiFAST Probe Hi-ROX kit, Bioline, UK), 1µl of premixed primer/probe (TaqMan Gene Expression Assays, Life Technologies), 1µl of cDNA template and 8µl of RNase free water were prepared. Again all procedures were performed on ice to avoid RNA degradation and were performed with RNase-free materials. Mastermix contains the reagents necessary to perform PCR, including DNA polymerase, dNTPs, stabilisers and magnesium chloride (enzyme co-factor). The addition of the ROX (5-carboxy-X-rhodamine) fluorophore allows for the normalisation of non-PCR associated fluctuations in fluorescence. The plate was centrifuged at 500 x g for 1 minute and then incubated for 20secs at 95°C before going through 40 cycles of PCR of 1 second at 90°C followed by 20secs at 65°C to allow primers to anneal and new strands to extend. Experiments were performed using an Applied Biosystems StepOnePlus™ Real-time PCR system machine.

2.3.17 RT-PCR quality control

To minimise assay errors due to incorrect pipetting, each RT-PCR reaction was performed in triplicate. If the threshold cycle (Ct, see below) differed by greater than 1.0 within triplicate samples, that well was excluded from further analysis.

For each 96-well PCR plate, a no-template control (NTC) triplicate experiment was performed to ensure there was no DNA contamination within the mastermix, primer/probe or water used in the experiments. To ensure no gDNA contamination of the RNA preparation used to make the cDNA template, an RNA-template reaction was performed for representative samples.

Relative quantitative RT-PCR calculations assume that the reaction efficiency of the primer/probe is 100%, with an acceptable range of 90% to 110%. Primers were validated by measuring Ct for 1/10 serially diluted cDNA concentrations, plotted on a log10 scale. The slope of this curve can be used to calculate the efficiency of each primer via the equation:

$$\text{Efficiency} = 10^{(-1/\text{slope})} - 1$$

The R^2 co-efficient of the standard curve is a measure of the degree of fit and therefore of replicate reproducibility; it should be >0.98. Figure 2.8 and table 2.2 demonstrate primer validation results for the primers used in these experiments.

Primer	Slope	Efficiency	R-squared
FXR	-3.273	102.1%	1.00
SHP	-3.193	105.7%	0.99
IBABP	-3.17	106.8%	0.97
IL-8	-3.127	108.8%	0.99
MLCK	-3.279	101.8%	1.00
GAPDH	-3.349	98.9%	0.96

Table 2.2; Primer efficiency and goodness of fit (R^2) for primers used in chapter 2. See fig 2.8

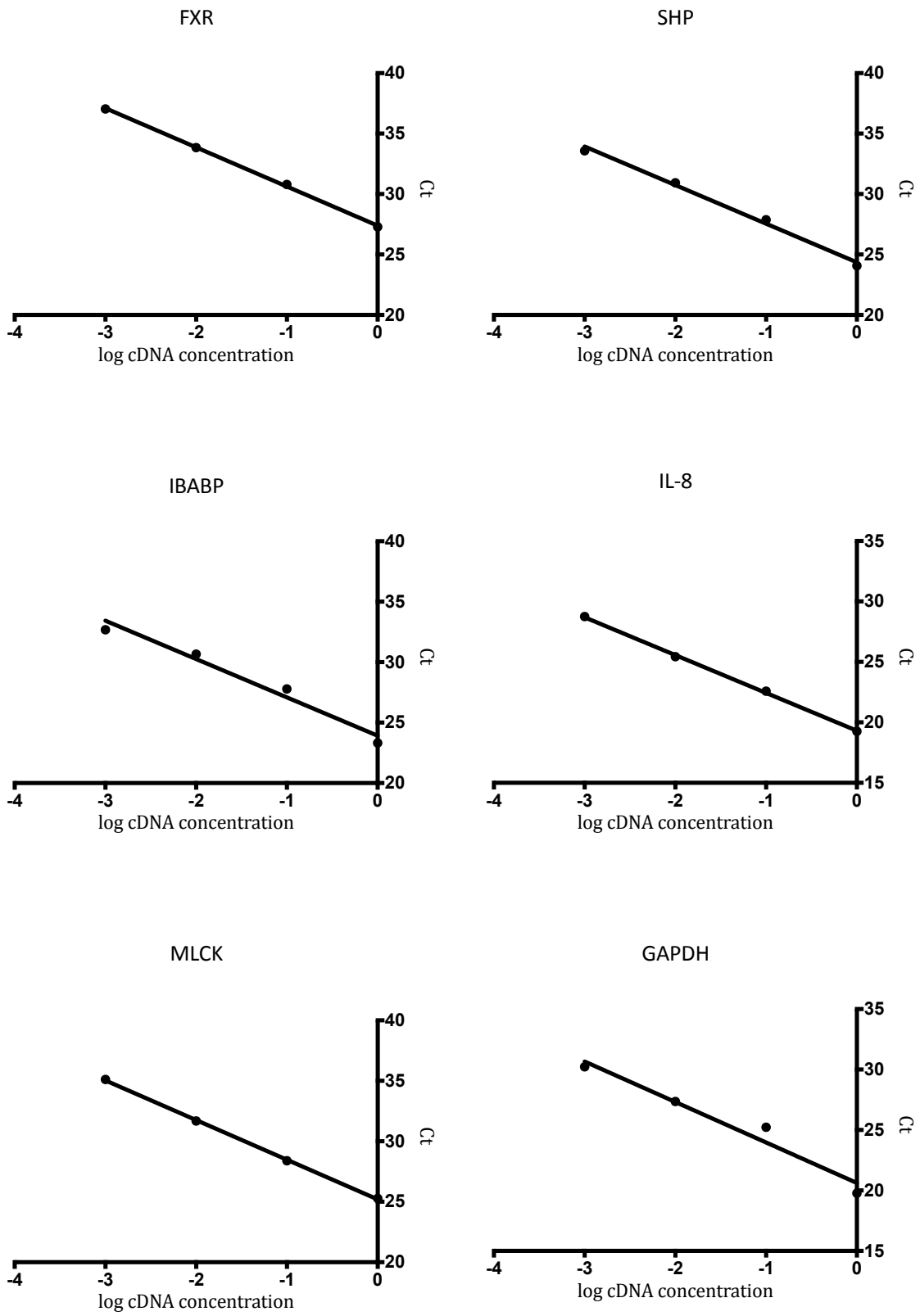

Figure 2.8; Primer validation experiments for primers used in chapter 2. Threshold cycle is measured for serial dilutions of cDNA. See table 2.2 for R^2 and efficiency calculation

2.3.18 Threshold cycle and relative quantification

An RT-PCR experiment creates an amplification plot with fluorescence on the *y*-axis and cycle number on the *x*-axis. The reaction can be divided into 3 phases; a baseline phase during which there is little change in the fluorescent signal, which remains barely detectable; an exponential phase, during which 'perfect' PCR is occurring with the concentration of DNA doubling every cycle; finally, a plateau phase when reagents begin to be depleted and DNA replication begins to slow (see figure 2.9).

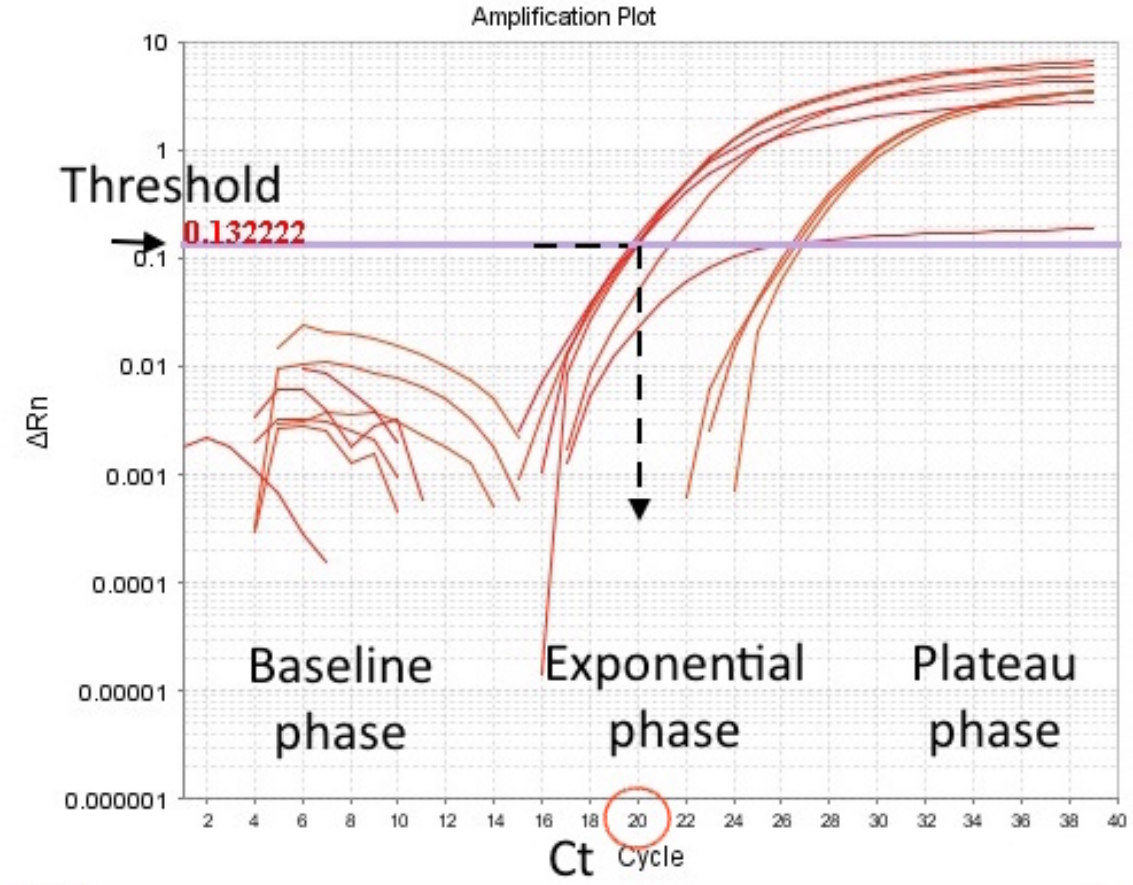

Figure 2.9; See text for detail. An example of an RT-PCR amplification plot to demonstrate the concept of threshold cycle (Ct). In this example, highest concentration gives Ct 20.

The threshold cycle (Ct) is the cycle number at which the fluorescent signal crosses a determined level. Samples with a higher concentration of DNA at baseline will cross the Ct earlier than samples with lower levels of DNA at baseline. The Ct is

determined during the exponential phase and is constant across all samples to allow relative quantification.

To measure the expression levels of mRNA for each gene of interest in the different samples, relative quantification was used. This method compares the expression of the gene of interest (e.g. TNFα) in comparison to a standard or reference gene (also known as a housekeeper gene). The expression of the reference gene should remain stable throughout the samples, being unchanged by any intervention. The quantity of the gene of interest, relative to the reference gene, can then be compared between a control sample and an intervention sample. Relative quantification is faster than absolute quantification and doesn't rely on the production of sensitive standard curves.

The choice of reference gene is, however, critically important in the analysis of the results. In these experiments, the commonly used reference gene for glyceraldehyde 3-phosphate dehydrogenase (GAPDH) was used(Barber et al., 2005).

2.3.19 Fold change calculations and statistical analyses

Relative quantification was calculated using the ΔΔCt method as described by Livak and Schmittgen(Livak and Schmittgen, 2001). From triplicate samples, a mean Ct was calculated for each biological sample. The relative expression of the gene of interest (GOI) in comparison to the reference gene (ΔCt) was then calculated by the equation:

$$\Delta Ct = \text{mean } Ct_{GOI} - \text{mean } Ct_{reference}$$

The change in relative gene expression between control and intervention groups (ΔΔCt) can then be calculated as:

$$\Delta\Delta Ct = \Delta Ct_{intervention} - \Delta Ct_{control}$$

The ratio of the GOI in the intervention group relative to the GOI in the control group (the fold change), is then given by:

$$\text{Fold Change} = 2^{-\Delta\Delta Ct}$$

This converts the results to a logarithmic scale (e.g. 2 fold increase, 4 fold decrease etc.) and, therefore, represented error bars should be interpreted with caution. A fold change of greater than 2 is thought to be biologically significant.

Unpaired Student's *t*-tests, two-way ANOVA (analysis of variance) and non-linear regression analyses were calculated using Prism version 6.0e, Graphpad software, San Diego. All P values were 2-tailed, and a P value of 0.05 or less was considered to be statistically significant.

2.4 Results

2.4.1 Optimisation of a Caco-2 polarised monolayer model

Serial measurements of the TEER of 12 different monolayers were made over a period of 30 days, from seeding to full differentiation. Figure 2.10 demonstrates the mean (n=12) increase in TEER over time as the monolayer matures and intercellular TJs form to decrease monolayer permeability. The Caco-2 monolayers formed high levels of unit area resistance with a best-fit peak resistance of approximately 2,700Ω/cm^2 and a subsequent slow decline in resistance up to 30 days.

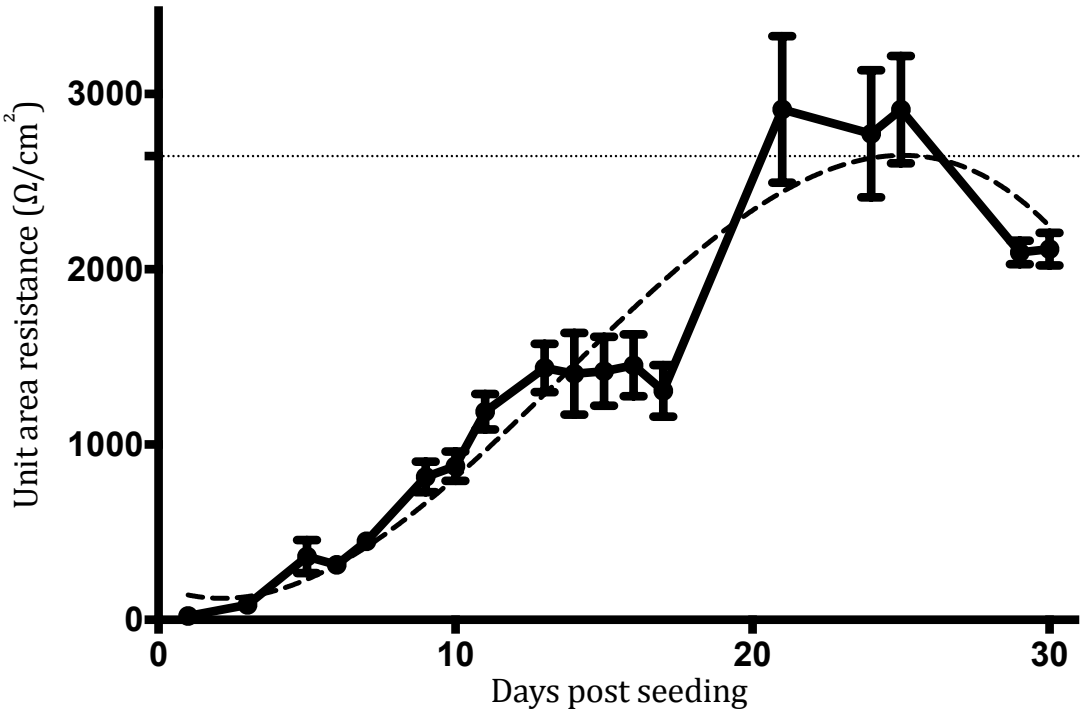

Figure 2.10; Mean TEER of Caco-2 polarised monolayers with time. Dashed line is best-fit by non-linear regression. Dotted line marks zenith of best-fit line. (For each data point, n=12, standard error of mean [SEM]).

In order to model the effect of CD associated inflammatory cytokines on gut epithelial permeability, the TEER was measured at several time points following exposure of the fully differentiated (> 21 day post seeding), polarised monolayer to IFNγ, TNFα and IL-6.

Figure 2.11 demonstrates the effect on mean TEER (n=4), over time, of 100ng/ml of cytokine, added to the basolateral compartment. The results are presented as change in TEER normalised to a baseline of 1.0. An untreated control group is presented as a comparison. For each cytokine, there is a significant decrease in the epithelial permeability, over the 120 hours of the experiment, in comparison with control (by two-way ANOVA, IFNγ $p < 0.0001$, TNFα $p < 0.0001$, IL-6 $p < 0.0001$).

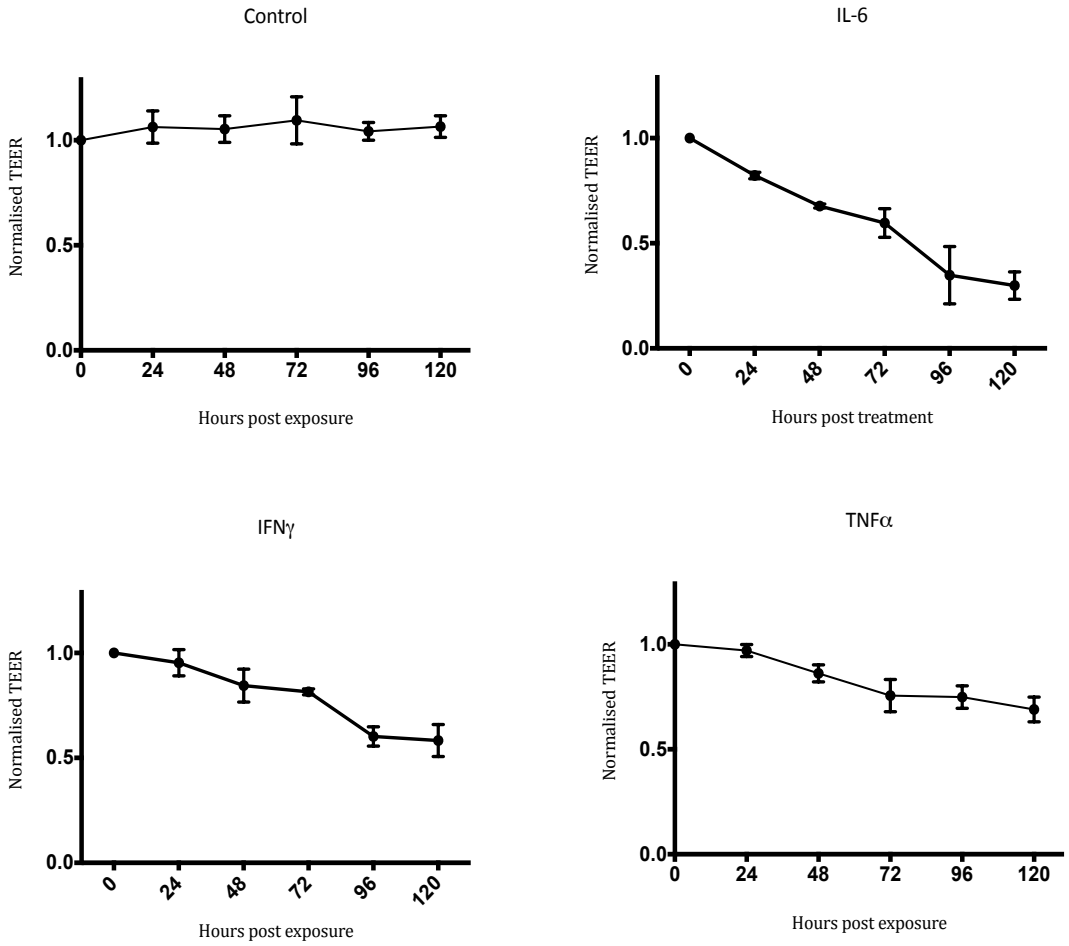

Figure 2.11; The mean change in TEER over time (normalised to 1.0) for Caco-2 monolayers exposed to 100ng/ml of IL-6, IFNγ or TNFα in comparison to control (n=4, error=SEM). TEER is significantly different between cytokine treated and control groups (2-way ANOVA p<0.0001).

There is a dose-response relationship between the concentration of inflammatory cytokine and the reduction in TEER. Figure 2.12 demonstrates the mean TEER at 48 hours for different concentrations of cytokine. It can be seen that cytokine at 10ng/ml and 100ng/ml produces a significant reduction in TEER, as compared with control, for all of the cytokines tested. At concentrations of 1ng/ml, there is no significant difference in TEER as compared with control. Table 2.3 demonstrates the results from unpaired Student's *t*-tests, with 95% confidence intervals, for the TEER at 48 hours for each concentration of cytokine tested in comparison with control.

Cytokine	Concentration	P-value	95% Confidence interval
TNF α	0ng/ml	N/A	N/A
	1ng/ml	0.180	-243.5 to 930.1
	10ng/ml	*0.011	337.4 to 1406
	100ng/ml	**0.002	524.5 to 1203
IFN γ	0ng/ml	N/A	N/A
	1ng/ml	0.266	-231.4 to 634.6
	10ng/ml	**<0.001	1003 to 1573
	100ng/ml	**<0.001	1001 to 1571
IL-6	0ng/ml	N/A	N/A
	1ng/ml	0.336	-291.4 to 669.4
	10ng/ml	**0.002	755.5 to 1694
	100ng/ml	**0.001	936.2 to 1866

Table 2.3; A table to demonstrate the results of unpaired Student's t-tests for different concentrations of cytokine versus control (0ng/ml) for TEER at 48 hours in Caco2 monolayers (results given to 3 decimal places).

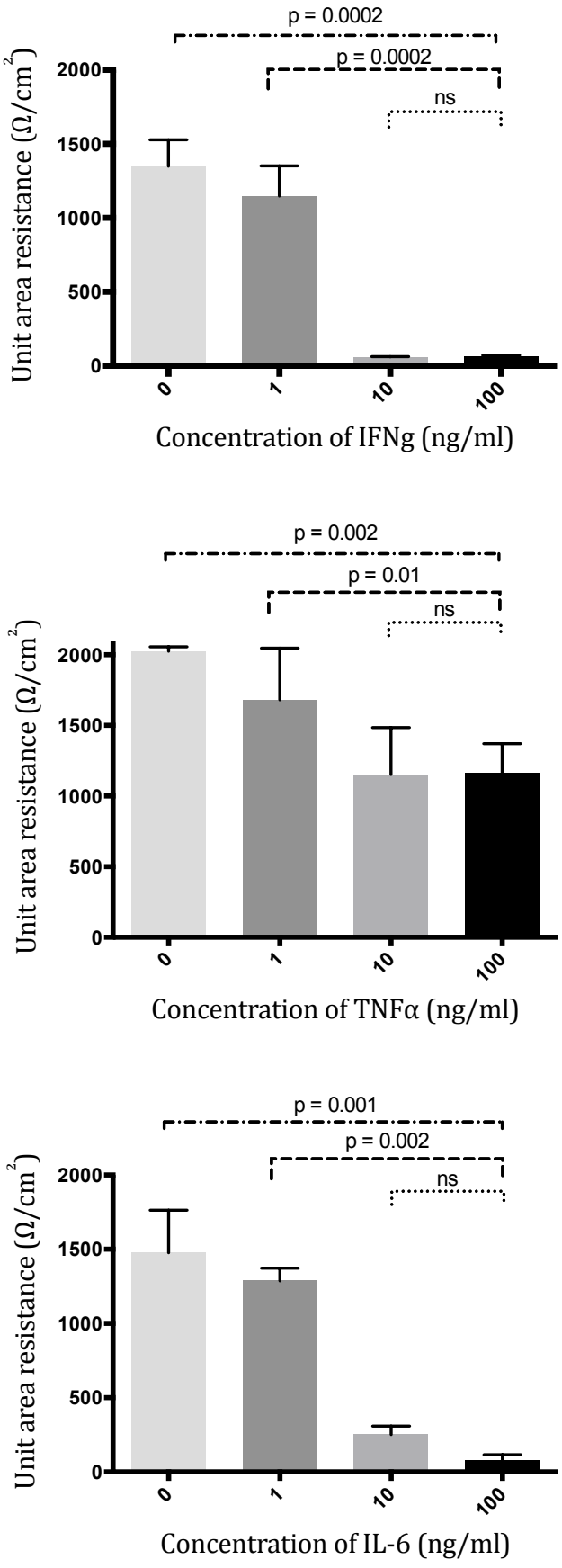

Figure 2.12; The mean TEER of polarised Caco-2 monolayers at 48 hours after stimulation with different concentrations of CD associated cytokines (n=4, SEM, 2-tailed unpaired t-tests)

An LDH release assay demonstrated that the disruption to the epithelial barrier observed when monolayers were challenged with cytokine was not caused by cell death and subsequent cell lysis, as seen in figure 2.13.

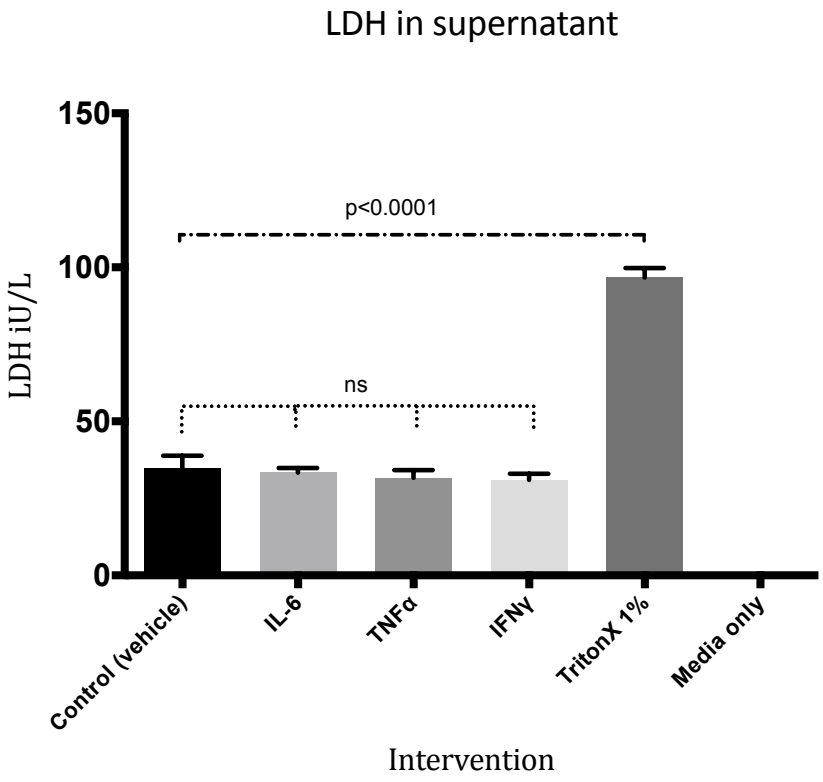

Figure 2.13; LDH release assay for polarised Caco-2 monolayers stimulated with 100ng/ml of IL-6, TNFα or IFNγ. Controls are monolayers treated with vehicle (PBS), TritonX 1% (positive control) and fresh, untreated growth media (negative control)

2.4.2 6-ECDCA and GW4064 agonise FXR in both Caco-2 and HT29 cells

A measure of FXR activity was performed by assaying the expression of FXR downstream targets, SHP and IBABP.

On stimulation with the FXR agonists 6-ECDCA and GW4064, both Caco-2 and HT29 cells demonstrated an increase in the level of mRNA for SHP and IBABP, in comparison to vehicle (DMSO) treated cells (see figures 2.14 and 2.15). As described in section 2.2.13, relative gene expression was calculated to give a fold change in mRNA levels between control and FXR agonist treated groups.

In Caco-2 cells, both 10μM 6-ECDCA and 10μM GW4064 were able to induce a positive fold change in FXR, SHP and IBABP, which was greater at 24 hours than at 48 hours (figure 2.14). Under these experimental conditions, 6-ECDCA had greater downstream effects on SHP and IBABP expression than GW4064. 6-ECDCA induced a positive fold change of 2.5 in FXR, 41.3 in SHP and 29.3 in IBABP at 24 hours. In comparison, GW4064 induced a positive fold change of 8.9 in FXR, 2.1 in SHP and 8.9 in IBABP at 24 hours.

However, when the same experimental conditions were applied to HT29 cells, slightly different results were observed. Unlike Caco-2 cells, neither of the FXR agonists was able to induce auto-upregulation of FXR in HT29 cells, with in fact a biologically significant fold reduction in relative FXR mRNA (see figure 2.15).

The EC_{50} of both FXR agonists is close to 0.1μM. Therefore, experiments were repeated using this lower dose, to test whether the observed results were due to any potential cytotoxicity induced by higher concentrations of agonist. The 0.1μM dose of both agents was also unable to upregulate FXR expression in HT29 cells.

The downstream FXR targets were, however, positively induced at 24 hours, with the higher 10μM concentration of both agonists demonstrating a greater effect. Only a small positive fold change was found at 24 hours for SHP, of 2.2 for 6-

ECDCA and 1.2 for GW4064. IBABP mRNA expression, however, was strongly induced with fold changes of 42.3 and 216.1 for 6-ECDCA and GW4064 respectively, at 24 hours (see figure 2.15).

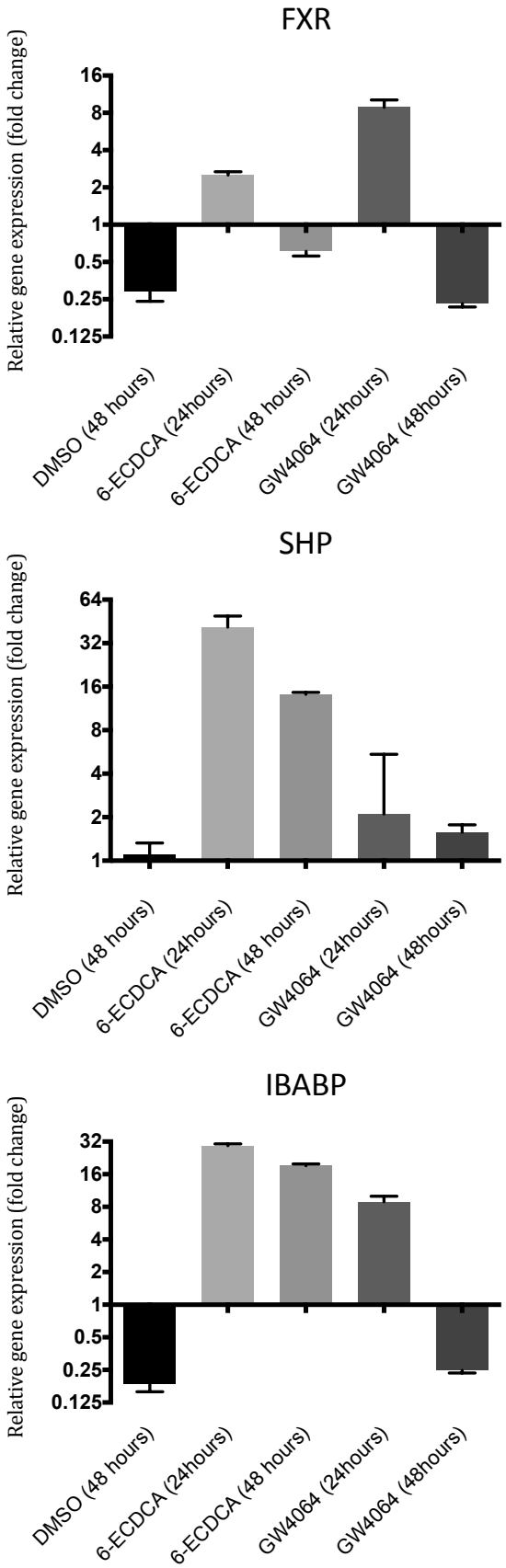

*Figure 2.14; The relative gene expression (as fold change) of FXR and its downstream targets, SHP and IBABP, in **Caco-2** cells treated with 6-ECDCA (10µM) or GW4064 (10µM) 24 and 48 hours post exposure (n=3, SEM, y-axis is log scale).*

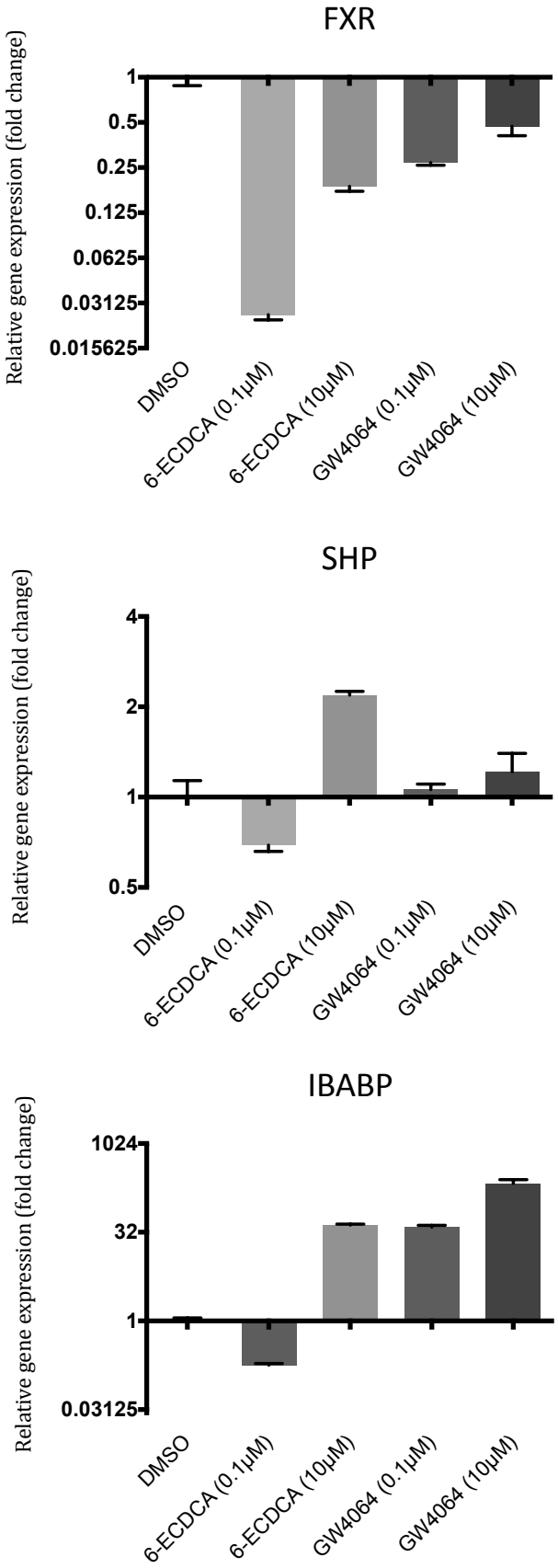

*Figure 2.15; The relative gene expression (as fold change) of FXR and its downstream targets, SHP and IBABP, in **HT29** cells treated with 6-ECDCA (0.1μM & 10μM) or GW4064 (0.1μM & 10μM) 24 hours post exposure (n=3, SEM, y-axis is log scale).*

2.4.3 Activation of FXR does not maintain Caco-2 monolayer permeability when disrupted with inflammatory cytokines

In order to assay whether FXR agonism could maintain epithelial barrier function when disrupted with CD associated cytokines, TEER was measured in the Caco-2 monolayer model after insult with IFNγ, TNFα and IL-6 both with and without 6-ECDCA.

Figures 2.16, 2.17 and 2.18 demonstrate the epithelial barrier dysfunction, as measured by TEER, on exposure to IL-6, IFNγ or TNFα, during the period of observation (up to 11 days).

The TEER remained stable or increased in the control (DMSO treated) or 6-ECDCA -alone treated monolayers. There is a significant reduction in the TEER, compared with 6-ECDCA –alone treatment, when monolayers are exposed to 100ng/ml IL-6, IFNγ or TNFα (two-way ANOVA, variance from baseline $p < 0.001$).

Pre-treatment of monolayers with 6-ECDCA, at either 10μM or 1μM, did not ameliorate the reduction in TEER observed when monolayers were stressed by inflammatory cytokine. Data are only shown for monolayers exposed to 1μM 6-ECDCA. There was no significant difference, as tested by two-way ANOVA, between the inflammatory cytokine treated groups and the cytokine plus 6-ECDCA intervention groups.

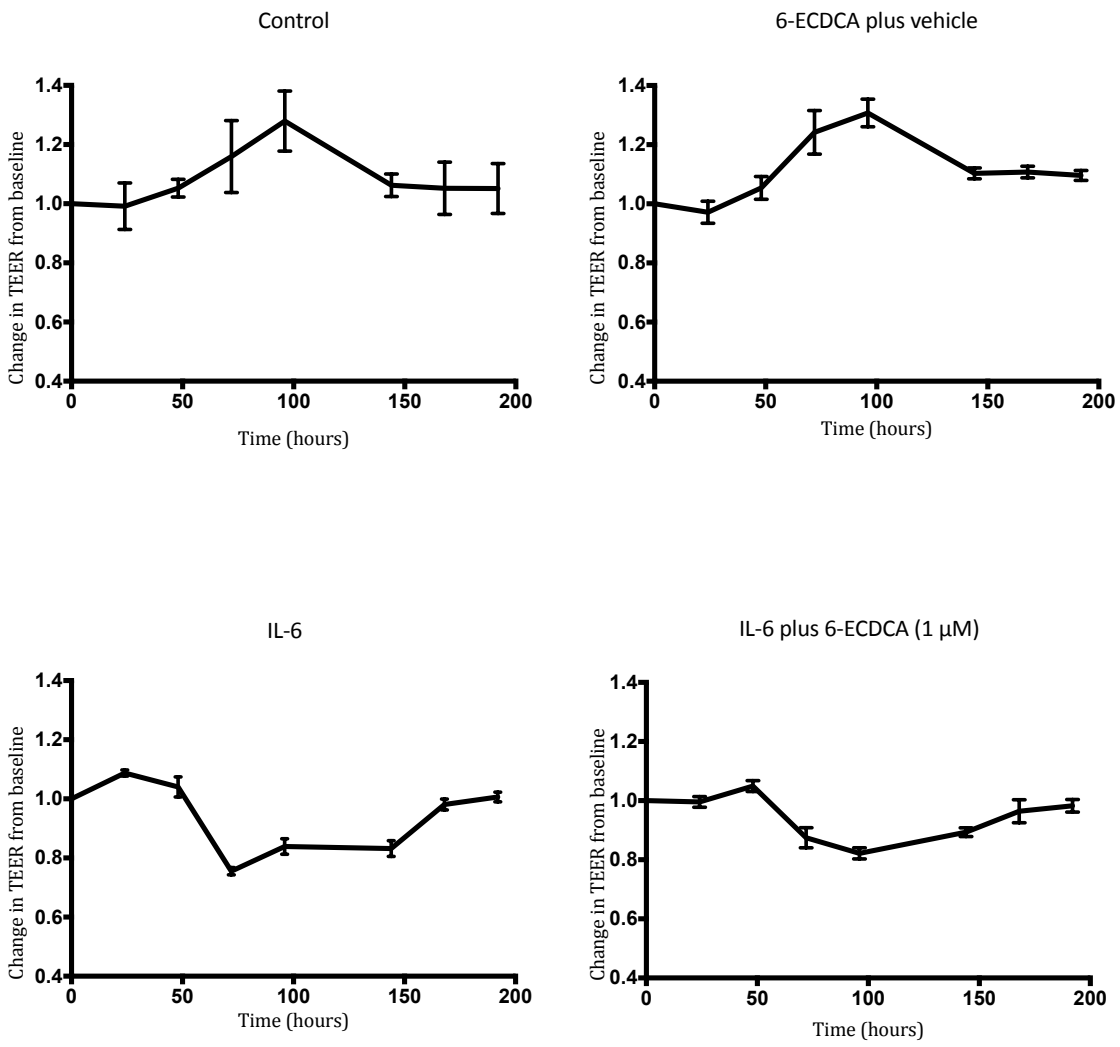

Figure 2.16; Mean TEER for polarised Caco-2 monolayers treated with IL-6 (100ng/ml) +/- 6-ECDCA (1µM), or control (n=4, SEM). There is a significant reduction in TEER from control for IL-6 exposed monolayers (Two-way ANOVA p<0.001). The reduction in TEER was also significantly different in the IL-6 plus 6-ECDCA monolayers.

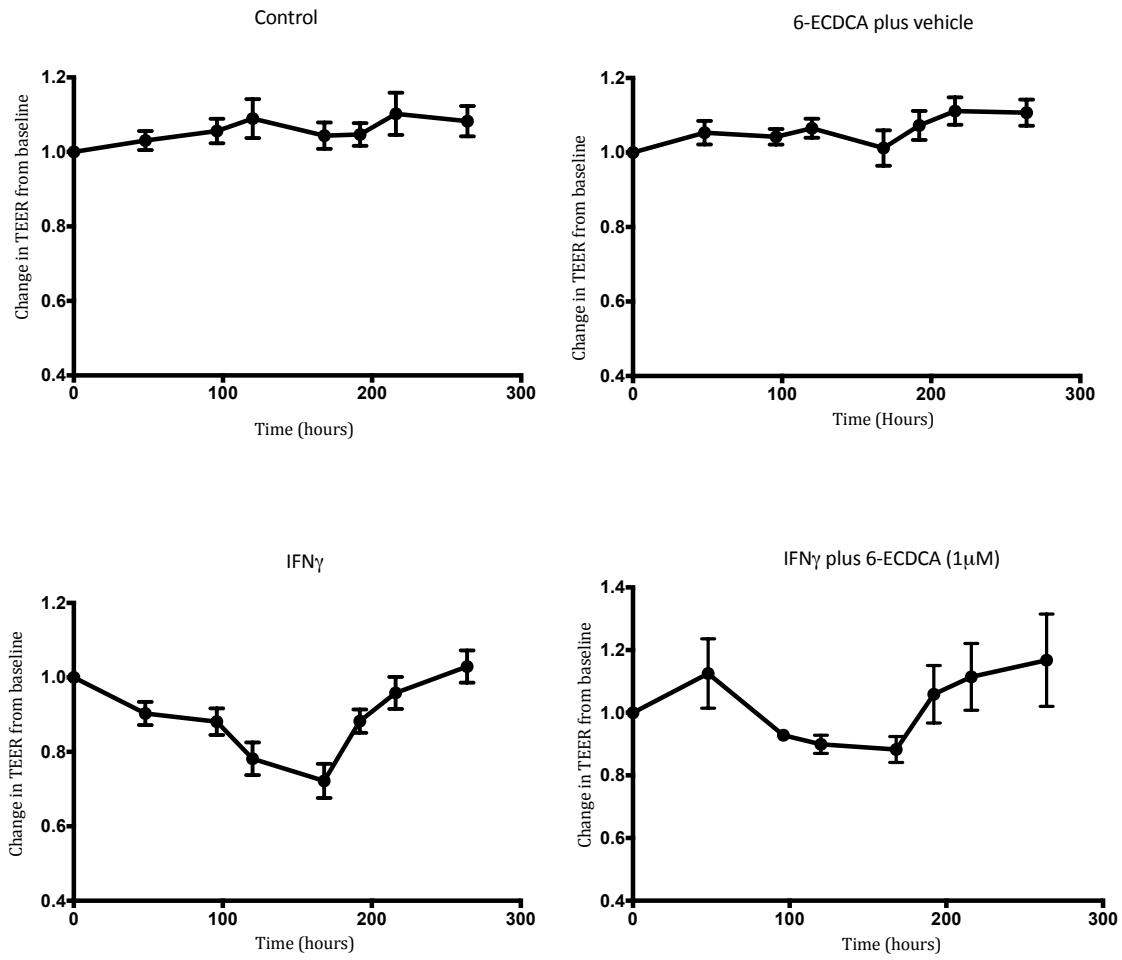

Figure 2.17; Mean TEER for polarised Caco-2 monolayers treated with IFNγ (100ng/ml) +/- 6-ECDCA (1μM), or control (n=4, SEM). There is a significant reduction in TEER from control for IFNγ exposed monolayers (Two-way ANOVA p<0.001). The reduction in TEER was also significantly different in the IFNγ plus 6-ECDCA monolayers.

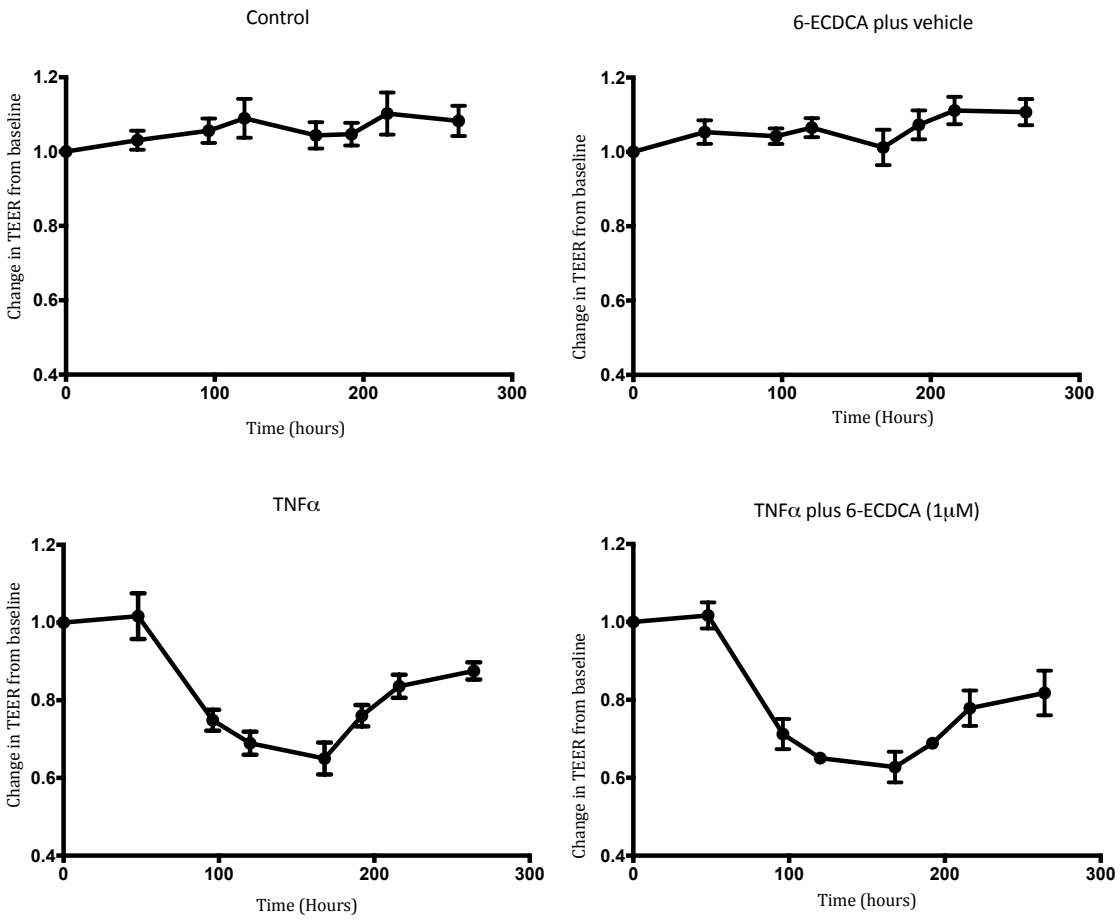

Figure 2.18; Mean TEER for polarised Caco-2 monolayers treated with TNFα (100ng/ml) +/- 6-ECDCA (1μM), or control (n=4, SEM). There is a significant reduction in TEER from control for TNFα exposed monolayers (Two-way ANOVA p<0.001). The reduction in TEER was also significantly different in the TNFα plus 6-ECDCA monolayers.

Lucifer yellow assays failed to demonstrate any significant difference in paracellular flux between vehicle (DMSO) treated, inflammatory cytokine treated or inflammatory cytokine plus 6-ECDCA (10μM) treated monolayers. Figure 2.19 demonstrates the basolateral supernatant fluorescence as a percentage of the apical supernatant fluorescence following treatment with IL-6, IFNγ or TNFα +/- 6-ECDCA. A positive control with 1% Triton-X treated monolayers was significantly different (2-tailed *t*-test, p=0.0026, 95% CI 0.61-0.95).

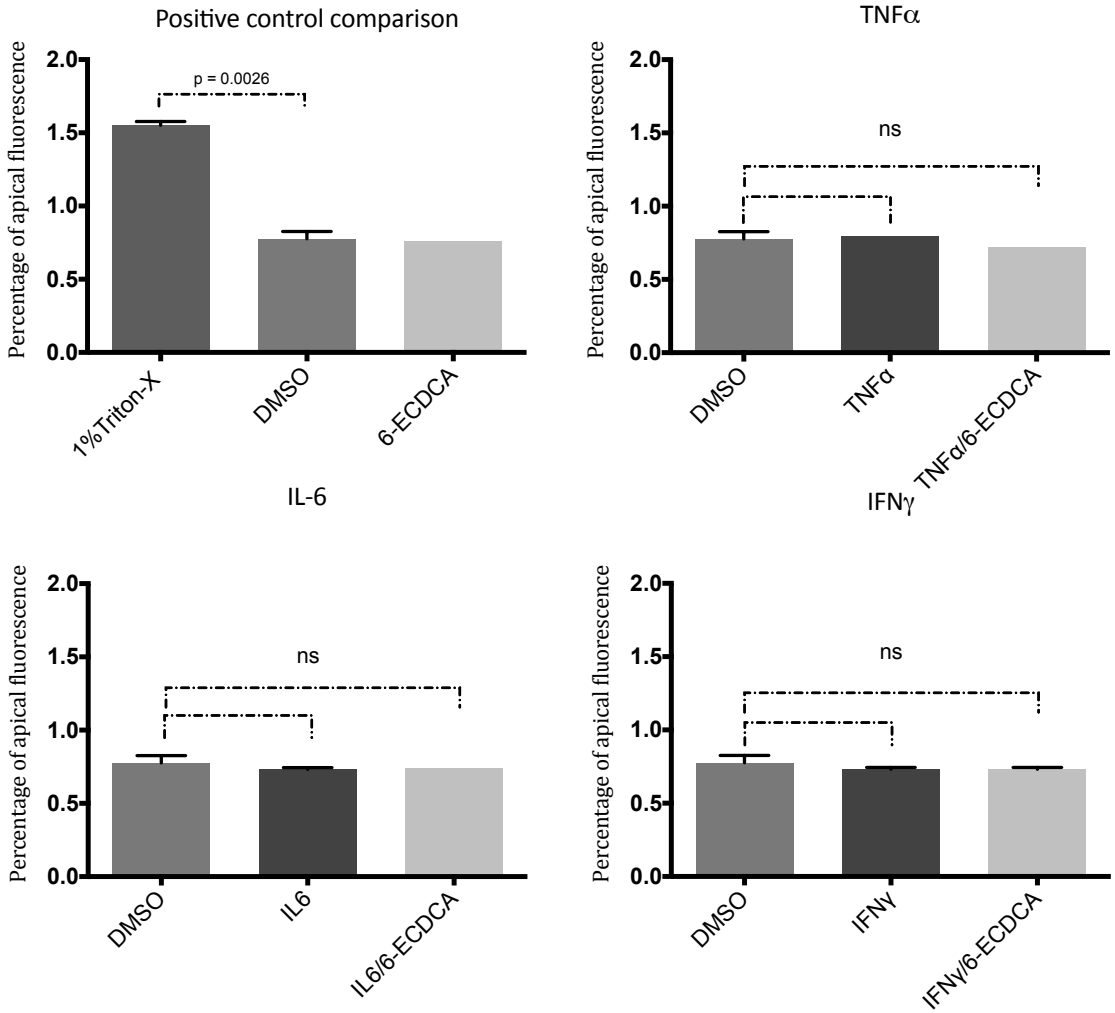

Figure 2.19; Lucifer yellow flux assay in polarised Caco-2 monolayers after exposure to TNFα, IL-6 or IFNγ +/- 6-ECDCA (10μM) or vehicle (DMSO). 1% Triton-X is included as a positive control. The flux of LY into the basolateral compartment is expressed as a percentage of the apical compartment fluorescence (n=3, SEM, t-test).

2.4.4 Activation of FXR maintains Caco-2 cell morphology

Bright-field microscopy revealed no differences in the morphology of in-situ Caco-2 monolayers when treated with cytokine with or without FXR agonist as compared to control. However, exposure did disrupt cell morphology when monolayers were examined in cross-section via electron microscopy.

Figure 2.20 (pages 85-86) shows bright-field microscopy of cells treated with vehicle (DMSO), 100ng/ml IL-6, IFNγ or TNFα, 6-ECDCA (10μM), cytokine with 6-ECDCA and 1% Triton-X as a positive control. Intact cell junctions are clearly visible. Also visible are the numerous vacuoles typical of Caco-2 cells grown in monolayers. In the 1% Triton-X treated images, the junctions between cells are obviously disrupted.

Transmission electron microscopy (TEM) of Caco-2 demonstrates a well-differentiated polarised monolayer with enterocyte-like microvilli on the apical surface (figure 2.22). Also visible are the apical TJ complex and the invaginated cell-cell junctions.

TEM reveals that cells stressed for 48 hours with IL-6 and IFNγ show morphological changes as compared with vehicle treated monolayers, with multiple infra-TJ complex fissures within the cell-cell junctions (see white arrow, figure 2.22b). Almost no morphological changes were seen (either 0 or 1 per 20 junctions measured) in monolayers stressed with TNFα.

As described in section 2.3.5, a standardised, blinded method was used to determine the number of cell-cell junction fissures per 20 sections imaged. Exposure of the monolayers to 6-ECDCA for 24 hours prior to stimulation with IL-6 or IFNγ reduced the number of morphological re-arrangements, maintaining the epithelial barrier (see fig 2.21). This was significant in the IFNγ group ($p = 0.03$

95% CI 10.23-74.77), but failed to reach significance in the IL-6 group (p = 0.08 95% CI -9.01-59.02), where only a trend was observed. There were no morphological re-arrangements in control (PBS) or 6-ECDCA only treated monolayers. The raw data are presented in table 2.3 and demonstrates the reliability of findings between the two independent, blinded researchers.

Figure 2.20 (pages 86 and 87); Bright-field microscopy (10x) of in-situ Caco-2 monolayers following treatment with A) 6-ECDCA, B) vehicle, C) IFNγ, D) IL-6, E) TNFα, F) 1% Triton-X. There are no morphological differences between control and cytokine treated monolayers. The cell-cell junctions are clearly visible (black arrows). 1% Triton-X treated monolayers, shown as a positive control, demonstrate grossly disrupted cell-cell junctions (white arrows).

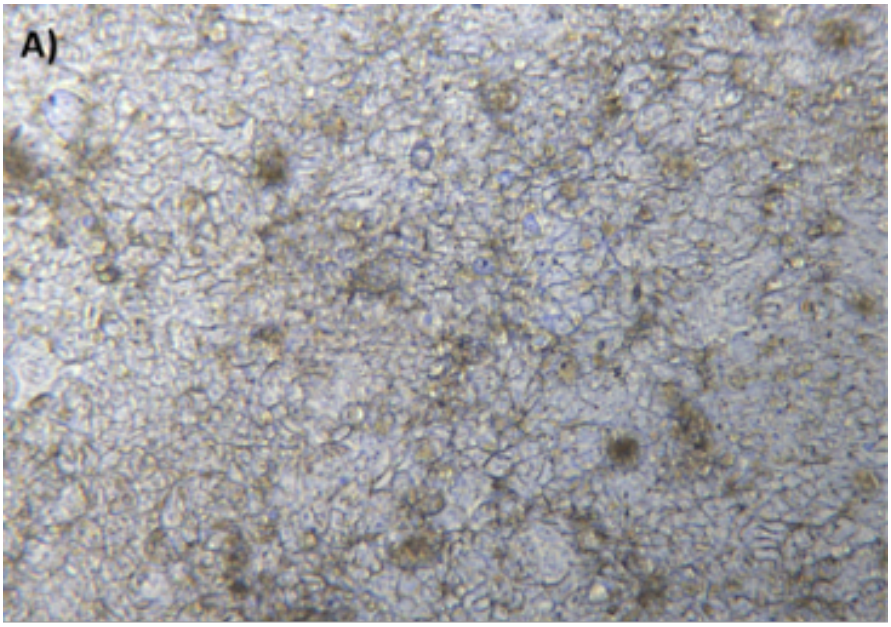
A)

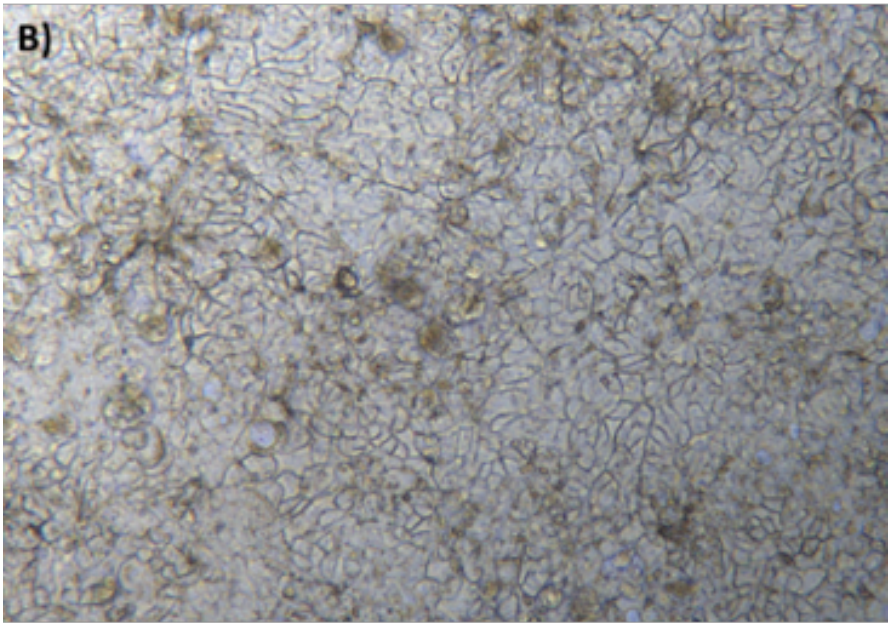
B)

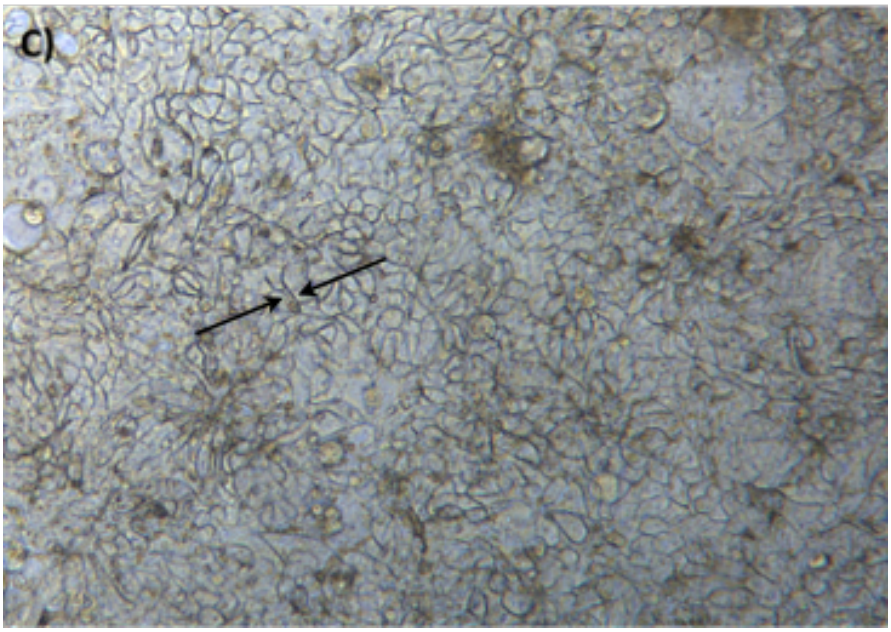
C)

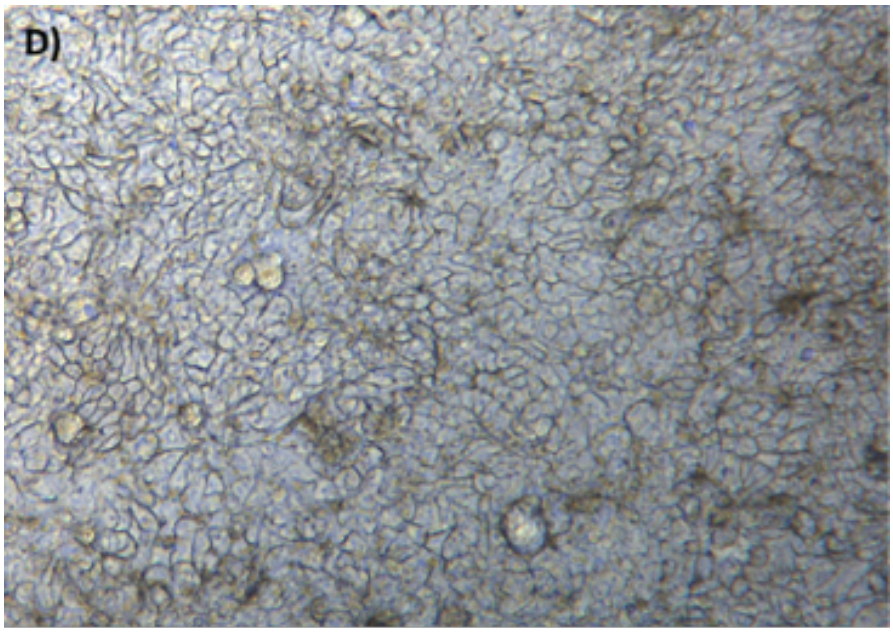
D)

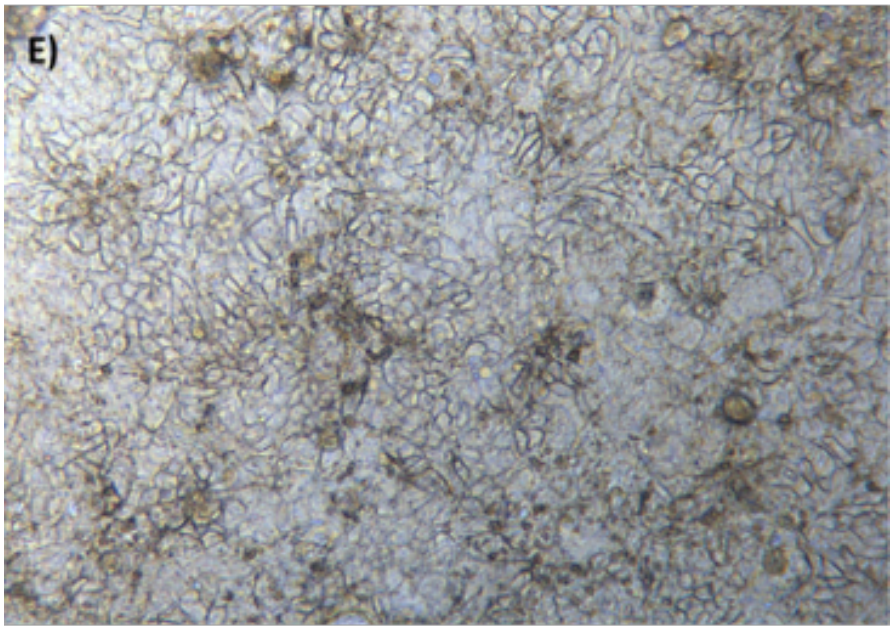
E)

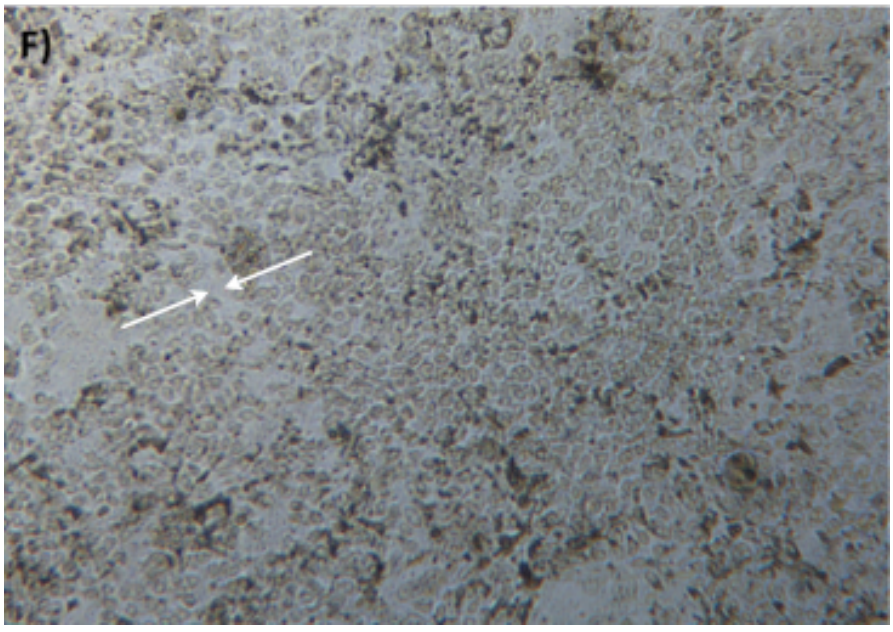
F)

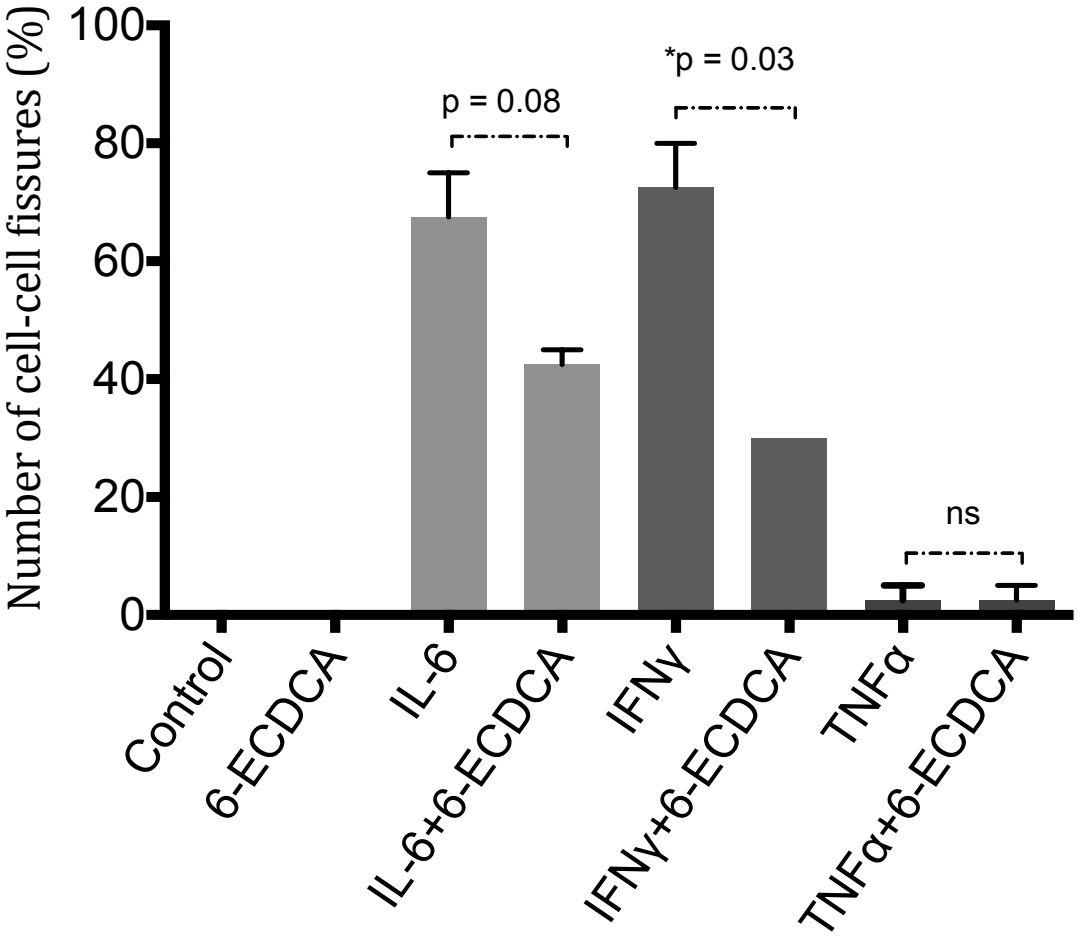

	Control	6-ECDCA	IL-6	IL6/6-ECDCA	IFNγ	IFNγ/6-ECDCA	TNFα	TNFα/6-ECDCA
Researcher 1	0	0	12	8	13	6	1	1
Researcher 2	0	0	15	9	16	6	0	0

Figure 2.21 & Table 2.3; Number (absolute or %) of cell-cell fissures seen at TEM (n=20, SEM, t-test) for Caco-2 monolayers stimulated with cytokine or vehicle +/- FXR agonist (6-ECDCA). Counted by two independent researchers, with blinding as to the intervention.

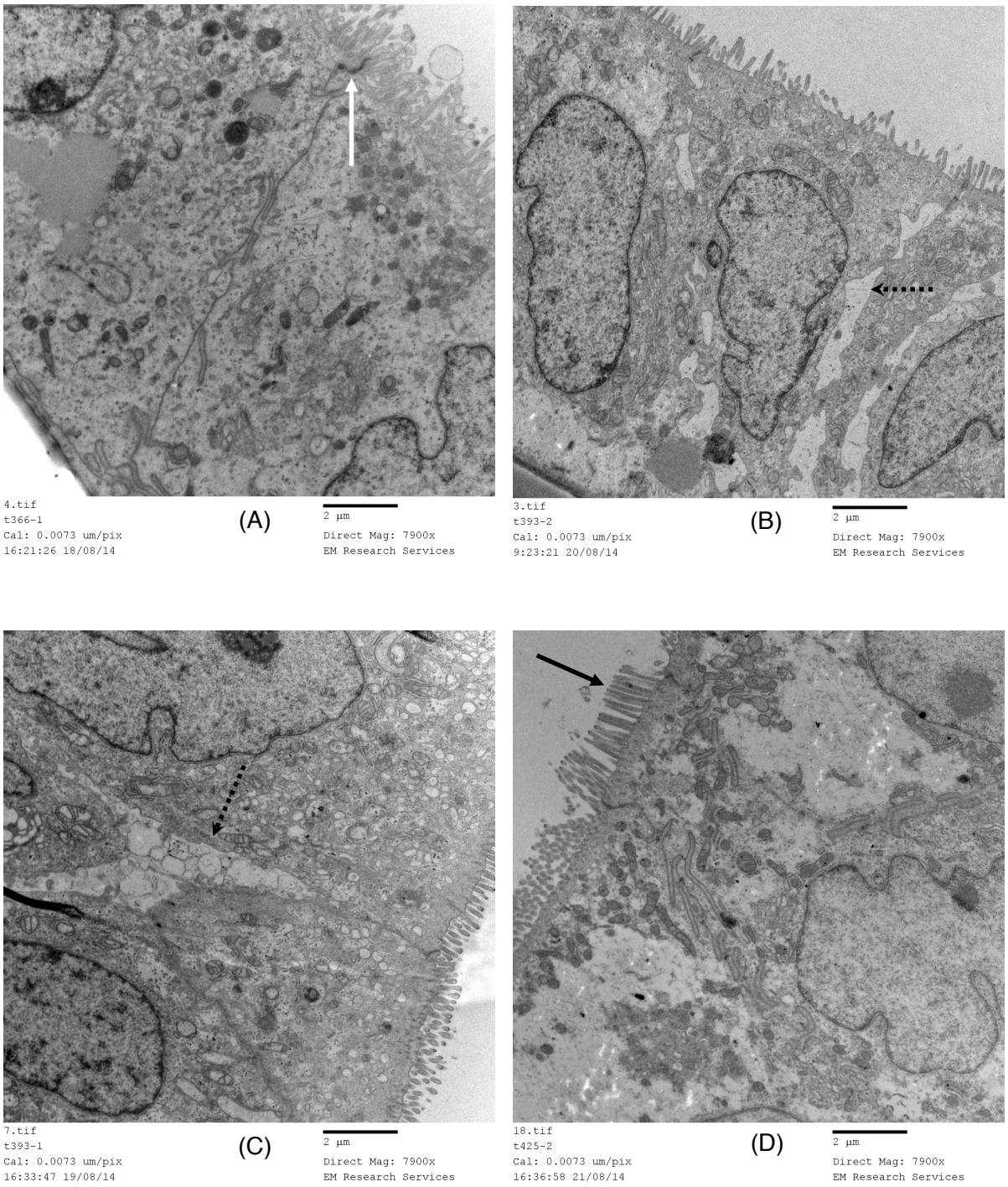

Figure 2.22; TEM images demonstrating examples of Caco-2 polarised monolayers with intervention groups (A) control, (B) IFNγ, (C) IL-6, (D) IFNγ + 6-ECDCA, (E) IL-6 + 6-ECDCA (overpage). Microvilli (black arrow), TJ complex (white arrow) and cell-cell junction fissures (dashed arrows) are highlighted. In control and FXR agonist only groups, there were no cell-cell junction fissures. Stress with IL-6 and IFNγ (B and C) produced multiple fissures. Treatment with FXR agonist (6-ECDCA) reduced the number of observed cell-cell junction fissures (D & E)

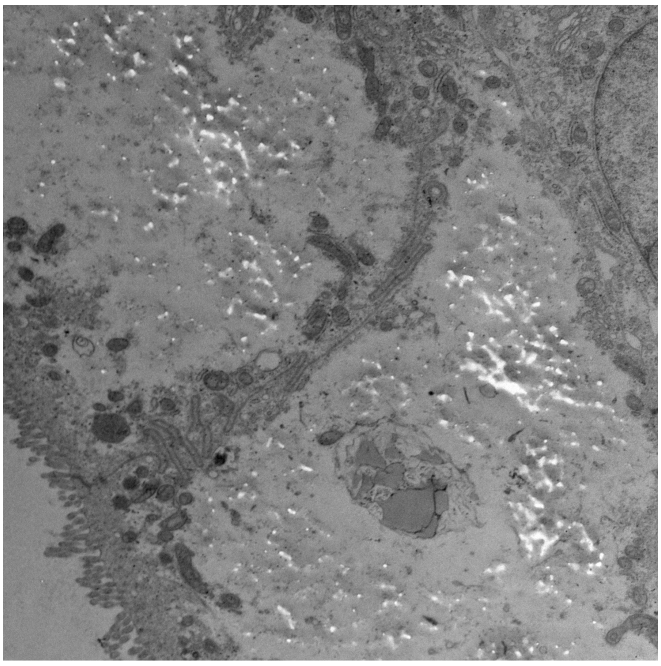

10.tif
t425-3
Cal: 0.0073 um/pix
9:38:10 22/08/14

(E)

2 µm
Direct Mag: 7900x
EM Research Services

2.4.5 Activation of FXR may inhibit cytokine induced upregulation of MLCK

In order to test whether FXR agonism maintained Caco-2 monolayer morphology via a mechanism involving cytoskeletal re-arrangement facilitated by MLCK, RT-PCR was performed for MLCK mRNA following stimulation with IL-6, IFNγ or TNFα with and without 6-ECDCA. Unfortunately, data was only collected for monolayers exposed to IL-6, due to methodological problems in extracting RNA of sufficient quantity or quality (see section 2.3.9).

When stimulated with IL-6, Caco-2 cells grown in culture as a polarised monolayer, demonstrated a marked increase in the relative gene expression of MLCK with a positive fold change of 435.4 (figure 2.23). When cells were pre-treated with 6-ECDCA for 24 hours, the IL-6 induced upregulation of MLCK was completely abolished.

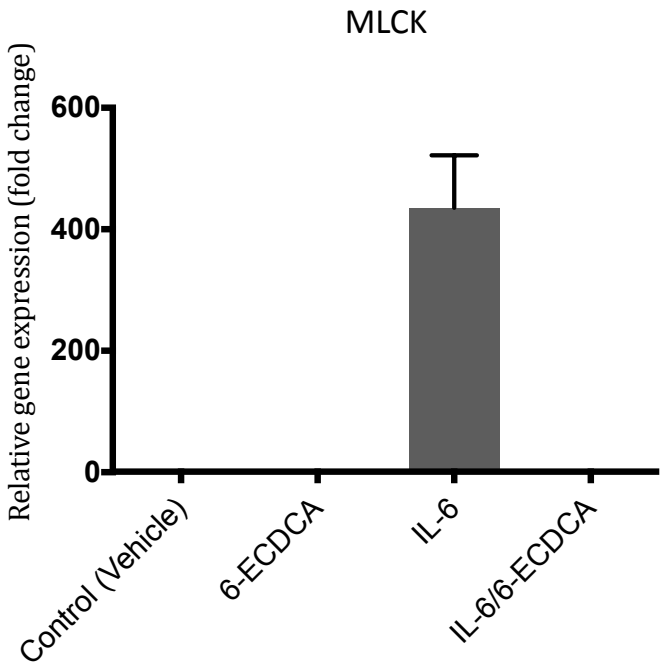

Figure 2.23; Relative gene expression for MLCK, as measured by RT-PCR, in Caco-2 cells grown as a polarised monolayer following exposure to vehicle, FXR agonist (6-ECDCA) and IL-6 +/- FXR agonist (6-ECDCA) (n=3, SEM)

2.4.6 Optimisation of HT29 as a model of IL-8 secretion

In response to stress, epithelial cells up-regulate innate immune mechanisms, including the production of the neutrophil chemo-attract cytokine IL-8. In order to model the effect FXR agonism may have on the production of IL-8 when gut epithelial cells were stressed with CD associated cytokines, several optimisation experiments were performed using different stressors and cell lines.

Like other researchers, Caco-2 cells were found to be relatively un-responsive to stimulation with IFNγ, TNFα, IL-6 or LPS, as measured by ELISA for IL-8 (results not shown).

HT29 cells were, however, found to be highly responsive to TNFα. On co-culture with TNFα, significantly more IL-8 could be detected, in comparison with control, in cell supernatant (p=0.0005 95% CI 3727-6540) (figure 2.24).

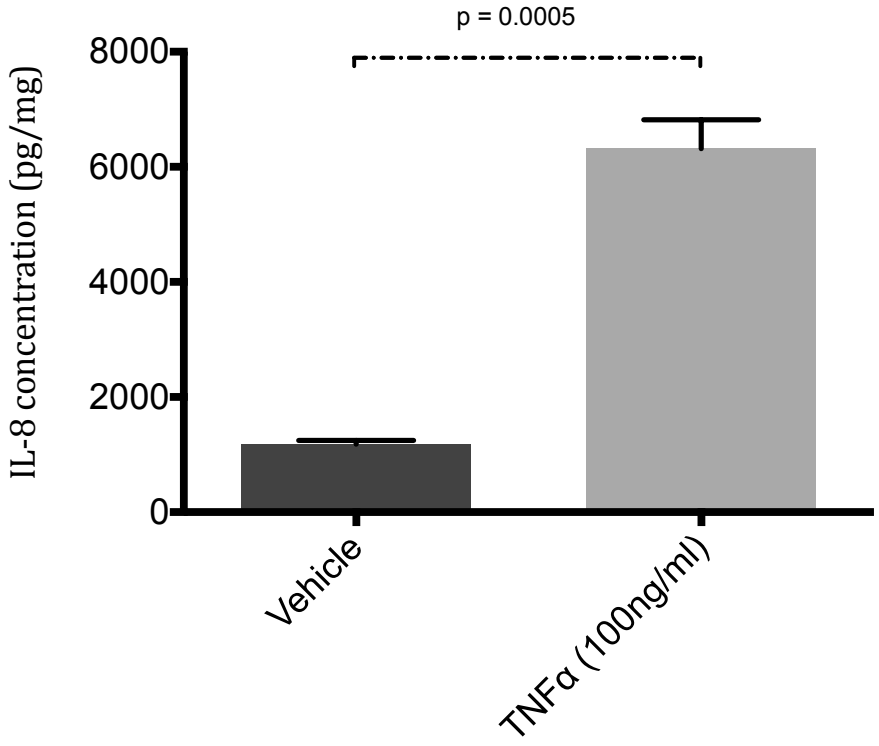

Figure 2.24; IL-8 production by HT29 cells when cultured with growth media containing 100ng/ml TNFα in comparison with control (SEM, n=3, Student's t-test).

2.4.7 FXR agonism reduces the IL-8 response induced by TNFα in HT29 cells

In order to assess the effect of FXR agonism on the production of IL-8, HT29 cells were cultured with TNFα following 24 hours of co-culture with different concentrations of GW4064 or 6-ECDCA, with or without the FXR antagonist guggulsterone. The IL-8 response was measured both at a protein level (by ELISA) and at a gene expression level (by RT-PCR).

When HT29 cells were pre-treated with high doses of GW4064 (10μM), the IL-8 response, as measured by ELISA, to TNFα was reduced to baseline (p=0.0004, 95% CI 3936-6728)(figure 2.25). However, lower doses of GW4064 (0.1μM and 1μM) had no significant effect on the concentration of IL-8.

Guggulsterone was able to reverse the attenuating effect of GW4064 (10μM), with significantly more TNFα-induced IL-8 detected (p = 0.0005, 95% CI 2423-4174)(figure 2.25). Treatment with GW4064 alone had no effect on the baseline IL-8 concentration.

Measurement of IL-8 gene expression confirmed the findings measured at a protein level. As measured by RT-PCR, the higher dose of GW4064 reduces to baseline the up-regulation of IL-8 mRNA associated with TNFα stimulation (figure 2.25).

There is an inverse dose-response relationship between the co-treatment concentration of GW4064 and the TNFα-induced expression of IL-8. Again, co-treatment with guggulsterone reverses the attenuating effect of GW4064 (10μM), this time measured at an mRNA copy level.

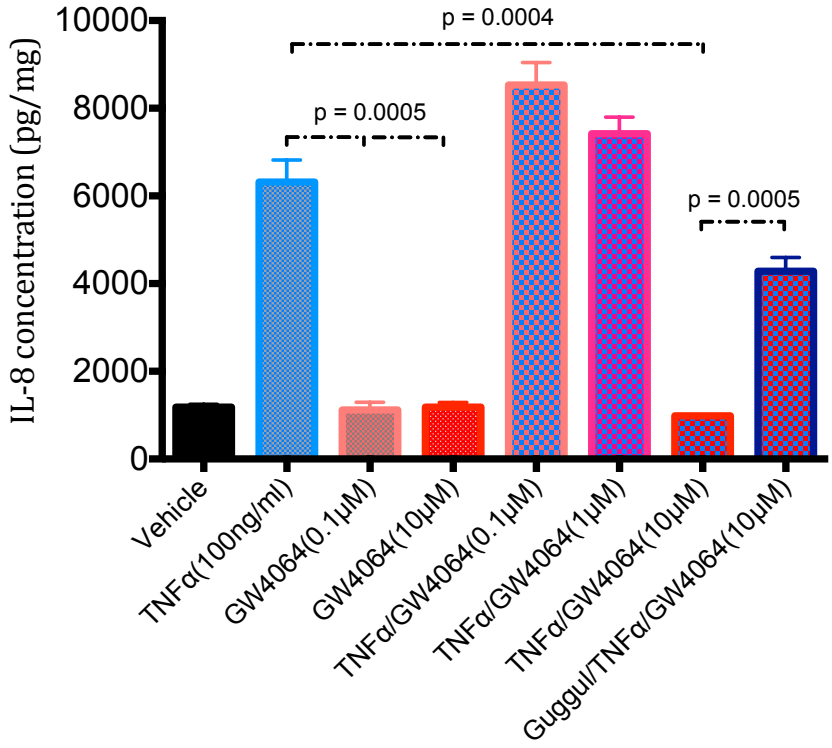

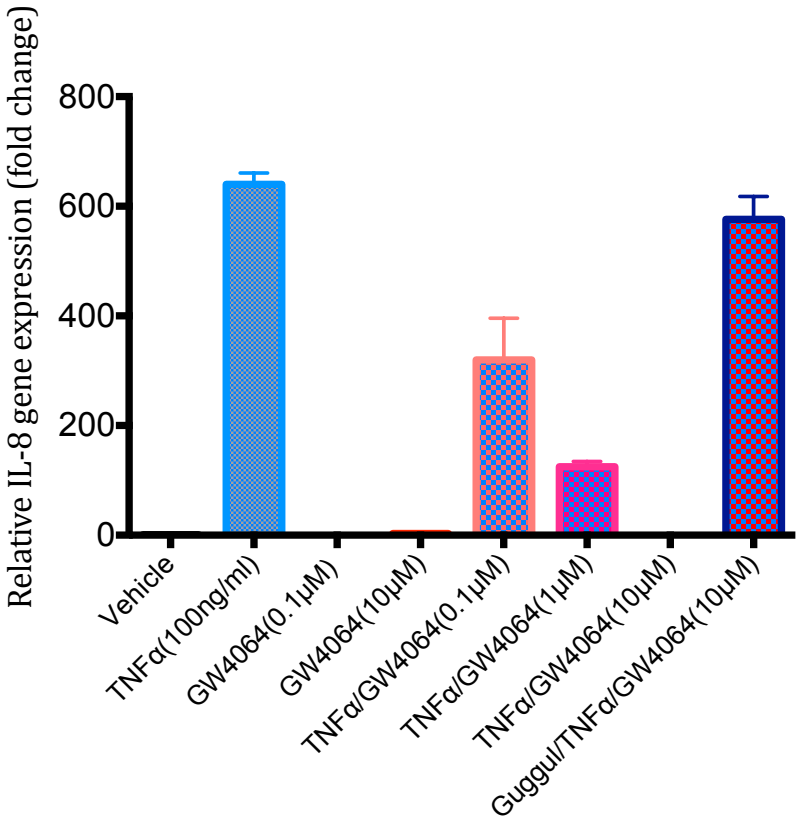

Figure 2.25; Graphs to demonstrate the concentration (ELISA) and gene expression (RT-PCR) of IL-8 in HT29 cultured with TNFα and/or GW4064. 'Guggul' is the FXR antagonist guggulsterone. (n=3, SEM, t-tests)

Under the same experimental conditions, a different dose-response relationship was observed between the concentration of 6-ECDCA and IL-8 production, as compared with GW4064 (see figure 2.26).

The lowest concentration of 6-ECDCA (0.1μM) used in this assay, was observed to reduce the TNFα induced IL-8 production to the baseline level. This observation was replicated at an mRNA level. This in comparison to GW4064 in which the highest dose (10μM) had this effect.

The highest dose of 6-ECDCA (10μM) induced the paradoxical effect of increasing the amount of IL-8 secreted on stressing cells with TNFα. 6-ECDCA (10μM) alone had no effect on the production of IL-8. This apparently synergistic effect was observed at an mRNA level and was a consistent finding when the experiment was replicated on three separate occasions. Antagonising 6-ECDCA 10μM with guggulsterone reduced the concentration of IL-8 to the level seen when cells were stimulated with TNFα alone.

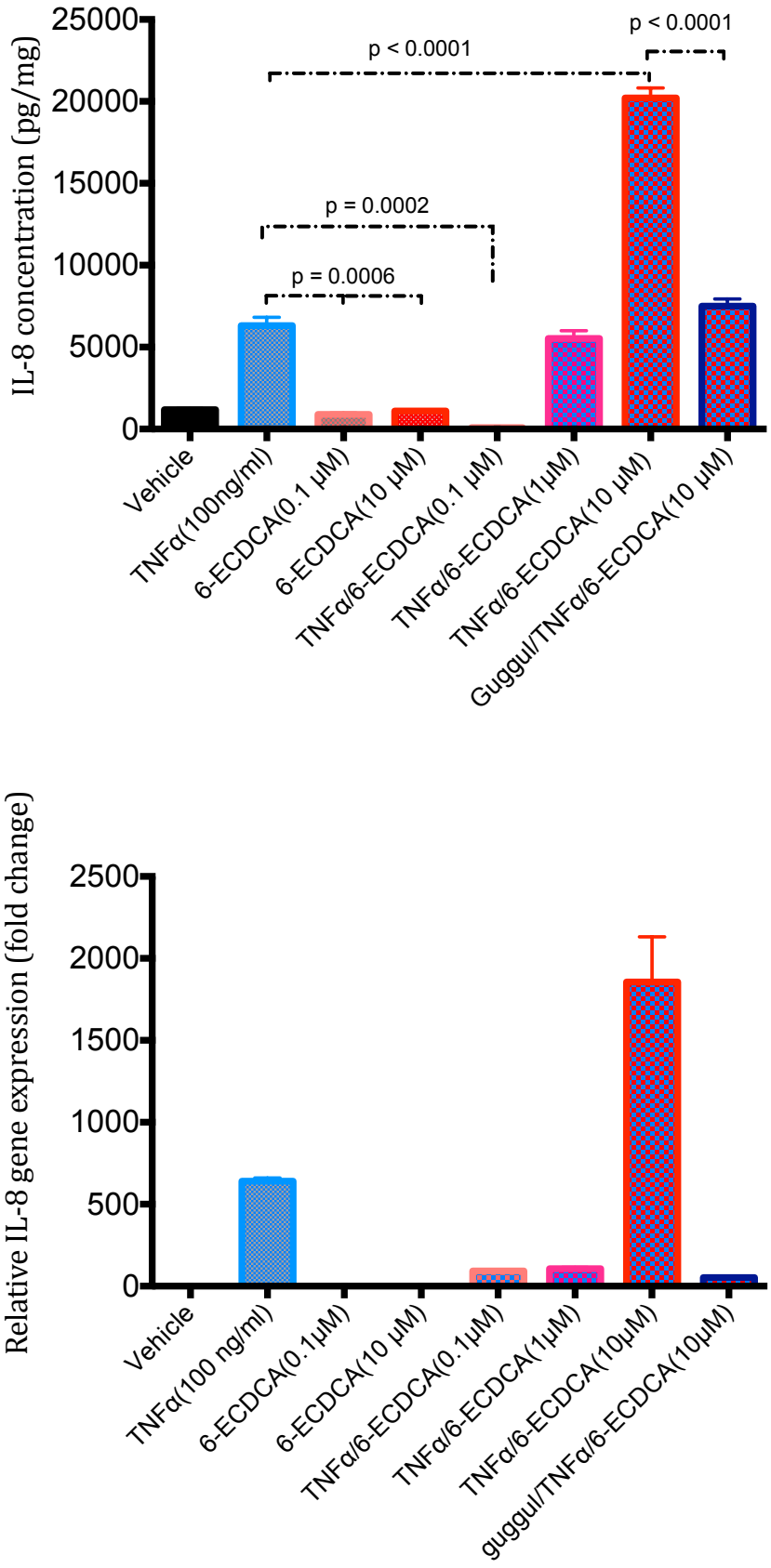

Figure 2.26; Graphs to demonstrate the concentration and gene expression of IL-8 in HT29 cultured with TNFα and/or 6-ECDCA. 'Guggul' is the FXR antagonist guggulsterone. (n=3, SEM, t-tests)

2.5 Discussion

Gut epithelial barrier dysfunction is a crucial factor in the aetiopathogenesis of CD(Zeissig et al., 2007, Su et al., 2009, Hedin et al., 2012). A dysfunctional barrier allows microorganisms to translocate from the lumen into the mucosa, driving an inflammatory response(Soderholm et al., 2004, McGuckin et al., 2009). These experiments, in human, gut-derived epithelial cell lines, provide evidence that FXR agonism can maintain the epithelial barrier when exposed to CD associated inflammatory cytokines by i) inhibiting disruption of cell morphology and ii) attenuating the innate immune response of IL-8 production.

A reproducible model of inflammatory cytokine induced epithelial barrier dysfunction was optimised in Caco-2 cells grown as a polarised monolayer. This technique was new to our group and is now being used in other areas of research within the laboratory.

Evidence from RT-PCR experiments demonstrates that both 6-ECDCA and GW4064 act as FXR agonists, as shown by significant upregulation of downstream SHP and IBABP target gene expression, in two different epithelial cell lines. Differences were seen in FXR agonism between the two, different compounds, but also between different cell lines. In Caco-2 cells, 6-ECDCA induced a greater fold change in downstream genes than GW4064, with its greatest effect seen when measured at 24 hours, compared with 48 hours. The assay was performed at these time points to allow FXR activation, translocation of the receptor to the nucleus with subsequent RNA transcription and processing of downstream targets. It is of course, possible that downstream activation occurs before 24 hours, with preliminary results from another group in the laboratory suggesting, in particular, that SHP levels increase much sooner after FXR agonism than 24 hours.

These results confirmed the findings of previous studies in demonstrating that FXR activation induces its own expression in Caco-2 cells(Gadaleta et al., 2011b). However, the positive auto-regulation of FXR was not present in HT29 cells, in which a fold reduction in FXR mRNA was observed for both FXR agonist compounds across a 100 fold dose range. Caco-2 and HT29 are of course phenotypically different cell types with different origins. HT29 are thought to be a more crypt-derived epithelial cell, with Caco-2 a more mature, villous like epithelial cell. It may be that FXR auto-regulation in different epithelial cell types is contradictory in-vivo, but this would need further investigation to determine. One could hypothesise that such a mechanism could be related to the increased BA uptake higher in the epithelial villous rather than the crypt. An alternative explanation would be that, in HT29 cells, IBABP and SHP are under the control of another nuclear receptor, agonised off target by the FXR agonist compounds.

The null hypothesis, that FXR agonism could not maintain the epithelial barrier when stressed by IFNγ, TNFα or IL-6, was proved when measured by epithelial electrical resistance. A functional assay using the paracellular flux of a cell impermeable molecule failed as a model as no difference between control and cytokine induced epithelial dysfunction could be demonstrated.

However, FXR agonism did maintain epithelial morphology when cells were stressed with the inflammatory cytokines IL-6 and IFNγ, as measured by TEM. Cytokine induced cytoskeletal re-arrangement occurs due to contractions in the actin-myosin ring, regulated by the phosphorylation of myosin II regulatory light chain (MLC) by MLCK(Cunningham and Turner, 2012). I hypothesised that FXR agonism may maintain cell morphology by inhibiting MLCK at a transcriptional level. Unfortunately, only data for Caco-2 co-cultured with IL-6 were produced

due to problems with RNA extraction. However, these preliminary results show that IL-6 induced MLCK transcription is reduced by FXR activity. Recently, IL-6 has been shown to increase phosphorylated-MLC(Zahs et al., 2013). By inhibiting the transcription of MLCK, FXR may act to maintain the epithelial barrier by preventing cytokine induced cytoskeletal re-arrangement of the actin-myosin ring.

Published literature suggests that TNFα should also induce changes in the cytoskeleton(Cunningham and Turner, 2012), but this finding was not observed in this study. It may be that TNFα induced morphological change may occur sooner and resolve prior to the 48-hour time point used in these experiments.

It is interesting to note that FXR agonism had no effect on the loss of TEER induced by inflammatory cytokine, but did maintain epithelial morphology. This suggests that the cellular mechanism by which TEER is reduced is not wholly related to cytoskeletal re-arrangement. Presumably other factors, such as changes in claudin protein expression at the TJ complex, are responsible for the increase in ion flux seen after epithelia are stressed with cytokine. If FXR agonism maintains epithelial barrier homeostasis in-vivo, this is likely to be due to a process that involves cell morphology rather than via a process that only maintains the TJ itself. In addition, other processes, such as the effect on IL-8 production may be important in maintaining epithelial homeostasis.

These experiments, both at a transcriptional and protein level, were able to show that FXR agonism decreased the IL-8 response of HT29 cells to TNFα. Gut epithelial IL-8 production is an important innate immune mechanism. As a potent pro-inflammatory cytokine, IL-8 acts as a chemo-attractant for circulating neutrophils(Eckmann et al., 1993). This data set is in keeping with other studies in demonstrating an immuno-modulatory role for FXR(Vavassori et al., 2009,

Haselow et al., 2013). Demonstrating an attenuated IL-8 response to TNFα at both a transcript and protein level adds strength to the evidence that FXR has an immuno-modulating effect in gut epithelial cells. This is a potential mechanism by which FXR may act to maintain epithelial homeostasis. HT29 cells were used in these experiments as they demonstrate a more responsive secretory phenotype than Caco-2.

Again, differences in biological effect were observed between the two FXR agonists, this time with respect to the attenuation of TNFα induced IL-8 production. A more efficacious attenuating effect was observed for GW4064 at 10μM with lower doses being less effective. The opposite, however, was true for 6-ECDCA with the 0.1μM demonstrating complete attenuation of the IL-8 stress response. In fact, at high dose (10μM), 6-ECDCA with TNFα appeared to produce a synergistic response, with more IL-8 produced than with TNFα stimulation alone. This unusual finding was reproduced at a transcriptional level and was a consistent finding in three consecutive experiments. Therefore, I suspect that this finding is robust and does not reflect methodological error. It is possible that high doses of 6-ECDCA have an off target effect that would produce such a result or are directly toxic to the cell at high concentrations. It may be that, under these experimental conditions, a much lower dose range (e.g. from 0.01μM to 1μM) of the 6-ECDCA compound should have been assayed. The EC_{50} for 6-ECDCA is approximately 0.1μM. The dose range 0.1μM to 10μM was chosen as the higher dose of 6-ECDCA had produced the greatest increase in fold change for SHP and IBABP in HT29 cells in earlier experiments (figure 2.15).

There are several potential weaknesses with the data in this chapter. Only a model of inflammatory cytokine induced epithelial barrier dysfunction has been studied.

It is widely accepted that cytokines cause barrier dysfunction and that this in turn leads to the chronic inflammation of CD. However, the initial pathological process that leads to the development of CD is unknown and may not necessarily be inflammatory cytokine driven. For example, predisposing genetic factors (e.g. in autophagy) and the microbiota (e.g. AIEC and claudin 2 expression) may be more important in disease initiation or re-initiation in post-operative recurrence. It would be interesting to investigate the role of FXR in these circumstances. For instance, there is a putative mechanism by which FXR may promote autophagy pathways (via p62/sequestosome 1) and NOD2. This may form the basis of further research.

The finding that FXR agonism can ameliorate IL-6 induced upregulation of MLCK expression is of interest as it provides a potential molecular mechanism by which FXR may act to maintain the epithelial barrier. However, it is important to reproducibly prove this finding for other cytokines. The quality of RNA extracted from Caco-2 cells, grown as a polarised monolayer, was an ongoing problem. As discussed in the methods section, several different techniques to optimise RNA extraction were tried and I managed, towards the end of my laboratory time, to produce reliable results for IL-6 treated cells. Further work should collect the data for IFNγ and TNFα stimulated cells, perhaps at an earlier time point.

Some scientists have questioned the validity of the use of GAPDH as a reliably stable reference gene in RT-PCR experiments(de Jonge et al., 2007). If necessary, future studies could replicate this work using an alternative reference gene, such as ribosomal protein S13.

Finally, these are cell line studies and, therefore, provide only an estimate of the process of FXR activation *in-vivo*. The experiments are, by design, reductionist,

assaying only the function of these genetically abnormal epithelial cells, distinct from any interaction with the multiple other cell types in the gut mucosa. The next two chapters provide data from more complex models with experiments in mice and from primary human tissue.

In summary, however, these cell line models suggest that BA signalling via FXR acts to maintain the epithelial barrier by attenuating IL-8 production in response to cell stress and by maintaining epithelial cell morphology.

Chapter 3 – The Effect of FXR Agonism on Ileal Inflammation in a Mouse Model of Metabolic Syndrome

3.1 Abstract

Evidence from epidemiological and case-control studies implicate the western diet in the pathogenesis of Crohn's disease (CD). The pathological mechanism for this association is unknown. High-fat/high-sugar (HF/HS) feeding of mice induces a dysbiosis comparable to that seen in inflammatory bowel disease (IBD). The bile acid (BA) receptor, farnesoid X receptor (FXR), is central to the cross talk between the host and its microbiota. FXR has been shown to have an immuno-modulatory role in the GI tract.

The hypothesis was that disruption to BA signalling, induced by a HF/HS diet associated dysbiosis, is a potential mechanism linking dietary risk to the development of CD. The aims of this chapter were to investigate the effect of HF/HS feeding and FXR agonism on ileal inflammation in a mouse model of obesity.

Evidence is presented demonstrating that animals fed a western-like diet express more ileal inflammatory cytokine. There is a trend to suggest that supplementation of a western-lifestyle diet with an FXR agonist reduces diet-induced inflammatory cytokine expression in the mouse ileum.

3.2 Introduction and aims

A high fat, high sugar (HF/HS) content diet is associated with CD pathogenesis in several case-control studies(Hou et al., 2011). Epidemiological data demonstrates an increased risk of developing CD for populations exposed to a western lifestyle, which is in turn associated with a HF/HS diet(Probert et al., 1992).

The so-called metabolic syndrome of obesity, diabetes mellitus type II, essential hypertension, dyslipidaemia and non-alcoholic steato-hepatitis (NASH) is also associated with a HF/HS diet(Bhatia et al., 2012). Obesity is a low grade, chronic inflammatory condition in which macrophages and adipocytes are activated, producing inflammatory cytokines such as TNFα, IL-1 and IL-6(Wellen and Hotamisligil, 2005, Cani et al., 2007). High fat feeding of mice produces an endotoxaemia associated with an increase in epithelial permeability(Cani et al., 2007, Cani et al., 2008). Increased epithelial permeability is a central tenet in the pathogenesis of IBD(McGuckin et al., 2009). In patients with CD, an accumulation of peri-enteric fat, known as 'creeping fat', is often observed around areas of inflammed tissue. Creeping fat is metabolically active and produces inflammatory cytokines such as TNFα and IL-6(Martinez-Medina et al., 2014).

The American Lifestyle-Induced Obesity Syndrome (ALIOS) animal model was developed to study the development of NASH in mice(Tetri et al., 2008). The ALIOS model resembles a typical 'fast-food' diet, being rich in trans-fats and high fructose corn syrup, in association with reduced energy expenditure. This model has been shown to closely resemble the metabolic syndrome, with genetically normal mice developing obesity, fatty liver disease, hyperinsulinaemia and hypercholesterolaemia(Tetri et al., 2008, Dowman et al., 2014).

Experiments in this chapter were intended to explore the potential association between dietary risk factors, BA dysmetabolism and ileal inflammation. The

hypothesis was that mice fed an ALIOS diet would develop evidence of ileal inflammation and, furthermore, that supplementation of feed with an FXR agonist would attenuate any observed diet-induced inflammation.

The main aims of the experiments in this chapter were, therefore, to:

1. Demonstrate ileal inflammation in a mouse model of diet-induced obesity;
2. To assess the ability of Px-102 to act as an FXR agonist and upregulate downstream gene expression, and;
3. To assay the effect of FXR agonism on any observed ileal inflammation induced by HF/HS feeding, by measuring cytokine gene expression.

3.3 Methods

3.3.1 Animal care

Animal husbandry was performed by members of Dr H Reeves' research group under licence from the Home Office, in keeping with the requirements of the Animals (Scientific Procedures) Act 1986 (ASPA). All animal care, including animal sacrifice, was performed in the Comparative Biology Centre (CBC), Newcastle University by members of Dr Reeves' team or by university staff in the CBC. The CBC ensures that animals are housed and cared for appropriately and that research is performed in such a way to minimise any adverse effects on the animals.

After being culled, the whole GI tract from each mouse was gifted to our group in order to perform the experiments described in this chapter. The author assisted in the dissection of the GI tract and was responsible for subsequent handling of this tissue. The author was not responsible for animal care, animal handling or Schedule 1 killing.

3.3.2 Mouse strain – C3H/He

The mice used in this study were the genetically inbred mouse strain C3H/He, purchased from Harlan Laboratories, Wisconsin. The C3H/He is a widely used laboratory mouse strain which has previously been studied in models of IBD(Bilger et al., 2004, Difedele et al., 2005). Importantly, with regards to this study, unlike other C3H strains, C3H/He mice express a normal TLR4 (LPS sensing) receptor complex(The Jackson Laboratory, 2015). In a model of diet induced obesity it is expected that there will be an associated change in the microbiota and, therefore, the expression of normal bacterial sensing molecules is important when assessing gut inflammatory responses.

C3H/He mice are often used to study carcinogenesis in the liver and the mammary gland. In tangent with these experiments, Dr Helen Reeves' team (NICR, Newcastle University) was studying the role of FXR agonism in the inhibition of the formation of hepatocellular carcinoma (HCC). C3H/He spontaneously develop HCC, with 30-50% of mice affected by 2 years of age(Bilger et al., 2004).

3.3.3 Study design

Animals were maintained in the CBC, Newcastle University, in a temperature and humidity controlled environment. A standard, 12 hours diurnal light cycle was applied. In contrast to the Tetri et al description of the ALIOS model, unmodified, standard cages were used. The animals were checked daily and weighed weekly.

Mice were fed either standard (control) chow or ALIOS feed from arrival at age 6 to 8 weeks. Feed and drinking water was provided ad-libitum with feeds supplied by Harlan Laboratories (tables 3.1 and 3.2). The control mice were fed a diet containing normal levels of fat (6.2% by weight) and no trans-fats (TD.110196 6% Soybean Oil Diet, see table 3.1 for full detail). The ALIOS mice were fed a diet enriched with fat (23.2% by weight) and trans-fat in the form of hydrogenated vegetable oil (6.6% by weight; TD.110201 22% HVO Diet (VI), see table 3.2 for full detail).

Mice in the control arm were given normal drinking water. ALIOS animals were given drinking water equivalent to high fructose corn syrup (55% fructose, 45% glucose by weight) at a concentration of 42 g/l.

At 24 weeks of age, intervention groups had their diet supplemented with the non-steroidal, small molecule FXR agonist, Px-102 (Phenex Pharmaceuticals AG, Germany) at a concentration of 1mg/kg or 5mg/kg of feed. Mice were maintained

on the control or ALIOS diets, with or without the FXR agonist, up to 42 weeks of age.

Following ASPA Schedule 1 killing at 42 weeks, mice were weighed and then a midline laparotomy incision was made. The GI tract was sectioned at the distal oesophagus and the rectum and the whole GI tract was removed en-bloc and stored in a 50ml Falcon tube at -80°C for later RNA extraction. The visceral adipose tissue was also section and weighed. The GI tract from 44 mice was obtained. Figure 3.1 gives an overview of the study design and the numbers of animal in each group.

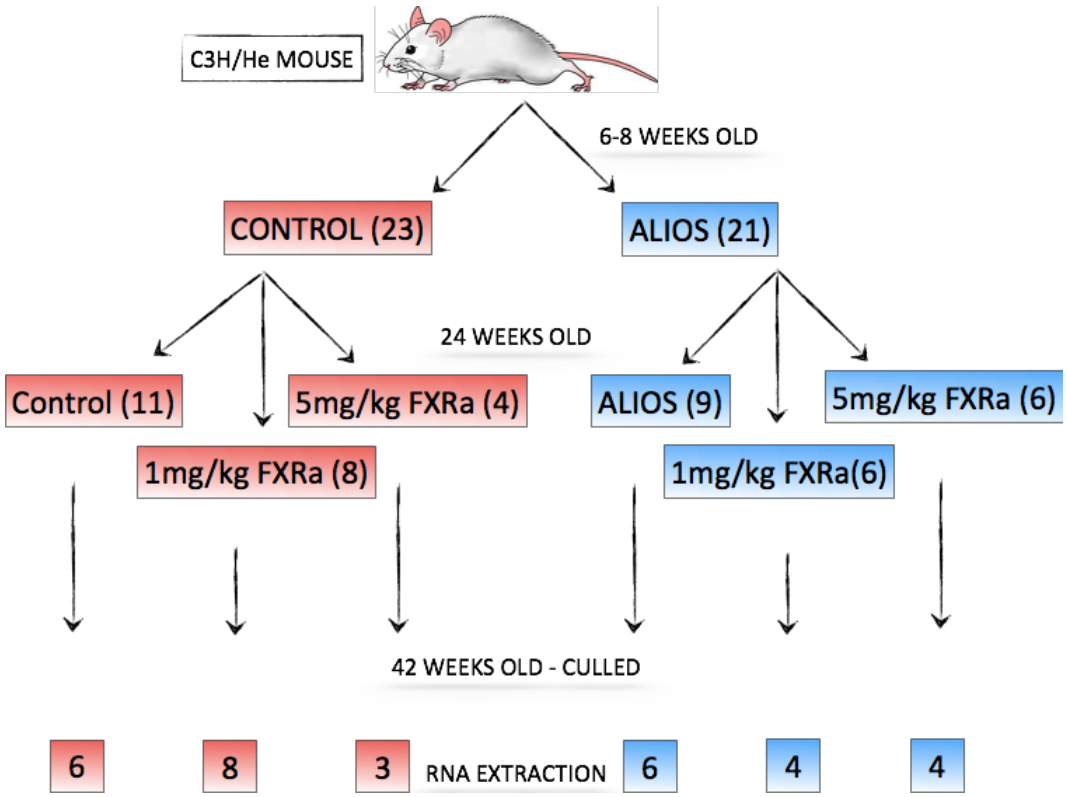

Figure 3.1; Schematic to represent study design for mouse feeding regimen. C3H/He mice were fed ALIOS diet or a control diet from 6 to 8 weeks of age. At 24 weeks, feed was either supplemented with a Px-102 (FXR agonist - FXRa), at a dose of 1mg/kg or 5mg/kg of feed, or was continued without the addition of the FXR agonist. At 42 weeks, mice were culled as per ASPA Schedule 1 guidance. Mouse total body weight and visceral adipose tissue weight was measured. The GI tract was dissected and RNA was extracted from the ileum as described in the text. Sufficient quality RNA was extracted in only 31 of the 44 mice, with the distribution as demonstrated.

Formula	g/Kg
Casein	183.0
DL-Methionine	2.7
Sucrose, fine ground	100.0
Corn Starch	431.2751
Maltodextrin	130.0
Soybean Oil	60.0
Cellulose	50.0
Mineral Mix, AIN-93G-MX (94046)	36.8
Calcium Phosphate, dibasic	2.72
Niacin	0.051
Calcium Pantothenate	0.027
Pyridoxine HCl	0.012
Thiamin HCl	0.0105
Riboflavin	0.0105
Folic Acid	0.0033
Biotin	0.0003
Vitamin B_{12} (0.1% in mannitol)	0.042
Vitamin E, DL-alpha tocopheryl acetate (500 IU/g)	0.15
Vitamin A Palmitate (500,000 IU/g)	0.0135
Vitamin D_3, cholecalciferol (500,000 IU/g)	0.0033
Vitamin K_1, phylloquinone	0.0015
Choline Bitartrate	3.17
TBHQ, antioxidant	0.01

Footnote

A control for TD.110201 without trans fat and with reduced sucrose. Protein, minerals and vitamins are adjusted so that they are equivalent to levels in TD.110201 when compared on the basis of kcal density. The exception is vitamin E which is kept the same in both diets (because it was intentionally reduced in TD.06303, which these diets are based on).

Selected Nutrient Information[1]	% by weight	% kcal from
Protein	16.2	17.6
Carbohydrate	62.0	67.3
Fat	6.2	15.1
Kcal/g 3.7		

[1] Values are calculated from ingredient analysis or manufacturer data

Table 3.1; Control diet constituents (from Harlan Laboratories product literature)

Formula	g/Kg
Casein	230.0
DL-Methionine	3.4
Sucrose, fine ground	212.9277
Corn Starch	80.0
Maltodextrin	140.0
Vegetable Shortening, hydrogenated (Primex)	220.0
Soybean Oil	10.0
Cellulose	50.0
Mineral Mix, AIN-93G-MX (94046)	46.0
Calcium Phosphate, dibasic	3.3
Niacin	0.063
Calcium Pantothenate	0.0336
Pyridoxine HCl	0.0147
Thiamin HCl	0.0126
Riboflavin	0.0126
Folic Acid	0.0042
Biotin	0.0005
Vitamin B_{12} (0.1% in mannitol)	0.0525
Vitamin E, DL-alpha tocopheryl acetate (500 IU/g)	0.15
Vitamin A Palmitate (500,000 IU/g)	0.0168
Vitamin D_3, cholecalciferol (500,000 IU/g)	0.0042
Vitamin K_1, phylloquinone	0.0016
Choline Bitartrate	3.96
TBHQ, antioxidant	0.046

Footnote

Modification of TD.06303 with vitamins increased for irradiation. Hydrogenated vegetable oil (HVO) is about 30% trans-fat, giving this diet approximately 6.6% trans-fat by weight.

Selected Nutrient Information[1]	% by weight	% kcal from
Protein	20.4	17.7
Carbohydrate	42.8	37.1
Fat	23.2	45.2
Kcal/g 4.6		

[1] Values are calculated from ingredient analysis or manufacturer data

Table 3.2; ALIOS diet constituents (from Harlan Laboratories product literature)

3.3.4 Ileal preparation

The whole GI tract from distal oesophagus to rectum was stored at -80°C prior to ileal preparation. There was concern that thawing of samples to room temperature would degrade ileal RNA. Therefore, samples were thawed to -20°C for 16 hours in 6ml of RNA*later*-ICE Frozen Tissue Transition Solution (Ambion, Life Technologies), in a 50ml Falcon tube, prior to dissection. Care was taken to ensure that the tissue was fully submerged in an adequate volume of transition solution. The transition solution allows dissection and tissue homogenisation as the tissue becomes pliable and RNA stabilised at -20°C. After transitioning the tissue for 16 hours, the manufacturers claim that the tissue RNA will then be stable for up to 30 minutes at room temperature(Life Technologies Product Literature, 2014).

Following overnight storage in the RNA*later*-ICE Frozen Tissue Transition Solution, the ileum was sectioned at the ileo-caecal valve and then at 2 cm proximal to produce a short segment of dissected terminal ileum. Peri-enteric fat was trimmed from the serosal surface of the ileum to prevent contamination of RNA extract with adipose tissue. Likewise, ileal contents were flushed out using the blunt edge of a syringe needle.

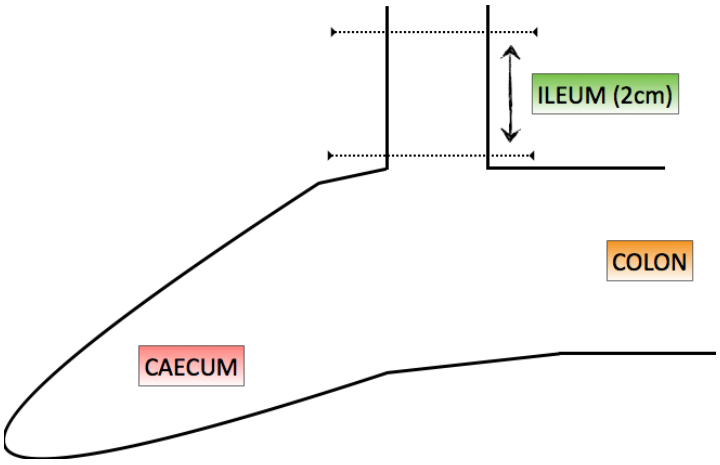

Figure 3.2; Schematic representation of mouse ileum. Caecum is a sac like structure distal to the ileum. Terminal ileum sectioned at the ileo-caecal junction and 2 cm more proximal.

3.3.5 RNA isolation

RNA was isolated using the RNeasy Fibrous Tissue Mini Kit by QIAGEN (74704) as per the manufacturers guidelines. All RNA work was performed using RNase-free reagents and equipment. Laboratory surfaces were cleaned with RNase decontamination solution (RNaseZap, Ambion, Life Technologies) prior to experiments and pipette filter tips were used.

Three ileal samples were weighed to ascertain that 2cm of ileal tissue weighed approximately 100mg. A 6mm length (approximately 30mg) of terminal ileum was dissected from the distal end of the sample and was suspended in 300µl of buffer RLT with β-mercaptoethanol (10µl per ml of buffer), in a 2.0ml Precellys ceramic bead kit tube (1.4/2.8mm beads), manufactured by Peqlab. The tissue was then homogenised using a Bertin Minilys tissue disruptor using 6 x 25 second cycles of disruption, with a 45 second rest between cycles. Samples were stored on ice between cycles of disruption. Following disruption, 590µl of RNase-free water and 10µl of proteinase-k was added to the homogenised solution and incubated in a pre-warmed heater block at 55°C for 10 minutes.

After incubation, the solution was spun at 10,000 x g for 3 minutes in a temperature controlled centrifuge at 4°C; the supernatant (~800µl) was transferred to a sterile, 1.5ml Eppendorf tube. 0.5 volumes of 100% ethanol was then added to the supernatant and the solution was gently mixed. 700µl of the sample was transferred to an RNA spin column, in a 2ml collection tube, and spun at 8,000 x g for 15 seconds. The flow through was discarded and 350µl of buffer RW1 was added and a further 8,000 x g for 15 second spin was performed. The flow though was again discarded.

The nucleic acid trapped within the spin column filter was then treated with a DNase I step. 80µl of solution, containing 10µl of DNase I in 70µl of buffer RDD,

was added to the spin column and left to incubate on the bench top for 15 minutes. After incubation, the DNase I solution was rinsed out with 350µl of buffer RW1, centrifuged at 8,000 x g for 15 seconds. The flow through was discarded. The spin column was then washed with two cycles of 500µl buffer RPE, spun for 8,000 x g for 15 seconds and 2 minutes respectively. Finally, the RNA was precipitated in 30µl of nucleic acid and RNase-free water and spun for 8,000 x g for 1 minute to collect the RNA containing precipitate in a fresh, 1.5ml Eppendorf.

3.3.6 RNA quantity and quality

As in chapter 2, the quantity and quality of extracted RNA was measured using a nanodrop spectrophotometer and also by gel electrophoresis.

For these experiments, A260/280nm and A260/230nm of 1.5 to 2.2 were accepted. In cases where the A260/230nm ratio was unacceptably low or the quantity of RNA was insufficient, the RNA extraction protocol was repeated using a further 6mm piece of ileum. Acceptable quality RNA could not be isolated for all specimens.

Gel electrophoresis was performed as described in the methods section of chapter 2. Gel electrophoresis was performed for optimisation steps and intermittently during RNA extraction to ensure RNA quality was maintained.

Figure 3.3 and 3.4 demonstrate examples of RNA spectrophotometry and electrophoresis for mouse RNA isolated using the above method.

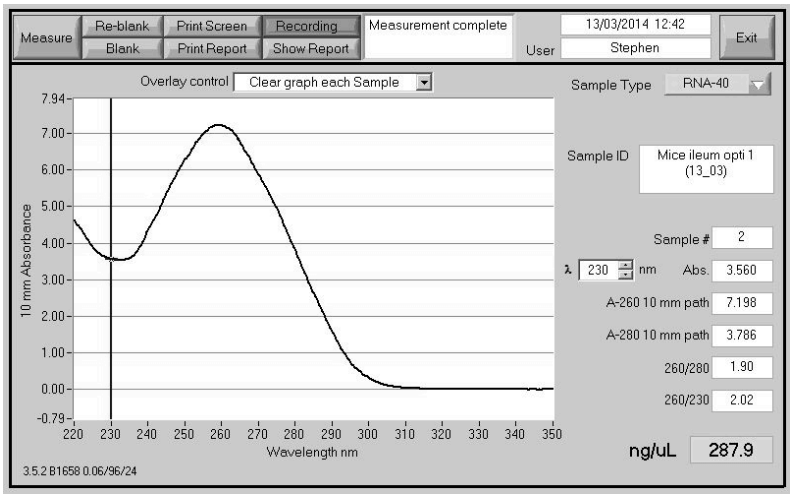

Figure 3.3; An example of Nanodrop spectrophotometry for mouse ileum RNA purified for the experiments in this chapter.

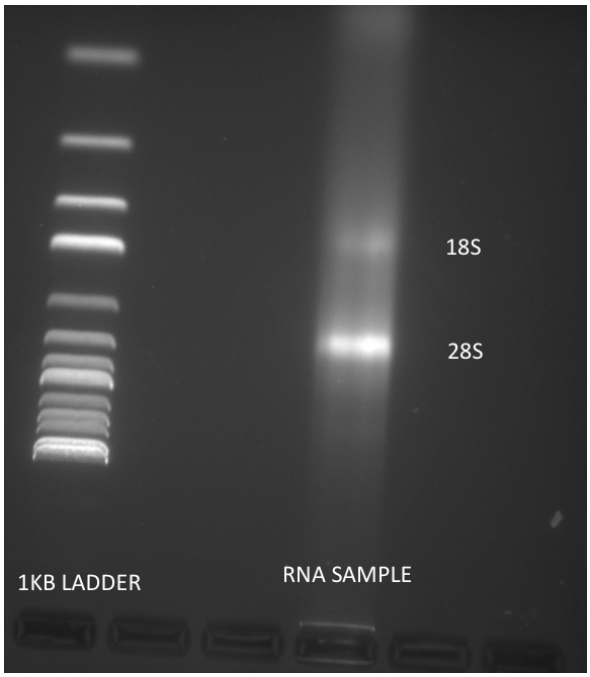

Figure 3.4; Gel electrophoresis of mouse ileum RNA purified for the experiments in this chapter. As in chapter 2, 16s and 28s ribosomal bands are highlighted beside DNA ladder

3.3.7 mRNA reverse transcription (cDNA synthesis)

Complementary DNA (cDNA) was prepared using the Tetro cDNA Synthesis Kit (Bioline) as described in the methods section of chapter 2, as per the manufacturers guidelines. As for RNA extraction, nuclease free equipment and reagents were used, surfaces were cleaned with RNase decontamination solution (RNaseZap, Ambion, Life Technologies) and filter pipette tips were used. All

procedures were performed on ice to minimize RNA degradation. cDNA samples were stored at -20°C for later use in the second part of two-step RT-PCR experiments.

3.3.8 Real-time reverse transcription polymerase chain reaction (RT-PCR)

The relative levels of mRNA for the inflammatory cytokines TNFα, IFNγ, IL-6 and IL-8 were measured to assess inflammation in the mice ilea. The relative mRNA level of FXR and its downstream targets, SHP and IBABP, was measured to assess the effect of Px-102 (FXR agonist, Phenex) in the mice ilea. Relative mRNA expression was measured using RT-PCR via a TaqMan-based chemistry assay (Life Technologies). The process of RT-PCR by a TaqMan-based assay is described in chapter 2.

Mouse specific, TaqMan Gene Expression Assays (pair of PCR primers and specific hydrolysis probe) to FXR, SHP, IBABP, TNFα, IFNγ, IL-6, IL-8 and β-actin were purchased from Life Technologies. The expression of β-actin was used as the reference (housekeeper) gene. Table 3.3 lists the primer/probes and their targets used in these experiments. In order to avoid false positive detection of genomic DNA (gDNA), TaqMan primers/probes that span exon-exon junctions (intron-splice sites) were used in these experiments.

Protein	Gene	Exon spanning	Primer/Probe
FXR	Nr1h4	yes	Mm00436425_m1
SHP	Nr0b2	yes	Mm00442278_m1
IBABP	Fabp6	yes	Mm00434315_m1
IFNγ	Ifng	yes	Mm01168134_m1
IL-6	Il6	yes	Mm00446190_m1
TNFα	Tnf	yes	Mm00443258_m1
IL-8	Cxcl15	yes	Mm04208136_m1
β -Actin	Actb	yes	Mm01205647_g1

Table 3.3; List of the genes of interest and their TaqMan primer/probes used in chapter 3

3.3.9 RT-PCR quality control

As described in chapter 2, the following steps were taken to ensure that consistent, good quality RT-PCR was performed; i) each RT-PCR reaction was performed in triplicate. If the cycle-threshold (Ct) differed by greater than 1.0 within triplicate samples, that well was excluded from further analysis; ii) A no-template control (NTC) triplicate experiment was performed to ensure there was no DNA contamination within the mastermix, primer/probe or water used in the experiments; iii) To ensure no gDNA contamination of the RNA preparation used to make the cDNA template, an RNA-template reaction was performed for representative samples (see figure 3.5). No gDNA or reagent contamination was demonstrated.

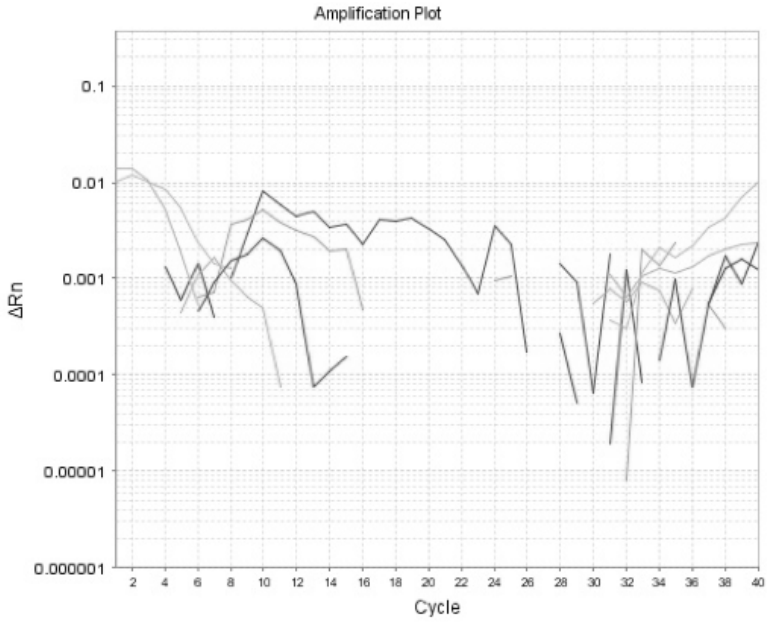

Figure 3.5; Amplification plot from RT-PCR experiment using an RNA only template to test for gDNA contamination of cDNA samples. No amplification product is detected.

Primers were validated by plotting a standard curve of Ct against serial dilutions of representative cDNA concentrations (log 10 scale), as described in chapter 2. The efficiency of the primer was calculated using the slope of the curve. The R^2 co-efficient, a measure of replicate reproducibility, should be >0.98. Figure 3.6 and table 3.4 demonstrate primer validation results for the primers used in these experiments. At low concentrations of DNA (less than 1/10th of the concentration used in the experiments) the primers for IL-6 and TNFα became inefficient.

Primer	Slope	Efficiency	R-squared
FXR	-3.122	109.1%	1.00
SHP	-3.419	96.1%	0.99
IBABP	-3.237	103.7%	1.00
IL-6	-3.226	104.2%	0.94
TNFα	-3.34	99.3%	0.98
IFNγ	-3.26	108.8%	0.99
IL-8	-3.263	102.5%	0.96
β -Actin	-3.255	102.9%	1.00

Table 3.4; Primer efficiency and goodness of fit (R^2) for primers used in chapter 3. See fig 3.5. For IL-6 and TNFα, the efficiency of slope 2 is expressed. Slope 2 covers the assay range of the primer required in these experiments.

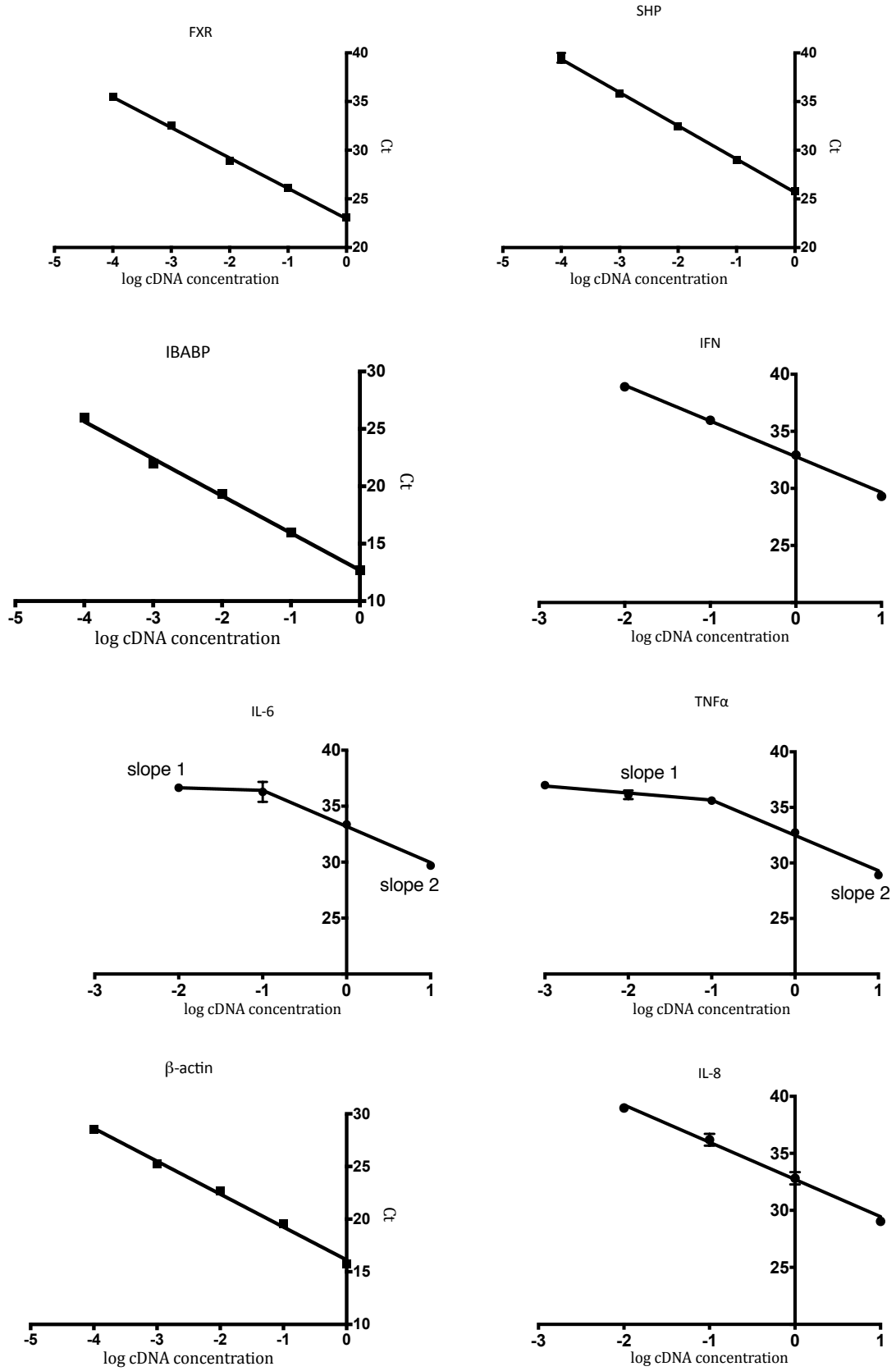

Figure 3.6; Primer validation experiments for primers used in chapter 3. Cycle threshold (Ct) is measured for serial dilutions of cDNA. See table 3.4 for R^2 and efficiency calculations

3.3.10 Relative quantification and statistical analyses

Relative quantification was used to calculate the relative expression of the genes of interest, as described in chapter 2. The choice of reference gene is critically important in the analysis of the results. For experiments in this chapter, the commonly used mouse reference gene *Actb* (β - Actin) was utilised(Kouadjo et al., 2007).

Relative quantification was calculated using the ΔΔCt method as described by Livak and Schmittgen(Livak and Schmittgen, 2001). A Ct was calculated for each biological sample by calculating the mean result from triplicate PCR wells.

The relative expression of the gene of interest (GOI) in comparison to the reference gene (ΔCt) was then calculated by the equation:

$$\Delta Ct = Ct_{GOI} - Ct_{reference}$$

For each control or intervention mouse, a ΔCt was calculated for each GOI. These individual replicate ΔCt values were then used in a Student's *t*-test to test the difference between control and different interventions.

For control and intervention groups, the mean Ct_{GOI} and mean $Ct_{reference}$ was determined. To calculate the relative quantification (ΔΔCt) of gene expression between the control diet group and the intervention groups (ALIOS diet, FXR agonist supplementation) first the mean ΔCt for control and intervention groups was calculated. For each GOI the mean ΔΔCt was then calculated as:

$$\text{mean } \Delta\Delta Ct = \text{mean } \Delta Ct_{\text{ intervention}} - \text{mean } \Delta Ct_{\text{ control}}$$

Additive error is propagated as the standard error (SE) of the differences of the mean (SEM). This can be calculated by the equation:

$$\Delta\Delta Ct \text{ SE} = \sqrt{\text{Error (control)}^2 + \text{Error (intervention)}^2}$$

Where:

$$\text{Error (control)} = \sqrt{SEM_{reference}^2 \times SEM_{GOI}^2}$$

$$\text{Error (intervention)} = \sqrt{SEM_{reference}^2 \times SEM_{GOI}^2}$$

Finally, the fold change in relative gene expression can be calculated as:

$$\text{Fold change} = 2^{\text{mean}\Delta\Delta Ct}$$

Fold change is a relative ratio and therefore, normally distributed error bars cannot be meaningfully represented on a bar chart (fold change is not normally distributed). In order to represent the degree of SE, but also to give an idea of relative ratio changes, data are presented both as ΔΔCt values with error and as fold change.

Unpaired Student's *t* tests, Chi-squared tests, Fisher's exact tests, regression analysis and Pearson correlation were calculated using Prism version 6.0e, Graphpad software, San Diego. All P values were 2-tailed, and a P value of 0.05 or less was considered statistically significant.

3.4 Results

3.4.1 Study animals

Of the 44 mice in the study, RNA from 13 of the mice was of insufficient quantity or quality and so these samples were discarded from RT-PCR analysis. If the initial concentration of cDNA was too low, the level of cytokine gene product became undetectable and could not be analysed.

To exclude the effect of intervention on RNA extraction, both Fisher's exact test and chi-squared tests were performed for the quality of RNA (good or poor) versus control diet/ALIOS diet and FXR agonist/no FXR agonist (tables 3.5 and 3.6). There was no significant difference between the groups demonstrating that any analysis of results is not confounded by the effect of intervention on RNA quality.

	RNA good	**RNA poor**	
FXR agonist +ve	19	5	24
FXR agonist -ve	12	8	20
	31	13	44

Table 3.5; Contingency table, chi-squared test not significantly different, Fisher's test p=0.199

	RNA good	**RNA poor**	
ALIOS diet	14	7	21
Control diet	17	6	23
	31	13	44

Table 3.6; Contingency table, chi squared test not significantly different, Fisher's test p=0.743

The relative gene expression of inflammatory cytokines and FXR, along with its downstream targets, was measured in 31 mice. The body weight and visceral

adipose tissue weight was measured in all 44 mice. Table 3.7 demonstrates these characteristics for all mice in the study.

Animal ID	Intervention	RT-PCR	Body Weight (grams)	VAT Weight (grams)
9218L	Control	Yes	39.8	0.4
9218R	Control	No	35.7	0.3
9217N	Control	No	47.9	0.5
9217B	Control	Yes	41.6	0.6
9217L	Control	No	44.7	0.7
9217R	Control	No	47.5	0.5
9218B	Control	No	30.0	0.2
9839B	Control	Yes	43.5	0.3
9839R	Control	Yes	44.8	0.7
9839L	Control	Yes	39.2	1.2
9839N	Control	Yes	43.0	0.6
9224N	ALIOS	Yes	49.6	1.5
9224B	ALIOS	Yes	47.9	2.4
9224R	ALIOS	No	47.9	1.2
9226N	ALIOS	No	50.8	1.7
9226B	ALIOS	No	45.8	2.5
9226R	ALIOS	Yes	53.7	1.8
9226L	ALIOS	Yes	45.5	2.3
9299N	ALIOS	Yes	51.0	1.2
9299R	ALIOS	Yes	57.1	1.8
9838L	Control+1mg/kg FXRa	Yes	37.4	1.0
9838R	Control+1mg/kg FXRa	Yes	44.9	0.5
9838N	Control+1mg/kg FXRa	Yes	42.4	0.4
9843R	Control+1mg/kg FXRa	Yes	40.8	0.4
9843B	Control+1mg/kg FXRa	Yes	49.1	0.5
9843L	Control+1mg/kg FXRa	Yes	43.2	0.4
9843N	Control+1mg/kg FXRa	Yes	43.2	1.2
9838B	Control+1mg/kg FXRa	Yes	40.5	3.3
9845N	Control+5mg/kg FXRa	Yes	44.1	0.5
9845R	Control+5mg/kg FXRa	No	43.3	0.9
9845B	Control+5mg/kg FXRa	Yes	43.4	0.7
9845L	Control+5mg/kg FXRa	Yes	47.9	0.6
9841N	ALIOS+1mg/kg FXRa	No	44.4	1.9
9841B	ALIOS+1mg/kg FXRa	Yes	44.6	1.8
9836B	ALIOS+1mg/kg FXRa	Yes	51.5	1.5
9841L	ALIOS+1mg/kg FXRa	No	49.4	2.5
9841R	ALIOS+1mg/kg FXRa	Yes	41.6	1.7
9298R	ALIOS+1mg/kg FXRa	Yes	49.3	1.6
9837L	ALIOS+5mg/kg FXRa	No	37.5	1.7
9842R	ALIOS+5mg/kg FXRa	Yes	48.6	1.6
9842N	ALIOS+5mg/kg FXRa	Yes	49.2	1.0
9837R	ALIOS+5mg/kg FXRa	Yes	43.7	1.9
9837N	ALIOS+5mg/kg FXRa	Yes	44.7	3.2
9837B	ALIOS+5mg/kg FXRa	No	45.9	2.8

Table 3.7; Mice characteristics, including identifier, intervention (FXRa is FXR agonist), yes = used for RT-PCR, No = not used for RT-PCR, measurement of weight and visceral adipose tissue (VAT)

3.4.2 Mice fed a HF/HS diet were heavier with more visceral fat

At 42 weeks, mice in the ALIOS group were significantly heavier than control mice (mean weight of 49.9 g versus mean weight of 41.6 g, p = 0.0009, 95% CI 3.91-12.71). In addition, ALIOS mice had stored significantly more visceral fat (mean VAT weight 1.8 g versus 0.5 g, p < 0.0001, 95% CI 0.99-1.70), as seen in figure 3.7.

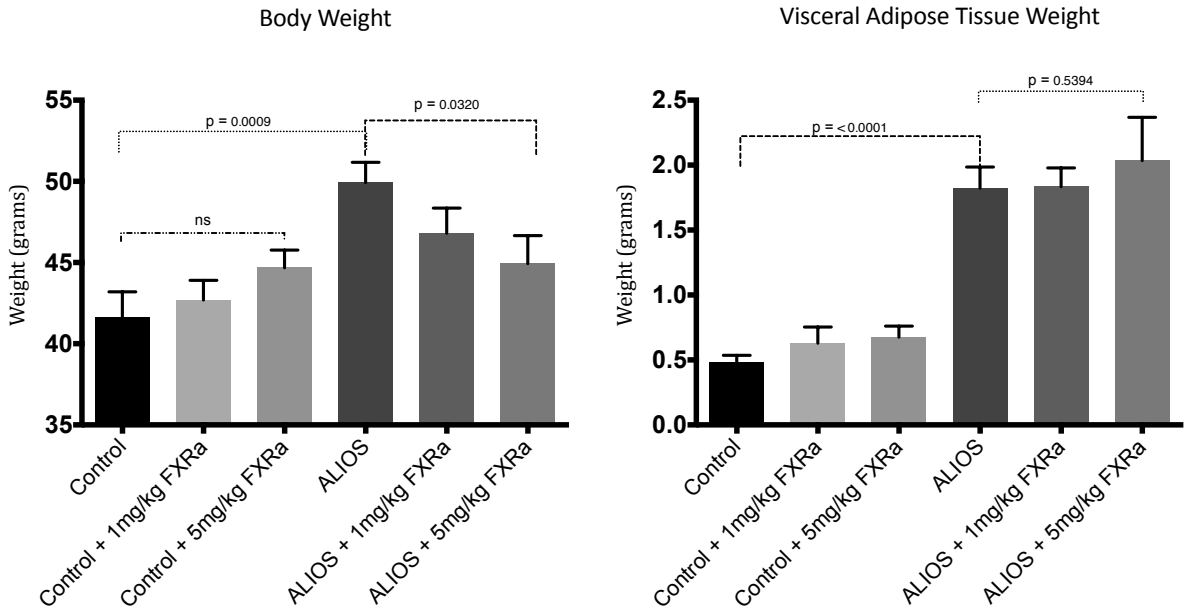

Figure 3.7; Body weight and visceral adipose tissue weight for mice fed control or ALIOS diet, with or without different concentrations of FXR agonist (FXRa). (n=44, SEM, t-tests)

From these data, the supplementation of HF/HS diet with the FXR agonist significantly reduced the body weight (p = 0.032, 95% CI 0.50-9.48), but not the visceral fat, of mice on the ALIOS diet. The reduction in body weight in the FXR agonist supplemented ALIOS groups, is significant only for the high dose (5mg/kg), but not for the low dose (1mg/kg) of FXR agonist (p=0.032, p=0.141 respectively).

3.4.3 Increased body fat is associated with higher levels of inflammatory cytokine expression in the ileum

Body weight and VAT weight were compared with cytokine expression for mice in the control and ALIOS group. Mice treated with an FXR agonist were excluded

from this analysis to avoid the potential confounding effect FXR agonism may have on gene expression (n=12).

As seen in figure 3.8, there was a positive correlation between the weight of accumulated mouse visceral adipose tissue and relative inflammatory cytokine expression in the ileum. The positive correlation is significantly deviated from 0 for TNFα and IFNγ (p=0.049, p=0.021), but falls short of significance for IL-6 and IL-8 (p=0.178, p=0.07).

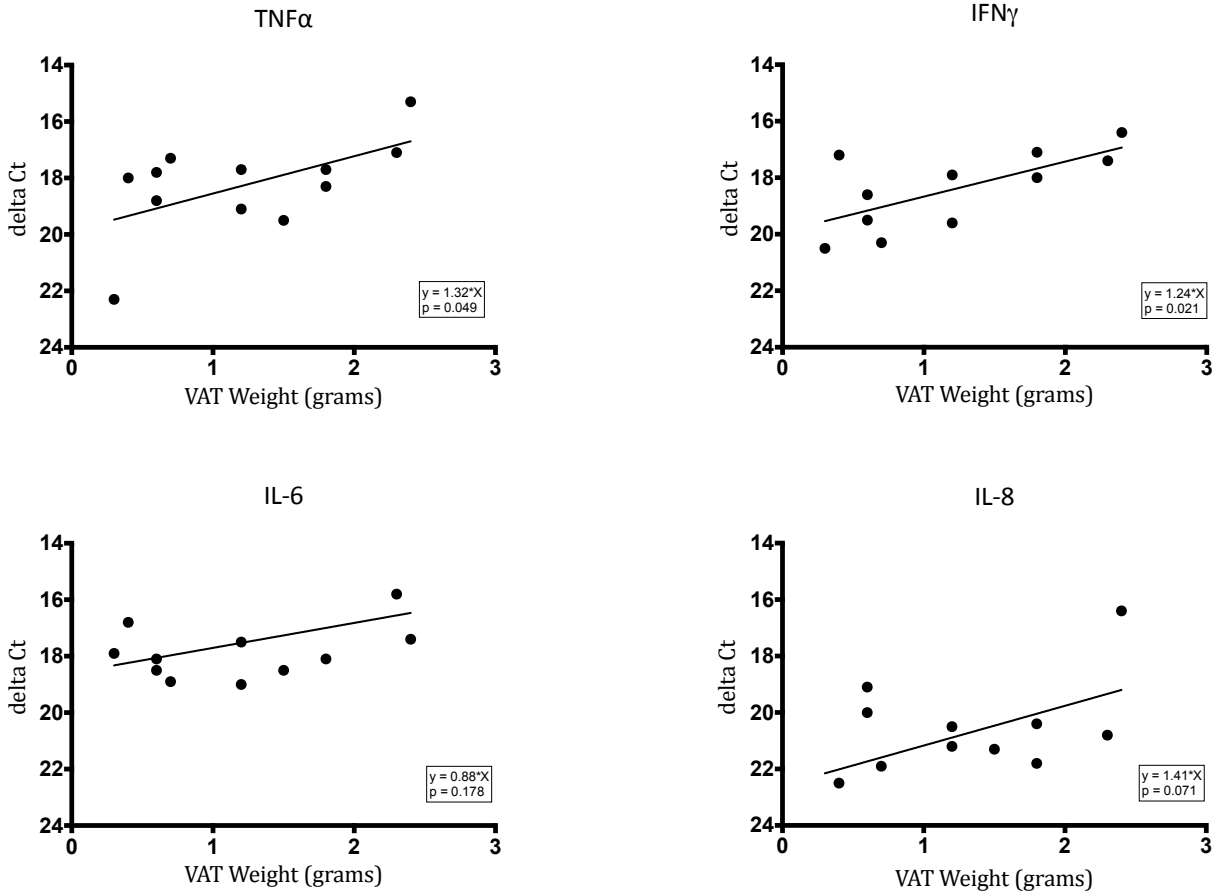

Figure 3.8; Correlation between visceral adipose tissue weight and delta Ct (as measure of relative gene expression) for TNFα, IFNγ, IL-6 and IL-8. Note y-axis is inverted as lower ΔCt values equate to higher levels of relative gene expression. (n=12, linear regression analysis)

Figure 3.9 presents the association between total body weight and the relative gene expression of CD associated inflammatory cytokine in the mouse ileum. A positive trend to increasing gene expression with increased weight was

demonstrated, but the correlation is relatively weak. None of the correlations deviated significantly from 0.

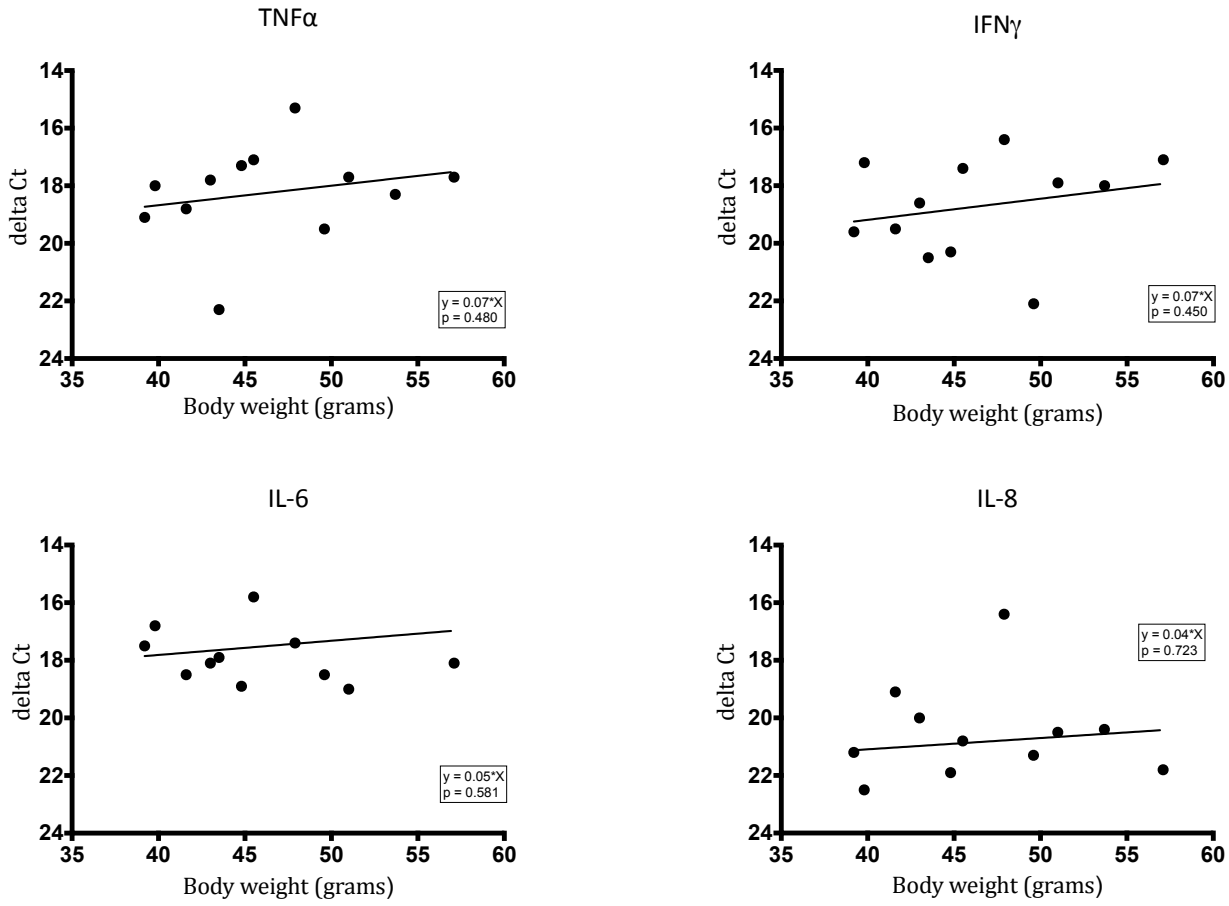

Figure 3.9; Correlation between body weight and ΔCt (as measure of relative gene expression) for TNFα, IFNγ, IL-6 and IL-8. Note y-axis is inverted as lower ΔCt values equate to higher levels of relative gene expression.(n=12, linear regression analysis)

3.4.4 There is evidence that FXR activity is decreased in the ileum of mice fed a HF/HS diet

The relative expression of FXR and its downstream targets, SHP and IBABP, was measured to assess the effect of HF/HS feeding on FXR activity. As described in section 3.3.9, relative gene expression was calculated to give a fold change in mRNA levels between control and intervention groups. A fold change of greater than 2, or less than 0.5, is thought to be biologically relevant(Inagaki et al., 2006).

The relative mRNA levels of FXR, SHP and IBABP were all reduced in the ALIOS group as compared with control, with a fold decrease of 0.51, 0.18 and 0.44 respectively (see figure 3.10). This fold decrease was significant for IBABP ($p=0.04$). The decreased trend observed for FXR and SHP was not significant ($p=0.30$ and $p=0.34$ respectively).

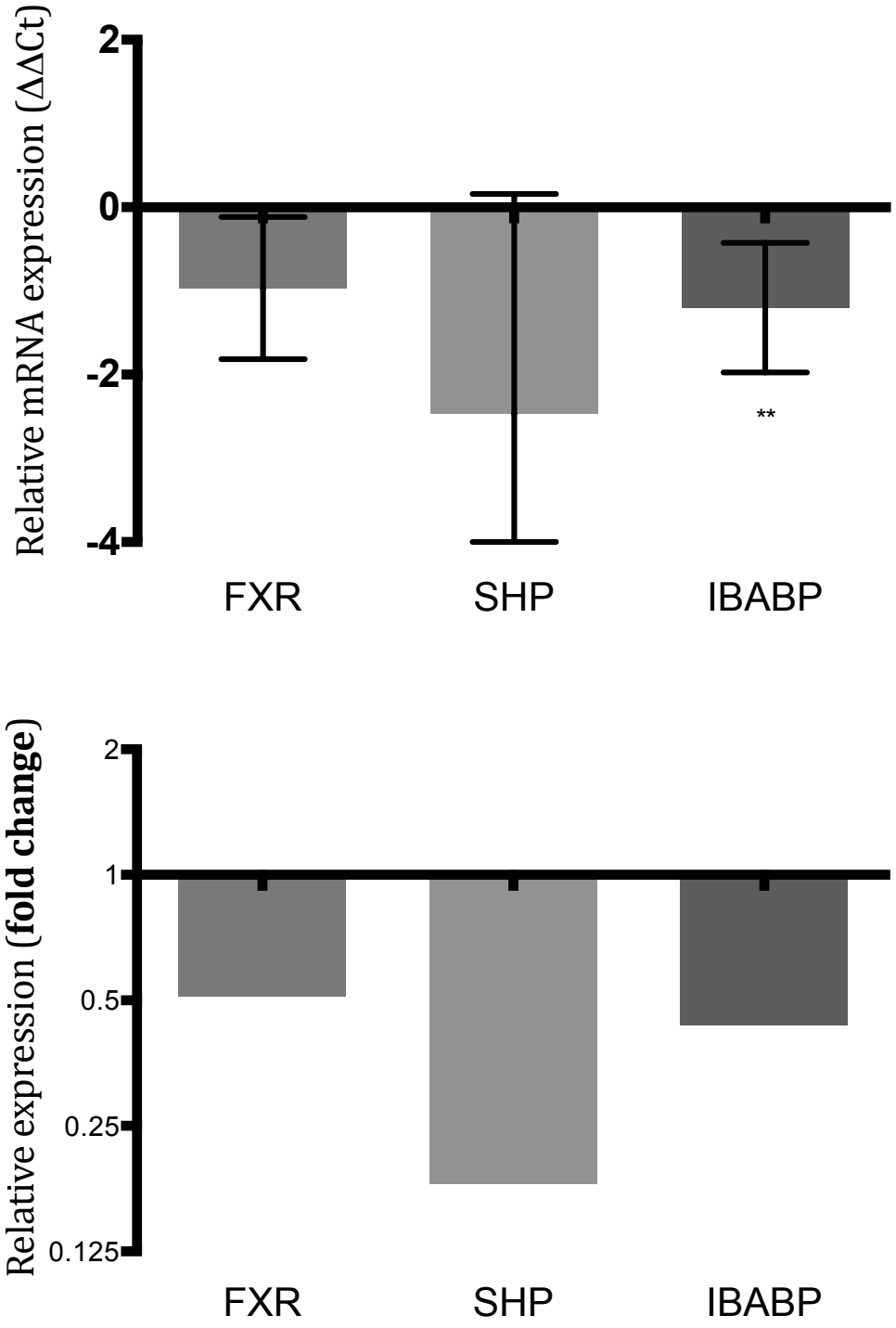

*Figure 3.10; The relative gene expression of FXR and its downstream targets in ileum of mice fed a diet rich in fat and sugar (ALIOS) as compared with mice fed a control diet. The data are presented both as a fold change and as delta delta Ct to allow the representation of the degree of error.(n=12, **significant by t-test, SE – see section 3.3.10)*

3.4.5 There is a trend to suggest that Ileal inflammatory cytokine gene expression is elevated in mice fed a HF/HS diet

Mice fed a HF/HS diet in the ALIOS group demonstrate increased levels of ileal TNFα, IFNγ, IL-6 and IL-8 mRNA in comparison to control.

In the ALIOS group, ileal mRNA levels of TNFα, IFNγ and IL-8 were increased by a factor of 2 or more (2.49, 2.17 & 2.43 respectively), whilst IL-6 was increased by a factor of 1.87, as compared with control mice (see figure 3.11).

Due to the broad range of delta Ct values within each sample, the propagation of error was large. This is demonstrated by the size of the error bars on the lower graph that demonstrates the relative expression by ΔΔCt method, figure 3.11.

There was a consistent trend to increased levels of relative ileal mRNA expression for TNFα, IFNγ, IL-6 and IL-8 in the ALIOS group as compared to control. However, this finding was not significant for any of the cytokines assayed (TNFα p=0.19, IFNγ p=0.28, IL-6 p=0.35, IL-8 p=0.26).

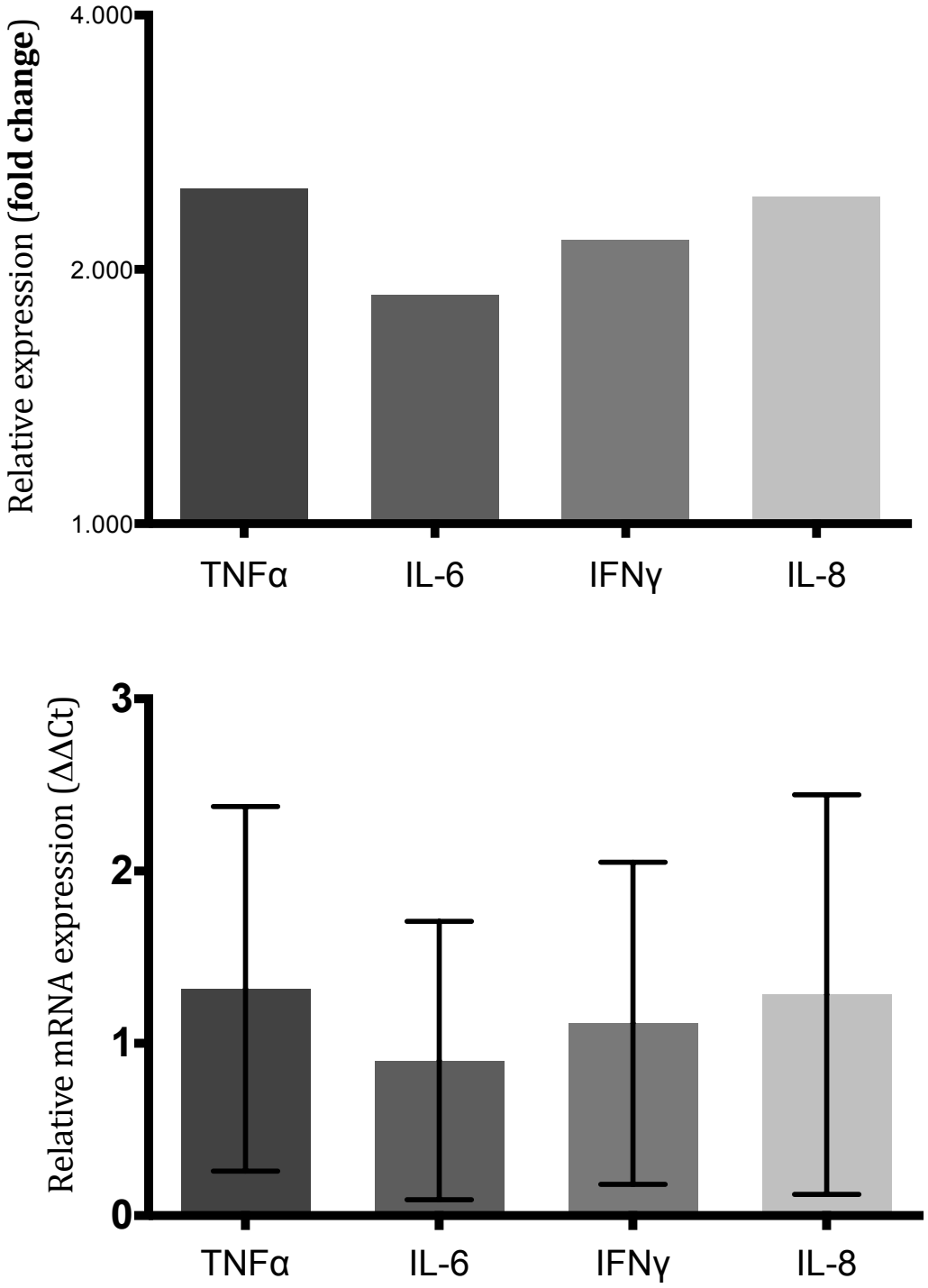

Figure 3.11; The relative gene expression of CD associated inflammatory cytokine in ileum of mice fed a diet rich in fat and sugar (ALIOS) as compared with mice fed a control diet. The data are presented both as a fold change and as delta delta Ct to allow the representation of the degree of error. (n=12, SE – see section 3.3.10)

3.4.6 High dose, but not low dose, FXR agonist induced FXR activation

The relative expression of FXR, SHP and IBABP were measured to assess the activity of the FXR agonist. TNFα, acting via NF-κB, can inhibit FXR

expression(Gadaleta et al., 2011a). Therefore, in order to assess whether the FXR agonist supplementation of feed produced a biological effect in the mouse ilea, the levels of FXR and its downstream genes were measured in the control diet and the control with FXR agonist groups (n=17). The ALIOS fed groups with FXR agonist were excluded from analysis due to the potential confounding factor of any inflammatory suppression of FXR activity.

Figure 3.12 and 3.13 demonstrate the effect of the two doses of FXR agonist supplemented feed on the expression of FXR, SHP and IBABP. Again, the data are presented as a relative fold change, but also as the mean ΔΔCt value with SE represented by error bars.

The higher, 5mg/kg, dose of FXR agonist induced a significant increase in ileal IBABP expression with a fold increase of 2.0 ($p = 0.01$). At this dose, there was also a trend towards increased relative expression levels of SHP (fold change 1.05) and FXR (fold change 1.52). These changes were not significantly different ($p=0.96$ and $p=0.40$ respectively) and only an increased trend was suggested. The increase in IBABP and the trend to increased levels of FXR and SHP demonstrate that the 5mg/kg dose agonised FXR in the mouse ileum.

The 1mg/kg dose of FXR agonist did not increase FXR, SHP or IBABP expression levels. In fact, there was the paradoxical observation of significantly reduced downstream IBABP gene expression, suggesting relative inhibition of FXR activity. A trend to reduced expression of FXR and SHP was also suggested. There was a 0.57 fold decrease in FXR ($p=0.32$), 0.31 fold decrease in SHP ($p=0.32$) and a significant 0.41 fold decrease in IBABP ($p=0.03$).

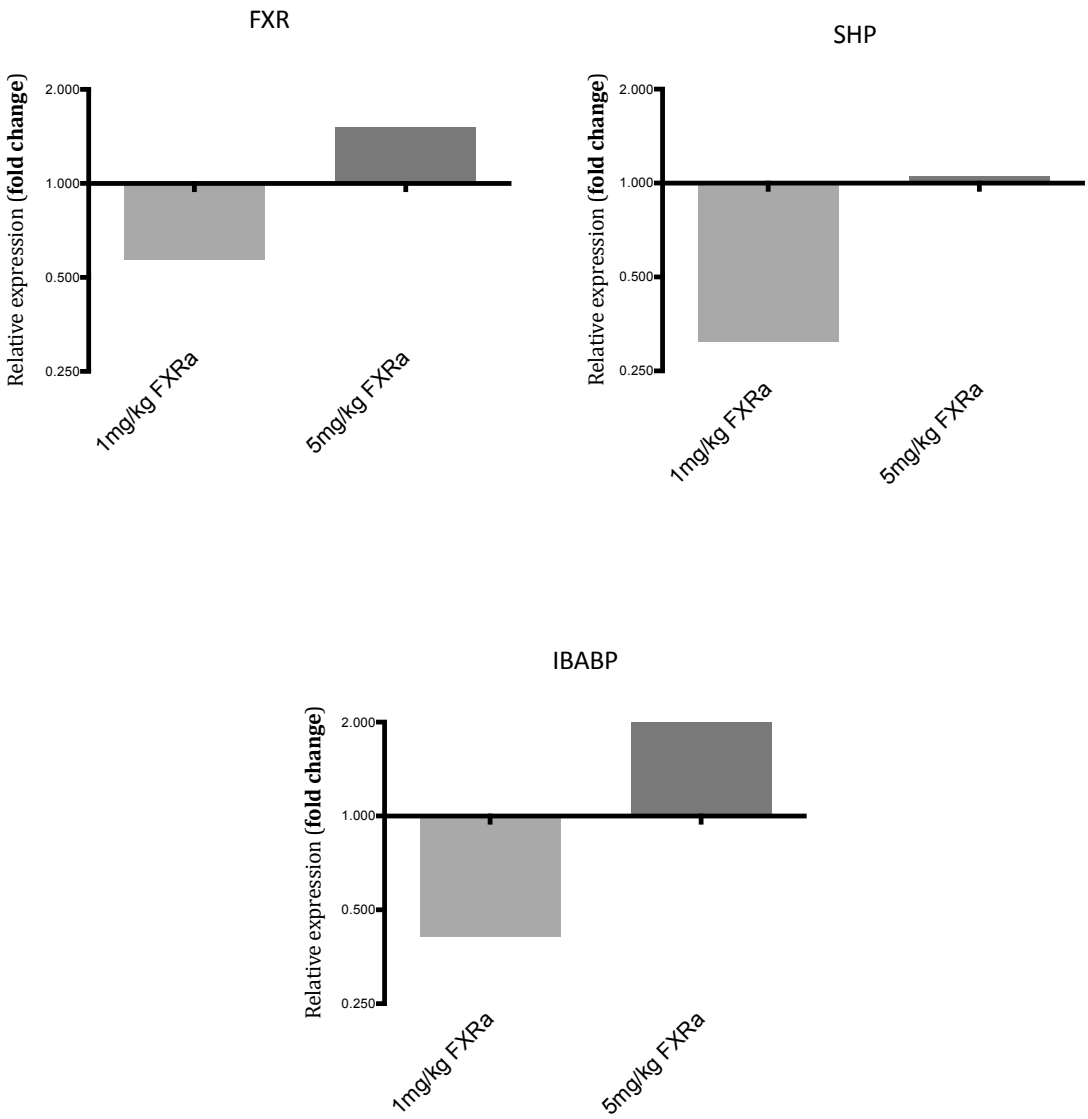

Figure 3.12; The effect of 1mg/kg or 5mg/kg FXR agonist (FXRa) on the relative expression of ileal FXR, SHP and IBABP in mice fed a control diet, as compared with mice fed control diet alone. SHP and IBABP are downstream of FXR and are a measure of FXR activity. Results are presented as a fold change. (n=17)

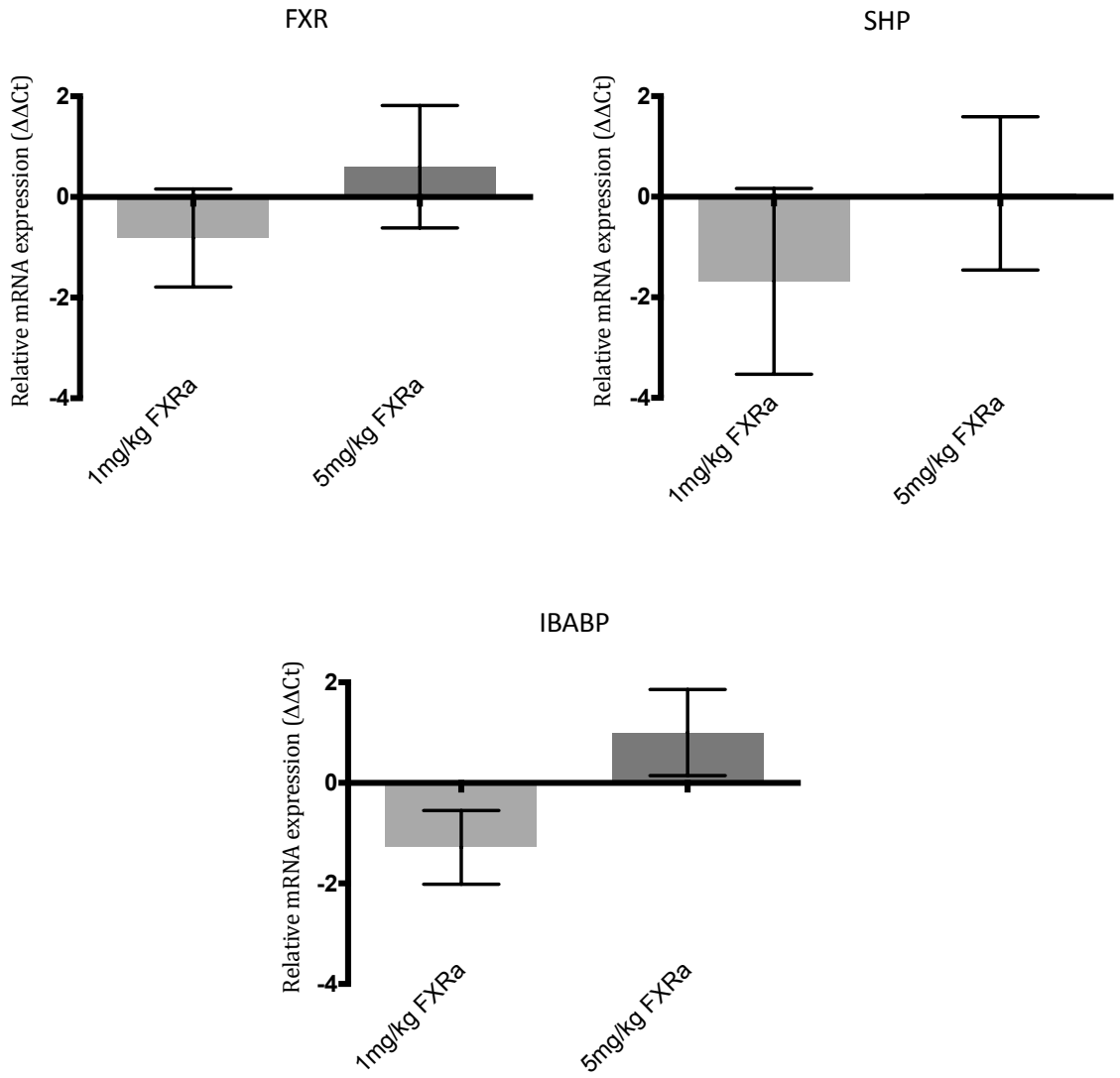

Figure 3.13; The effect of 1mg/kg or 5mg/kg FXR agonist (FXRa) on the relative expression of ileal FXR, SHP and IBABP in mice fed a control diet, as compared with mice fed control diet alone. SHP and IBABP are downstream of FXR and are a measure of FXR activity. Results are presented as mean ΔΔCt with error bars to represent SE. (n=17)

Taken together, these results suggest that the FXR agonist was biologically active in the mouse ilea. However, only the higher, 5mg/kg dose was able to agonise FXR under these experimental conditions.

3.4.7 There is a trend suggesting attenuated levels of ileal cytokine expression in HF/HS fed mice when treated with an FXR agonist

The level of inflammatory cytokine expression in the ilea of ALIOS mice was measured with and without the FXR agonist supplemented feed in order to assess the effect of FXR on HF/HS associated inflammation.

Results in section 3.4.4 demonstrated that ALIOS fed mice have higher relative levels of ileal inflammatory cytokine expression compared with control diet mice. When diet was supplemented with the FXR agonist, there was a trend for the ALIOS induced increase in inflammatory cytokine expression to be attenuated. Figure 3.14 and 3.15 demonstrates the effect of 5mg/kg or 1mg/kg FXR agonist in the ALIOS mice.

In the 5mg/kg FXR agonist supplemented group, the expression of TNFα, IFNγ and IL-6 was reduced from a relative fold increase of 2.49 to 1.43, 2.17 to 1.93 and 1.86 to 1.53 respectively. For IL-8 there was increase in the relative fold change from 2.43 to 2.76. None of these changes were significantly different (TNFα $p=0.51$, IFNγ $p=0.90$, IL-6 $p=0.81$, IL-8 $p=0.85$).

In the 1mg/kg FXR agonist supplemented group, there was an observed reduction in the relative expression of each cytokine assayed. The expression of TNFα, IFNγ, IL-6 and IL-8 was reduced from a relative fold increase of 2.49 to 0.43, 2.17 to 0.74, 1.86 to 0.93 and 2.43 to 0.79 respectively. Again, none of the changes were statistically significant (TNFα $p=0.20$, IFNγ $p=0.27$, IL-6 $p=0.32$, IL-8 $p=0.26$).

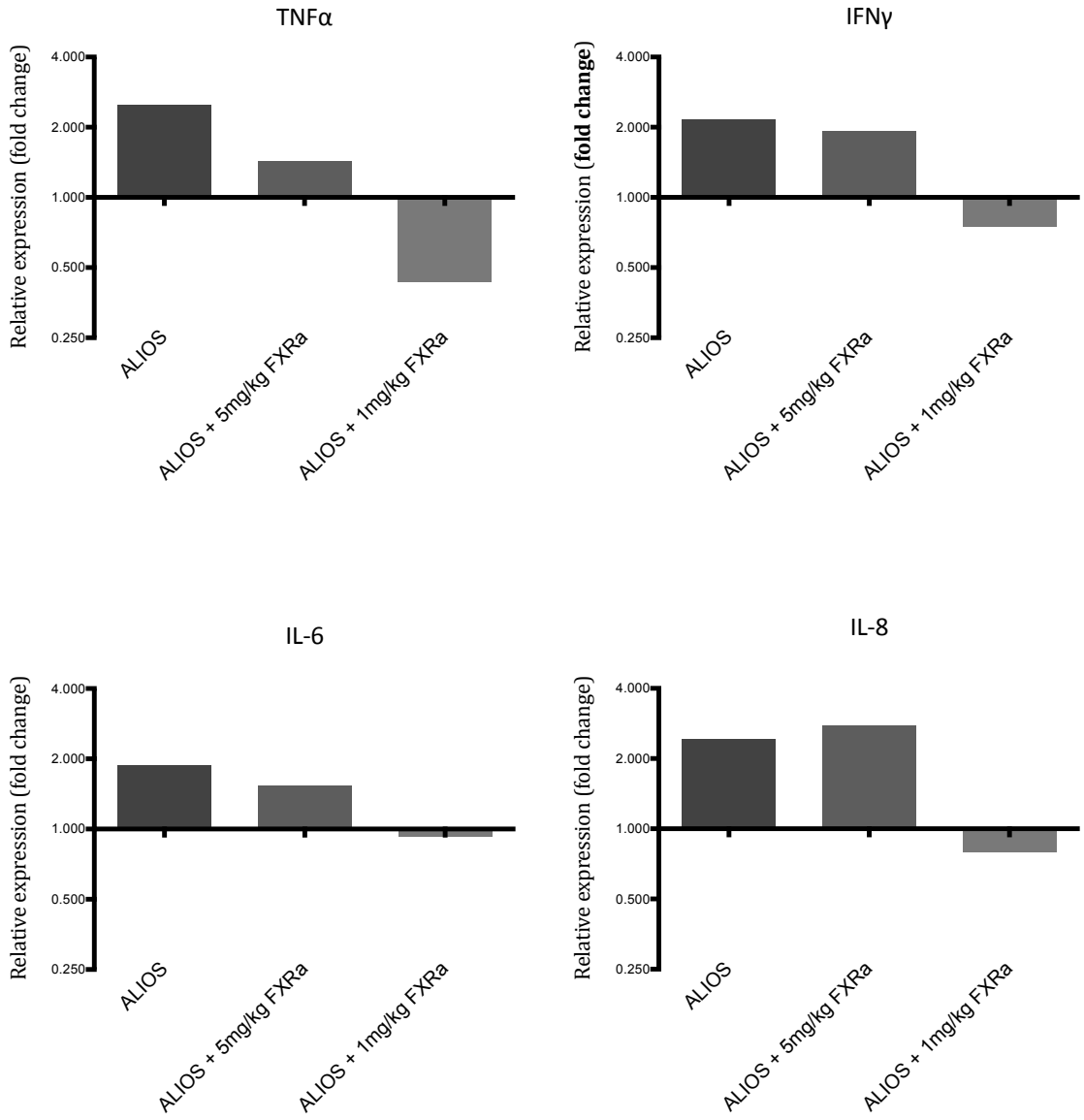

Figure 3.14; The effect of ALIOS diet with or without 1mg/kg FXR agonist (FXRa) or 5mg/kg FXR agonist on the relative gene expression of TNFα, IFNγ, IL-6 and IL-8 in the ilea of mice. Results are presented as a fold change. (n=14)

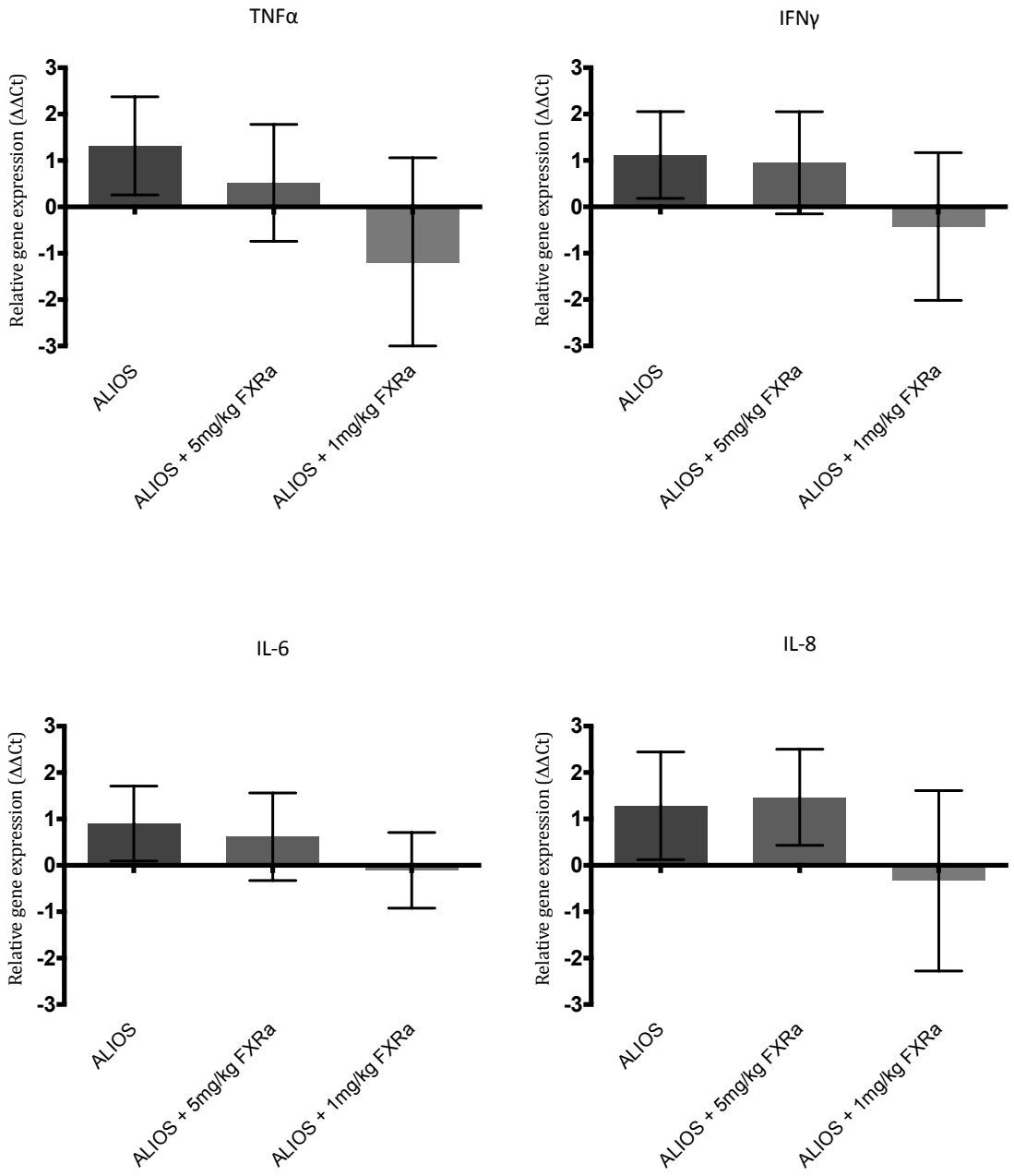

Figure 3.15; The effect of ALIOS diet with or without 1mg/kg FXR agonist (FXRα) or 5mg/kg FXR agonist on the relative gene expression of TNFα, IFNγ, IL-6 and IL-8 in the ilea of mice. Results are presented as mean ΔΔCt with error bars to represent SE. (n=14)

3.4.8 High dose FXR agonist may cause an increase in ileal cytokine expression

The level of inflammatory cytokine expression in control mice was measured with and without the FXR agonist supplemented feed. The finding that there was an inverse dose response, such that 1mg/kg FXR agonist appeared to have a greater effect on reducing cytokine expression in ALIOS mice than 5mg/kg of FXR agonist, suggested that high dose FXR agonism might have a toxic, cytokine stimulating effect.

Figure 3.16 and 3.17 demonstrate that in the 5mg/kg FXR agonist supplemented group, the expression of TNFα, IFNγ, IL-6 and IL-8 was increased with a relative fold change of 5.3, 2.2, 2.7 and 2.0 respectively, as compared with control. None of these changes were significantly different (TNFα p=0.18, IFNγ p=0.14, IL-6 p=0.12, IL-8 p=0.52).

In the 1mg/kg FXR agonist supplemented group, there was little change from control with fold changes of 1.7, 1.1, 0.94 and 1.9 for TNFα, IFNγ, IL-6 and IL-8 respectively (TNFα p=0.39, IFNγ p=0.88, IL-6 p=0.87, IL-8 p=0.41).

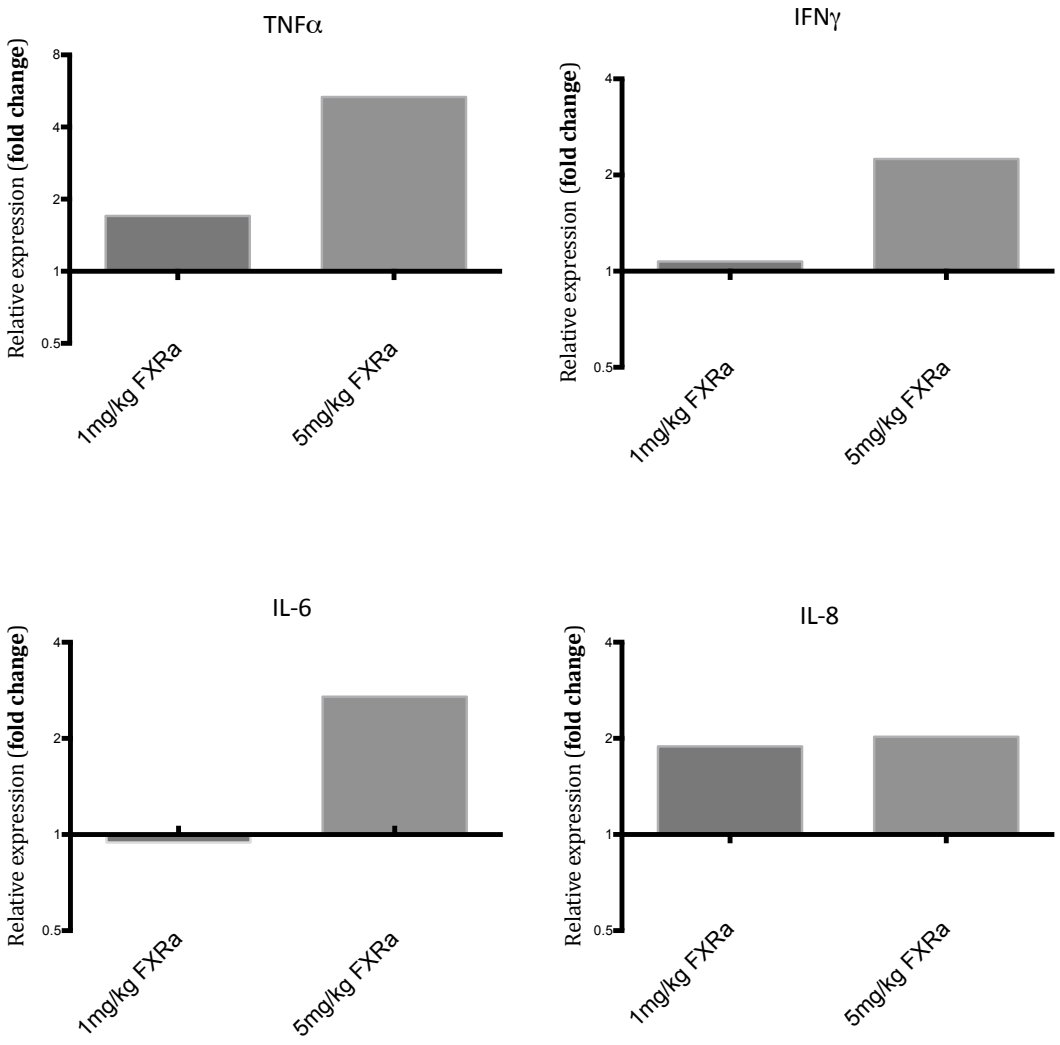

Figure 3.16; The effect of 1mg/kg FXR agonist (FXRa) or 5mg/kg FXR agonist on the relative gene expression of TNFα, IFNγ, IL-6 and IL-8 in the ilea of control mice. Results are presented as a fold change (n=17)

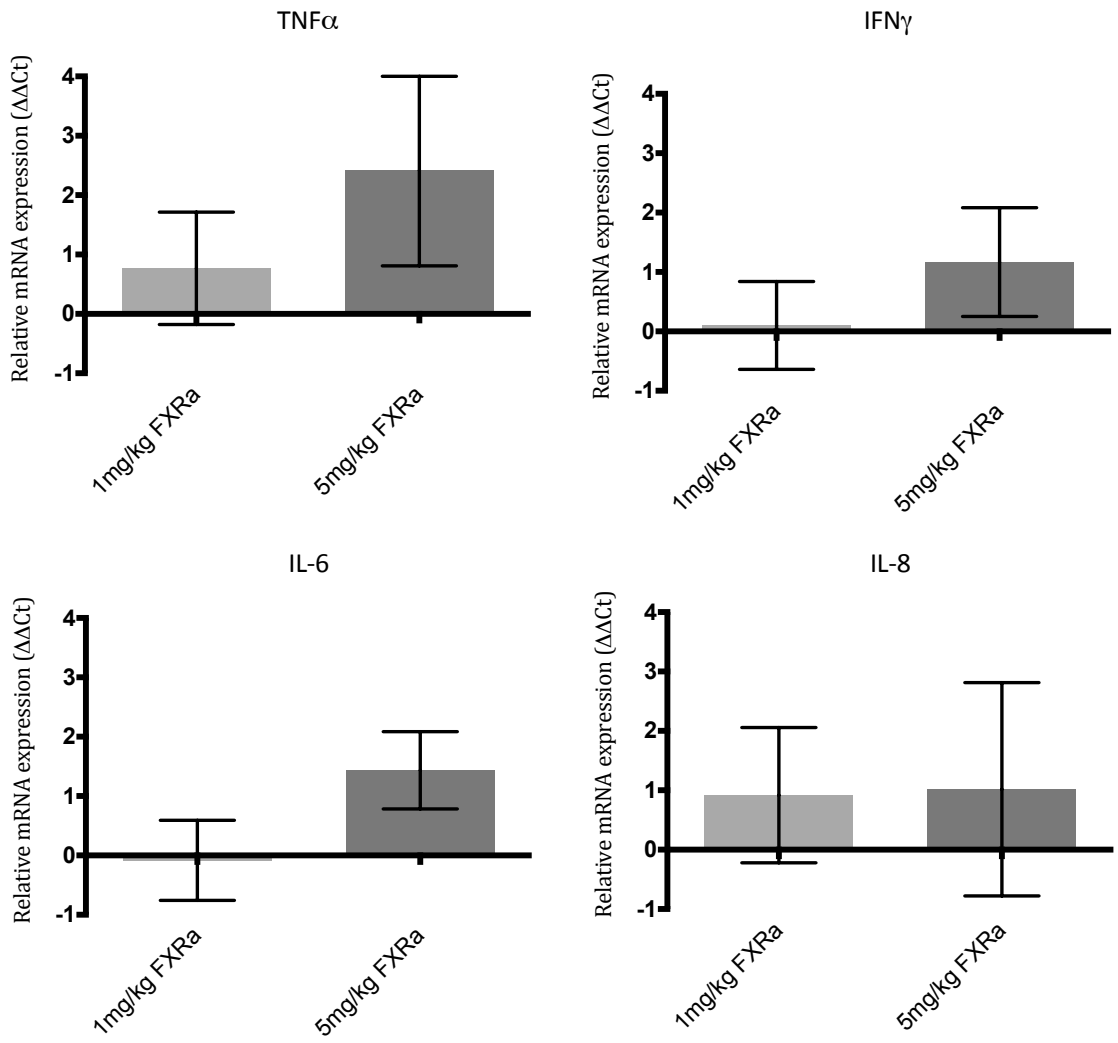

Figure 3.17 The effect of 1mg/kg FXR agonist (FXRa) or 5mg/kg FXR agonist on the relative gene expression of TNFα, IFNγ, IL-6 and IL-8 in the ilea of control mice. Results are presented as mean ΔΔCt with error bars to represent SE. (n=17, SE)

3.5 Discussion

The high fat/high sugar (HF/HS) content western diet is associated with an increased risk of developing CD(Hou et al., 2011). The pathological mechanism by which a HF/HS may induce small bowel inflammation is unknown, but disruption to BA signaling due a diet-induced dysbiosis has been postulated(Duboc et al., 2013). The aims of this chapter were to assess for evidence of ileal inflammation associated with a western diet and to assay the effect of promoting ileal BA signaling, using an FXR agonist, in this model system.

Evidence from these mouse studies is in keeping with the hypothesis that disruption to BA signalling, induced by a HF/HS diet associated dysbiosis, is a mechanism linking diet to the development of CD. The ALIOS model has previously been shown to induce physiological changes similar to those found in patients with the metabolic syndrome, of obesity, hyperinsulinaemia and dyslipidaemia(Dowman et al., 2014). Data presented here, demonstrates an associated increase in the expression of CD associated inflammatory cytokines, whilst the activity of FXR was reduced, in the ilea of mice fed a HF/HS, western diet. There was a strong, significant correlation between the amount of visceral fat and the mRNA levels of TNFα and IFNγ expressed in the ileum. IL-6 and IL-8 levels were also associated with the accumulation of visceral fat, but the correlation was less strong. This finding is concordant with the work of Hotamisligil et al and others(Hotamisligil et al., 1993, Wellen and Hotamisligil, 2005), who have demonstrated that the obese state is one of a low grade inflammatory process, with increased circulating LPS and cytokine expression in the liver and subcutaneous tissue. In these experiments, trimming of serosal fat prior to tissue homogenisation ensured that the extracted ileal RNA was representative of the

cells in the ileum. The homogenised ileal tissue therefore included enterocytes, intra-epithelial lymphocytes and antigen presenting cells, rather than peri-enteric fat. In this respect, this model is much less reductionist than the chapter 2 experiments with human gut derived epithelial cell lines.

This study did not measure the microbiome and so a direct relationship between ileal inflammation and a diet-induced dysbiosis has not been demonstrated. However, these findings build on work by Ding et al who have previously demonstrated an increase in ileal TNFα mRNA levels in HF fed conventional mice, but not germ free mice, demonstrating the importance of the microbiome in promoting gut inflammation(Ding et al., 2010).

The upregulation of the FXR downstream gene, IBABP, demonstrates that supplementing feed with the FXR agonist was able to increase the activity of FXR, for the higher, 5mg/kg, dose of the compound.

In the HF/HS fed mice, there was a decrease in the activity of FXR as demonstrated by a significant decrease in the expression of IBABP and a decreased trend in the expression of SHP and FXR. This is merely an association with the increase in the inflammatory cytokine expression and does not demonstrate causation.

However, there is a trend to suggest that the diet-induced increase in ileal cytokine expression may be attenuated by treatment with the FXR agonist, particularly for the 1mg/Kg FXR agonist dose. This was only a trend and did not reach statistical significance. This trend is concordant with the hypothesis that BA dysmetabolism is a potential mechanism by which HF/HS diet increases the risk of CD.

As measured by its downstream activity, only the high dose of Px-102 was able to significantly agonise FXR. In the study design, the FXR agonist was added to the chow and not lavaged. Therefore, there is possibly some variability in the amount

of drug individual mice received. However, average drug dosing should have been similar between animals. It is difficult to explain the observation that the 1mg/kg dose of Px-102 seemed to antagonise FXR. The standard error of the mean in this group is large, representing a large range of values, and may contain unrepresentative outliers. However, with only a small number of samples, it is impossible to statistically identify any potential outliers (e.g. by using a statistical test such as the Grubb's test).

There is the suggestion of an inverse dose response for the attenuation of cytokine expression, with the 1mg/kg FXR agonist apparently producing a greater effect than the 5mg/kg dose. Also, there is the suggestion that the 5mg/kg FXR agonist dose in control animals increased cytokine expression. As both findings were only a trend, it is difficult to analyse this finding. However, it is possible that the higher dose is producing an antagonising effect. This may be as a result of an off-target effect or as a cell stressor (bile acids are detergent molecules) at high concentrations. A similar potential toxic effect was seen with high doses of 6-ECDCA on IL-8 production by HT29 cells in chapter 2. A repeat experiment using a larger sample would provide a clearer answer.

ALIOS feeding over 42 weeks was associated with a significant increase in body weight and visceral fat, as expected. Interestingly, treatment with the FXR agonist was observed to inhibit this total weight gain, whilst visceral fat mass was unchanged. Presumably, the ALIOS diet mice treated with the FXR agonist failed to gain weight in some other body compartment, such as liver, muscle, bone or other fat compartment. Again, this observation should be investigated further.

There are potential weaknesses in the methodology of these studies. The data presented are from a mouse model that closely resembles the western diet that has

been associated with CD pathogenesis. However, unlike patients with CD, the C3H/He mouse strain is genetically normal with respect to its predisposition to ileitis or colitis. Future studies may try to remedy this by using a genetic CD animal model, such as the TNF $^{\Delta ARE}$ (Pizarro et al., 2003) mouse, with the ALIOS diet. These experiments have not demonstrated that the increase in inflammatory cytokine expression associated with HF/HS feeding induced an actual ileitis. Expression levels of cytokine mRNA does not necessarily equate to changes in protein level and, when it does, may not lead to actual tissue inflammation. Unfortunately, storage of the GI tract post-resection, with a slow freezing process, disrupted tissue architecture such that histology or protein assay could not be performed reliably. Any future studies should attempt to assess for histological evidence of inflammation.

Due to difficulties extracting high quality RNA, the sample size was small. This, allayed to the large biological variability in mRNA expression between animals, meant that results were not statistically significant. Trends were observed, but these should be statistically verified by repeating a similar study with a greater sample size.

In summary, this chapter provides tentative evidence to suggests that treatment with an FXR agonist may correct the disruption to BA signalling induced by HF/HS feeding, dysbiosis and BA dysmetabolism. Studies of FXR activity using primary tissue from patients with CD may provide further evidence for the role of disrupted BA signalling in the pathogenesis of the disease.

Chapter 4 – FXR Activity In Patients With Ileal Crohn's Disease

4.1 Abstract

The role of farnesoid X receptor (FXR) in the aetiopathogenesis of inflammatory bowel disease (IBD) has been, up until now, studied mainly in cell line and animal models. There are few studies on the role of FXR using primary tissue from patients with Crohn's disease (CD).

Ex-vivo organ culture of small intestinal mucosa has been used to study a variety of GI diseases, including CD. The technique of ileal organ culture allows the study of immune function in an architecturally preserved primary tissue sample.

The broad aims of this chapter were, therefore, to assay FXR activity in patients with ileal CD and to optimise an *ex-vivo* ileal mucosa culture model in order to study the role of FXR agonism on cytokine secretion by primary gut epithelial tissue.

These studies demonstrate that FXR expression and activity is decreased in the ilea of patients with ileal CD as compared with controls. An *ex-vivo* explant model was optimised as described in the methods section. There is no evidence, from this initial pilot study, to support the hypothesis that FXR agonism can reduce TNFα-induced mucosal inflammatory cytokine secretion.

4.2 Introduction and aims

The results presented in chapters 2 and 3 are of experiments performed using epithelial cell-line and mouse models. A more accurate prediction of the role of FXR in ileal CD may be provided by studies utilising primary tissue from patients with the disease. The studies of FXR agonism presented here are intended to be, in part, proof of concept to show that primary ileal tissue can be successfully cultured and experimentally manipulated *ex-vivo*.

There are only a few studies of the role of FXR using primary tissue from patients with CD. Nijmeijer et al. demonstrated that FXR activity, as measured by SHP expression, is lower in the ilea of patients with a Crohn's colitis as compared with healthy controls(Nijmeijer et al., 2011). There are no published data on the role of FXR in patients presenting with ileal CD, the most common site for disease activity. This dearth of studies may be because access to primary ileal tissue is more difficult than access to mucosal tissue from the colon, due in part to technical issues (e.g. reaching the ileum during colonoscopy), but also due to the ethics of biopsying normal ileal tissue in healthy controls.

The organ culture of small intestinal mucosal biopsies, originally described by Browning and Trier(Browning and Trier, 1969), has been used to study a variety of small bowel enteropathies. This technique has been used successfully to study GI diseases as diverse as coeliac disease, necrotising enterocolitis, bile acid malabsorption and IBD(Nanthakumar et al., 2000, Monteleone et al., 2001, Fina et al., 2011, Zhang et al., 2013). This model provides an architecturally preserved epithelial layer, complete with its associated stromal and immune cells (e.g. M-cells, dendritic cells, IELs, macrophages). This allows the experimental manipulation of the intact human mucosa, providing a more holistic model of mucosal immune function than simple epithelial cell-line models. There was no

expertise in organ tissue culture within our group prior to this thesis, but it was felt that this would provide a good model system for the study of FXR agonism in ileal CD.

The hypotheses were that FXR and downstream gene expression would be reduced in the ilea of patients with CD as opposed to controls; that the cytokine milieu from diseased tissue would be more pro-inflammatory than control; and that co-culture with an FXR agonist would attenuate the response of primary tissue to stimulation with inflammatory cytokine.

Therefore, the aims of the experiments in this chapter were:

1. To optimise an *ex-vivo* ileal mucosa culture model.
2. To assay the effect of FXR agonism using this optimised model as a proof of concept pilot study.
3. To compare FXR activity in patients with ileal CD as compared with control.

4.3 Methods

4.3.1 Ethics and consent

Samples were collected and stored in accordance with the Human Tissue Act (2004), with approval from the Local Research Ethics Committee (LREC - Newcastle and North Tyneside). The Hepatopancreatobiliary (HPB) and Gastroenterology research groups at Newcastle University have an agreement, from the LREC, to collect and store research samples without the need to obtain specific consent for individual projects (REC number 10/H0906/41). The project was approved by the HPB/Gastroenterology Biobank Committee prior to the collection of any samples. Details of all projects falling within the remit of the HPB/Gastroenterology Biobank are submitted to the LREC as part of an annual report for audit and review. A copy of the Biobank submission request proforma can be found in the appendix.

Patient consent was obtained in accordance with the General Medical Council's 'Good Medical Practice' guidance(GMC, 2013). A patient information leaflet explaining the process was provided to all participants. Prior to their procedure, all patients provided written, informed consent for their tissue to be stored and analysed. A copy of the patient information leaflet and patient consent form can be found in the appendix.

4.3.2 Patient recruitment and control group

Included in the study were consecutive patients undergoing right hemi-colectomy or ileo-caecal resection, for colonic cancer or ileal CD. Patients were recruited at the Royal Victoria Infirmary, Newcastle upon Tyne, between March and July 2014. In total, ileal samples were collected from 11 patients, 6 patients with CD and 5 patients with some form of colonic or caecal tumour.

Patients undergoing ileo-caecal resection or right hemi-colectomy for cancer were included as controls. This patient group was chosen as a control group to circumvent the ethical problem of collecting ileal tissue from healthy patients. Whilst ileal tissue can be readily reached by the colonoscope, routinely biopsying normal ileal tissue is contra-indicated due to the small, but theoretically increased risk of variant Creutzfeld-Jacob disease transmission from prion proteins prevalent in Peyer's patches within the ileum(Rutter, 2005). Collecting ileal control samples from healthy human individuals, with no clinical indication for biopsy, could, therefore, be potentially unethical.

Abundant ileal tissue can, however, be accessed from patients undergoing surgical resection for cancer. As justification for using this control group, published evidence demonstrates that, whilst FXR expression is reduced within cancer tissue itself, it is unaltered in the surrounding GI tissue unaffected by cancer(Modica et al., 2008, A. M. Bailey et al., 2014).

There were no exclusion criteria. Patient demographics were collated at the time of recruitment to the study. Data as to final histological diagnosis, disease phenotype (stricturing, penetrating etc.) and medical treatment (including use of biological) was recorded using patient records at a later date. Patient identifiable information was stored in a separate site file within the Newcastle upon Tyne NHS Foundation Trust.

4.3.3 *Ex-vivo* organ culture of ileal mucosa

By combining elements from several of the published techniques, a variety of optimisation experiments were performed. These experiments included the histological comparison of tissue following; i) culture with different formulations of growth media with, for example CMRL 1066 or RPMI with and without HEPES

buffer, gentamycin and hydrocortisone; ii) sample preparation as a full-thickness specimen (all mucosal and serosal layers), as a dissected mucosal-role (all mucosa with serosa removed) or with biopsy forceps (epithelial and stromal layer) and; iii) tissue supported either completely submerged in growth media, on chemokine filters in a 6 well plate or on organ tissue culture plates with a nylon filter to provide an air-liquid interface. At 40 hours, the mucosal tissue samples were formalin fixed and paraffin embedded (FFPE). Sections were then stained with H&E and viewed microscopically to assess for histological architecture and enterocyte viability. Examples of these optimisation H&E sections are presented in the results section (figure 4.7). Standard ELISA experiments were also performed for IL-6 and IL-8 as described in chapter 2.

4.3.4 Final protocol

Following right hemi-colectomy or ileo-caecal resection, a $2cm^2$ longitudinal section of ileum was dissected from the surgically resected ileo-caecal specimen. Care was taken to avoid the ileo-caecal resection margin, as per clinical pathology guidance. Dissection of the sample for experimentation was performed in the operating theatre as soon as the ileo-caecum was removed from the abdominal cavity to minimise ischaemic time. The resected piece of ileum was then suspended in ice-cold growth media and transported on ice to the laboratory immediately. Growth media consisted of CMRL 1066 (Gibco, Life Technologies) supplemented with 25 mM HEPES buffer (Sigma), 10% heat inactivated FCS (Biosera), 2mM L-glutamine, 100units/ml penicillin and 100μg/ml streptomycin (all Sigma).

The tissue was washed on an orbital shaker in 35ml of ice-cold PBS containing 100units/ml penicillin and 100µg/ml streptomycin for 1 minute. The ice-cold PBS was replaced and the washing step was repeated.

The mucosal surface of the ileal section was identified and 8 mucosal biopsies were taken using Radial Jaw 4 Biopsy Forceps (Boston Scientific, Alajuela, Costa Rica). The use of forceps standardised the sample size to 8mm and was also found to produce a mucosal sample that was thin enough to allow diffusion of oxygen and nutrients.

Two biopsies were snap frozen by submersion in liquid nitrogen-cooled isopentane, then placed in cryovials and frozen in liquid nitrogen before storage at -80 ^{o}C.

Six biopsies were mounted on individual 100µm nylon filters (BD Falcon) with the luminal, mucosal surface facing uppermost. Filters were then placed on the central well of a sterile organ culture plate (BD Falcon) as shown in figure 4.1; 2 ml of growth media was added to the central well, to just cover the tissue sample by capillary action, and 1 ml of growth media was added to the moat, to prevent samples from dehydrating. The organ culture plates were incubated in 5% CO^2 humidified atmosphere at 37^{o}C. The growth media was changed after 12 hours and the supernatant was collected in a 1.5ml Eppendorf and stored at -80 ^{o}C for later cytokine analysis. At 12 hours, vehicle (DMSO) or 1µM 6-ECDCA was added to the mucosal surface of the biopsy sample and the plates were returned to the incubator. At 24 hours, TNFα 100ng/ml was added to the growth media in the organ culture plate well. At 40 hours, the supernatant was again harvested and stored in a 1.5ml Eppendorf at -80 ^{o}C. The biopsy samples were snap frozen as described above and stored at -80 ^{o}C

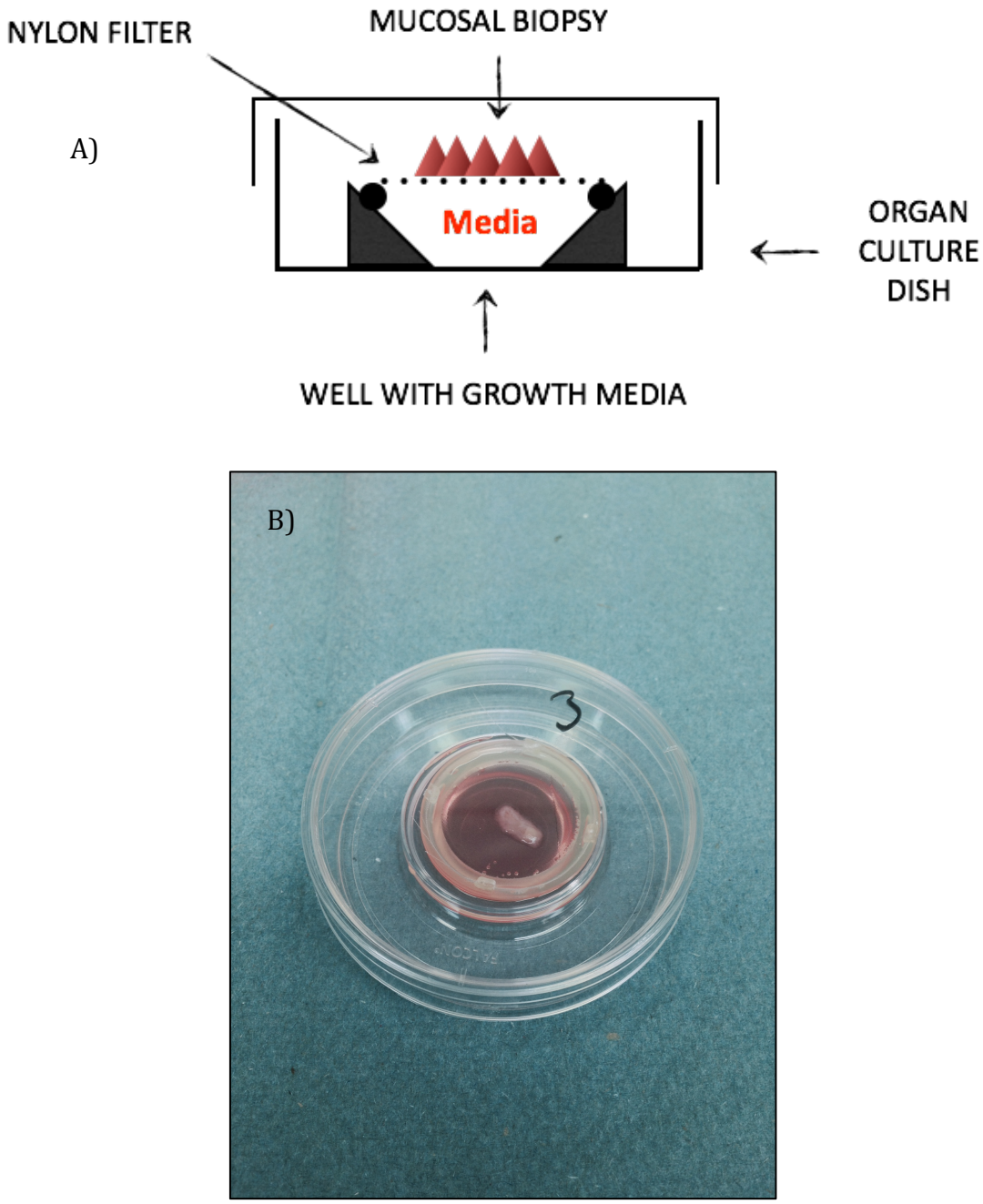

Figure 4.1; A) Schematic representation of organ culture dish with biopsy placed on nylon filter, epithelial surface uppermost. B) Photograph of sample on filter in organ culture dish. Well is filled with growth media such that it is drawn over the mucosal sample by capillary action.

4.3.5 Real-time reverse transcription polymerase chain reaction (RT-PCR)

RNA was isolated using the RNeasy Mini Kit and the RNase-Free DNase Set, by QIAGEN (74104, 79254), as per the manufacturers guidelines. All RNA work was performed using RNase-free reagents and equipment. Laboratory surfaces were

cleaned with RNase decontamination solution (RNaseZap, Ambion, Life Technologies) prior to experiments and pipette filter tips were used.

RNA was extracted from ileal biopsy samples that had been snap frozen immediately following resection and washing and then stored at -80 ^{o}C. Two mucosal biopsy samples, from each patient, were removed from the freezer and suspended in 600µl of buffer RLT with β-mercaptoethanol (10µl per ml of buffer), in a 2.0ml Precellys ceramic bead kit tube (1.4/2.8mm beads), manufactured by Peqlab. The tissue was then homogenised using a Bertin Minilys tissue disruptor using 4 x 25 second cycles of disruption, with a 45 second rest between cycles. Samples were stored on ice between cycles of disruption. A 700µl solution of 70% ethanol was then added to the supernatant and the solution was gently mixed. Next, 700µl of the sample was transferred to an RNA spin column, in a 2ml collection tube, and spun at 8,000 x g for 15 seconds. The flow through was discarded and 350µl of buffer RW1 was added and a further 8,000 x g for 15 second spin was performed. An 80µl solution, containing 10µl of DNase I in 70µl of buffer RDD, was added to the spin column and left to incubate on the bench top for 15 minutes. After incubation, the DNase I solution was rinsed out with 350µl of buffer RW1, centrifuged at 8,000 x g for 15 seconds. The flow through was discarded. The spin column was then washed with two cycles of 500µl buffer RPE, spun for 8,000 x g for 15 seconds and 2 minutes respectively. A drying step was performed with the spin column in a fresh 2ml collection tube, spun at 8,000 x g for 1 minute. Finally, the RNA was precipitated in 30µl of nucleic acid and RNase-free water and spun for 8,000 x g for 1 minute to collect the RNA containing precipitate in a fresh, 1.5ml Eppendorf. The quantity and quality of extracted RNA was measured using a Nanodrop spectrophotometer and also by gel

electrophoresis as described in chapter 2. A spectrophotometer example of RNA purified using this method is demonstrated in figure 4.2.

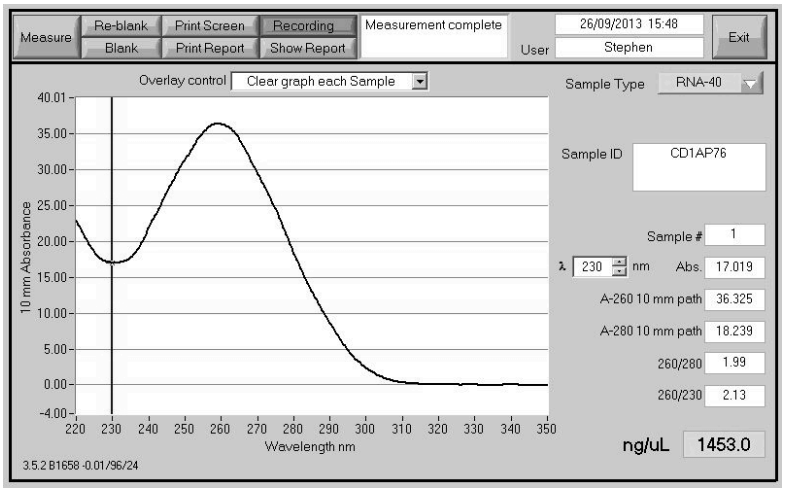

Figure 4.2; A Nanodrop spectrophotometer reading as an example to demonstrate the purity of RNA isolated from human ileal biopsy as described in the text.

Complementary DNA (cDNA) was prepared using the Tetro cDNA Synthesis Kit (Bioline) as described in chapter 2. The subsequent cDNA was then used as the template to perform TaqMan-based (Life Technologies) RT-PCR experiments, as previously described in chapter 2. From the ileal samples of each patient, the relative mRNA level of FXR, IBABP, SHP, TNFα, IL-6 and IL-8 were measured. GAPDH was used as the reference (housekeeper) gene. Table 4.1 shows the primer/probes used in these experiments. Quality control was performed as described in chapter 2 (e.g. triplicate samples, no template control [NTC] and primer validation).

Protein	Gene	Exon spanning	Primer/Probe
FXR	NR1H4	yes	Hs01026590_m1
SHP	NR0B2	yes	Hs00222677_m1
IBABP	FABP6	yes	Hs01031183_m1
IL-6	IL6	yes	Hs00985639_m1
IL-8	IL8	yes	Hs00174103_m1
GAPDH	GAPDH	yes	Hs02758991_g1

Table 4.1; List of genes of interest and TaqMan primer/probes used in chapter 4

Primer efficiency validation plots were produced for the human TaqMan primer/probes for FXR, IBABP, SHP, IL-8, IL-6, TNFα and GAPDH. As described in chapter 2, the efficiency for each primer can be calculated using the slope of the standard curve and should be in the acceptable range 90% to 110%. The goodness of fit (R^2) should be greater than 0.98. Figure 4.3 and table 4.2 demonstrate the validation plots and primer efficiency for each primer/probe used in these experiments.

Primer	Slope	Efficiency	R-squared
FXR	-3.273	102.1%	1.00
SHP	-3.193	105.7%	0.99
IBABP	-3.17	106.8%	0.97
IL-8	-3.127	108.8%	0.99
MLCK	-3.279	101.8%	1.00
GAPDH	-3.349	98.9%	0.96

Table 4.2; Primer efficiency and goodness of fit (R^2) for primers used in chapter 4. See fig 4.3

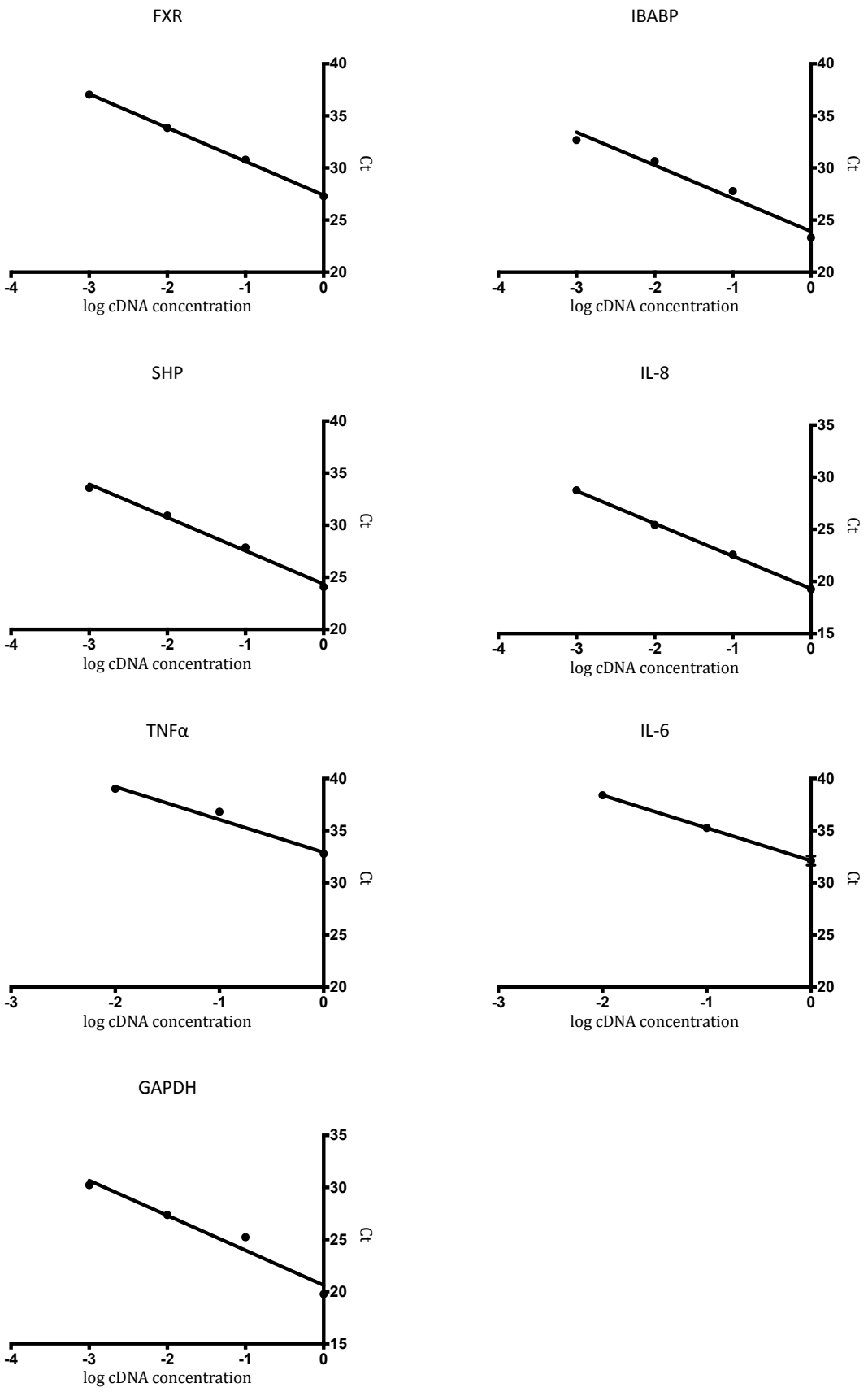

Figure 4.3; Primer validation experiments for primers used in chapter 4. Threshold cycle is measured for serial dilutions of cDNA. See table 4.2 for R^2 and efficiency calculation

Relative quantification was used to calculate the relative expression of the genes of interest, as described in chapters 2 and 3. Relative quantification was calculated using the ΔΔCt method as described by Livak and Schmittgen(Livak and Schmittgen, 2001). As in chapter 3, in order to represent the degree of SE, but also to give an idea of relative ratio changes, data are presented both as ΔΔCt values with error and as fold change.

4.3.6 Detection of pro-inflammatory cytokines using a multi-array, electro-chemical luminescence assay

A panel of pro-inflammatory cytokines was measured in the supernatant from the organ culture experiments.

A cytokine assay for IFN-γ, IL-1β, IL-6, IL-8, IL-12p70, IL-13 and TNF-α was performed using a V-PLEX Multi-Spot Assay System (K15049D, Meso Scale Diagnostics, Maryland, U.S.A.). This is a sandwich assay (capture antibody, detection antibody with electrochemiluminescent probes) performed in pre-prepared plates with all 7 cytokines being assayed in each well. Figure 4.4 is a schematic representation of the process in the product literature provided by the manufacturer.

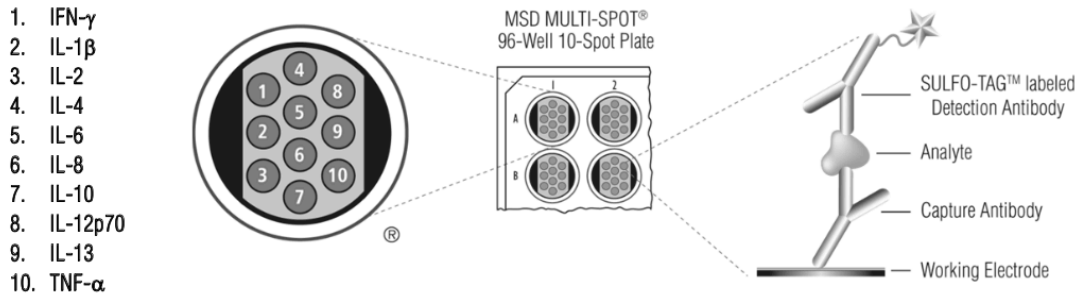

Figure 4.4; A schematic demonstrating the placement of capture antibody in each well of an MSD mutli-array plate (left) and sandwich detection assay with electro-luminescent detection antibody, cytokine (analyte) and capture antibody (right).

The cytokine assay was performed as per the manufacturer's guidelines. A calibrating serial dilution was prepared by adding 1000µl Diluent 2 to the lyophilized calibrator vial, to produce the highest calibrator. The highest calibrator was then serially diluted 1:4, using Diluent 2, a further 5 times. Diluent 2 is used as a zero calibrator. The detection antibody solution was prepared by adding 60µl of each detection antibody (Anti-hu IFN-γ, IL-1β, IL-6, IL-8, IL-12p70, IL-13 and TNF-α antibodies) to 2400µl of Diluent 3.

50µl of sample (either supernatant or homogenised tissue) or calibrator was added to each well of a V-PLEX plate and incubated at room temperature for 2 hours on an orbital shaker. The plate was washed x3 in an automated plate washer (Thermo Fisher), using a wash buffer comprised of 1800ml water, 200ml 1% PBS and 1ml Tween-20. 25µl of detection antibody solution was added to each well and incubated for a further 2 hours, at room temperature, on an orbital shaker. The plate was washed 3x and then 150µl of Read Buffer T was added to each well. The plate was then read in a SECTOR Imager 2400 machine (Meso Scale Diagnostics).

A Pierce BCA Protein Assay (Thermo Scientific), as described in chapter 2 (section 2.3.8), was performed. The mean protein mass per tissue sample was found to be 0.88 +/- 0.27 mg/ml. Results from the cytokine detection assays were then converted from concentration of cytokine per volume of supernatant (pg/ml) to concentration of cytokine per mass of protein (pg/mg).

4.3.7 Statistics

Unpaired Student's *t*-tests and linear regression analyses were calculated using Prism version 6.0e, Graphpad software, San Diego. All P values were 2-tailed, and a P value of 0.05 or less was considered statistically significant. The cytokine assay

data set was tested for outliers using the ROUT method (Q=1.0%), as described by Motulsky and Brown, in Prism version 6.0e, Graphpad software, San Diego(Motulsky and Brown, 2006).

4.4 Results

4.4.1 Study patient demographics

Enrolled in the study were 6 patients with CD (mean age 53 +/- 18 years, all female) and 5 patients with a caecal cancer (mean age 68 +/- 19 years) as controls. There was no significant difference in age between the two groups (p=0.21). The majority of patients included in the study were female (9/11). No patients refused consent to enter the study and there is no gender bias for either the risk of developing colorectal cancer or CD.

Tables 4.3 and 4.4 demonstrate patient demographics for CD patients and controls, including disease phenotype, medical treatment at time of surgery and final histology.

Two patients (1 with CD and 1 control) were used for organ culture optimisation studies. Tissue from the other 9 patients (5 CD, 4 control) was used in the organ culture experiments. RNA of sufficient quality was only isolated from 8 patients (5 CD and 3 control) for RT-PCR experiments.

Patient Identifier	Age	Gender	Diagnosis	Disease Site	Phenotype	Treatment	Histology	Experiments
CD47 PR	67	F	Crohn's disease	Ileocaecal	Stricturing	Nil	Stricturing, mildly active	PCR/Organ culture
CD45 ER	69	F	Crohn's disease	Ileocaecal and perianal	Stricturing	Thiopurine	Stricture, active inflammation	PCR/Organ culture
CD75 SD	39	F	Crohn's disease	Terminal ileal disease	Stricturing	Steroids	Stricture, active inflammation	PCR/Organ culture
CD85 SC	29	F	Crohn's disease	Terminal ileal	Fistulating	Anti-TNFα	Severe, active disease	PCR/Organ culture
CD45 LB	69	F	Crohn's disease	Terminal ileal and perianal	Fistulating	Steroids	Perforated stricture	PCR/Organ culture
CD72 CM	42	F	Crohn's disease	Ileocaecal	Stricturing	Thiopurine/ Anti-TNFα	Stricture, active disease	Optimisation
Mean age (+/-SD)	53 (+/- 18)							

Patient Identifier	Age	Gender	Diagnosis	Histology	Experiments
Ctrl80 RD	34	M	Neuroendocrine tumour of appendix	Unremarkable ileum, appendicectomy. 2/21 nodes mets. disease (NET)	PCR/Organ culture
Ctrl38 ML	76	F	Caecal adenocarcinoma	Moderately differentiated adenoca. Dukes'A	PCR/Organ culture
Ctrl43 LB	71	F	Caecal adenocarcinoma	Poorly differentiated adenoca. pT3, N0	PCR/Organ culture
Ctrl40 SL	74	M	Caecal adenocarcinoma	Poorly differentiated adenoca. pT4b, N1	Organ culture
Ctrl31 ER	83	F	Caecal adenocarcinoma	Poorly differentiated adenoca. pT3 N0. Dukes B.	Optimisation
Mean age (+/-SD)	68 (+/-19)				

Tables 4.3 (previous page) and 4.4 (this page); characteristics of patients enrolled in the studies of FXR activity in ileal mucosa in chapter 4

4.4.2 FXR expression and FXR activity is decreased in patients with ileal Crohn's disease

Figure 4.5 demonstrates that there was significantly less FXR expression in patients with ileal CD as compared with controls (p=0.004,). In addition, the activity of FXR, as measured by the downstream gene expression of SHP and IBABP, was also significantly reduced (p=0.02 and p=0.02 respectively). Two-tailed *t*-tests, were performed by comparing ΔCt values for each biological sample. Figure 4.5 demonstrates relative mRNA levels of FXR, SHP and IBABP expression in comparison with control patients, as expressed as a ΔΔCt value. As detailed in chapter 2, ΔΔCt is the difference in the relative expression level of the gene of interest between the intervention group (those with CD) and the control group (those without CD).

Figure 4.6 demonstrates the change in relative expression, as compared with controls, as a fold change. A fold reduction of 0.04 was found for FXR, 0.11 for SHP and 0.01 for IBABP. Error bars are not included, as SE becomes meaningless when the calculation to non-normally distributed data is made.

Data are presented in both formats (ΔΔCt and fold change) to allow an appreciation of the degree of error in addition to the fold increase or decrease.

4.4.3 There is a trend to increased levels of inflammatory cytokine in the ileal mucosa of patients with Crohn's disease

There was a trend suggesting increased relative mRNA levels of the inflammatory cytokines IL-6, TNFα and IL-8 in the ileal mucosa of patients with CD as compared with controls (see figures 4.5 and 4.6). A fold change of 3.96 was found for IL-6, 3.36 for TNFα and 6.44 for IL-8. However, two-tailed *t*-tests are not significantly different (IL-6 p = 0.44, TNFα p = 0.51, IL-8 p = 0.24) and therefore the null

hypothesis is not disproved. Figures 4.5 and 4.6 demonstrate the relative mRNA levels of IL-6, TNFα and IL-8 expression in comparison with control patients, expressed both as a ΔΔCt value and as a fold change. Again, data are presented in both formats to allow an appreciation of the degree of error in addition to the fold increase or decrease.

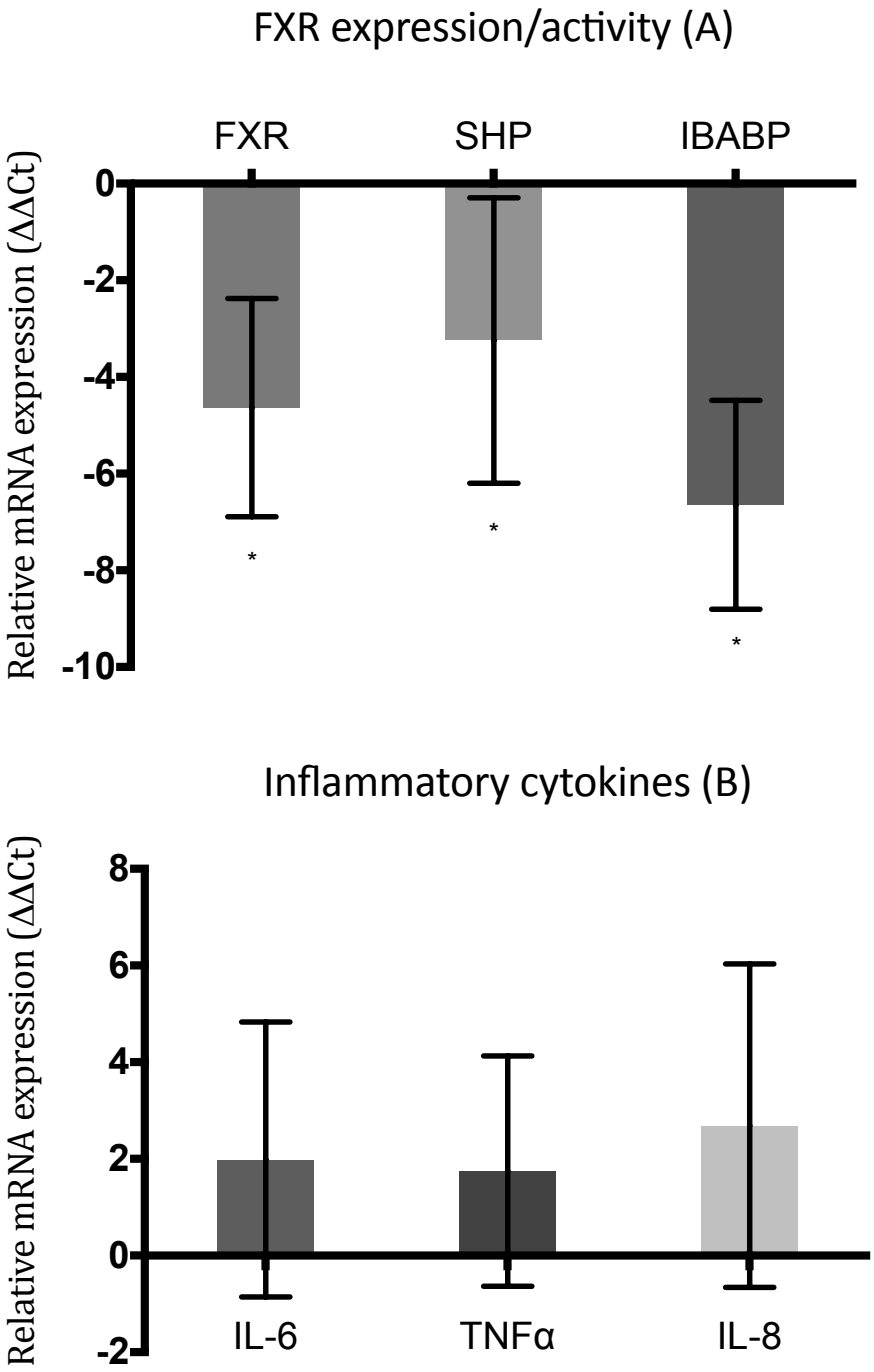

*Figure 4.5; Relative mRNA levels (ΔΔCt) of FXR and its downstream targets (A) and inflammatory cytokines (B) in the ileal mucosa of patients with CD as compared with controls.(n=8, SE, * p<0.05 t-tests)*

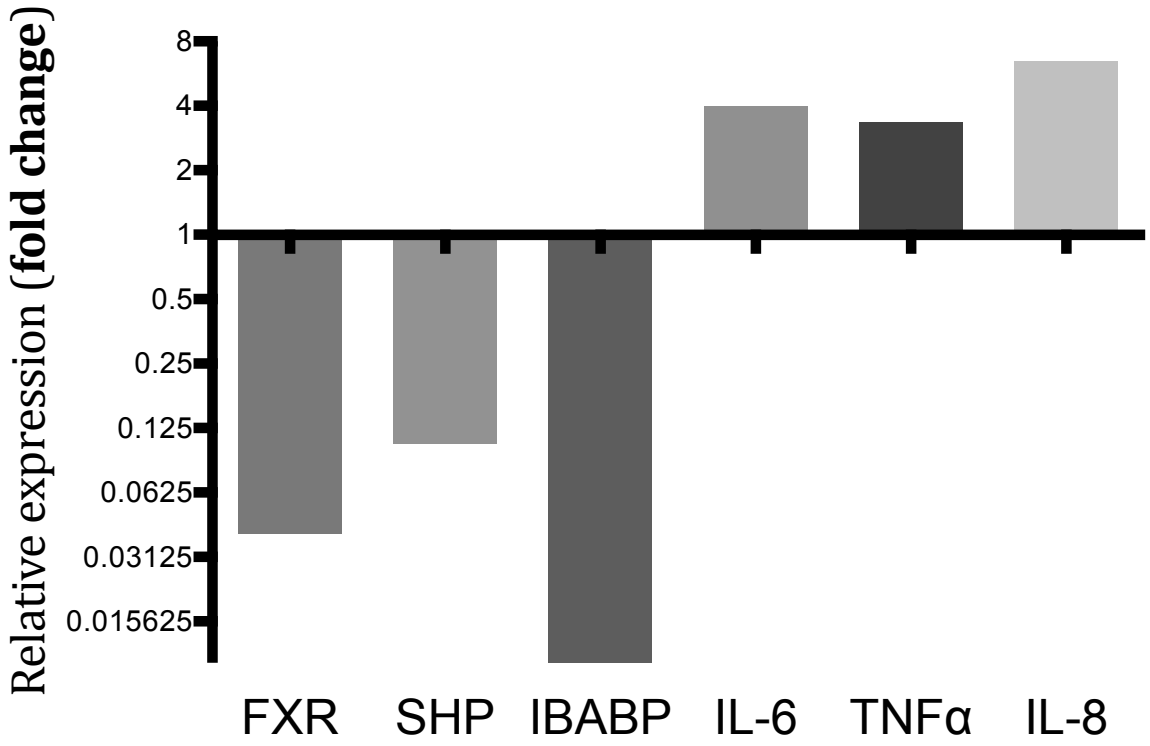

Figure 4.6; Relative mRNA levels of FXR and downstream genes with inflammatory cytokine in the ileal mucosa of patients with CD, in comparison with control. Expressed as a fold change. (n=8)

4.4.4 Short-term, *ex-vivo* ileal explant culture is biologically viable

Optimisation experiments were performed as described in section 4.3.3. The addition of hydrocortisone and/or gentamycin to the growth media had no effect either on the histology or the production of IL-6 and IL-8 as measured by sandwich ELISA (results not shown). The results from a variety of experiments demonstrate that the ex-vivo explant culture protocol can be used to study BA signaling via FXR.

4.4.4.i H&E stains demonstrate viable enterocytes at 40 hours

A variety of micrographs of H&E stained ileal explant tissue are demonstrated in figure 4.7. Micrographs from initial optimisation experiments are presented to demonstrate dead tissue with few, if any, viable enterocytes. The crypts are empty, with barely any nucleated enterocytes, in keeping with severe ischaemic injury (see figure 4.7 A & B). In these images the tissue has been sectioned in a saggital plane (crypts and villi longitudinally).

Explant cultured tissue using the developed protocol is also shown (see figure 4.7 D & E). In these micrographs, the villi have been sectioned in a transverse plane. Abundant, nucleated enterocytes can be clearly seen with associated goblet cells and inflammatory cells within the lamina propria.

The difference in the planes of sectioning was due to the orientation of the tissue when embedded within the paraffin block. Ideally, to allow a better comparison, H&E sections should have been presented using the same orientation, but unfortunately these were not available.

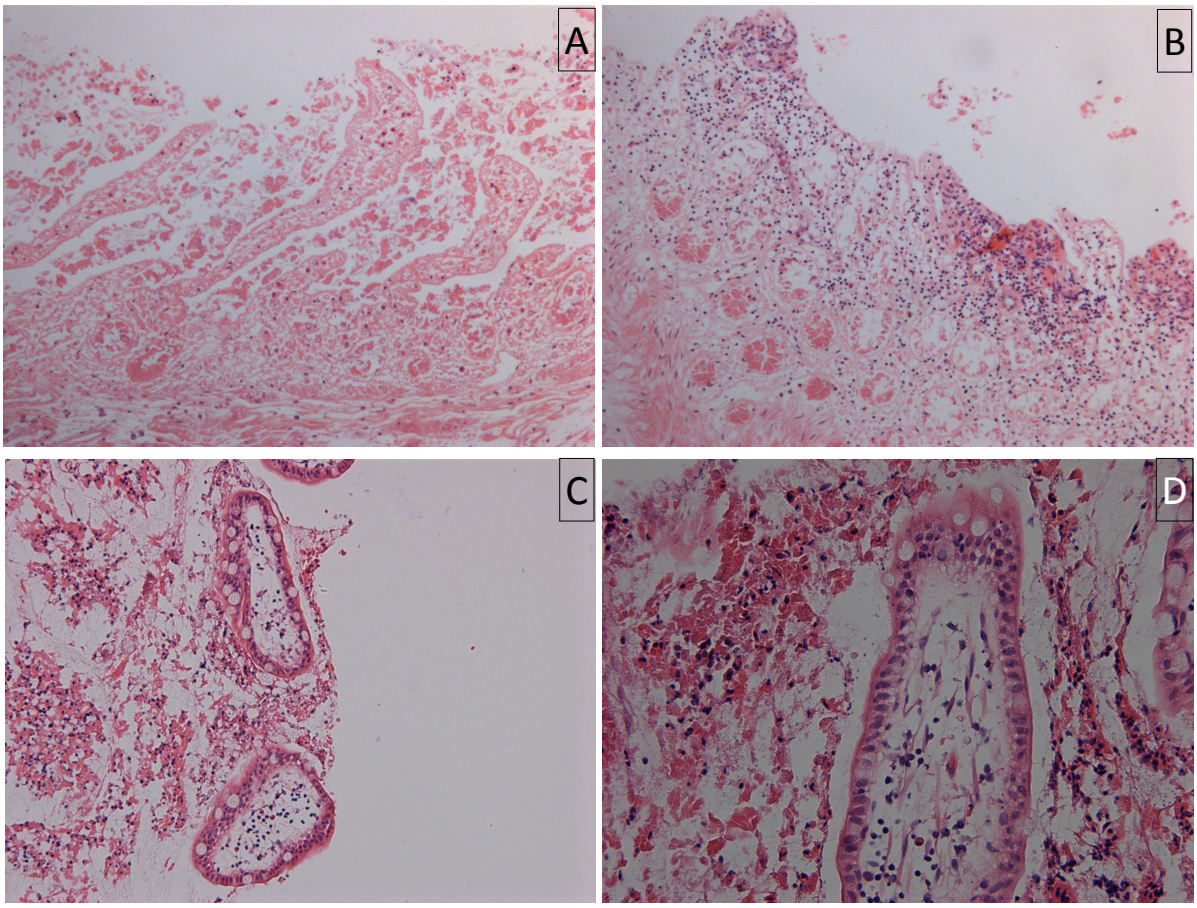

Figure 4.7 (A-D); H&E stains (x10 to x20 magnification) of ileal explant tissue culture. Slides A & B are from optimisation steps at 40 hours and demonstrate ischaemic, dead tissue with few if any viable enterocytes (saggital plane). The crypts are largely denuded. Slides C & D are from cultured tissue at 40 hours using the final protocol (villi sectioned in transverse plain). Abundant nucleated viable enterocytes and associated goblet cells can be seen.

4.4.4.ii Ileal tissue from CD patients produces higher concentrations of inflammatory cytokine than control

The concentration of a panel of inflammatory cytokines was measured in the supernatant from ex-vivo cultured ileum at 12 hours. In keeping with the expected finding, the secretion of inflammatory cytokine was higher from the ileal tissue of patients with CD as compared with controls (see figure 4.8 a, b). This difference was significant for TNFα, IL-12p70 and IL-13 ($p = 0.04$ 95% CI 1.06-53.33, $p = 0.03$ 95% CI 0.69-6.49 and $p = 0.02$ 95% CI 4.21-22.91, respectively). Whilst not significantly different, there was a consistent trend for increased concentrations of IFNγ, IL-6, IL-1β and IL-8 in the supernatant from the cultured ileal mucosa of CD patients versus control.

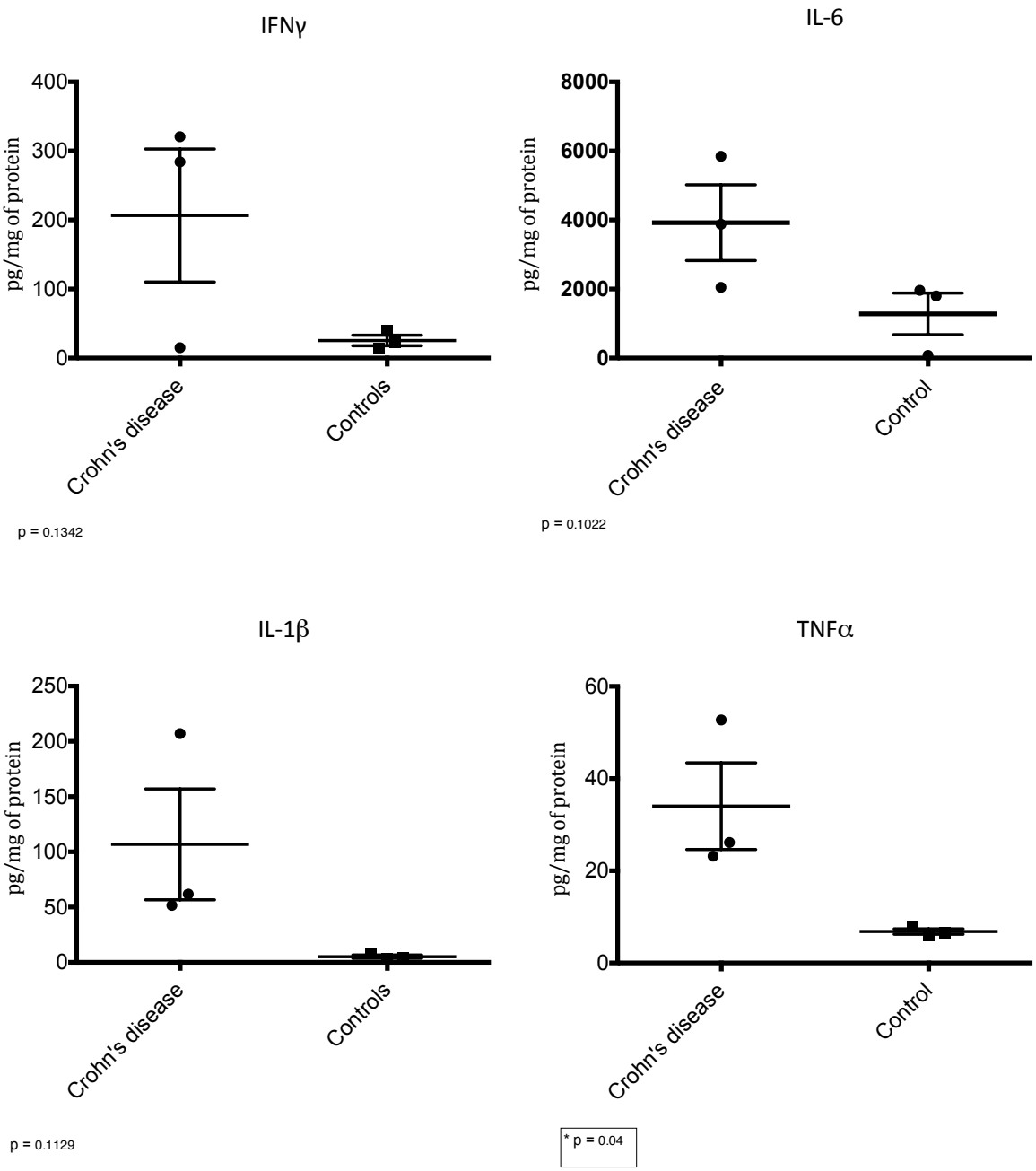

Figure 4.8 (a); The concentration of IFNγ, IL-6, IL-1β and TNFα in the supernatant from 12 hours organ culture of tissue from patients with Crohn's disease versus control. (n=9, SEM, outliers tested by ROUT method)

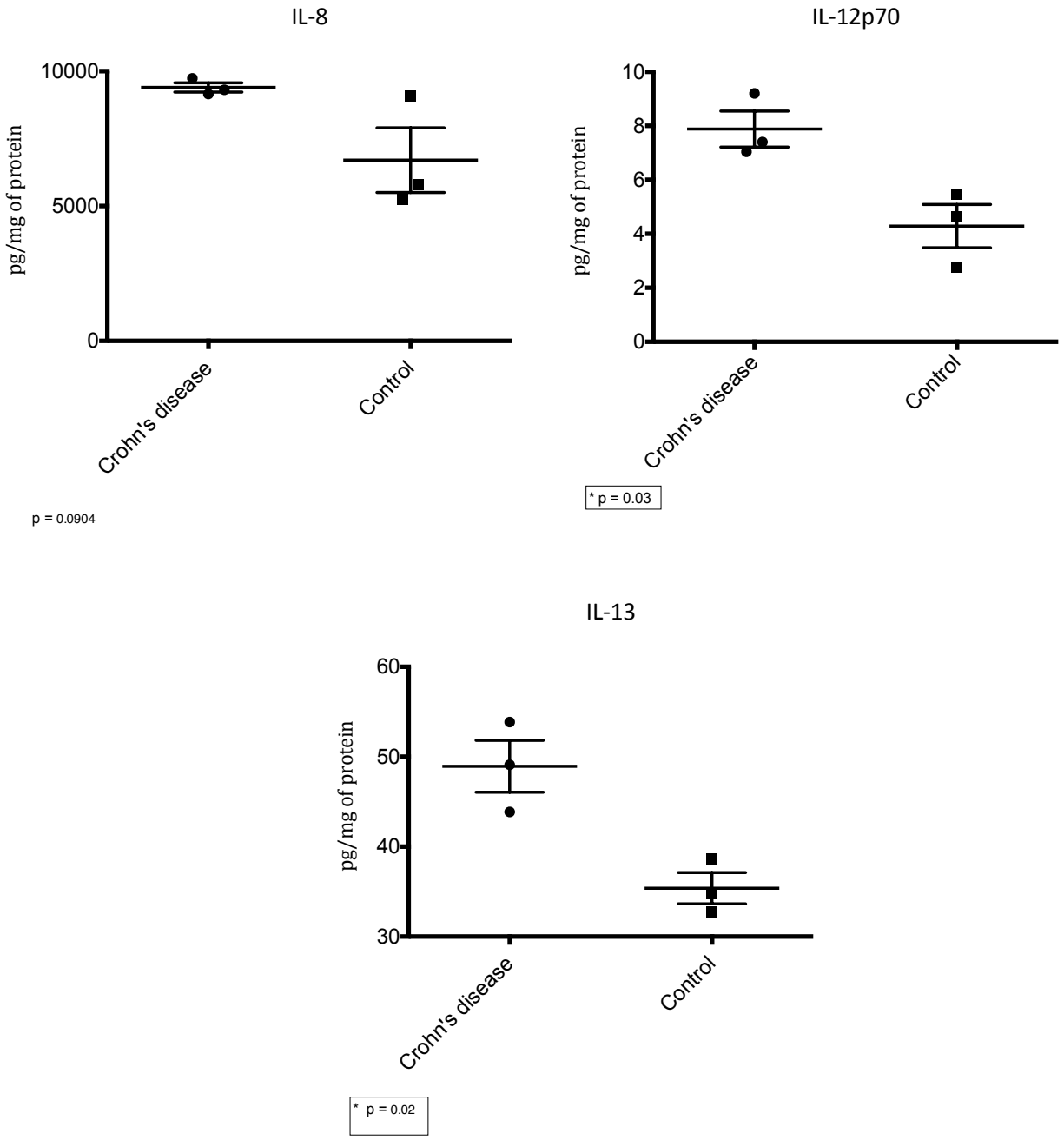

Figure 4.8 (b); The concentration of IL-8, IL-12p70 and IL-13 in the supernatant from 12 hours organ culture of tissue from patients with Crohn's disease versus control. (n=9, SEM, outliers tested by ROUT method)

4.4.4.iii Evidence that explanted ileal tissue will produce cytokine when stimulated with TNFα

The concentration of a panel of inflammatory cytokines was measured in the supernatant from ex-vivo cultured ileum after 16 hours of co-culture with TNFα, 40 hours after resection. Figure 4.9 (a & b) demonstrates the concentration of

cytokine in TNFα stimulated tissue in comparison with a vehicle (DMSO) control. There is a significant increase in the production of IL-12p70 and IL-13 ($p = 0.04$ 95% CI 0.15-7.24 and $p = 0.01$ 95% CI 2.90-15.99, respectively) when tissue is stimulated with TNFα. It can be seen that there is a trend for increased levels of cytokine production in the TNFα stimulated group for all of the other inflammatory cytokines assayed, although these changes fail to reach significance. The highly significant increase in the concentration of TNFα ($p<0.0001$), following TNFα stimulation, acts as a positive control for the assay. The concentration of TNFα in the supernatant should clearly increase after the addition of 100ng/ml of TNFα to the organ culture dish. The IL-8 concentration is at, or above, the detection level for the assay and therefore cannot be interpreted. A repeat assay utilising a dilute supernatant sample for IL-8 was not repeated due to the high cost of the V-PLEX plate.

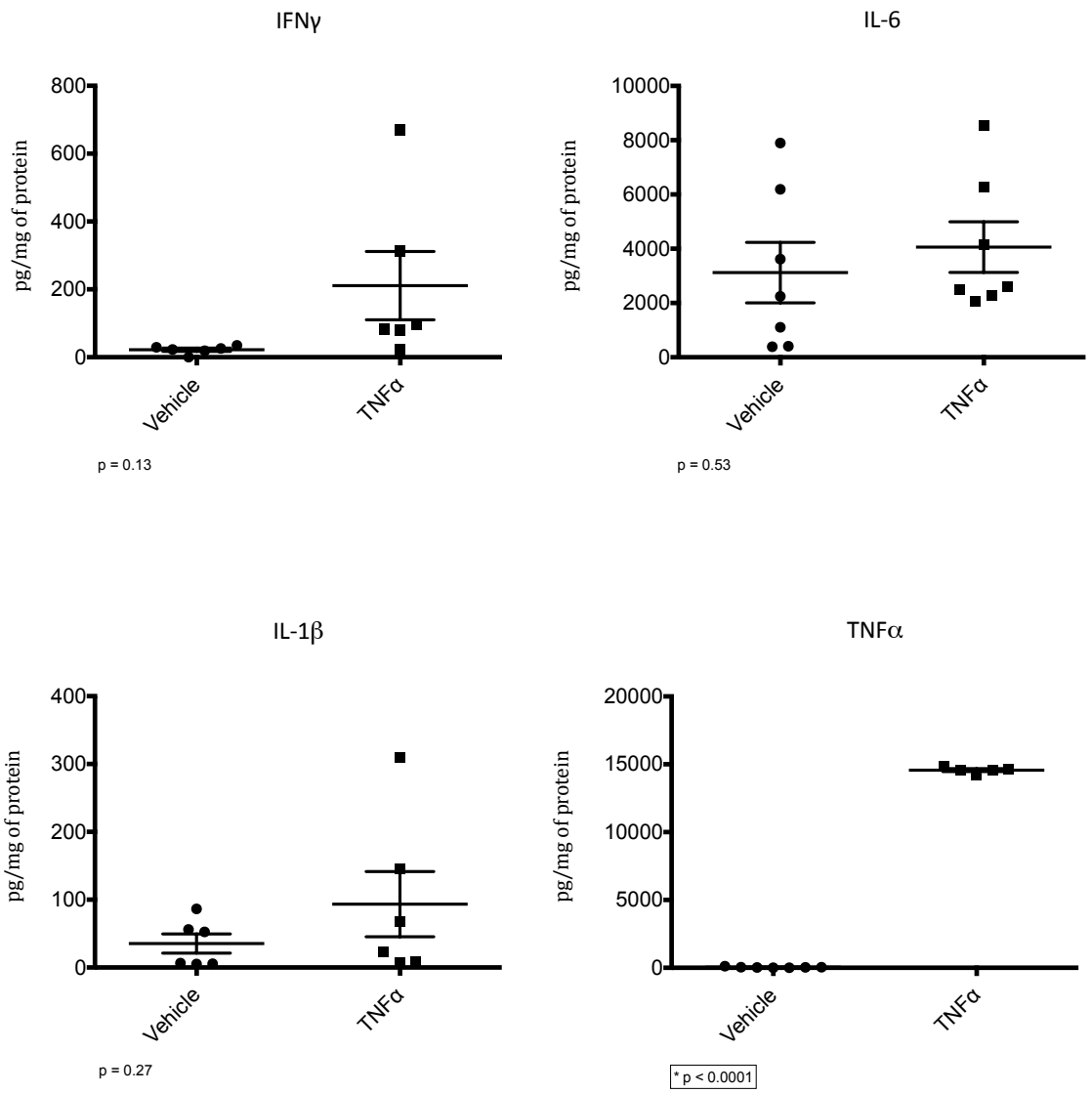

Figure 4.9 (a); Concentration of IFNγ, IL-6, IL-1β and TNFα in the supernatant from ileal tissue cultured with TNFα (100ng/ml), for 16 hours, in an organ culture model. Assays for TNFα and IL-8 are at the upper limit of detection. (n=14, SEM, outliers tested by ROUT)

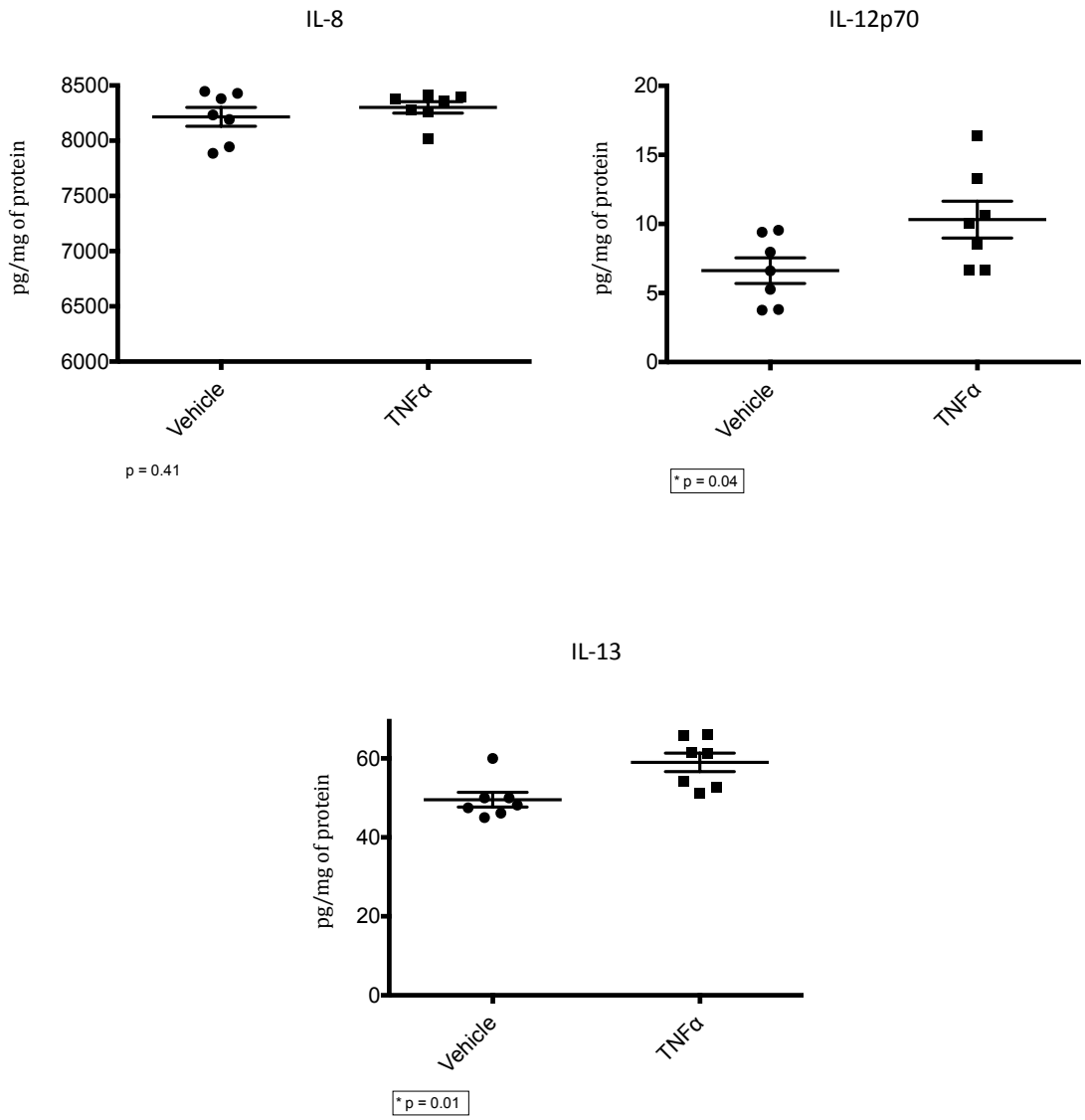

Figure 4.9 (b); Concentration of IL-8, IL-12p70 and IL-13 in the supernatant from ileal tissue cultured with TNFα (100ng/ml), for 16 hours, in an organ culture model. (n=14, SEM, outliers tested by ROUT)

4.4.5 Pilot data suggests that FXR agonism does not ameliorate the pro-inflammatory milieu associated with TNFα stimulation

The concentration of a panel of inflammatory cytokines was measured in the supernatant from ex-vivo cultured ileum following 12 hours of pre-treatment with 6-ECDCA (1μM) or vehicle (DMSO) followed by stimulation with TNFα for 16 hours.

From this pilot data set, treatment with an FXR agonist did not ameliorate the inflammatory cytokine production of human ileal mucosa after stimulation with TNFα, as demonstrated in figure 4.10. There was no statistical difference between the cytokine concentrations from TNFα stimulated tissue treated with 6-ECDCA versus TNFα stimulated tissue treated with vehicle. No consistent trend could be demonstrated between treatment and intervention groups, with a decrease in IL-1β and IFNγ, but an increase in IL-12, IL-13 and IL-6.

Again, the TNFα concentration acted as a positive control group. Likewise, IL-8 is at the limits of the assay detection level and therefore cannot be interpreted.

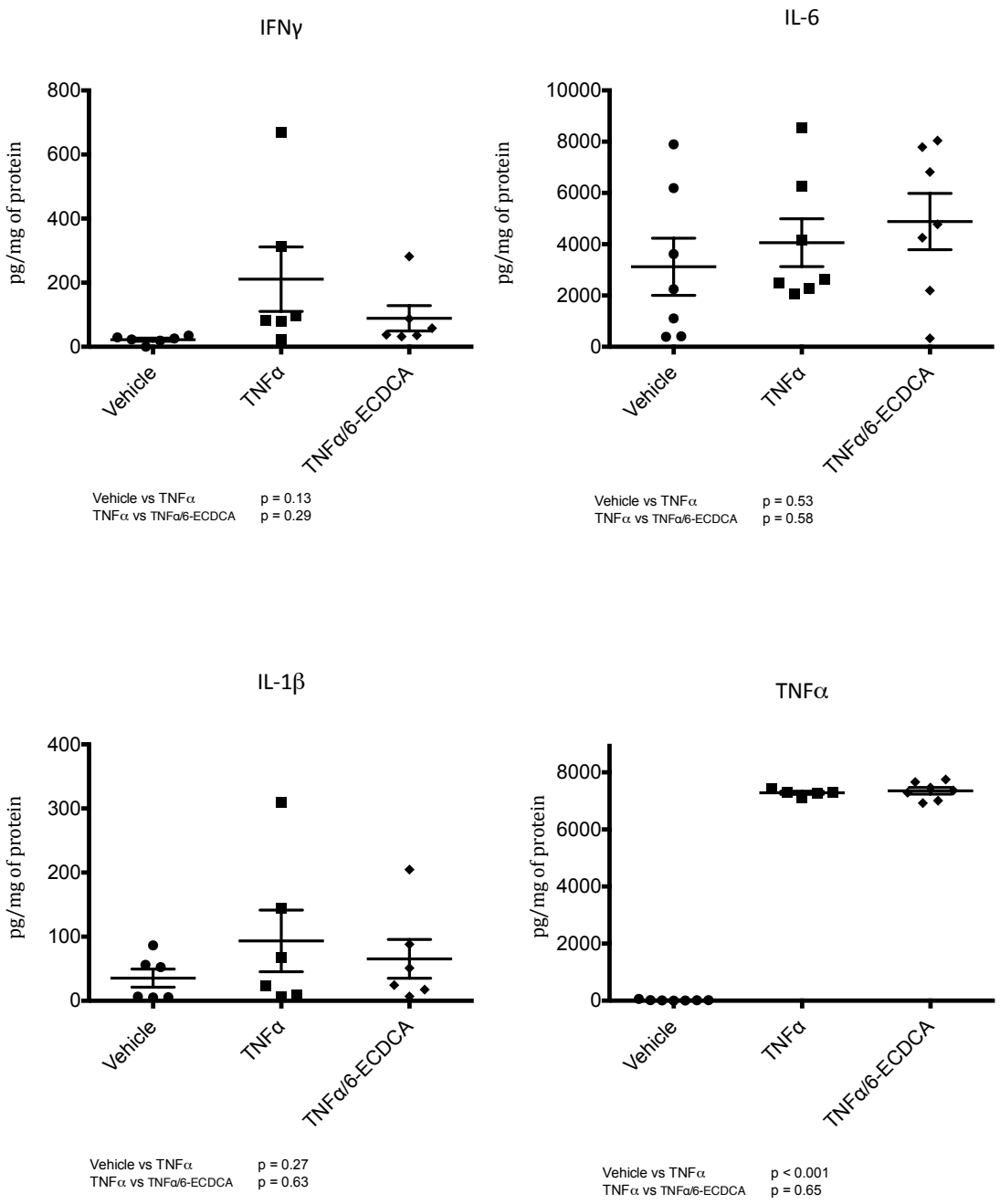

Figure 4.10 (a); The concentration of CD associated cytokines (IFNγ, IL-6, IL-1β and TNFα) in the supernatant of ex-vivo cultured ileal mucosal tissue after stimulation with TNFα in the presence or absence of 6-ECDCA. The concentration of TNFα is at the limit detection in this assay.

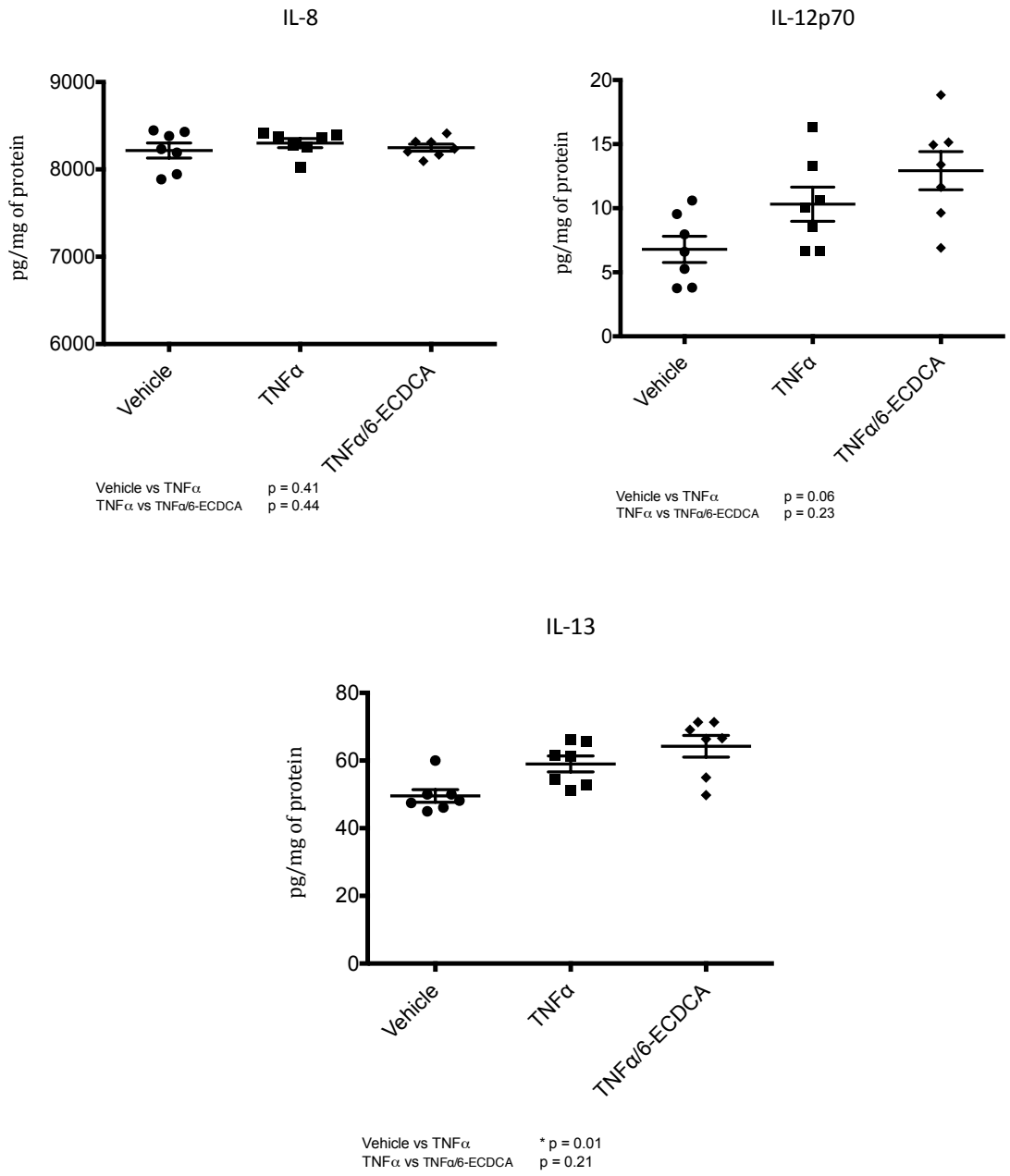

Figure 4.10 (b); The concentration of CD associated cytokines (IL-8, IL-12p70 and IL-13) in the supernatant of ex-vivo cultured ileal mucosal tissue after stimulation with TNFα in the presence or absence of 6-ECDCA. The concentration of IL-8 is at the limit detection in this assay.

4.5 Discussion

There is little published evidence regarding FXR activity in patients with CD. The *ex-vivo* culture of ileal mucosa is a good model in which to study the role of FXR in primary tissue as it allows the experimental manipulation of whole ileal mucosa under controlled conditions.

The aims of this chapter were to optimise an *ex-vivo* ileal mucosal culture model, to assay the role of FXR using this model and to measure the activity of FXR in patients with ileal CD.

This chapter has demonstrated that FXR expression and activity is reduced in the ilea of patients with ileal CD. These patients were undergoing ileal resection for complications of CD and all patients had active inflammation when the histology was examined. This is in keeping with Nijmeijer et al. who demonstrated that FXR activity was suppressed in the ileal mucosa of patients with quiescent CD colitis (rather than ileitis)(Nijmeijer et al., 2011).

Pilot data demonstrates that the technique of *ex-vivo* organ culture of ileal mucosa can be used to study the role of FXR agonism in GI inflammation and fibrosis. This technique was successfully optimised and is new to our laboratory group. However, the pilot data presented here does not support the hypothesis that FXR agonism can attenuate the response of primary tissue to stimulation with inflammatory cytokine. Further study, using a larger sample and different concentrations or different types of FXR agonist would provide a more complete answer.

The finding that FXR expression and activity is reduced in the ileum of patients with CD is in keeping with the hypothesis that a dysregulated BA signalling cascade may predispose to inflammation within the gut mucosa. There is some cell-line

evidence to suggest that FXR may induce its own expression(Modica et al., 2010). Therefore, a reduction in primary BA signaling within the terminal ileum would lead to a reduction in FXR mRNA levels in addition to a reduction in the expression of its downstream targets.

However, FXR is antagonised by NF-κB, a common end point in multiple pro-inflammatory cellular pathways(Gadaleta et al., 2011a). In addition, in active inflammation, the villous architecture is denuded and BA uptake reduced. Therefore, an alternative hypothesis would be that the process of inflammation in CD suppresses FXR expression and activity. In order to help unravel this causality conundrum, the *ex-vivo* organ culture experiments were designed to test whether FXR agonism could reverse the pro-inflammatory effect of stimulation with TNFα. Unfortunately, the sample size is too small to answer this question and so data are presented as part of a pilot study.

By applying a variety of different methods from published descriptions, the optimisation of an ileal mucosa organ culture technique is an important outcome from this thesis. This is a good model of the immune function of the mucosa *ex-vivo*. It is less reductionist than an epithelial cell line model, as all cell types within the mucosa are included, yet allows for a similar degree of experimental manipulation. It is, of course, still only an approximation of the *in-vivo* mucosa, being starved of a blood supply and neuro-humoral inputs.

The evidence that the organ culture model is viable up until 40 hours includes the H&E FFPE sections and the functional data that are in keeping with what would be expected. *Ex-vivo* ileal tissue from patients with active CD produces more pro-inflammatory cytokine than control. In addition, there is evidence that the cultured ileal tissue remains metabolically active as it produces more inflammatory cytokine when stimulated with TNFα. Significantly for IL-12, the

main driver of Th1 differentiation and IL-13. IL-13 is a pro-inflammatory, pro-fibrotic Th2 cytokine that has been shown to be important in the pathogenesis of fistulae in CD(Jovani et al., 2013). There is also a trend for all other effector cytokines assayed to increase when tissue is stimulated with TNFα.

Missing from the optimisation studies is a measure of FXR expression following a period of *ex-vivo* culture. An assumption has been made that FXR is no more affected by a period of relative ischaemia than other cellular receptors. A simple immunohistochemical stain and/or RT-PCR experiment for FXR expression should be performed to confirm that FXR is still expressed in the enterocytes at 40 hours.

There are limitations affecting these experiments. In general, the sample size is too small to determine significance in several assays, although significance for some cytokine concentrations is demonstrated in association with the same trend for others. The small sample size meant that analyses of cytokine response to TNFα stimulation could not be subdivided into CD versus control. It would be of interest to determine whether CD patients respond to TNFα stimulation with or without FXR agonism in the same way as controls. The statistical problem encountered when the sample size is small is well demonstrated by the gender ratio in the study group. Consecutive patients were entered into the study, no patients refused consent and there is no significant gender bias in the presentation of CD or of caecal cancer. The preponderance of females within the study group can, therefore, only be explained as a statistical quirk.

Another criticism is with the choice of cancer patients as 'healthy' controls. The justification for the choice of control group is explained in the methods section. There is published evidence demonstrating that FXR expression is unaltered in cancer patients in areas of tissue unaffected by the cancer itself(Modica et al., 2008); for example, in a patient with caecal adenocarcinoma, the ileal expression

of FXR is the same as a healthy volunteer. However, this evidence was not tested specifically in our control cohort. In addition, there may well have been a low level inflammatory stimulus associated with the cancer that could, theoretically, confound the results. Future studies should mitigate against this by attempting to ethically gain ileal tissue from patients with non-inflammatory conditions.

In the cytokine assays, the concentration of IL-8 was found to be at or above the level of detection for the assay. Given the findings in chapter 2 with regards an FXR induced reduction of IL-8 production, it would be interesting to repeat these experiments using a serial dilution of supernatant until any differences in IL-8 concentration could be determined. This was not repeated for the thesis due to the cost of further V-PLEX plates and also time constraints.

In summary, FXR activity was decreased in the ileal of patients with CD as compared with controls. An ex-vivo organ culture technique for small bowel epithelium was optimised. Whilst, the treatment of ileal mucosa with 1μM 6-ECDCA did not appear to ameliorate the cytokine secretion associated with TNFα stimulation, these are pilot data and requires further study. It could be that an alternative dose (e.g. 0.1μM) of 6-ECDCA, a longer incubation time, a smaller dose of TNFα or even a different FXR agonist altogether would demonstrate a positive effect.

Chapter 5 – Conclusions

5.1 Introduction

The aetiopathogenesis of Crohn's disease (CD) remains incompletely understood. There is a need for safer, more efficacious treatments in the management of CD. Advancing our understanding of the mechanisms and risk factors determining the development of CD will aid in the development of these potential, new therapeutic compounds.

In this thesis, evidence has been presented regarding the role of farnesoid X receptor (FXR) in the aetiopathology of ileal CD. Three strata of experiments, gut-derived epithelial cell line models, an animal model of dietary risk and human ileal mucosal tissue, have been used. This evidence supports the hypothesis that disrupted bile acid signalling, via FXR, may predispose to the development of ileal CD by impairing gut epithelial homeostasis.

In this final chapter, the overarching hypothesis and supporting evidence is explained. A discussion of the thesis limitations and plans for future work is also outlined.

5.2 The overarching hypothesis

Figure 5.1 represents the overarching hypothesis with the healthy state demonstrated in figure 5.1A and the pre-disposing, at risk state demonstrated in figure 5.1B.

Under normal conditions, a 'healthy' microbiota (healthy is, as yet, scientifically undefined) metabolises primary BA's in the ileo-caecum. Central to the normal human–microbiotal co-metabolism of BA's is the BA receptor, FXR, found in high concentration within villous enterocytes of the ileum(Nicholson et al., 2005, Inagaki et al., 2006). FXR has pleiotropic roles including the control of BA metabolism in the liver, via FGF19, and the control of glucose and energy metabolism(de Aguiar Vallim et al., 2013). Importantly, evidence has also demonstrated that FXR is a modulator of intestinal innate immune function(Vavassori et al., 2009). Appropriate activation of FXR by primary BAs acts to maintain epithelial homoestasis.

In the pre-disposing state, a HF/HS western diet leads to alterations in the microbiome (a dysbiosis) and alters BA production. This dysbiosis disrupts the human–microbiotal co-metabolism of BA's, leading to a decrease in FXR signalling and activation of its downstream pathways. This leads to a disruption in BA metabolism, and, more importantly, impairs gut immune system homeostasis. The epithelial barrier becomes more permeable to bacteria within the gut lumen. Innate immune cells and epithelial cells are more responsive to stressful stimuli (such as LPS and muramyl dipeptide), with the secretion of pro-inflammatory effector cytokines that predispose to inflammation and induce further leakiness of the epithelial barrier. In patients with a genetic predisposition to the development of CD, these changes may induce the chronic, relapsing inflammation that is the hallmark of the disease.

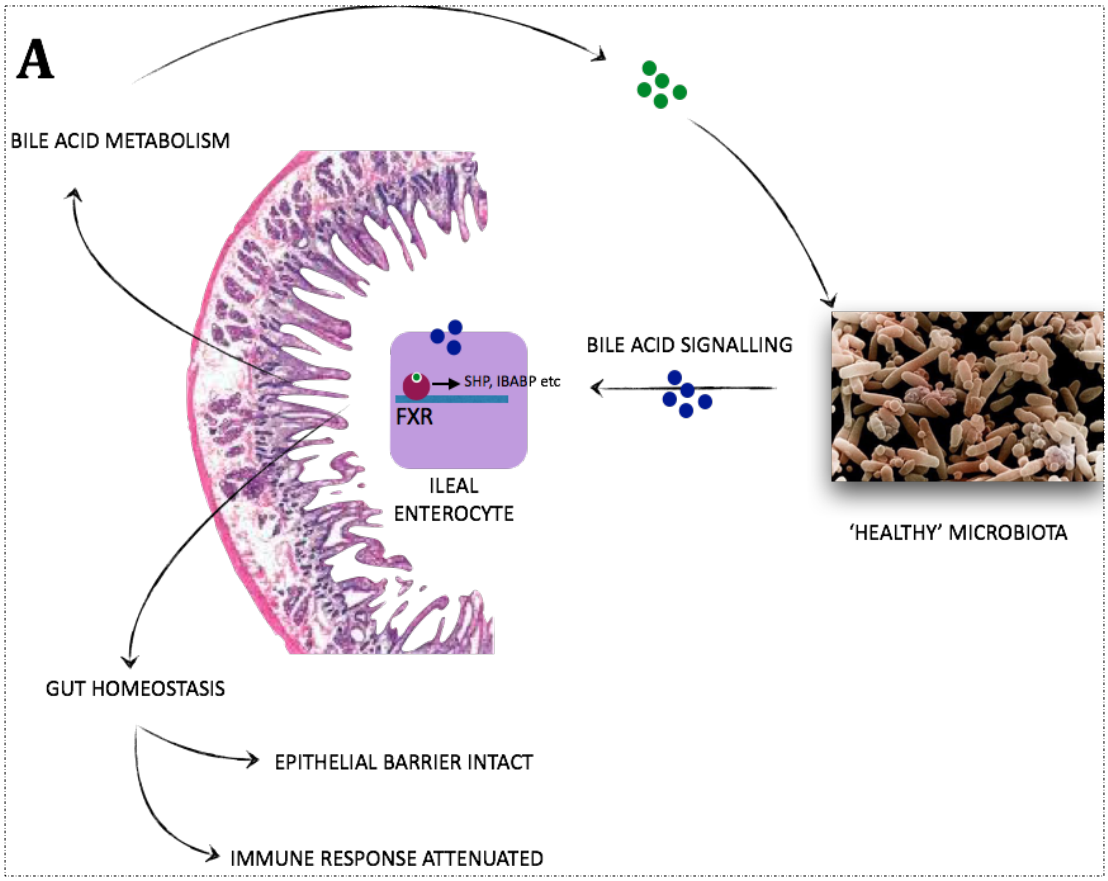

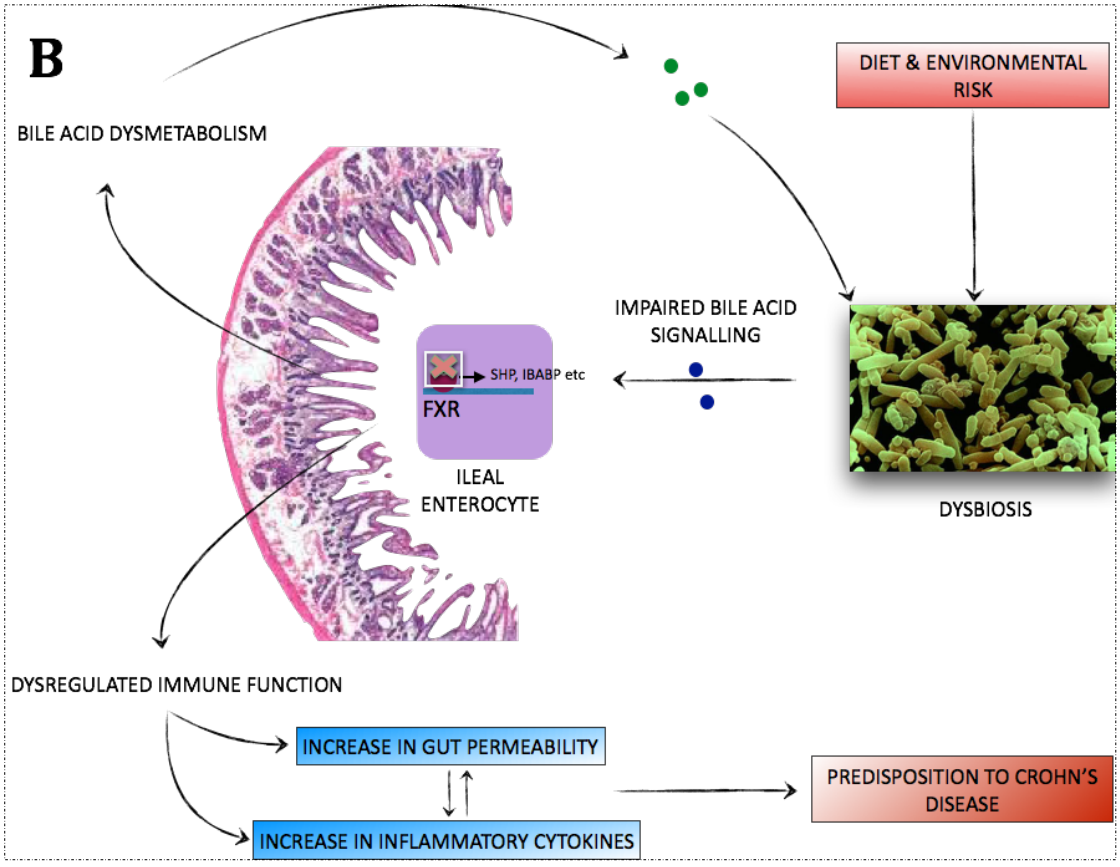

Figure 5.1; Diagram to represent potential role of impaired BA signalling in pathogenesis of CD. 'A' is normal, healthy state. 'B' is state imposed by diet-induced dysbiosis. Other environmental risk factors include exposure to antibiotics, smoking and vitamin D deficiency.

5.2.1 Data to support the hypothesis

The role of a dysbiosis and impaired BA signalling in the pathogenesis of CD is supported both by the current published literature and the findings presented in this thesis. Epidemiological data and case-control series have demonstrated that a western diet is a risk factor in the development of CD(Gibson and Shepherd, 2005, Hou et al., 2011). High fat/high sugar (HF/HS) feeding of mice will induce a dysbiosis similar to that found in humans with IBD(Martinez-Medina et al., 2014). Duboc et al demonstrated an impaired BA metabolism in association with a typical IBD dysbiosis in patients with active IBD(Duboc et al., 2013). In a mouse model of NASH, an antibiotic-induced dysbiosis altered ileal BA composition with subsequent inhibition of intestinal FXR signalling(Jiang et al., 2015). BA signalling via FXR is central to the communication between the mammalian host and its microbiota, facilitating the human-microbial co-metabolism of BA's(Nicholson et al., 2005, Martin et al., 2007). In this thesis, I have demonstrated, in a diet-induced obesity animal model, that HF/HS feeding could induce ileal cytokine expression. This increase in cytokine expression may be reduced by activation of FXR, suggesting that the diet-induced inflammatory stimulus may be mediated by impaired FXR signalling. Whilst these data do not reach statistical significance, the trend suggesting that supplementing feed with an FXR agonist can ameliorate the diet-induced inflammatory cytokine expression is in keeping with the overall hypothesis.

Several studies have demonstrated the immuno-modulatory function of FXR. In a bile duct ligation animal model, the translocation of bacteria to mesenteric lymph nodes is reduced by treatment with an FXR agonist(Inagaki et al., 2006). In an FXR knockout mouse model, there is an increase in lamina propria inflammatory cells and an increase in inflammatory cytokine expression(Vavassori et al., 2009). In

animal studies, an FXR agonist was able to attenuate the effects of a DSS and TNBS induced colitis(Gadaleta et al., 2011b). Several aspects of the data presented in this thesis supports the current published evidence. I have demonstrated that FXR agonism reduces the potent neutrophil chemo-attractant IL-8 response of epithelial cells when stressed with TNFα. A variety of published evidence has demonstrated that immune cell types exposed to an FXR agonist were refractory to stimulation with LPS(Vavassori et al., 2009, Gadaleta et al., 2011b, Haselow et al., 2013). The findings regarding an attenuated epithelial IL-8 response would appear to be another mechanism by which FXR maintains innate immune homeostasis in the ileum.

Disruption to the epithelial barrier is central to the pathogenesis of CD(McGuckin et al., 2009). It has previously been shown that FXR acts to maintaining the epithelial barrier, although the molecular mechanism is unknown. Here, I have begun to unravel this question by demonstrating that FXR agonism maintains epithelial cell morphology in a cell line model of cytokine-induced epithelial barrier disruption. In experiments with IL-6, it would appear that maintenance of epithelial morphology is via a mechanism involving, at least in part, the inhibition of MLCK expression.

Finally, I have demonstrated, for the first time in patients with ileal CD, that there is a decrease in the expression and activity of FXR in the ileum. The same pattern is demonstrated in mice fed a HF/HS diet, with a decrease in the activity of FXR and an increase in CD associated inflammatory cytokine expression.

5.2.2 Data against the hypothesis

In the only published data regarding BA metabolism in patients with IBD, an impairment in the transformation of primary BAs to secondary BAs was demonstrated(Duboc et al., 2013). This might suggest that it is a lack of secondary BAs that predisposes or drives an inflammatory process. Secondary BAs are only weak FXR agonists and therefore, this finding would not fit the overarching hypothesis. However, the study by Duboc did not measure BA species in the ileo-caecum, but instead measured faecal BAs. Faecal BAs may not be representative of BA dysmetabolic changes occurring in the ileo-caecum. TGR5 is antagonised by these secondary BA's and therefore a study of the role of this receptor in gut inflammation would be of interest.

The finding that FXR knockout mice do not develop IBD(Vavassori et al., 2009) would suggest that impaired BA signalling alone is not responsible for the development of chronic inflammation. Other predisposing factors, genetic, immune or environmental are clearly required in addition. As suggested in chapter 1 (sections 1.2.6 to 1.2.8), there is evidence that the microenvironment may impact on intestinal homeostasis in a number of different ways, for example in a reduction in butyrate producing bacteria. Several studies have demonstrated a CD associated dysbiosis in which several butyrate producing species (e.g. *faecalibacterium prausnitzii*) are reduced(Joossens et al., 2011). In some studies, but not others, butyrate has been shown to have anti-inflammatory properties(Marteau, 2013). These alternative mechanisms, by which a dysbiosis may induce inflammation, are not explained by disrupted FXR signalling. It is possible that more than one mechanism may be important.

The data presented from the *ex-vivo* organ culture model does not support the overarching hypothesis. No attenuation of mucosal inflammatory cytokine

production could be demonstrated when tissue was treated with an FXR agonist. However, the data is limited by a small sample size and use of heterogeneous mucosal samples. Further work is needed in this area.

Also, in a cell line model of the epithelial barrier, exposure to an FXR agonist did not maintain epithelial electrical resistance when the epithelial layer was stressed with cytokine. Presumably, whilst the FXR agonist could maintain cell morphology, there were still cytokine-induced alterations within the TJ complex that allow the paracellular flow of charged ions. If we accept the hypothesis that FXR maintains epithelial homeostasis within the gut, it is presumably not by a mechanism that maintains seal-forming claudin expression at the TJ.

5.3 Limitations of the thesis

In several experiments, in particular the animal data, only trends have been demonstrated, with any findings failing to reach significance. This may be because the trends are fictitious, with no real difference between control and the intervention. Sample sizes were small and often the underlying biological variability large. Therefore, a larger sample size is required in order to demonstrate whether there is any real difference between control and intervention groups. Sample size was limited in chapter 4 by the time taken to enroll enough control and CD patients in the study. In chapter 3, a major failure was in the storage of tissue after en-bloc resection of the GI tract. Unfortunately, due to a variety of circumstances, the GI tract was not snap frozen, but instead slowly frozen to -80°C. This impaired RNA quality and despite the use of the frozen tissue transition solution, good quality RNA could only be extracted from a subset of mice in the study.

Much of the data in chapters 3 and 4 makes use of the technique of RT-PCR. Whilst this is a powerful laboratory technique, able to detect very small changes in mRNA levels, I recognise that it has its limitations. Only a single reference gene was used and perhaps, ideally, a second reference gene to control for changes in expression between control groups and intervention should have been included. There has been some criticism of the use of both GAPDH and β-actin as reference genes as their expression is not as uniformly stable as previously thought(de Jonge et al., 2007). However, no such criticism for the use of these genes in studies investigating GI tissue In addition, RT-PCR will only provide an assessment of changes in relative gene expression. This is not, therefore, a direct measure of inflammation. It would have been more methodologically robust if a measurement of tissue inflammation, in both the mouse and primary tissue experiments, by histological assessment for example, had been used.

Much was accomplished in the 2 years of research that contributed to this thesis, including the optimisation of an *ex-vivo* ileal mucosa culture model that was new to our group. However, there are some time-limited, omissions in the data. It would have been preferable to study other cytokines in addition to IL-6 in the RT-PCR experiments regarding MLCK expression. Another omission is in the study of IL-8 secretion in the *ex-vivo* organ culture experiments. The primary mucosal samples produced huge concentrations of IL-8, above the level of assay detection, in both control and intervention groups. Given the finding that FXR agonists could inhibit IL-8 secretion in HT29 cells, an analysis of IL-8 production in the primary tissue would have been very interesting. Unfortunately, cost limited experiments to a single V-PLEX plate and so I did not get chance to repeat the assay with a diluted supernatant in order to ascertain whether there was any difference in IL-8 concentration between control and intervention groups.

Finally, an analysis of the BA species and the dysbiosis induced by HF/HS feeding was not performed, due a lack of access to high performance liquid chromatography-mass spectrometry and 16s pyrosequencing. These are areas to be explored in the future and research groups from King's College, and Imperial College, London have approached the group with a view to collaborating on such studies.

5.4 Questions arising from the data and future work

Other than the areas mentioned above, there are a variety of further areas for research suggested by this thesis.

In chapter 2, an apparent synergistic relationship is demonstrated between high doses of FXR agonist (10μM 6-ECDCA) and TNFα stimulation with regards IL-8 production. If FXR agonists are to be translated into use as therapeutic compounds in IBD, it would be important to investigate this finding further, as supra-therapeutic doses of the compound may in fact be pro-inflammatory.

Other environmental co-factors, in addition to impaired FXR signalling, may be important in the development of IBD. Much interest has focused recently on the role of vitamin D in the development of chronic inflammatory immune conditions(Mouli and Ananthakrishnan, 2014, S. Wu et al., 2014). Given that vitamin D receptor (VDR) is a nuclear receptor, similar in structure to FXR, it may be that a deficiency in both pathways may produce a synergistic pro-inflammatory phenotype.

As discussed in chapter 1 (section 1.5.4), a wealth of recent data has demonstrated that defective autophagy is an important process in the development of CD(Fritz et al., 2011). FXR interacts with NOD2, via p62/Sequestosome 1, which both targets polyubiquitinated proteins to the autophagosome and also acts to maintain the

half-life of NOD2(Williams et al., 2012, Park et al., 2013). A study of the role of FXR in promoting autophagy would also be of scientific and clinical interest.

An investigation into the role of FXR signalling as an anti-fibrotic pathway could be of great clinical significance. Epithelial-mesenchymal transition (EMT) describes a process during which fully differentiated epithelial cells undergo a phenotypic change to develop mesenchymal cell (e.g. fibroblast) features(Radisky, 2005). EMT is both pro-inflammatory and pro-fibrotic and can disrupt the epithelial barrier and so is of great interest in CD. An EMT-like process has been described in the formation of CD associated fisulae(Bataille et al., 2008) and an EMT induced fibrosis has been described in a mouse model of CD(Flier et al., 2010). Clinically, fibrosis and fistula are important, difficult to manage sequelae of CD. Certain EMT-like epithelial cell markers, such as αSMA and TIMP-1, were found to be upregulated in the FXR knockout model described by Vavasorri and colleagues(Vavassori et al., 2009). Given these findings, a study of the role of FXR as an anti-fibrotic, EMT inhibiting molecule would be both interesting and potentially clinically useful.

Finally, an important question raised by this thesis is with regards the role of ileo-caecal resection in the management of CD. Approximately 80% of patients with CD will end up with a surgical resection to treat either uncontrolled inflammation or stricturing/penetrating disease(Rutgeerts, 2003). The most common site for disease activity is within the ileo-caecum and therefore an ileo-caecal resection is the most commonly performed operation. Post-operative disease recurrence is extremely common, usually at the site of the surgical anastomosis. Recurrence can be rapid and aggressive with 30% of patients demonstrating evidence of inflammation within the anastomosis at 3 months post surgery and 80% of patients by 1 year(Baert et al., 2003, Van Assche and Rutgeerts, 2004). More

importantly, 15-45% of patients will require further surgery by 3 years and up to 65% will require further surgery at 10 years(Rutgeerts, 2003). To date, no medical intervention has consistently been shown to reduce the need for surgery.

Post ileo-caecal resection, the expression of FXR is upregulated in the colon(Dekaney et al., 2008). For this reason, it has been argued that removing the ileo-caecum may provide an immuno-protective effect in the colon(Wildenberg and van den Brink, 2011). However, the extent to which FXR is upregulated in the colon is unknown and, in addition, FXR-activating primary BAs are rapidly metabolised to secondary BAs in the colon. Therefore, the extent to which FXR is active within the colon post resection is unclear.

Given that FXR in the ileum is immuno-modulatory, it may well be that surgical resection of the ileo-caecum will actually predispose patients with CD to the development of further disease. This would fit with the observation that post-operative recurrence is common and can occur rapidly. FXR agonist treatment of post-operative patients in order to prevent recurrence is an intriguing therapeutic possibility and warrants further investigation.

5.5 From bench to bedside

Given both the current published data and the evidence demonstrated in this thesis, is it reasonable to propose FXR agonists as a treatment option in active CD?

FXR agonists, in the form of 6-ECDCA, have entered phase II and phase III clinical trials in cholestatic liver diseases, like PBC, and in NASH(Nevens et al., 2014, Neuschwander-Tetri et al., 2015). Adverse outcome reporting in these trials has been favourable other than the commonly reported problem of pruritus. The development of pruritus would appear to be a dose related effect with between 23%-80% of patients affected with doses ranging from 10 to 50mg of 6-ECDCA. A

small, phase I study has been conducted in patients with quiescent Crohn's colitis (9 patients and 12 controls), again with 6-ECDCA. This trial was able to demonstrate that pharmacological activation of the FXR receptor was feasible in patients with CD(van Schaik et al., 2012).

There is, however, still scientific information that it would be useful to answer, such as the role of high dose FXR agonists on the stimulation of IL-8 from epithelial cells. Another potential safety concern is the potential for FXR agonists to predispose to the development of hepatocellular carcinoma (HCC), induced by FGF19 overexpression. FGF19 is a hormonal signal, stimulated in the intestine by FXR, which completes a negative feedback loop by reducing gallbladder contraction and inhibiting BA neosynthesis in the liver. Overexpression of FGF19 has been associated with the development of HCC in both animal models and in humans(Schaap et al., 2015). It is feasible that over-promotion of FXR could lead to high levels of FGF19 which in turn is carcinogenic.

Aside from these safety concerns, is the question as to whether FXR agonists would be effective in reducing inflammation in patients with CD? The evidence presented here suggests that FXR maintains epithelial homeostasis. It is perhaps more likely, therefore, that the clinical utility of an FXR agonist may be to reduce the risk of relapse for patients who are already in disease remission. Even further in the future is the potential for FXR agonists to be used to reduce the risk of disease development, perhaps in people identified via genetic testing or with multiple environmental risk factors, as being at high risk.

Appendix

1. Application to the HPB/GI Biobank Committee
2. Copy of patient information leaflet
3. Copy of patient consent form

Appendix 1: Proforma for submitting a request to collect/use samples in the Hepatopancreatobiliary (HPB) tissue bank by research groups in Newcastle University

Request to perform research in Newcastle University using samples collected as part of the HPB tissue bank

Written by:	Dr Helen Reeves (HLR) NICR Newcastle University	Version 1	**March 2010**
	HLR	**Version 2**	**4TH July 2010**

Background

Approval has been obtained from Newcastle and North Tyneside Research Ethics Committee to perform research on samples collected as part of the HPB (Hepatopancreatobiliary) groups based in Newcastle University without the need to obtain specific consent for individual projects. However, it is a condition of this approval that details of the projects included are submitted to the LREC as part of an annual report, when they will be reviewed to ensure that they fall within the remit described in the accompanying protocol (Biological studies of samples).

In order to do this please complete the sections below and send this form by e-mail to Professor Alastair Burt (A.D.Burt@ncl.ac.uk). Applications will be considered by Professor Burt and designated individuals forming part of an approval committee. The committee will include informed individuals from Newcastle University and the Newcastle Hospitals NHS Foundation Trust, who are able to act as independent assessors. The purpose of the review is to ensure that the work proposed does not duplicate ongoing studies in Newcastle, is adequately funded and has a reasonable prospect of producing meaningful results. Every effort will made to decide on the suitability of projects within 4-6 weeks. If access to samples is denied the reasons for this will be explained in writing.

Please note that results of laboratory investigations covered by this protocol specifically exclude any which would be used to influence the treatment of individual patients.

Contact details

Name of Principal Investigator	*Dr J C Mansfield*
e-mail	*john.mansfield@nuth.nhs.uk*
Telephone	*1912336161*
Address	*Ward 48 office, level 6 Leazes Wing* *Dept of Gastroenterology* *RVI*

Project details

Title of project	*The role of bile acids in the aetiopathology of inflammatory bowel disease*
Source and amount of funding	*Department of gastroenterology, NUTH, £25,000*
Place where research will be conducted	*Newcastle University and NUTH*
Sponsor (eg NHS Trust)	*NUTH*
Details of peer review (eg through funding peer review or local research committee).	*This is an MD project that has been peer reviewed for approval by Prof J Kirby, Prof Julia Newton (Dean of Clinical Medicine) and Dr C Ward*

Abstract (no more than 500 words). Please attach copy of full application and /or research protocol if available

Inflammatory Bowel Disease (IBD)
The inflammatory bowel diseases, Crohn's disease and ulcerative colitis, are chronic, relapsing inflammatory conditions effecting the gastrointestinal (GI) tract. The aetiopathology of IBD is incompletely understood but is thought to be due, in part, to epithelial barrier dysfunction. There is a clinical need for safer, more efficacious treatments in IBD.

The role of BAs in inflammation
Primary BA's are detergents to allow the absorption of dietary fats. In addition, BA's also act as signaling molecules regulating their own metabolism, glucose metabolism, lipid metabolism and immune function. FXR acts as a transcription factor for a variety of anti-inflammatory genes. In FXR KO mice, epithelial barrier function is impaired. Also, treatment with an FXR agonist protects against colitis in a mouse model. FXR agonists also inhibit proinflammatory cytokine production by epithelial cells in-vitro.

This study aims to investigate the role BA's play in maintaining epithelial barrier function via the nuclear receptor FXR.

Planned Methodology
To define the importance of primary bile acids as mediators of inflammation in IBD, quiescent disease and in healthy controls, ex vivo tissue will be collected during ileo-colonoscopy/flexible sigmoidoscopy, or operative intervention performed as part of planned clinical care. This will include ileo-colonic biopsies from patients with IBD and controls (those attending endoscopy and no abnormality found during the test). Resection specimens will be obtained from patients undergoing operative intervention for IBD, and control patients undergoing resection for diverticular disease or colorectal carcinoma (normal tissue will be taken from margins of specimen in the case of carcinoma).
Tissue samples will be subjected to digestion and real time quantitative PCR will performed. Some tissue will be formalin fixed and processed for immunohistochemistry.

Is the proposed project a pilot study or a more substantive project?
Substantive project

Have power calculations been performed, and if so how?
This is an observational study and so a power calculation is not possible. It is envisaged that 20 to 30 patient samples will be collected.

Are the results likely to contribute to a publication in the near future? If so, please give brief details.
If significant findings, aim to submit for publication within the next two years.

Sample details

Number and type required (eg bone marrow, blood, CSF, other)	Biopsy samples from colon and ileum (initially 20 patients)	Ileo-colonic resection specimens	Paraffin embedded tissue slides	
Minimum size of sample (eg cell number or quantity of RNA, DNA or protein)	A minimum of 2 biopsies from each patient	Ideally 10cm by 5cm depending on size of resection specimen and NHS requirements		
Please justify, including details of power equations where performed				

To be completed by Biobank manager/committee Sample availability - How many samples are available of the type requested? Are you aware of other projects which are likely to benefit form the use of samples of this nature?	
Date application received	
Date sent for approval	
Date of approval decision	
Outcome	

Electronic versions of this form may be obtained from Professor Alastair Burt (A.D.Burt@ncl.ac.uk) or Research Co-ordinator Diane Walia; Research Study Co-ordinator, Hepatology, Freeman Hospital, Tel: 0191 21 31568. E-mail: Diane.Walia@nuth.nhs.uk.

Newcastle University
The Medical School,
Framlington Place,
Newcastle-upon-Tyne,
NE2 4HH, U.K.

PATIENT INFORMATION SHEET
The hepatopancreatobiliary (HPB) and gastroenterology (GI) tissue bank.

The collection and storage of diagnostic samples and those taken during therapy, to support research into Hepatopancreatobiliary (HPB), gastrointestinal (GI) or retroperitoneal disease.

Introduction

Although progress has been made in understanding the development of chronic diseases and cancer in the last 20 years, we still have a lot to learn if we are to detect diseases sooner and improve the treatments available for affected people in the future. Many of our research projects use blood, body fluids, tissues or cells to help us understand what is wrong. In order to help with our research, in Newcastle we are co-ordinating a local collection of stored blood, fluids and tissues, taken at the time of routine tests or planned operations, but which are extra to those needed for diagnosis. In particular, we undertake or collaborate with a variety of laboratory based research projects into chronic diseases and cancers of the hepatopancreatobiliary (HPB) and gastroinstestinal (GI) systems. The HPB system includes the liver, pancreas, gall bladder and biliary tree, while the GI system includes the esophagus, stomache, small and large bowel. We also study those tissues in the retroperitoneal space, behind the liver and abdominal organs. To enable us to carry out this research, we would like to collect samples from people who are undergoing investigation or treatment of a part of these systems.

We therefore invite you to give permission for a small amount of the samples which we take from you as part of your normal investigation or treatment to be kept for a variety of research projects to help us understand your disease. The samples we keep come from material left over after we have completed our routine hospital tests or treatment. In some cases we may ask if we can take a small amount of extra material at the same time as routine samples (eg. Blood), but this will not involve an extra procedure.

All of the research that we do has been approved by our tissue bank committee and will be regularly monitored by them, with annual reporting to the local research ethics committee who has approved the collection. Occasionally we also send samples to other researchers in the UK or abroad. We only do this if the research they are undertaking has also been approved by their local research ethics committee. Research does sometimes involve the testing of your DNA, but your identity will not be revealed to the research team. Our research is not conducted for moneymaking purposes, but it may be that some results, once published, will be of value to commercial companies, eg. in the development of new treatments.

This work will not directly benefit you but may help patients with similar diseases to you in the future. You do not have to give permission for your samples to be stored. If you decline, it will not affect your medical care in any way at all.

What will happen if I take part?

If you give your consent for samples to be stored and used for research purposes, these will be taken from material left over after routine elective tests or treatments have been performed. An extra sample eg. blood would only be taken at a time when other samples were being taken for clinical reasons. Samples would be taken at various stages, including at your first visit, but may also be taken at any follow-up or treatment visits. The amounts needed are very small (2-4 teaspoonfuls of blood or aspirated fluid,) and the taking of them should not affect your health in anyway. If you are having a biopsy or an operation to remove some tissues, we may save a very small part of that which is surplus to diagnostic needs. Again, this would be a very small amount – the size of a 0.5-1cm piece of spaghetti for a biopsy, or small pea-sized samples if you are having tissues surgically removed.

What will happen to my specimens?

The samples will be stored in the HPB tissue bank or at another research laboratory approved for a similar purpose. These samples may be stored for many years before they are used. They may be used to extract DNA (the genetic

material inside a cell) which will also be stored. The samples are stored and labelled with a code number, which means that the only link between the sample code and any medical information is held securely by the doctor who is the principal investigator for the project co-ordinating your samples collection. This may be at Newcastle University in a secure location, or in the Newcastle Hospitals NHS Foundation Trust, depending on where the principal investigator responsible for collecting your tissues is based. Coded samples may be released from the tissue bank for approved research projects in other research laboratories, but only if the laboratory has approval for their research from their local ethical committee.

Researchers may be given access to some information about your health and diagnosis, but they will not have any personal information that will enable them to identify you. Similarly, any results from research projects will not be traceable back to you by the researcher. All coded information on you will be kept in accordance with current national regulations (the Data Protection Act and Caldicott guidelines).

How do I know that my samples will only be used for ethically approved medical research?

Approval has been given by the local research ethics committee to perform research in Newcastle-upon-Tyne on samples in the HPB tissue bank. The nature of this research will be regularly monitored by the tissue bank committee. Samples will only be released to other research centres if they can confirm that their research is ethically approved in a similar fashion.

Will I be told of the results of research tests on my samples?

No. Nor will the results be given to any hospital doctor or practitioner. The research tests will not form any part of your medical treatment or record. The overall results of the research projects will be published in the scientific literature. In the future, if the research showed that there was a test which might be useful, it may – after independent review and validation – become part of standardised NHS care for all people with similar conditions.

What will happen to the information gathered about me?

No personal identifiable information about you will be given to the scientists doing the research tests and any research carried out on your tissues that is linked to your condition will be done in a strictly anonymous way. Information from your medical notes relating to your diagnosis, treatment or response to treatment will be kept stored in a strictly confidential manner according to the Data Protection Act within the NHS Trust responsible for your care.

What are the possible risks of taking part?

There are usually no extra risks involved in collecting samples stored for research. The numbers of biopsies required will be kept to a minimum and additional needle punctures for research blood tests will be avoided. Tissues taken at the time of an operation are from the part removed, after the surgery is complete.

Are there any possible benefits?

The information learned from studies using specimens obtained from you may help to improve treatment for future patients with similar conditions and possibly lead to the prevention of these diseases developing.

Do I have to take part?

No. Your participation is entirely voluntary. Whether or not you decide to allow your tissues to be stored for research will not affect the care you are given. If you give consent and then change your mind, any of your samples remaining will be disposed of, usually by incineration.

What should I do if I have any concerns about taking part?

If you have any problems, concerns or questions about this study, please feel free to speak to the medical and nursing staff who are responsible for your care. Alternatively, you may contact the Designated Individual responsible for all Human Tissues research performed in Newcastle-upon-Tyne, Professor A G Hall on (0191) 246 4411, who will put you in touch with appropriate clinical investigator to address your query.

NO CELLS, TISSUES OR BODILY MATERIAL WILL BE TAKEN OR STORED FOR RESEARCH WITHOUT YOUR AGREEMENT

Newcastle University
The Medical School,
Framlington Place,
Newcastle-upon-Tyne,
NE2 4HH, U.K.

PATIENT CONSENT FORM
The hepatopancreatobiliary (HPB) and gastroenterology (GI) tissue bank.

The collection and storage of diagnostic samples and those taken during therapy, to support research into hepatopancreatobiliary (HPB), gastrointestinal (GI) and retroperitoneal disease.

You are attending your NHS Trust for investigation and treatment. During this process, both now and in the future, you may give blood samples or undergo and additional procedure, depending on your condition (eg. tissue aspiration or biopsy or a surgical procedure). These procedures are performed both to help diagnose, but also to monitor, your condition. Sometimes tissues are removed at a time of surgery, as a treatment.

Once your sample has been taken for diagnostic, monitoring or treatment purposes, there may be some sample remaining. This remaining sample is very valuable for research. We therefore ask for your consent to use this remaining sample for research, by making a gift of it to our research tissue bank. In some cases we may also ask if we can obtain a small amount of extra material specifically for research purposes. These samples will only ever be taken at the same time as any routine procedures and will not involve any undue extra risk. A leaflet is available containing more information about the use of these samples and describing our policy for the safe keeping of tissue gifted in this way.

Your diagnosis and treatment will not be adversely affected in any way by giving consent. Any research studies in which your samples are used will have been approved by our local research ethics committee or an equivalent organisation. This is to ensure that the research is justified and meets current ethical standards. Research will be conducted anonymously, which means that your samples will be identified only by a code. Your personal details will not be accessible to researchers. Your confidentiality will be respected at all times.

In addition to collecting your surplus sample and clinical information, we may ask you to complete a questionnaire if it is relevant to your condition. You may be asked to complete a questionnaire at the hospital at the time of your scheduled visit, or to take it home with you, returning it at your next visit. Data collected for research purposes, including clinical information, that generated by your samples, as well as answers to questionnaires, will always remain anonymous, with all of you data being identifiable only by a code.

We may use your samples and data in association with commercial research partners but human tissues are never sold (this is illegal). Our partnerships are organised on a not-for-profit basis, with any resulting benefits being used directly to improve patient care or to enable us to perform more research. Although the research will not be conducted for the purposes of making money it is possible that some of the results, once published, will be of value to commercial companies, for example in the development of new tests or treatments.

Most of the research conducted using the samples we obtain is conducted in the UK but as the work we undertake is part of an international effort we sometimes send samples to centres outside the country- for example to mainland Europe or the USA. If you do not wish your samples, information or data to leave the country you can indicate this on the form we ask you to sign.

Use of your tissue or cells for research in this way will not influence your treatment directly. Withholding consent will not affect your diagnosis or treatment in any way. If you do not wish to give consent, we guarantee that any sample surplus to needs for diagnosis is disposed of appropriately, following national guidelines.

I agree to the use of my sample(s) after diagnosis for research: **YES / NO**

If yes, please answer the following questions ***(Please circle one response to each question)***

The patient should complete the whole of this sheet himself/herself

- Have you read and understood the patient information sheet? **Yes/No**
  (Please take a copy home with you to keep)
- Have you had an opportunity to discuss the tissue bank and ask questions? **Yes/No**
- Have you had satisfactory answers to your questions from Prof/Dr/Sr ……..? **Yes/No**
- Do you understand that you are free to withdraw your consent from the tissue bank at any time, without having to give a reason and without affecting your future medical care? **Yes/No**
- Do you agree to donate samples in excess of what is required for medical purposes and for these to be stored for future use in approved research projects? **Yes/No**
- Do you agree to donate small extra samples specifically for research purposes and for these to be stored for future use in approved research projects? **Yes/No**
- Do you understand that you will not be told the results of any tests which may be carried out on your samples ? **Yes/No**
- Do you give permission for your medical notes to be looked at, in relation to your condition, by an NHS professional (doctor or research nurse), where it is relevant to research about your condition and your stored sample(s)? **Yes/No**
- Do you give permission for your GP to be contacted if it is relevant to your having donated samples to the research tissue bank. **Yes/No**
- Do you give permission for your medical information (data) to be stored? **Yes/No**
- Do you give permission for samples to be sent to centres outside the UK? **Yes/No**
- A de-identified sample of DNA obtained from your blood may be sent to a laboratory for detailed genetic analysis. The remainder of your DNA, as well as your de-identified genetic information and medical information (data), may be stored for an unlimited amount of time. Your data and DNA may be shared with other qualified researchers, including academic, commercial, domestic and foreign researchers, who have received appropriate approval. Your data and DNA might be used for research on any disease, health condition or risk factor. Do you give permission for storage and use of your data and DNA in this way?

  Yes/No

_____ _____ _____
Name of Patient Date Signature & Hospital Number

_____ _____ _____
Name of Person taking consent Date Signature

1 for patient; 1 for researcher; 1 to be kept with hospital notes

Research Co-ordinator Contact Details:
Diane Walia; Research Study Co-ordinator; Hepatology; Freeman Hospital; Tel: 0191 21 31568;
Diane.Walia@nuth.nhs.uk

Publications

1. 'Activation of the bile acid receptor, farnesoid X receptor, does not maintain the epithelial barrier in a human cell line', **Speight, R.A.**, Lamb, C.A., Mansfield, J.C., Kirby, J.A.; IBD 2014: Thinking Out of the Box, Falk Symposium 192, Paris, May 2014; *Digestive Diseases* 2014, Vol. 32, s1
   Abstract voted as 'poster of distinction'

2. 'Activation of the bile acid receptor, farnesoid X receptor, may reduce ileal inflammatory cytokine expression in an animal model of diet-induced obesity', **Speight, R.A**., Whitehead, A., Patman, G., Mansfield, J.C., Reeves, H., Kirby, J.A.; 2nd Digestive Disorders Federation Conference 22–25 June 2015, *Gut* 2015, vol 64, s1
   Abstract accepted as oral presentation

3. 'Activation of the bile acid receptor, farnesoid X receptor, maintains gut epithelial cell morphology, possibly via inhibition of myosin light chain kinase expression', **Speight, R.A**., Davey, T., White, K., Kirby, J.A., Mansfield, J.C.; 2nd Digestive Disorders Federation Conference 22–25 June 2015, *Gut* 2015, vol 64, s1
   Abstract accepted as poster presentation

4. 'Farnesoid X receptor agonism modulates gut epithelial innate immune response', **Speight, R.A**., Barker, C.E., Palmer, J.M., Mansfield, J.C., Kirby, J.A.; *submitted* to United European Gastroenterology Week Conference 24-28 October 2015, *UEG Journal* 2015, vol 3, s1
   Abstract accepted as poster presentation
5. 'Novel Bile Acid Therapeutics for the Treatment of Chronic Liver Diseases', Hegade, S., **Speight, R.A**., Jones, D.E.J. *Therapeutic Advances in Gastroenterology* 2015 (in press)

Activation of the bile acid receptor, farnesoid-x receptor, does not maintain the epithelial barrier in a human cell line

R A Speight[1,2] C A Lamb[1,2] J C Mansfield[2,3] J A Kirby[1]

1 Applied Immunobiology and Transplantation Research Group, ICM, Newcastle University, UK; 2 Department of Gastroenterology, Newcastle u Tyne Hospitals Trust, UK; 3 Institute of Genetic Medicine, Newcastle University, UK

Introduction

The aetiopathology of inflammatory bowel disease (IBD) is incompletely understood, but is characterised by epithelial barrier dysfunction and immune dysregulation in a genetically susceptible host (Brant 2011). Exposure to a western diet, bacterial dysbiosis and bile acid (BA) dysmetabolism have been implicated in the pathogenesis of IBD (Trauner, Fickert et al. 2013). Farnesoid X receptor (FXR) is a BA receptor which promotes gut homeostasis by maintaining the epithelial barrier and exerting anti-inflammatory effects (Gadaleta, van Erpecum et al. 2011). The mechanism by which FXR maintains the epithelial barrier is not known. IBD associated inflammatory cytokines, such as TNFα, IL-1β, and IFNγ are known to disrupt epithelial barrier function (Adams 1993, Ma 2004).The aim of this study was to assay the effect of FXR agonism in an *in-vitro* human model of epithelial barrier dysfunction.

Methods

Fully differentiated (>21 day old) Caco-2 cells were cultured as a polarised monolayer on hanging cell culture inserts. Transepithelial electrical resistance (TEER), a marker of epithelial barrier function, was measured in the presence or absence of the pro-inflammatory cytokines TNFα and IFNγ with or without an FXR agonist. Enzyme-linked immunosorbent assay (ELISA) was performed for IL-8 following stimulation with IL-1β with or without an FXR agonist.

Results

Inflammatory cytokines reduced the TEER, as expected. There was no statistical difference (ANOVA) in the TEER between the groups treated with the FXR agonist and those without (figure 1). In terms of IL-8 production, the Caco-2 cells were unresponsive to stimulation with both TNFα and IFNγ. IL-1β stimulation induced a significant increase in IL-8. The level of IL-8 production was increased when cells were treated with the FXR agonist (figure 2).

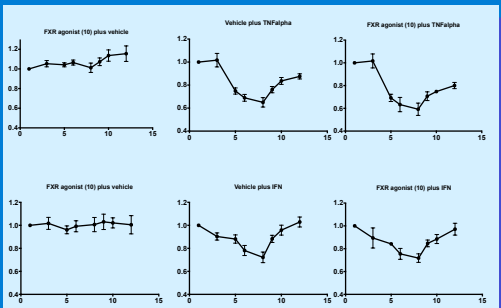

Fig.1: Change in transepithelial electrical resistance (normalised to 1.0), with time (in days), following exposure to tumour necrosis factor alpha or interferon gamma in the presence or absence of 10 microM FXR agonist and control.

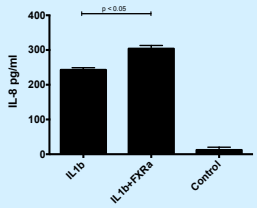

Fig. 2: IL-8 production in response to exposure with IL-1β with and without FXR agonist

Discussion

From this provisional data, in a human cell line model, FXR agonism does not ameliorate the epithelial barrier dysfunction induced by TNFα and IFNγ, as measured by TEER. The chemotactic cytokine IL-8 is readily induced by IL-1β. Rather than attenuating this response, the FXR agonist, in this assay, would seem to increase the level of IL-8 produced. These findings will be explored further in further epithelial cell lines and in primary tissue.

References

Adams, R B, et al (1993). IFNgamma Modulation of Epithelial Barrier Function; time course, reversibility and site of cytokine binding. *The Journal of Immunology 150(6): 2356-2363*

Brant, S R (2011). Update on the heritability of inflammatory bowel disease: the importance of twin studies. *Inflamm Bowel Dis* 17(1):1-5

Gadelata, R M, et al (2011). Farnesoid X receptor activation inhibits inflammation and preserves the intestinal barrier in inflammatory bowel disease. *Gut* 60(4):463-472

Ma, T Y, et al (2004). TNF-alpha induced increase in intestinal epithelial tight junction permeability requies NF kappa B activation. *Am J Physiol Gastrointest Liver Physiol*, 294:938-947

Trauner, M, et al (2013) Bile acids as modulators of gut microbiota linking dietary habits and inflammatory bowel disease: a potentially dangerous liaison. *Gastroenterology* 144(4): 844-846

The Newcastle upon Tyne Hospitals NHS
NHS Foundation Trust

Newcastle University

Activation of the bile acid receptor, Farnesoid-x receptor, may reduce ileal cytokine expression in an animal model of diet-induced obesity

R A Speight [1 2], A Whitehead [3], G Patman [3], J C Mansfield [2], H Reeves [3], J A Kirby [1]

1) ICM, Newcastle University, 2) Gastroenterology, Newcastle u Tyne NHS Foundation Trust, 3) NICR, Newcastle University, Newcastle u Tyne, United Kingdom

Discussion

- HF/HS feeding increases expression of ileal inflammatory cytokines in model of diet-induced obesity
- FXR agonist may reduce the cytokine expression induced by HF/HS feeding
  - Potential risk factor modificatio
- Possible FXR mechanisms:
  - Attenuated epithelial IL-8 response to stimulation
  - Maintains epithelial morphology
  - Inhibits various primary human immune cell types

Activation of the bile acid receptor, farnesoid-X receptor, maintains gut epithelial cell morphology, possibly via inhibition of myosin light chain kinase expression

R A Speight[1,2] T Davey[3] K White[3] J C Mansfield[2] J A Kirby[1]

1 Institue of Cellular Medicine, Newcastle University, UK; 2 Department of Gastroenterology, Newcastle u Tyne Hospitals Trust, UK; 3 Electron Microscopy Research Services, Newcastle University, UK

Introduction

By inducing epithelial barrier dysfunction, IBD associated inflammatory cytokines increase the leakiness of the gut mucosa, driving chronic inflammation1. Epithelial permeability increases, in part, due to cell-cell junction re- arrangement, mediated by myosin light chain kinase (MLCK)2. FXR agonism has been shown to maintain the epithelial barrier in a mouse model of colitis3. The aim of this study was to assay the effect of FXR agonism on epithelial cell morphology in a human, gut-derived epithelial model of barrier dysfunction.

Methods

Fully differentiated Caco-2 cells were cultured as a polarised monolayer and treated with TNFα, IFNγ or IL-6 with or without INT747 (FXR agonist, Intercept Pharmaceuticals). At 48 hours, transmission electron microscopy (TEM) was performed to assess for morphological re-arrangement of the cell-cell junction. Two independent researchers, blinded as to intervention, counted the number of morphological re-arrangements in 20 samples, chosen at random. RNA was isolated from IL-6 treated monolayers and the expression of MLCK was measured by RT-PCR (ΔΔCt method). Unpaired t-tests were calculated using Prism version 6.0e. All P values were 2-tailed, and a P value of 0.05 or less was considered significant.

Results

FXR agonism reduced the number of epithelial cell-cell junction fissures (fig 1) for monolayers stressed with IFNγ (73% to 30%) and IL-6 (70% to 43%). This was significant in the IFNγ group (p = 0.03), but failed to reach significance in the IL-6 group (p = 0.08). There were no, or few, morphological re-arrangements in control, INT747 only or TNFα treated monolayers (fig 2). Cells stressed with IL-6 demonstrated a significant increase in the relative expression of MLCK (fold increase 435.4). The IL-6 induced upregulation of MLCK was completely abolished by co-treatment with INT747 (fig 3).

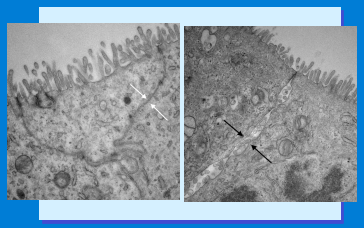

Fig 1: Examples of electron micrographs of normal cell-cell junction (left) and cell-cell junction fissure (right) in epithelial monolayer

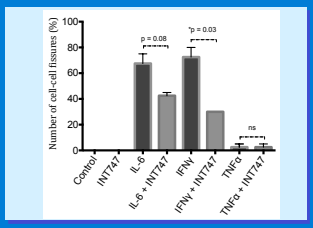

Fig 2: % of cell-cell fissures seen at TEM (n=20) for monolayers stimulated with cytokine or vehicle +/- FXR agonist.

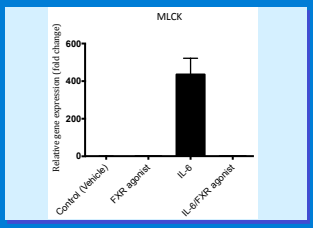

Fig 3: Relative gene expression for MLCK in monolayers following exposure to vehicle, FXR agonist or IL-6 +/- FXR agonist

Discussion

Evidence is presented to demonstrate that FXR acts to maintain human, gut-derived epithelial cell morphology after stress with IFNγ and IL-6, probably via a mechanism involving the regulation of MLCK expression. FXR agonists are potential therapeutic compounds in the management of IBD.

References

1. Capaldo CT et al. Bioch. Bioph. Acta 2009:1788; 864-871
2. Cunningham KE et al. Ann. N.Y. Acad. Sci. 2012:2058;34-42
3. Gadaleta RM et al. Gut 2011;60:463-472

Farnesoid X receptor agonism modulates gut epithelial innate immune response

R A Speight[1,2], C Barker[1], J Palmer[1], J C Mansfield[2], J A Kirby[1]

1 Applied Immunobiology and Transplantation Research Group, ICM, Newcastle University, UK, 2 Department of Gastroenterology, Newcastle u Tyne Hospitals Trust, UK

Introduction

Disruption to the epithelial barrier is central to the pathophysiology of IBD (Zeissig et al., 2007, Su et al., 2009). A variety of innate immune mechansims contribute to the maintenance of the epithelial barrier. When stressed, either by pathogens or by inflammatory cytokine, gut epithelial cells produce IL-8 which acts as a chemo-attractant for circulating polymorphonucleocytes (Eckmann et al., 1993). Farnesoid X receptor (FXR) is a bile acid (BA) receptor which promotes gut homeostasis by maintaining the epithelial barrier and exerting anti-inflammatory effects (Gadaleta et al., 2011). The mechanism by which FXR maintains the epithelial barrier is not known.

Methods

The aim of this study was to assay the effect of FXR agonism on the production of IL-8 by human gut-derived epithelial cells, in response to cytokine stress.

HT29 cells were cultured with media containing an FXR agonist (GW4064) or control (vehicle) with or without an FXR antagonist (guggulsterone). Following exposure to the FXR agonist +/- guggulsterone, HT29 cells were stimulated with growth media containing TNFα. IL-8 was measured both at a protein level by ELISA and a transcriptional level by RT-PCR.

Results

In the control group, gut epithelial cells produced high levels of IL-8 when exposed to TNFα (6,316+/-870 pg/mg). Concomitant treatment with an FXR agonist at high dose (GW4064 10μM) completely abolished this IL-8 response (p=0.0004). Lower doses of FXR agonist (0.1μM, 1μM) had no significant effect on the concentration of IL-8. (continued)

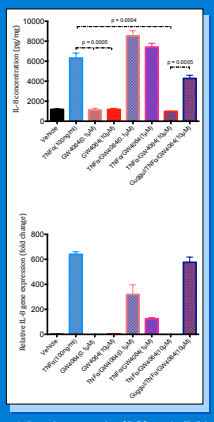

Fig. Concentration and gene expression of IL-8 from gut epithelial cells

(Results continued)

Guggulsterone was able to reverse the attenuating effect of high dose FXR agonist, with significantly more IL-8 detected in co-treated cells (p=0.0005). Measurement of the relative gene expression of IL-8 confirmed the findings observed at the protein level (TNFα alone: fold change 640+/-20, TNFα+FXR agonist: fold change 0.08+/-0.02) (See figure).

Discussion

These experiments demonstrate that FXR activation decreases the IL-8 response of human gut-derived epithelial cells to TNFα at a transcriptional level. Gut epithelial IL-8 expression is an important innate immune mechanism and this data is in keeping with other studies in demonstrating an immuno-modulatory role for FXR (Vavassori et al., 2009, Haselow et al., 2013). This is a potential mechanism by which FXR may act to maintain epithelial homeostasis.

References

Eckmann, L., et al. (1993), *Infect Immun.*, 61(11), pp. 4569-4574
Gadaleta, R. M., et al. (2011), *Gut*, 60(4), pp. 463-72
Haselow, K., et al. (2013), *J Leukoc Biol*, 94(6), pp. 1253-64
Su, L., et al. (2009) *Gastroenterology*, 136(2), pp. 551-63
Vavassori, P., et al. (2009), *J Immunol*, 183(10), pp. 6251-61
Zeissig, S., et al. (2007), *Gut*, 56(1), pp. 61-72

UNITED EUROPEAN GASTROENTEROLOGY ueg week
23rd United European Gastroenterology Week
October 24 – 28, 2015 | Barcelona, Spain

References

Acosta-Rodriguez, E. V., Rivino, L., Geginat, J., et al. (2007) 'Surface phenotype and antigenic specificity of human interleukin 17-producing T helper memory cells', *Nat Immunol,* 8, pp. 639-646.

Adams, R. B., Planchon, S. M. and Roche, J. K. (1993) 'IFN-gamma Modulation of Epithelial Barrier Function; Time Course, Reversibility and Site of Cytokine Binding', *The Journal of Immunology,* 150(6), pp. 2356-2363.

Albenberg, L. G., Lewis, J. D. and Wu, G. D. (2012) 'Food and the Gut Microbiota in IBD: A Critical Connection', *Current Opinion in Gastroenterology,* 28(4).

Ananthakrishnan, A. N. (2013) 'Environmental Risk Factors for Inflammatory Bowel Disease', *Gastroenterology & Hepatology,* 9(6), pp. 367-374.

Ananthakrishnan, A. N., Khalili, H. and De Silva, P. S. (2012) 'Higher dietary fibre intake is associated with lower risk of Crohn's disease but not ulcerative colitis - a prospective study', *Presented at Digestive Disease Week,* Abstract 863.

Annunziato, F., Cosmi, L., Liotta, F., et al. (2008) 'The phenotype of human Th17 cells and their precursors, the cytokines that mediate their differentiation and the role of Th17 cells in inflammation', *Int Immunol,* 20, pp. 1361-1368.

Baert, F., D'Haens, G. and Rutgeerts, P. (2003) 'Postoperative prevention of recurrence of Crohn's disease', *Inflammatory Bowel Disease: From Bench to Bedside*. USA: Springer Science Business Media, pp. 1369-1373.

Bailey, A. M., Zhan, L., Maru, D., et al. (2014) 'FXR silencing in human colon cancer by DNA methylation and KRAS signaling', *Am J Physiol Gastrointest Liver Physiol,* 306(1), pp. G48-58.

Bailey, J. R., Bland, P. W., Tarlton, J. F., et al. (2012) 'IL-13 promotes collagen accumulation in Crohn's disease fibrosis by down-regulation of fibroblast MMP synthesis: a role for innate lymphoid cells?', *PLoS One,* 7(12), pp. e52332.

Barber, R. D., Harmer, D. W., Coleman, R. A., et al. (2005) 'GAPDH as a housekeeping gene: analysis of GAPDH mRNA expression in a panel of 72 human tissues', *Physiol Genomics,* 21, pp. 389-395.

Bataille, F., Rohrmeier, C., Bates, R., et al. (2008) 'Evidence for a role of epithelial mesenchymal transition during pathogenesis of fistulae in Crohn's disease', *Inflamm Bowel Dis,* 14(11), pp. 1514-27.

Berg, R. D. (1995) 'Bacterial translocation from the gastrointestinal tract', *Trends in Microbiology,* 3, pp. 149-154.

Bhatia, L. S., Curzen, N. P., Calder, P. C., et al. (2012) 'Non-alcoholic fatty liver disease: a new and important cardiovascular risk factor?', *Eur Heart J.,* 33(10), pp. 1190-1200.

Bilger, A., Bennett, L. M., Carabeo, R. A., et al. (2004) 'A potent modifier of liver cancer risk on distal mouse chromosome 1: linkage analysis and characterization of congenic lines', *Genetics,* 167(2), pp. 859-66.

Bjorkoy, G., Lamark, T., Brech, A., et al. (2005) 'p62/SQSTM1 forms protein aggregates degraded by autophagy and has a protective effect on huntingtin-induced cell death', *J Cell Biol,* 171(4), pp. 603-14.

Boom, R., Sol, C. J., Salimans, M. M., et al. (1990) 'Rapid and Simple Method for Purification of Nucleic Acids', *J Clin Microbiol,* 28(3), pp. 495-503.

Brand, S. (2009) 'Crohn's disease: Th1, Th17 or both? The change of a paradigm: new immunological and genetic insights implicate Th17 cells in the pathogenesis of Crohn's disease', *Gut,* 58(8), pp. 1152-67.

Brant, S. R. (2011) 'Update on the heritability of inflammatory bowel disease: the importance of twin studies', *Inflamm Bowel Dis,* 17(1), pp. 1-5.

Browning, T. H. and Trier, J. S. (1969) 'Organ Culture of Mucosal Biopsies of Human Small Intestine', *J Clin Invest.,* 48, pp. 1424-1432.

Bruewer, M., Luegering, A., Kucharzik, T., et al. (2003) 'Proinflammatory Cytokines Disrupt Epithelial Barrier Function by Apoptosis-Independent Mechanisms', *The Journal of Immunology,* 171(11), pp. 6164-6172.

Cani, P. D., Amar, J., Iglesias, M. A., et al. (2007) 'Metabolic endotoxemia initiates obesity and insulin resistance', *Diabetes,* 56(7), pp. 1761-72.

Cani, P. D., Bibiloni, R., Knauf, C., et al. (2008) 'Changes in gut microbiota control metabolic endotoxemia-induced inflammation in high-fat diet-induced obesity and diabetes in mice', *Diabetes,* 57(6), pp. 1470-81.

Cao, H. and Shockey, J. M. (2012) 'Comparison of TaqMan and SYBR Green qPCR methods for quantitative gene expression in tung tree tissues', *J Agric Food Chem,* 60(50), pp. 12296-12303.

Capaldo, C. T. and Nusrat, A. (2009) 'Cytokine regulation of tight junctions', *Biochim Biophys Acta,* 1788(4), pp. 864-71.

Capello, A., Moons, L. M., Van de Winkel, A., et al. (2008) 'Bile acid-stimulated expression of the farnesoid X receptor enhances the immune response in Barrett esophagus', *Am J Gastroenterol,* 103, pp. 1510-1516.

Chassaing, B., Koren, O., Carvalho, F. A., et al. (2014) 'AIEC pathobiont instigates chronic colitis in susceptible hosts by altering microbiota composition', *Gut,* 63(7), pp. 1069-80.

Cho, I. and Blaser, M. J. (2012) 'The human microbiome: at the interface of health and disease', *Nat Rev Genet,* 13(4), pp. 260-70.

Chomczynski, P. and Sacchi, N. (1987) 'Single-step method of RNA isolation by guanidinium thiocyanate-phenol-chloroform extraction', *Anal Biochem,* 162(1), pp. 156-159.

Clark, E., Hoare, C., Tanianis-Hughes, J., et al. (2005) 'Interferon-gamma induces translocation of commensal Escherichia coli across gut epithelial cells via a lipid raft-mediated process', *Gastroenterology,* 128, pp. 1258-1267.

Claus, S. P., Ellero, S. L., Berger, B., et al. (2011) 'Colonization-induced host-gut microbial metabolic interaction', *MBio,* 2(2), pp. e00271-10.

Clayburgh, D. R., Barrett, T. A., Tang, Y., et al. (2005) 'Epithelial myosin light chain kinase-dependent barrier dysfunction mediates T cell activation-induced diarrhea in vivo', *J Clin Invest,* 115(10), pp. 2702-15.

Cosnes, J. (2004) 'Tobacco and IBD: relevance in the understanding of disease mechanisms and clinical practice', *Best Practice & Research Clinical Gastroenterology,* 18(3), pp. 481-496.

Crawley, M. L. (2010) 'Farnesoid X receptor modulators: a patent review', *Expert Opin Ther Patents,* 20(8), pp. 1047-1057.

Crohn, B. B., Ginzburg, I. and Oppenheimer, G. D. (1932) 'Regional Ileitis: a pathological and clinical entity', *Journal of the American Medical Association,* 99, pp. 1323-1329.

Cunningham, K. E. and Turner, J. R. (2012) 'Myosin light chain kinase: pulling the strings of epithelial tight junction function', *Ann N Y Acad Sci,* 1258, pp. 34-42.

Dalmasso, G., Charrier-Hisamuddin, L., Nguyen, H. T., et al. (2008) 'PepT1-Mediated Tripeptide KPV Uptake Reduces Intestinal Inflammation', *Gastroenterology,* 134(1), pp. 166-178.

Dalziel, T. K. (1913) 'Chronic Interstitial Enteritis', *British Journal of Medicine,* 2, pp. 1068-1079.

de Aguiar Vallim, T. Q., Tarling, E. J. and Edwards, P. A. (2013) 'Pleiotropic roles of bile acids in metabolism', *Cell Metab,* 17(5), pp. 657-69.

De Filippo, C., Cavalieri, D., Di Paola, M., et al. (2010) 'Impact of diet in shaping gut microbiota revealed by a comparative study in children from Europe and rural Africa', *Proc Natl Acad Sci U S A,* 107(33), pp. 14691-6.

de Jonge, H. J., Fehrmann, R. S., de Bont, E. S., et al. (2007) 'Evidence based selection of housekeeping genes', *PLoS One,* 2(9), pp. e898.

Dekaney, C. M., von Allmen, D. C., Garrison, A. P., et al. (2008) 'Bacterial-dependent up-regulation of intestinal bile acid binding protein and transport is FXR-mediated following ileo-cecal resection', *Surgery,* 144, pp. 174-181.

Denizot, J., Sivignon, A., Barreau, F., et al. (2012) 'Adherent-invasive Escherichia coli induce claudin-2 expression and barrier defect in CEABAC10 mice and Crohn's disease patients', *Inflamm Bowel Dis,* 18(2), pp. 294-304.

Devkota, S., Wang, Y., Musch, M. W., et al. (2012) 'Dietary-fat-induced taurocholic acid promotes pathobiont expansion and colitis in Il10-/- mice', *Nature,* 487(7405), pp. 104-8.

Difedele, L. M., He, J., Bonkowski, E. L., et al. (2005) 'Tumor Necrosis Factor α Blockade Restores Growth Hormone Signaling in Murine Colitis', *Gastroenterology,* 128(5), pp. 1278-1291.

Ding, S., Chi, M. M., Scull, B. P., et al. (2010) 'High-Fat Diet: Bacteria Interactions Promote Intestinal Inflammation Which Precedes and Correlates with Obesity and Insulin Resistance in Mouse', *PLoS One,* 5(8), pp. e12191.

Dowman, J. K., Hopkins, L. J., Reynolds, G. M., et al. (2014) 'Development of hepatocellular carcinoma in a murine model of nonalcoholic steatohepatitis induced by use of a high-fat/fructose diet and sedentary lifestyle', *Am J Pathol,* 184(5), pp. 1550-61.

Duboc, H., Rajca, S., Rainteau, D., et al. (2013) 'Connecting dysbiosis, bile-acid dysmetabolism and gut inflammation in inflammatory bowel diseases', *Gut,* 62(4), pp. 531-9.

Eckmann, L., Kagnoff, M. F. and Fierer, J. (1993) 'Epithelial cells secrete the chemokine interleukin-8 in response to bacterial entry', *Infect Immun.,* 61(11), pp. 4569-4574.

Eeckhaut, V., Machiels, K., Perrier, C., et al. (2013) 'Butyricicoccus pullicaecorum in inflammatory bowel disease', *Gut,* 62(12), pp. 1745-52.

Fasano, A. (2012) 'Leaky gut and autoimmune diseases', *Clin Rev Allergy Immunol,* 42(1), pp. 71-8.

Fava, F. and Danese, S. (2011) 'Intestinal microbiota in inflammatory bowel disease: Friend or foe?', *World Journal Of Gastorenterology,* 17(5), pp. 557-566.

Fina, D., Franze, E., Rovedatti, L., et al. (2011) 'Interleukin-25 production is differently regulated by TNF-alpha and TGF-beta1 in the human gut', *Mucosal Immunol,* 4(2), pp. 239-44.

Fiorucci, S., Rizzo, G., Antonelli, E., et al. (2005) 'A farnesoid x receptor-small heterodimer partner regulatory cascade modulates tissue metalloproteinase inhibitor-1 and matrix metalloprotease expression in hepatic stellate cells and promotes resolution of liver fibrosis', *J Pharmacol Exp Ther,* 314(2), pp. 584-95.

Flier, S. N., Tanjore, H., Kokkotou, E. G., et al. (2010) 'Identification of epithelial to mesenchymal transition as a novel source of fibroblasts in intestinal fibrosis', *J Biol Chem,* 285(26), pp. 20202-12.

Fogh, J. and Trempe, G. (1975) 'Human Tumor Cells In Vitro', *Plenum (J.Fogh, ed.)*, pp. 115-141.

Franke, A., McGovern, D. P., Barrett, J. C., et al. (2010) 'Genome-wide meta-analysis increases to 71 the number of confirmed Crohn's disease susceptibility loci', *Nat Genet,* 42(12), pp. 1118-25.

Fries, W., Muja, C., Crisafulli, C., et al. (2008) 'Dynamics of enterocyte tight junctions: effect of experimental colitis and two different anti-TNF strategies', *Am J Physiol Gastrointest Liver Physiol,* 294, pp. 938-947.

Fritz, T., Niederreiter, L., Adolph, T., et al. (2011) 'Crohn's disease: NOD2, autophagy and ER stress converge', *Gut,* 60(11), pp. 1580-8.

Fuss, I. J., Neurath, M. F., Boirivant, M., et al. (1996) 'Disparate CD4+ Lamina Propria (LP) Lymphokine Secretion Profiles in Inflammatory Bowel Disease', *Journal of Immunology,* 157, pp. 1261-1270.

Gadaleta, R. M., Oldenburg, B., Willemsen, E. C., et al. (2011a) 'Activation of bile salt nuclear receptor FXR is repressed by pro-inflammatory cytokines activating NF-kappaB signaling in the intestine', *Biochim Biophys Acta,* 1812(8), pp. 851-8.

Gadaleta, R. M., van Erpecum, K. J., Oldenburg, B., et al. (2011b) 'Farnesoid X receptor activation inhibits inflammation and preserves the intestinal barrier in inflammatory bowel disease', *Gut,* 60(4), pp. 463-72.

Gadaleta, R. M., van Mil, S. W., Oldenburg, B., et al. (2010) 'Bile acids and their nuclear receptor FXR: Relevance for hepatobiliary and gastrointestinal disease', *Biochim Biophys Acta,* 1801(7), pp. 683-92.

Gibson, P. R. and Shepherd, S. J. (2005) 'Personal view: food for thought--western lifestyle and susceptibility to Crohn's disease. The FODMAP hypothesis', *Aliment Pharmacol Ther,* 21(12), pp. 1399-409.

Glasser, A. L., Boudeau, J., Barnich, N., et al. (1999) 'Invasive ability of an Escherichia coli strain isolated from ileal mucosa of a patient with Crohn's disease', *Infect Immun.,* 67, pp. 5529-5537.

GMC (2013) *Good Medical Practice - Consent to research*. http://www.gmc-uk.org/guidance/ethical_guidance/5993.asp.

Goodwin, B., Jones, S. A., Price, R. R., et al. (2000) 'A Regulatory Cascade of the Nuclear Receptors FXR, SHP-1, and LRH-1 Represses Bile Acid Biosynthesis', *Mol Cell,* 6, pp. 517-526.

Hambruch, E., Miyazaki, M., Miyazaki-Anzia, S., et al. (2013) 'FXR agonist Px-102 improves steatosis in NAFLD mouse models', *Presented at APASL Liver Week, Singapore, Malaysia*.

Hanuer, S. B. (2006) 'Inflammatory Bowel Disease: Epidemiology, Pathogenesis, and Therapeutic Opportunities', *Inflamm Bowel Dis,* 12(1), pp. S3-S9.

Hart, A. L., Al-Hassi, H. O., Rigby, R. J., et al. (2005) 'Characteristics of Intestinal Dendritic Cells in Inflammatory Bowel Diseases', *Gastroenterology,* 129(1), pp. 50-65.

Haselow, K., Bode, J. G., Wammers, M., et al. (2013) 'Bile acids PKA-dependently induce a switch of the IL-10/IL-12 ratio and reduce proinflammatory capability of human macrophages', *J Leukoc Biol,* 94(6), pp. 1253-64.

Hedin, C. R., Stagg, A. J., Whelan, K., et al. (2012) 'Family studies in Crohn's disease: new horizons in understanding disease pathogenesis, risk and prevention', *Gut,* 61(2), pp. 311-8.

Hidalgo, I. J., Raub, T. J. and Borchardt, R. T. (1989) 'Characterization of the human colon carcinoma cell line (Caco-2) as a model system for intestinal epithelial permeability', *Gastroenterology,* 96, pp. 736-749.

Hofmann, A. F. (2009) 'Chronic diarrhoea caused by idiopathic bile acid malabsorption: an explanation at last.', *Expert Rev. Gastroenterol. Hepatol.,* 3(5), pp. 461-464.

Hofmann, A. F. and Eckmann, L. (2006) 'How bile acids confer gut mucosal protection against bacteria', *Proc Natl Acad Sci U S A,* 103(12), pp. 4333-4.

Holland, P. M., Abramson, R. D., Watson, R., et al. (1991) 'Detection of specific polymerase chain reaction product by utilizing the 5'----3' exonuclease activity of Thermus aquaticus DNA polymerase', *Proc Natl Acad Sci U S A,* 88(16), pp. 7278-7280.

Hotamisligil, G. S., Arner, P., Caro, J. F., et al. (1995) 'Increased adipose tissue expression of tumor necrosis factor-alpha in obesity and insulin resistance', *J Clin Invest.,* 95(5), pp. 2409-2415.

Hotamisligil, G. S., Shargill, N. S. and Spiegelman, B. M. (1993) 'Adipose expression of tumor necrosis factor-alpha: direct role in obesity-linked insulin resistance', *Science,* 259, pp. 87-91.

Hou, J. K., Abraham, B. and El-Serag, H. (2011) 'Dietary intake and risk of developing inflammatory bowel disease: a systematic review of the literature', *American Journal of Gastroenterology,* 106, pp. 563-573.

Hugot, J., Chamaillard, M., Zouali, H., et al. (2001) 'Association of NOD2 leucine-rich repeat variants with susceptibility to Crohn's disease', *Nature,* 411, pp. 599-603.

Huttenhower, C., Kostic, A. D. and Xavier, R. J. (2014) 'Inflammatory bowel disease as a model for translating the microbiome', *Immunity,* 40(6), pp. 843-54.

Inagaki, T., Moschetta, A., Lee, Y. K., et al. (2006) 'Regulation of antibacterial defense in the small intestine by the nuclear bile acid receptor', *Proc Natl Acad Sci U S A,* 103(10), pp. 3920-5.

Islam, K. B., Fukiya, S., Hagio, M., et al. (2011) 'Bile acid is a host factor that regulates the composition of the cecal microbiota in rats', *Gastroenterology,* 141(5), pp. 1773-81.

Jiang, C., Li, F., Zhang, L., et al. (2015) 'Intestinal farnesoid X receptor signaling promotes nonalcoholic fatty liver disease', *J Clin Invest.,* 125(1), pp. 386-402.

Jones, B. V., Begley, M., Hill, C., et al. (2008) 'Functional and comparative metagenomic analysis of bile salt hydrolase activity in the human gut microbiome', *Proc Natl Acad Sci U S A,* 105(36), pp. 13580-5.

Joossens, M., Huys, G., Cnockaert, M., et al. (2011) 'Dysbiosis of the faecal microbiota in patients with Crohn's disease and their unaffected relatives', *Gut,* 60(5), pp. 631-7.

Jostins, L. and Ripke, S. and Weersma, R. K., et al. (2012) 'Host-microbe interactions have shaped the genetic architecture of inflammatory bowel disease', *Nature,* 491(7422), pp. 119-24.

Jovani, M., Fiorino, G. and Danese, S. (2013) 'Anti-IL-13 in inflammatory bowel disease: from the bench to the bedside', *Curr Drug Targets,* 14(12), pp. 1444-1452.

Jumarie, C. and Malo, C. (1991) 'Caco-2 cells cultured in serum-free medium as a model for the study of enterocytic differentiation in vitro', *Jnl Cell Physiol.,* 149, pp. 24-33.

Kannegati, T. D., Lamkanfi, M., Nunez, G., et al. (2007) 'Intracellular NOD-like receptors in the host defense and disease', *Immunity,* 27, pp. 549-559.

Katsuma, S., Hirasawa, A. and Tsujimoto, G. (2005) 'Bile acids promote glucagon-like peptide-1 secretion through TGR5 in a murine enteroendocrine cell line STC-1', *Biochem. Biophys. Res. Commun.,* 329(1), pp. 386-390.

Keita, A. V., Salim, S. Y. and Jiang, T. (2008) 'Increased uptake of non-patho- genic E. coli via the follicle-associated epithelium in longstanding ileal Crohn's disease', *Jnl Pathology,* 2008(215), pp. 135 - 144.

Khor, B., Gardet, A. and Xavier, R. J. (2011) 'Genetics and pathogenesis of inflammatory bowel disease', *Nature,* 474(7351), pp. 307-17.

Khurana, S., Raufman, J. P. and Pallone, T. L. (2011) 'Bile acids regulate cardiovascular function', *Clin Transl Sci,* 4(3), pp. 210-8.

Kiesslich, R., Duckworth, C. A., Moussata, D., et al. (2012) 'Local barrier dysfunction identified by confocal laser endomicroscopy predicts relapse in inflammatory bowel disease', *Gut,* 61(8), pp. 1146-53.

Konkel, J. E. and Chen, W. (2011) 'Balancing acts: the role of TGF-beta in the mucosal immune system', *Trends Mol Med,* 17(11), pp. 668-76.

Kouadjo, K. E., Nishida, Y., Cadrin-Girard, J. F., et al. (2007) 'Housekeeping and tissue-specific genes in mouse tissues', *BMC Genomics,* 8, pp. 127.

Lee, J. W., Wang, P., Kattah, M. G., et al. (2008) 'Differential Regulation of Chemokines by IL-17 in Colonic Epithelial Cells', *J Immunol,* 181, pp. 6536-6545.

Lees, C. W., Barrett, J. C., Parkes, M., et al. (2011) 'New IBD genetics: common pathways with other diseases', *Gut,* 60(12), pp. 1739-53.

Leone, V., Chang, E. B. and Devkota, S. (2013) 'Diet, microbes, and host genetics: the perfect storm in inflammatory bowel diseases', *J Gastroenterol,* 48(3), pp. 315-21.

Leong, R. W. L., Lau, J. Y. and Sung, J. J. Y. (2004) 'The Epidemiology and Phenotype of Crohn's Disease in the Chinese Population', *Inflamm Bowel Dis,* 10(5), pp. 646-651.

Levine, B. and Kroemer, G. (2008) 'Autophagy in the pathogenesis of disease', *Cell,* 132, pp. 27-42.

Licharowicz, A. M. and Mayberry, J. F. (1988) 'Antoni Lesniowski and his contribution to regional enteritis (Crohn's disease)', *Journal of the Royal Society for Medicine,* 81(8), pp. 468-470.

Life Technologies Product Literature 2014. RNAlater®-ICE Frozen Tissue Transition Solution.

Livak, K. J. and Schmittgen, T. D. (2001) 'Analysis of Relative Gene Expression Data Using Real-Time Quantitative PCR and the 2−ΔΔCT Method', *Methods,* 25(4), pp. 402-408.

Lorenzo-Zuniga, V., Bartoli, R., Planas, R., et al. (2003) 'Oral bile acids reduce bacterial overgrowth, bacterial translocation, and endotoxemia in cirrhotic rats', *Hepatology,* 37(3), pp. 551-7.

Ma, T. Y., Boivin, M. A., Ye, D., et al. (2005) 'Mechanism of TNF-{alpha} modulation of Caco-2 intestinal epithelial tight junction barrier: role of myosin light-chain kinase protein expression', *Am J Physiol Gastrointest Liver Physiol,* 288(3), pp. G422-30.

Ma, T. Y., Iwamoto, G. K., Hoa, N. T., et al. (2004) 'TNF-alpha-induced increase in intestinal epithelial tight junction permeability requires NF-kappa B activation', *Am J Physiol Gastrointest Liver Physiol,* 286(3), pp. G367-76.

Maeda, S., Hsu, L. C., Liu, H., et al. (2005) 'Nod2 mutation in Crohn's disease potentiates NF-kappaB activity and Il-1beta processing', *Science,* 307, pp. 734-738.

Makishima, M., Okamoto, A. Y., Repa, J. J., et al. (1999) 'Identification of a nuclear receptor for bile acids', *Sicence,* 21(284), pp. 1362-1365.

Mangelsdorf, D. J., Thummel, C., Beato, M., et al. (1995) 'The Nuclear Receptor Superfamily: The Second Decade', *Cell,* 83, pp. 835-839.

Manichanh, C., Rigottier-Gois, L., Bonnaud, E., et al. (2006) 'Reduced diversity of faecal microbiota in Crohn's disease revealed by metagenomic approach', *Gut,* 55, pp. 205-211.

Marteau, P. (2013) 'Butyrate-producing bacteria as pharmabiotics for inflammatory bowel disease', *Gut,* 62, pp. 1673.

Martin, F. P., Dumas, M. E., Wang, Y., et al. (2007) 'A top-down systems biology view of microbiome-mammalian metabolic interactions in a mouse model', *Mol Syst Biol,* 3, pp. 112.

Martinez-Medina, M., Denizot, J., Dreux, N., et al. (2014) 'Western diet induces dysbiosis with increased E coli in CEABAC10 mice, alters host barrier function favouring AIEC colonisation', *Gut,* 63(1), pp. 116-24.

McGuckin, M. A., Eri, R., Simms, L. A., et al. (2009) 'Intestinal barrier dysfunction in inflammatory bowel diseases', *Inflamm Bowel Dis,* 15(1), pp. 100-13.

Modica, S., Gadaleta, R. M. and Moschetta, A. (2010) 'Deciphering the nuclear bile acid receptor FXR paradigm', *Nucl Recept Signal,* 8, pp. e005.

Modica, S., Murzilli, S., Salvatore, L., et al. (2008) 'Nuclear bile acid receptor FXR protects against intestinal tumorigenesis', *Cancer Res,* 68(23), pp. 9589-94.

Molodecky, N. A., Soon, I. S., Rabi, D. M., et al. (2012) 'Increasing incidence and prevalence of the inflammatory diseases with time, based on systematic review', *Gastroenterology,* 142(1), pp. 46-54.

Monteleone, G., Kumberova, A., Croft, N. M., et al. (2001) 'Blocking Smad7 restores TGF-β1 signaling in chronic inflammatory bowel disease', *Journal of Clinical Investigation,* 108(4), pp. 601-609.

Mosmann, T. R., Cherwinski, H., Bond, M. W., et al. (1986) 'Definition According to Profiles of Lymphokine Activities and Secreted Proteins', *Journal of Immunology,* 136(7), pp. 2348-2357.

Motulsky, H. J. and Brown, R. E. (2006) 'Detecting outliers when fitting data with nonlinear regression – a new method based on robust nonlinear regression and the false discovery rate', *BMC Bioinformatics,* 7(123), pp. 1-20.

Mouli, V. P. and Ananthakrishnan, A. N. (2014) 'Review article: vitamin D and inflammatory bowel diseases', *Aliment Pharmacol Ther,* 39(2), pp. 125-36.

Muniz, L. R., Knosp, C. and Yeretssian, G. (2012) 'Intestinal antimicrobial peptides during homeostasis, infection, and disease', *Front Immunol,* 3, pp. 310.

Musch, M. W., Clarke, L. L., Mamah, D., et al. (2002) 'T cell activation causes diarrhea by increasing intestinal permeability and inhibiting epithelial Na+/K+-ATPase', *J Clin Invest.,* 110, pp. 1739-1747.

Nanthakumar, N. N., Fusunyan, R. D., Sanderson, I., et al. (2000) 'Inflammation in the developing human intestine: A possible pathophysiologic contribution to necrotizing enterocolitis', *Proc Natl Acad Sci U S A,* 97(11), pp. 6043-6048.

Neuschwander-Tetri, B. A., Loomba, R., Sanyal, A. J., et al. (2015) 'Farnesoid X nuclear receptor ligand obeticholic acid for non-cirrhotic, non-alcoholic steatohepatitis (FLINT): a multicentre, randomised, placebo-controlled trial', *The Lancet,* 385(9972), pp. 956-965.

Nevens, F., Andreone, P., Mazzella, G., et al. (2014) 'O168 the First Primary Biliary Cirrhosis (Pbc) Phase 3 Trial in Two Decades – an International Study of the Fxr Agonist Obeticholic Acid in Pbc Patients', *Journal of Hepatology,* 60(1), pp. S525-S526.

Nicholson, J. K., Holmes, E. and Wilson, I. D. (2005) 'Gut microorganisms, mammalian metabolism and personalized health care', *Nat Rev Microbiol.,* 3, pp. 431-438.

Nijmeijer, R. M., Gadaleta, R. M., van Mil, S. W. C., et al. (2011) 'Farnesoid X Receptor (FXR) Activation and FXR Genetic Variation in Inflammatory Bowel Disease', *PLoS One,* 6(8), pp. e23745.

Noguchi, E., Homma, Y., Kang, X., et al. (2009) 'A Crohn's disease- associated NOD2 mutation suppresses transcription of human IL10 by inhibiting activity of the nuclear ribonucleoprotein hnRNP-A1', *Nat Immunol,* 10, pp. 471-479.

Ogata, Y., Nishi, M., Nakayama, H., et al. (2003) 'Role of bile in intestinal barrier function and its inhibitory effect on bacterial translocation in obstructive jaundice in rats', *Journal of Surgical Research,* 115(1), pp. 18-23.

Ostaff, M. J., Stange, E. F. and Wehkamp, J. (2013) 'Antimicrobial peptides and gut microbiota in homeostasis and pathology', *EMBO Mol Med,* 5(10), pp. 1465-83.

Park, S., Ha, S. D., Coleman, M., et al. (2013) 'p62/SQSTM1 enhances NOD2-mediated signaling and cytokine production through stabilizing NOD2 oligomerization', *PLoS One,* 8(2), pp. e57138.

Parks, D. J., Blanchard, S. G., Bledsoe, R. K., et al. (1999) 'Bile acids: natural ligands for an orphan nuclear receptor', *Science,* 21(284), pp. 1365-1368.

Payne, C. M., Bernstein, C., Dvorak, K., et al. (2008) 'Hydrophobic bile acids, genomic instability, Darwinian selection, and colon carcinogenesis', *Clin Exp Gastro,* 1, pp. 19-47.

Pellicciari, R., Fiorucci, S., Camaioni, E., et al. (2002) '6alpha-Ethyl-Chenodeoxycholic Acid (6-ECDCA), a Potent and Selective FXR Agonist Endowed with Anticholestatic Activity', *J Medic Chem.,* 45(3569-3572).

Philpott, D. J. and Girardin, S. E. (2004) 'The role of Toll-like receptors and Nod proteins in bacterial infection', *Mol Immunol,* 41(11), pp. 1099-108.

Pizarro, T. T., Arseneau, K. O., Bamias, G., et al. (2003) 'Mouse models for the study of Crohn's disease', *Trends in Mol Med,* 9(5), pp. 218-222.

Pollan, M. (2013) 'Some of My Best Friends Are Germs', *New York Times*.

Probert, C. S., Jayanthi, V., Pollock, D. J., et al. (1992) 'Crohn's disease in Bangladeshi and Europeans in Britain: an epidemiological comparison in Tower Hamlets', *Postgrad Med J,* 68, pp. 914-920.

Radisky, D. C. (2005) 'Epithelial-mesenchymal transition', *J Cell Sci,* 118(Pt 19), pp. 4325-6.

Renga, B., Mencarelli, A., Migliorati, M., et al. (2011) 'SHP-dependent and -independent induction of peroxisome proliferator-activated receptor-gamma by the bile acid sensor farnesoid X receptor counter-regulates the pro-inflammatory phenotype of liver myofibroblasts', *Inflamm Res,* 60(6), pp. 577-87.

Richman, E. and Rhodes, J. M. (2013) 'Review article: evidence-based dietary advice for patients with inflammatory bowel disease', *Aliment Pharmacol Ther,* 38(10), pp. 1156-71.

Riedel, C. U., Foata, F., Philippe, D., et al. (2006) 'Anti-inflammatory effects of bifidobacteria by inhibition of LPS-induced NF-κB activation', *World J Gastroenterol,* 12(23), pp. 3729-3735.

Roberts, C. L., Keita, A. V., Duncan, S. H., et al. (2010) 'Translocation of Crohn's disease Escherichia coli across M-cells: contrasting effects of soluble plant fibres and emulsifiers', *Gut,* 59(10), pp. 1331-9.

Robinson, L. B., Wichelhausen, R. H. and Roizman, B. (1956) 'Contamination of Human Cell Cultures by Pleuropneumonialike Organisms', *Science,* 124, pp. 1147-1148.

Rottem, S. and Barile, M. F. (1993) 'Beware of Mycoplasmas', *Trends in Biotechnology,* 11, pp. 143-150.

Runkle, E. A. and Mu, D. (2013) 'Tight junction proteins: from barrier to tumorigenesis', *Cancer Lett,* 337(1), pp. 41-8.

Rutgeerts, P. (2003) 'Strategies in the prevention of post-operative recurrence in Crohn's disease', *Best Practice & Research Clinical Gastroenterology,* 17, pp. 63-73.

Rutgeerts, P., Goboes, K., Peeters, M., et al. (1991) 'Effect of faecal stream diversion on recurrence of Crohn's disease in the neoterminal ileum', *The Lancet,* 338, pp. 771-774.

Rutter, M. a. B. M. (2005) 'Terminal ileal biopsies should not be used to document extent of colonoscopic examination', *Gut,* 54, pp. 565-568.

Sato, H., Macchiarulo, A. and Thomas, C. e. a. (2008) 'Novel potent and selective bile acid derivatives as TGR5 agonists: biological screening, structure-activity reltaionships, and molecular modeling studies', *Jnl Med Chem,* 51, pp. 1831-1841.

Schaap, F. G., Jansen, P. L. and Olde Damink, S. W. (2015) 'FXR, intestinal FiXeR of hepatocellular carcinoma?', *Hepatology,* 61(1), pp. 21-3.

Schulzke, J. D., Gitter, A. H., Mankertz, J., et al. (2005) 'Epithelial transport and barrier function in occludin-deficient mice', *Biochim Biophys Acta,* 1669, pp. 34-42.

Sellon, R. K., Tonkonogy, S., Schultz, M., et al. (1998) 'Resident enteric bacteria are necessary for development of spontaneous colitis and immune system activation in interleukin-10-deficient mice', *Infect Immun.,* 66, pp. 5224-5231.

Soderholm, J. D., Olaison, G., Peterson, K. H., et al. (2002) 'Augmented increase in tight junction permeability by luminal stimuli in the non-inflamed ileum of Crohn's disease', *Gut,* 50, pp. 307-313.

Soderholm, J. D., Streutker, C., Yang, P. C., et al. (2004) 'Increased epithelial uptake of protein antigens in the ileum of Crohn's disease mediated by tumour necrosis factor-alpha', *Gut,* 53, pp. 1817-1824.

Sokol, H., Pigneur, B., Watterlot, L., et al. (2008) 'Faecalibacterium prausnitzii is an anti-inflammatory commensal bacterium identified by gut microbiota analysis of Crohn disease patients', *Proc Natl Acad Sci U S A,* 105(43), pp. 16731-6.

Sokol, H., Seksik, P., Furet, J. P., et al. (2009) 'Low counts of Faecalibacterium prausnitzii in colitis microbiota', *Inflamm Bowel Dis,* 15(8), pp. 1183-9.

Sokol, H., Seksik, P., Rigottier-Gois, L., et al. (2006) 'Specificities of the fecal microbiota in inflammatory bowel disease', *Inflamm Bowel Dis,* 12, pp. 106-111.

Sommers, S. C. and Korelitz, B. I. (1975) 'Mucosal-cell counts in ulcerative and granulomatous colitis', *Am J Clin Pathol,* 63, pp. 359-365.

Steenholdt, C., Brynskov, J., Thomsen, O. O., et al. (2014) 'Individualised therapy is more cost-effective than dose intensification in patients with Crohn's disease who lose response to anti-TNF treatment: a randomised, controlled trial', *Gut,* 63(6), pp. 919-27.

Strober, W. and Fuss, I. J. (2011) 'Proinflammatory cytokines in the pathogenesis of inflammatory bowel diseases', *Gastroenterology,* 140(6), pp. 1756-67.

Su, L., Shen, L., Clayburgh, D. R., et al. (2009) 'Targeted epithelial tight junction dysfunction causes immune activation and contributes to development of experimental colitis', *Gastroenterology,* 136(2), pp. 551-63.

Suenaert, P., Bulteel, V., Lemmens, L., et al. (2002) 'Anti-tumor necrosis factor treatment restores the gut barrier in Crohn's disease', *American Journal of Gastroenterology,* 97, pp. 2000-2004.

Suzuki, T. (2013) 'Regulation of intestinal epithelial permeability by tight junctions', *Cell Mol Life Sci,* 70(4), pp. 631-59.

Swann, J. R., Want, E. J., Geier, F. M., et al. (2011) 'Systemic gut microbial modulation of bile acid metabolism in host tissue compartments', *Proc Natl Acad Sci U S A,* 108 Suppl 1, pp. 4523-30.

Tazuke, Y., Drongowski, R. A., Teitelbaum, D. H., et al. (2003) 'Interleukin-6 changes tight junction permeability and intracellular phospholipid content in a human enterocyte cell culture model', *Pediatr Surg Int,* 19(5), pp. 321-5.

Tesori, V., Puglisi, M. A., Lattanzi, W., et al. (2013) 'Update on small intestinal stem cells', *World J Gastroenterol,* 19(29), pp. 4671-8.

Tetri, L. H., Basaranoglu, M., Brunt, E. M., et al. (2008) 'Severe NAFLD with hepatic necroinflammatory changes in mice fed trans fats and a high-fructose corn syrup equivalent', *Am J Physiol Gastrointest Liver Physiol,* 295(5), pp. G987-95.

The Jackson Laboratory (2015) *JAX Mice Database, 000635 C3H/HeOuJ*. Available at: http://jaxmice.jax.org/strain/000635.html.

Thomas, C., Gioiello, A., Noriega, L., et al. (2009) 'TGR5-mediated bile acid sensing controls glucose homeostasis', *Cell Metab,* 10(3), pp. 167-77.

Thorburn, A. N., Macia, L. and Mackay, C. R. (2014) 'Diet, metabolites, and "western-lifestyle" inflammatory diseases', *Immunity,* 40(6), pp. 833-42.

Turcotte, J., Wong, K., Mah, S. J., et al. (2012) 'Increased Epithelial Gaps in the Small Intestine Are Predictive of Hospitalization and Surgery in Patients With Inflammatory Bowel Disease', *Clinical and Translational Gastroenterology,* 3(e19).

Turksen, K. and Troy, T. C. (2004) 'Barriers built on claudins', *Jnl Cell Sci,* 117, pp. 2435-2447.

Turnbaugh, P. J., Ridaura, V. K., Faith, J. J., et al. (2009) 'The effect of diet on the human gut microbiome: a metagenomic analysis in humanized gnotobiotic mice', *Sci Transl Med,* 1(6), pp. 6ra14.

Urizar, N. L., Liverman, A. B., Dodds, D. T., et al. (2002) 'A natural product that lowers cholesterol as an antagonist ligand for FXR', *Science,* 296, pp. 1703-1706.

Van Assche, G. and Rutgeerts, P. (2004) 'Medical management of postoperative recurrence in Crohn's disease', *Gastroenterol Clin North Am,* 33(347-360).

Van Limbergen, J., Wilson, D. C. and Satsangi, J. (2009) 'The genetics of Crohn's disease', *Annu Rev Genomics Hum Genet,* 10, pp. 89-116.

van Schaik, F. D., Gadaleta, R. M., Schaap, F. G., et al. (2012) 'Pharmacological activation of the bile acid nuclear farnesoid X receptor is feasible in patients with quiescent Crohn's colitis', *PLoS One,* 7(11), pp. e49706.

Vavassori, P., Mencarelli, A., Renga, B., et al. (2009) 'The bile acid receptor FXR is a modulator of intestinal innate immunity', *J Immunol,* 183(10), pp. 6251-61.

Velcich, A., Yang, W., Heyer, J., et al. (2002) 'Colorectal cancer in mice genetically deficient in the mucin Muc2', *Science,* 295, pp. 1726-1729.

von Ahlfen, S. and Schlumpberger, M. (2010) 'Effects of low A260/A230 ratios in RNA preparations on downstream applications', *Gene Expression Newsletter (QIAGEN),* 15, pp. 7-8.

Wan, Y. Y. and Flavell, R. A. (2007) ''Yin-Yang' functions of TGF-beta and Tregs in immune regulation', *Immunol Rev,* 220, pp. 199-213.

Wang, F., Vallen Graham, W., Wang, Y., et al. (2005) *Am J Pathol,* 166(2), pp. 409-419.

Wang, W., Chen, J., Hollister, K., et al. (1999) 'Endogenous Bile Acids Are Ligands for the Nuclear Receptor FXR/BAR', *Molecular Cell,* 3, pp. 543-553.

Wang, Y. D., Chen, W. D., Wang, M., et al. (2008) 'Farnesoid X receptor antagonizes nuclear factor kappaB in hepatic inflammatory response', *Hepatology,* 48(5), pp. 1632-43.

Ward, J. B., Mroz, M. S. and Keely, S. J. (2013) 'The bile acid receptor, TGR5, regulates basal and cholinergic-induced secretory responses in rat colon', *Neurogastroenterol Motil,* 25(8), pp. 708-711.

Watanabe, M., Houten, S. M., Wang, L., et al. (2004) 'Bile acids lower triglyceride levels via a pathway involving FXR, SHP, and SREBP-1c', *The Journal of Clinical Investigation,* 113(10), pp. 1408-1418.

Weber, C. R. and Turner, J. R. (2007) 'Inflammatory bowel disease: is it really just another break in the wall?', *Gut,* 56, pp. 6-8.

Wehkamp, J., Salzman, N. H., Porter, E., et al. (2005) 'Reduced Paneth cell alph-defensins in ileal Crohn's disease', *Proc Natl Acad Sci U S A,* 102, pp. 18129-18134.

Wellcome Trust Case Control Consortium (2007) 'Genome-wide association study of 14,000 cases of seven common diseases and 3,000 shared controls', *Nature,* 447(7145), pp. 661-78.

Wellen, K. E. and Hotamisligil, G. S. (2005) 'Inflammation, stress and diabetes', *J Clin Invest.,* 115(5), pp. 1112-1119.

Wildenberg, M. E. and van den Brink, G. R. (2011) 'FXR activation inhibits inflammation and preserves the intestinal barrier in IBD', *Gut,* 60, pp. 432-433.

Williams, J. A., Thomas, A. M., Li, G., et al. (2012) 'Tissue specific induction of p62/Sqstm1 by farnesoid X receptor', *PLoS One,* 7(8), pp. e43961.

Wu, G. D., Chen, J., Hoffman, C., et al. (2011) 'Linking Long-Term Dietary Patterns With Gut Microbial Enterotypes', *Science,* 334(6052), pp. 105-108.

Wu, J., Xia, C., Meier, J., et al. (2002) 'The hypolipidemic natural product guggulsterone acts as an antagonist of the bile acid receptor', *Mol Endocrinol,* 16, pp. 1590-1597.

Wu, S., Zhang, Y. G., Lu, R., et al. (2014) 'Intestinal epithelial vitamin D receptor deletion leads to defective autophagy in colitis', *Gut*.

Xavier, R. J. and Podolsky, D. K. (2007) 'Unravelling the pathogenesis of inflammatory bowel disease', *Nature,* 448(7152), pp. 427-34.

Yoneno, K., Hisamatsu, T., Shimamura, K., et al. (2013) 'TGR5 signalling inhibits the production of pro-inflammatory cytokines by in vitro differentiated inflammatory and intestinal macrophages in Crohn's disease', *Immunology,* 139(1), pp. 19-29.

Zahs, A., Bird, M. D., Ramirez, L., et al. (2013) 'Anti-IL-6 antibody treatment but not IL-6 knockout improves intestinal barrier function and reduces inflammation following binge ethanol exposure and burn injury', *Shock,* 39(4), pp. 373-379.

Zeissig, S., Burgel, N., Gunzel, D., et al. (2007) 'Changes in expression and distribution of claudin 2, 5 and 8 lead to discontinuous tight junctions and barrier dysfunction in active Crohn's disease', *Gut,* 56(1), pp. 61-72.

Zhang, J. H., Nolan, J. D., Kennie, S. L., et al. (2013) 'Potent stimulation of fibroblast growth factor 19 expression in the human ileum by bile acids', *Am J Physiol Gastrointest Liver Physiol,* 304(10), pp. G940-8.

Zilbauer, M., Jenke, A., Wenzel, G., et al. (2011) 'Intestinal alpha-defensin expression in pediatric inflammatory bowel disease', *Inflamm Bowel Dis,* 17(10), pp. 2076-2086.

Zilbauer, M., Jenke, A., Wenzel, G., et al. (2010) 'Expression of human beta-defensins in children with chronic inflammatory bowel disease', *PLoS One,* 5(10), pp. e15389.